Design Guidelines for Multi-Stage Outlet Structures situated in Stormwater Attenuation Facilities of Residential Developments in South Africa: Physical Model Investigation

Marisa Myburgh

Thesis presented in fulfilment of the requirements for the degree Master of Engineering (Research) in the Faculty of Engineering at Stellenbosch University

Supervisor: Ms. A. Bosman
Department of Civil Engineering

December 2016

Declaration

By submitting this thesis electronically, I declare that the entirety of the work contained therein is my own, original work, that I am the sole author thereof (save to the extent explicitly otherwise stated), that reproduction and publication thereof by Stellenbosch University will not infringe any third party rights and that I have not previously in its entirety or in part submitted it for obtaining any qualification.

December 2016

Abstract

Flood attenuation controls are becoming a topic of interest and are more frequently being used within urban areas of South Africa, as local authorities bring into effect stormwater policies and legislation. Another reason for the interest is the increase of urban development, which increases the impervious area within a watershed, which in return increases the run-off. This could have detrimental effects on the morphology of rivers and streams due to erosion. Literature also points out that, due to effects of climate change, the future flow, for a return period corresponding to a similar pre-development period, could increase, and stormwater ponds will then be under designed. This scenario would increase the storage volume required for detention ponds which, due to spatial constrictions, would by then be difficult or impossible to increase. The importance of accurate calculation of future discharge from a multi-stage outlet thus becomes critical.

Attenuation facilities in the past were designed to control only a single recurrence interval (RI) design storm, such as the 50-year RI storm event. However, various metropolitan municipalities now instruct developers to implement on-site flood control structures, which must be capable of controlling run-off for a full range of design flows. Previous research reports concluded that multi-stage outlet structures were more effective at mimicking the pre-development flow during a range of storm events than a single outlet structure.

The aim of this research was to evaluate the hydraulic performance of a multi-stage outlet structure and to determine the optimal range of recurrence interval storms which the multi-stage outlet structure was capable of meeting while providing the pre-development flow rates. A 1:3 scaled physical model was constructed in order to verify that thee theoretical equations and design guidelines recommended in literature accurately calculate the flow through multi-stage outlet structures. Six different configurations of multi-stage outlet structures were tested in the hydraulic laboratory of Stellenbosch University to evaluate the control of discharge for a wider range of scenarios. The multi-stage outlet models were designed to control the flow to pre-development peaks for inland and coastal regions receiving either 400 mm, 700 mm or 1000 mm of mean annual precipitation.

It became evident from the physical model test results that multi-stage outlets consisting of discharge devices sized to control four of the RI storms (2- , 10-, 50- and 100-year), were sufficient to control all six (2- , 5-, 10-, 20- 50- and 100-year) RI storms. Thus, individual control devices were not required to control the intermediate RI storms (5- and 20-year storms), as the 2- and 10-year devices would control the outflow at the corresponding 5- and 20-year water surface elevations. Thus, designing discharge control devices to control the 2- and 10-year recurrence interval storms would shorten the iterative design process of the multi-stage outlet structure.

The experimental data indicated that corrections are required to be applied to the discharge coefficient for the low flow orifice. If the value of the actual discharge coefficient is higher than the

equation discharge coefficient (typically 0.61 for rectangular orifices), the outflow from the multi-stage outlet could exceed the design criteria.

The experimental data was used to further develop the spreadsheet-based model and Visual Studio program for practitioners to use when determining the discharge from multi-stage outlet structures. It can be concluded that the multi-stage outlet structures were effective at mimicking the pre-development flow during a full range of storm events for inland and coastal regions. The design of multi-stage outlet structures could, therefore, help to prevent erosion of the water bodies to which they discharge.

Opsomming

Vloedbeheermaatreëls vir stedelike gebiede in Suid-Afrika raak al hoe meer van belang omdat plaaslike owerhede se stormwaterbeleide dit vereis. ‘n Verdere rede vir belangstelling in vloedbeheermaatreëls is die toename in stedelike ontwikkeling, wat die indringbaarheid van stormwater in ‘n afloopgebied beïnvloed en die afloop vermeerder. Bogenoemde aspekte kan ‘n wesenlike invloed uitoefen op die morfologie en erosie van strome en riviere. Literatuur dui aan dat as gevolg van die effek van klimaatsverandering, kan die voor-ontwikkelingsvloei wat ooreenstem met soortgelyke herhaalperiodes in die toekoms, toeneem en stormwater vloedvertragingsdamme sal gevolglik onderontwerp word, tensy ingenieurs se bewustheid van veranderende omstandighede tred hou daarmee. Dié aspek sal aanleiding gee tot die genoodsaakte verhoging van die stoorkapasiteit van vloedvertragingsdamme. As gevolg van ruimtelike beperkings, sal die belangrikheid van akkurate berekening van die uitvloeie vir multi-fase uitlaatstrukture van kritieke belang wees.

In die verlede is vloedvertragingsfasiliteite ontwerp om slegs ‘n enkele herhaalperiode (RI) ontwerpstorm, soos die 1:50 jaar storm, te demp. Verskeie metropolitaanse owerhede vereis tans van ontwikkelaars om op-terrein vloedbeheerstrukture vir verskillende ontwerpvloeie te voorsien. Vorige navorsing het getoon dat vloedvertragingsfasiliteite wat ontwerp word met multi-fase uitlaatstrukture, meer effektief is vir die nabootsing van voor-ontwikkeling vloeie. Die ontwerp van hierdie multi-fase uitlaatstrukture kan dus help in die voorkoming van erosie.

Die doel van hierdie navorsing was om die hidrouliese werking van ‘n multi-fase uitlaatstruktuur te ondersoek, om te bepaal of die multi-fase uitlaatstruktuur die uitvloei van die vloedbeheerfasiliteit kan beperk vir storms van verskeie herhaalperiodes. Dit is belangrik om die kwantiteit van die stormwater so akkuraat as moontlik te beheer. Gevolglik is ‘n fisiese modelstudie onderneem, op ‘n 1:3 skaal, om te bepaal of die teoretiese vergelykings en ontwerphandleidings soos aanbeveel in die literatuur, gebruik kan word om die vloei deur multi-fase uitlaatstrukture akkuraat te kan bepaal. Ses verskillende konfigurasies van die multi-fase uitlaatstruktuur is getoets in Stellenbosch Universiteit se hidrouliese laboratorium om die beheer van die uitvloei vir ‘n wye reeks scenarios te evalueer.

Uit die fisiese model se toetsresultate blyk dit duidelik dat multi-uitlate, bestaande uit uitlaatstrukture wat ontwerp is om storms van vier verskillende herhaalperiodes te beheer, voldoende was om die storms van al ses herhaalperiodes te beheer. Daarom is individuele vloeibeheerstrukture om die intermediêre herhaal periode storms (d.i. 5- en 20-jaar storms) te beheer, onnodig, want as dit korrek ontwerp is, sal die multi-fase uitlaat die uitvloei van die ooreenstemmende 5- en 20-jaar watervlak hoogtes kontroleer. Dit verkort dus die iteratiewe ontwerpproses van die multi-fase uitlaatstruktuur.

Die eksperimentele data dui ook aan dat veranderings benodig word ten opsigte van die vloei koëffisiënt vir die gaatjiesplaat wat ontwerp is vir die 2-jaar herhaalperiode storm. Indien die werklike waarde van die vloei koëffisiënt hoër is as die teoretiese vloei koëffisiënt (tipies 0.61 vir reghoekige

ontwerpe) bestaan die moontlikheid dat die uitvloei van die multi-fase uitlaat die plaaslike owerhede se vereistes sal oorskry.

Die eksperimentele data is gebruik vir die verdere ontwikkeling van ‘n Excel sigblad gebaseerde model, asook ‘n Visual Studio program, wat gebruik kan word vir die bepaling van die uitvloei vanaf multi-fase uitlaatstrukture. Dit kan afgelei word van die eksperimentele resultate dat die multi-fase uitlaat struktuur suksesvol was in die demping van die na-ontwikkelingsvloei vloedpiek tot die voor-ontwikkelingsvloei vloedpiek vir storms van al ses herhaalperiodes wat getoets is (d.i. die 2-, 5-, 10-, 20-, 50- en 100-jaar storms) vir kus en binnelandse gebiede. Die ontwerp van multi-fase uitlaatstrukture in vloedvertragingsfasiliteite kan daarom help om erosie te voorkom in die waterliggame waarin dit uitvloei.

Acknowledgements

The author acknowledges the assistance and contributions of the following individuals without whom this research would not have been possible:

- Ms. A. Bosman, for her guidance, encouragement, and accessibility as my supervisor.
- Christiaan Visser, Johan Nieuwoudt, Marvin Lindoor and Ilyaaz Williams, the Hydraulic laboratory personnel of Stellenbosch University, for their work on the instrumentation, construction of the multi-stage models, and assistance with the model set-up.
- IMESA, for offering me a post-graduate bursary.
- Alvino DeMorney at Ithuba Engineering for providing a DN 300 pipe for the hydraulic laboratory tests.
- My parents and friends, for their emotional support and encouragement to enrol for a Master's degree.

Table of Contents

Declaration i
Abstract ii
Opsomming iv
Acknowledgements vi
List of Figures x
List of Table xii
List of Abbreviations xiii
List of Symbols xiv

1. Introduction ***1***
1.1 Thesis Background and Motivation of Study **1**
1.2 Research Objectives **3**

2. Literature Review ***4***
2.1 Introduction **4**
2.2 Detention and Retention Ponds **5**
2.2.1 Background 5
2.3 Multi-Stage Pond Outlet Structures **6**
2.3.1 Background 6
2.3.2 Devices used in the Design of Multi-Stage Outlet Structures 7
2.3.3 Summary of Best Practices for Design of Multi-Stage Outlet Structures 24
2.4 Trash Racks **27**
2.4.1 Background 27
2.4.2 Main Functions of Trash Racks 27
2.4.3 Trash Rack Design Procedure 28
2.4.4 Hydraulic Capacity of Drop Inlets with Trash Rack 31
2.5 Current Practices and Regulatory Requirements in South Africa **33**
2.6 Laws of Hydraulic Similitudes in Physical Models **35**
2.6.1 Implications of the Similarity Laws 35
2.6.2 Similarity Requirements for Multi-Stage Outlets 37
2.7 Summary of Literature Review **39**

3. Model Development: Pre- and Post-Development Hydrographs ***40***
3.1 Introduction **40**
3.2 Selection of Catchment Area **41**
3.2.1 Physical Characteristics of the Case Study Area 42
3.3 Sensitivity Analysis of Input Parameters **46**
3.3.1 Urban Run-Off Coefficient 46
3.3.2 Rural Run-Off Coefficient 47
3.3.3 Average catchment slope 49

3.3.4 Summary of Sensitivity Analyses 49

4. Preliminary Design Calculations 50

4.1 Introduction 50

4.2 Storage Volume Estimation 50

4.3 Stage-Storage Relationship 51

4.4 Sizing Calculations of the Multi-Stage Outlet Structure 51

4.4.1 Layout and Dimensions of Prototype Multi-Stage Outlet Structures 54

4.5 Design Results 55

4.5.1 Background 55

4.5.2 Computed Outflow of Multi-Stage Outlets in Coastal Regions 56

4.5.3 Computed Outflow of Multi-Stage Outlets in Inland Regions 61

4.5.4 Findings and Discussion of Design Results 65

5. Physical Model Study 67

5.1 Physical Model Layout 67

5.1.1 Experimental Set-up 68

5.2 Laboratory Apparatus 69

5.2.1 Discharge Measurement 69

5.2.2 Pressure Measurement 70

5.2.3 Water Level Measurement 71

5.3 Test Procedure 72

5.4 Limitations 73

5.5 Modelling Criteria Considering Scale Effects 73

6. Experimental Model Test Results and Analysis 75

6.1 Results of Model 3 77

6.1.1 Discharge Component of Model 3 Controlling the 2-year Storm Event 78

6.1.2 Discharge Component of Model 3 Controlling the 10-year Storm Event 80

6.1.3 Discharge Component of Model 3 Controlling the 50-year Storm Event 82

6.2 Summary of Experimental Results 86

7. Discussion and Findings of Test Results 88

7.1 Discharge Coefficient of the 2-year Storm Control Orifice 88

7.2 Discharge Coefficient of the 10-year Storm Control Orifice 93

7.3 50-year Storm Control Rectangular Weir 95

7.4 100-year Outlet Pipe 97

8. Conclusions and Recommendations 101

8.1 Conclusions 101

8.2 Recommended Multi-Stage Outlet Structure Design Guidelines 103

9. Future Research on the Design of Multi-Stage Outlet Structures 104

10. References 106

APPENDIX A: Concerns Related to Stormwater Quantity Control Facilities.....112

APPENDIX B: Scale Effects.....114

APPENDIX C: Sensitivity Assessment.....121

APPENDIX D: Flood Hydrology Results and Calculations.....126

APPENDIX E: Multi-Stage Outlet Design Sizing Calculations.....138

APPENDIX F: Preliminary Design Drawings of the Multi-Stage Outlets (Prototypes)....146

APPENDIX G: Drawings and Photographs of as-built Multi-Stage Outlet Models.....153

APPENDIX H: Experimental Test Results.....159

APPENDIX I: Experimental Test Data.....207

APPENDIX J: Evaluation of Experimental Stage-Discharge Curve with Target 214

APPENDIX K: Dimensional Analysis of Orifice Flow.....215

APPENDIX L: 50-year Control Rectangular Weir.....217

APPENDIX M: Visual Studio Program.....220

List of Figures

Figure 1.1: Examples of multi-stage outlet structures (adapted from Hotchkiss, 2015:31) 2
Figure 2.1: Schematic of the inflow and outflow flood hydrographs 4
Figure 2.2: Examples of detention (a) and retention (b) ponds (Hotchkiss, 2015:10) 5
Figure 2.3: Typical layout of a multi-stage outlet structure 6
Figure 2.4: Components of a multi-stage outlet structures (adapted from Headley and Wyrick, 2009:5) 7
Figure 2.5: Typical components of a multi-stage outlet structures (adapted from Headley and Wyrick, 2009:5) 8
Figure 2.6: Side view of effective head measurement at orifice outlet devices 8
Figure 2.7: Cross-section of circular weir (reproduced from SANRAL, 2013:9-15) 11
Figure 2.8: Comparison of Vatankhah (2010) with Barlow and Brandes (2012) (adapted from Barlow and Brandes, 2012:925) 12
Figure 2.9: Definition sketch of a perforated riser intake (reproduced from Iowa Stormwater Management Manual, 2009:8) 13
Figure 2.10: Broad-crested weir condition (adapted from SANRAL, 2013: 4-10) 16
Figure 2.11: Flow over a sharp-crested full-width rectangular weir (adapted form Chadwick et al., 2004:433) 18
Figure 2.12: Contracted rectangular weir (adapted from Chadwick et al., 2004:432) 19
Figure 2.13: Sharp-Crested weir affected by submergence (adapted from Knox County, 2008:7) 20
Figure 2.14: V-notch weir definition sketch 21
Figure 2.15 : Definition sketch of a Cipoletti Weir (adapted from Bengtson, 2011:23) 22
Figure 2.16: Definition sketch of a proportional weir (adapted from CSIR, 2000:6-34) 22
Figure 2.17: Head measurements for multi-stage riser outlet device (adapted from Virginia Department of Conservation and Recreation, 1999b:5-55) 23
Figure 2.18: Stage-discharge curve of a multi-stage outlet (Output from Hydrology…. Studio, 2014) 26
Figure 2.19: Riser flow diagrams (adapted from Virginia Department of Conservation and Recreation, 1999b) 26
Figure 2.20: Birdcage type trash racks (adapted from Headley and Wyrick, 2009:5) 27
Figure 2.21: Determination of the minimum rack size versus the outlet diameter (Urban Drainage and Flood Control District, 2010:270) 29
Figure 2.23: Weir flow condition around drop inlet (adapted from Hotchkiss, 2015:29) 32
Figure 3.1: Simplified triangular hydrograph for the rational method (adapted from SANRAL, 2013:3-30) 40
Figure 3.2: Typical size of communities in hectares (reproduced from ARC, 2014) 42
Figure 3.3 Approximation of the longest watercourse 43

Figure 4.1: Estimation of preliminary storage volume (adapted from McCuen et al., 2002:308) .. 51
Figure 4.2: Modelling methodology 52
Figure 4.3: Design criteria of the multi-stage outlets 54
Figure 4.4: Outflow results obtained from spreadsheet-based model and software 65
Figure 5.1: Glass flume and flow straightener bricks 68
Figure 5.2: Plan view of laboratory set-up 69
Figure 5.5: Tailwater produced by 100-year RI outlet pipe 71
Figure 5.6: Point gauge fixed in glass flume upstream of model 71
Figure 5.7: Moody Diagram indicating flow regime in outlet pipe 74
Figure 6.1: (a) Front view of flow patterns when riser overflows (b) Front view of Model 2, discharging at the 100-year water surface elevation 76
Figure 6.2: Model 6 discharging at the 100-year water surface elevation 76
Figure 6.3: Calculated and physically modelled stage-discharge relationship of Model 3 (prototype dimensions) 77
Figure 6.4: Stage-discharge curve for the 2-year control component of Model 3 79
Figure 6.5: Stage-discharge curve for the two 10-year control components of Model 3 ... 80
Figure 6.6: Relationship between the discharge and stage for the 50-year control component of Model 3 83
Figure 6.7: Model 3 operating at the 20-year water level (stage 1.089 m) 83
Figure 6.8: 10-year orifices partially submerged d/s at stage 1.251 m 84
Figure 6.9: Inflow (post-development) and outflow hydrographs used to estimate storage volume 87
Figure 7.1: Section views of water surface elevation inside riser of different models 88
Figure 7.2: Empirically-derived discharge coefficient versus the submergence ratio of the 2-year storm control orifice 89
Figure 7.3: Effect of the multi-stage outlet's configuration on C_d 91
Figure 7.5: Comparison of C_d with the large and small orifice equation 94
Figure 7.6: Formation of vortex at orifice opening 94
Figure 7.7: Stage-discharge relationship for the 50-year weir component of Model 3 96
Figure 7.8: Stage-discharge relationship of individual components of Model 6 98
Figure 7.9: Water elevation inside riser for (a) Model 6, (b) Model 5, (c) Model 4, and (d) Model 3 99
Figure 8.1:Stage-discharge plot showing the rating calculated and measured for Model 2 ... 103

List of Table

Table 2.1: Thin-walled orifice flow equations 12
Table 2.2: Discharge of culverts under inlet control (adapted from SANRAL, 2013) 14
Table 2.3: Values of coefficient C_W for Broad-Crested Weirs (Brater et al., 1996:5.25).... 16
Table 2.4: Discharge reduction factor (adapted form Ramamurthy, Tim and Rao, 1998:114) .. 17
Table 2.5: Bar shape factor, K_{g1} and K_{g2} fit curves (adapted from Iowa Stormwater Management Manual, 2009)..... 31
Table 2.6: Summary of the controlling design criteria 34
Table 2.7: Scalar relationships for models under Froude similitude (Webber: 1979:304). .. 36
Table 2.8: Equations to determine discharge for multi-stage outlet structures 39
Table 3.1: Summary of input parameters for hypothetical residential site 44
Table 3.2: Urban land use distribution 45
Table 3.3: Summary of pre- and post-development peak discharges 46
Table 3.4: Maximum difference in flood peaks due to change in C_2..... 47
Table 3.5: Test for sensitivity of MAP, pre-development scenario, coastal region..... 48
Table 3.6: Test for sensitivity of MAP, pre-development scenario, inland region 48
Table 4.1: Summary of peak outflow results – Coastal Region, 400 mm MAP..... 58
Table 4.2: Summary of peak outflow results – Coastal Region, 700 mm MAP..... 59
Table 4.3: Summary of peak outflow results – Coastal Region, 1000 mm MAP..... 60
Table 4.4: Summary of peak outflow results – Inland Region, 400 mm MAP 62
Table 4.5: Summary of peak outflow results – Inland Region, 700 mm MAP 63
Table 4.6: Summary of peak outflow results – Inland Region, 1000 mm MAP 64
Table 5.1: Summary of model identification 67
Table 6.1: Difference between theoretical and physically measured discharge of Model 3... 78
Table 6.2: Fractional change in dicharge from the 2-year orifice at the 2-year water level 79
Table 6.3: Percentage difference between theoretical and actual..... 81
Table 6.4: Fractional change in discharge at the 5-year water level 81
Table 6.5: Percentage difference between empirical and actual..... 81
Table 6.6: Fractional change in discharge at 10-year water level 82
Table 6.7: Percentage difference between theoretical and physical measured..... 84
Table 6.8: Fractional change in discharge at the 20-year water level..... 85
Table 6.9: Percentage difference between theoretical and actual..... 85
Table 6.10: Contribution of discharge coefficient and differential head to the percentage difference between theoretical and actual discharge at the 50-year water level..... 85
Table 6.11: Percentage difference between the theoretically estimated target stage and physical recorded stage..... 86
Table 6.12: Multiple correlation coefficient values for each multi-stage model test 87
Table 7.1: Theoretical equations to be used for calculations of multi-stage outlets..... 97

List of Abbreviations

ARC	Association for Residential Communities
ASCE	American Society of Civil Engineers
BMP	Best Management Practices
CCT	City of Cape Town
CSIR	Council for Scientific and Industrial Research
DN	Nominal Diameter
E	Euler number
JRA	Johannesburg Road Agency
MAP	Mean Annual Precipitation
NGL	Natural Ground Level
NWA	National Water Act
Re	Reynolds number
RI	Recurrence Interval
SANRAL	The South African National Roads Agency Limited
SI	International System of Units (metric units)
SSD	Stage-Storage-Discharge Relationship
UDFCD	Urban Drainage and Flood Control District
US	United Stated Code (imperial units)
USACE	United States Army Corps of Engineers
We	Weber number
WL	Water Level

List of Symbols

A	Cross-sectional area (m^2)
A_n	Net area through the rack bars / gross area of the racks and supports
A_o	Area of an orifice (m^2)
A_r	Ratio of the area of the bars to the area of the grate section
A_s	Total area of the side hole of a perforated riser (m^2)
A_t	Grate Open Area (m^2)
A_{ot}	Total Outlet Area (m^2)
B	Width inside of culvert or width of inlet box (m)
b	Total flow width (m)
b_c	Weir crest breadth
b_o	Width of a rectangular orifice
C_B	Inlet coefficient for culverts
C_d	Discharge coefficient
C_e	Effective discharge coefficient
C_H	Inlet coefficient for culverts
C_o	Dimensionless orifice discharge coefficient
C_s	Discharge coefficient for perforations
C_w	Dimensionless weir discharge coefficient (ranging from 0.27 to 0.38)
C_W	Weir coefficient (ranging from 1.35 to 1.83)
Clog	Clogging factor (ranging from 0 to 1)
D	Diameter (m)
d_s	Length of the perforated segment of the riser pipe (m)
e	Absolute wall roughness (mm)
f	Friction factor (Colebrook-White-Darcy-Weissbach Equation)
g	Acceleration of gravity (m/s^2)
h	Depth of flow (m)
h_1	Upstream flow depth above crest elevation (m)
h_2	Downstream flow depth above crest elevation (m)

h_e	Effective head acting on weir ($h_1 + K_H$)
h_i	Head relative to the orifice invert (m)
h_o	Effective head acting on orifice (m)
h_s	length of the perforated segment of the riser pipe (m)
h_T	Transition head (m)
H	Energy head, $h + v^2/2g$ (m)
H*	Normalised differential head
H_g	Head loss through grate (m)
H_1	Upstream energy level (m)
H_2	Downstream energy level (m)
K	Trash rack loss coefficient
K_{g1}	Bar shape factor
K_{g2}	Bar shape factor defined by fit curves
K_h	Small correction to the measured head (0 .001 m)
K_{in}	Inlet secondary loss coefficients
K_{out}	Outlet secondary loss coefficients
l	Characteristic linear dimension (m)
L	Length of culvert (m)
L_c	Longest watercourse (m)
L_b	Cumulative width of bars on grate (ft)
L_e	Effective weir length (m)
L_h	Horizontal grate length (ft)
L_R	Crest length of riser structure (m)
L_r	Geometric scale
L_w	Weir length (m)
M	Mass (kg)
m	Model
m	Metre
mm	Millimetre

m_t	Value measured in the physical model
m^3/s	Cubic metre per second
n	Manning roughness
n_o	The total number of samples in the dataset
p	Prototype
P_s	Weir crest height
p_t	Value obtained from spreadsheet-based computer model
q	Unit discharge ($m^3/s.m$)
Q	Discharge (m^3/s)
Q*	Normalized Discharge
Q_{ideal}	Ideal discharge over weir (m^3/s)
Q_s	Submerged flows (m^3/s)
Q_i	Peak inflow rate into the basin (m^3/s)
Q_o	Peak outflow rate out of the pond (m^3/s)
R	Hydraulic radius (m)
Re_r	Reynolds number of the prototype
R_t^2	Multiple correlation coefficient
S	Sensitivity (%)
s	Minimum clear spacing between bars (mm)
S_{av}	Average watercourse slope (0.01 m/m)
S_o	Slope of culvert bed (m/m)
T	Time interval (seconds)
Tc	Time of concentration
t_i	Duration of storage facility inflow (s)
t_{ci}	Time to peak of the inflow hydrograph (s)
t_{co}	Time to peak of the outflow hydrograph (s)
u	The power of the head in the head-discharge equation
V	Approach velocity of flow through trash rack, computed on gross area (m/s)
V_s	Storage volume estimate (m^3)

v	Approach velocity (m/s)
$\bar{v}$	Average flow velocity (m/s)
w	Maximum cross-sectional bar width facing the flow (mm)
x	Scale factor
Y_1	Upstream water level
Y_3	Downstream water level
ν	Kinematic viscosity ($\approx$1.13 x 10^{-6} m^2/s for water)
n	Open area ratio for the grate
σ	Surface tension of liquid
π	Pi
Π	h_1/D
%	Percentage
Δ	Change in parameter
θ	Angle of flow (degrees)
θ_g	Angle of the grate with respect to the horizontal (degrees)
ρ_r	Ratio between the densities of the prototype and the model

1. Introduction

1.1 Thesis Background and Motivation of Study

Urban development is largely responsible for significant changes in run-off characteristics due to the reduction of natural storage. Increased impervious cover in urban areas causes a reduction in the potential of infiltration and soil storage of rainwater. Land development reduces the natural storage of a watershed due to the removal of trees and vegetation, which in return reduces the volume of interception storage available. McCuen, Johnson and Ragan (2002:303) indicated that the primary changes in the timing of run-off, resulting from a reduction of natural storage, are a decrease in both the time to peak and the time of concentration.

Stormwater management is implemented to mitigate the detrimental effects of land development, with the intent of limiting peak flow rates from developed areas to the peak flows that existed prior to development. Detention and retention facilities are the most popular stormwater management practices. The post-development flood run-off hydrograph enters the pond at the upper end of the detention basin and an outlet structure then serves to limit the outflow rate (McCuen *et al*., 2002:303).

Attenuation facilities in the past were designed to control only a single recurrence interval (RI) design storm, such as the 50-year RI storm event. However, various metropolitan municipalities now instruct developers to implement on-site flood control structures, which must be able to control run-off for a full range of design flows (Hotchkiss, 2015:19). In particular, the more frequently occurring storm events (2-year RI) still exceed the pre-development peak run-off due to the designed outlet pipe diameter that is often too large to provide the essential attenuation for more frequent storm events (Sivanathan, Martens, Sivapalan and Davies, 2000:1).

A single stage outlet, which consists of a single pipe or culvert, could be designed to provide outflow at a rate equal to the pre-development peak stormwater run-off for a frequent storm event such as the 2-year or 5-year design storm. The less frequent events such as the 50-year or 100-year design storms would then be over controlled. Lafleur and McBean (1981:38) suggested that one design the outlet control system for a frequent storm event and then provide additional storage capacity for a less frequent storm event. Additional storage would necessitate the surface area of the pond being expanded, an undesirable prospect from the point of view of the developer. Another approach is multi-stage outlet control that is designed to control the run-off of storms of several recurrence intervals (McCuen,1998).

Common characteristics of the multi-stage outlet structure within the detention basin include a low-flow orifice near the base of the structure, a weir or orifice opening above the low-flow orifice for attenuating normal run-off volumes, and an emergency overflow spillway to pass the flow of extreme events (Headley and Wyrick, 2009:1).

Much research has been done on individual orifices, weirs and culverts, but the need to control storms with a particular range of recurrence intervals has led to the development of complex outlets, the hydraulic performance of which requires verification.

Several urban stormwater management manuals provide design techniques primarily in terms of increasing retention time, which manage discharge quality, rather than giving design guidelines for peak discharge management. However, when the land available for development is limited or expensive, a hydraulically efficient outlet structure would be required, with the stormwater treatment restricted to mechanical methods, such as trash racks. In this case, supplementary water quality treatment processes would be deferred to other locations in the drainage basin (Tullis, Olsen and Gardner, 2008). Furthermore, South African Stormwater management manuals contain little guidance with regard to designing the multi-stage outlet structures that mitigate the impact of new development for a wide range of storm events.

The design of multi-stage outlet structures is based on empirical, standard orifice and flat plate weir equations that seldom resemble the outlets they are intended to represent. Thick-walled concrete orifices and weirs are generally constructed to control the outflow from stormwater detention basins (Barlow and Brandes, 2015), the profile of which deviates from the requirements that must be met for using the standard sharp-edge orifice equation (thin-plate). Supplementary research is therefore required to improve the design of these structures so that it represents thick-walled multi-stage outlets. Literature also indicates that the outflow structures for stormwater detention basin vary widely within a single watershed (Headley and Wyrick, 2009:1). Figure 1.1 illustrates two examples of multi-stage outlet structures that function in the vicinity of Cape Town, South Africa. Why should there be such differences in the configuration of the outflow structures? This was a question that the current researcher wanted to explore in this study.

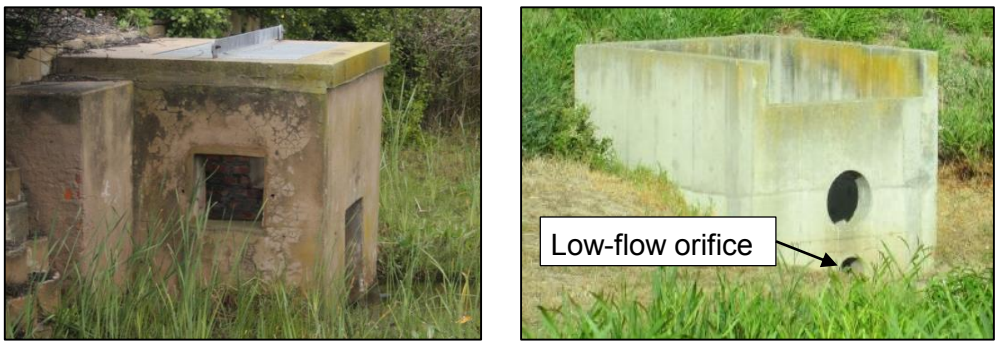

Figure 1.1: Examples of multi-stage outlet structures (adapted from Hotchkiss, 2015:31)

1.2 Research Objectives

This thesis aimed to provide guidelines to assist practitioners in the design of multi-stage outlets for a wide range (2-year to 100-year) of recurrence interval storms.

Various objectives were attained in order to meet this primary objective:

- Determine performance curves of several multi-stage outlet structures, which would reduce the post-development run-off hydrograph to the level of the pre-development (natural) run-off hydrograph for a full range of 2-, 5-, 10-, 20-, 50- and 100-year recurrence interval design storms.
- Determine the optimal range of recurrence interval storms that the multi-stage outlet structure was capable of meeting while providing the pre-development flow rates.
- Compare how the design of multi-stage outlet structure differed for coastal and inland regions and different amounts of mean annual precipitation (MAP) in South Africa.
- Incorporate the effects of a trash rack on the hydraulic performance of the multi-stage outlet structure.
- Analyse physical model data to determine whether a new set of equations of consistent form could be generated that would accurately describe the flow through the multi-stage outlet structure for all structure configurations.

To accomplish these objectives, physical models of typical multi-stage outlets were required that could accurately assess the outlet structures' geometric and hydraulic parameters, which in return would give insight into the outlets' capacity to discharge the water under a given head.

2. Literature Review

2.1 Introduction

The design of a storage facility depends on the target discharge, which is defined as the pre-development peak discharge (the peak of the green hydrograph in Figure 2.1). The goal of the design procedure of a multi-stage outlet structure is to ensure that the devices used in the multi-stage outlet structure are designed to limit the routed post-development peak discharge (red line in Figure 2.1) in order not to exceed the target discharge (McCuen *et al*., 2002:328).

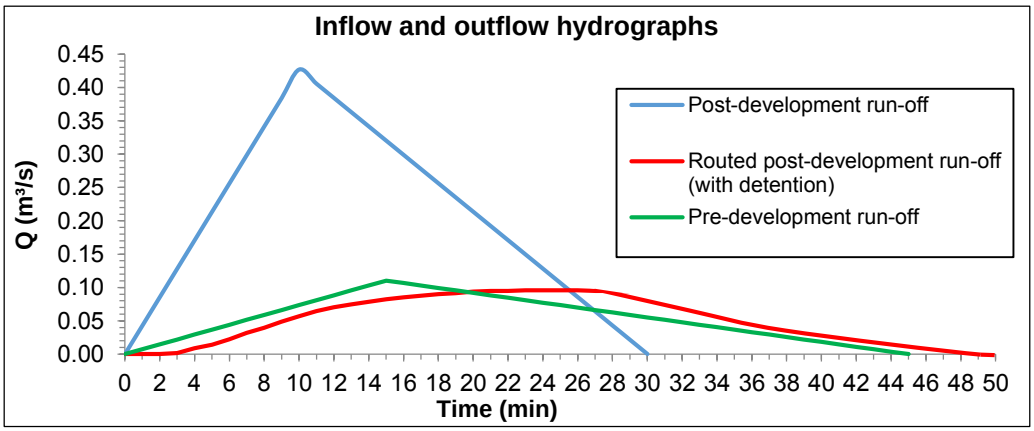

Figure 2.1: Schematic of the inflow and outflow flood hydrographs

Primary outlets dictate the nature of the release pattern from attenuation facilities for various inflows to which the facility is subjected. The design of the principal outlet is therefore critical in order to restrict the peak inflow to its pre-development (natural) level. A primary outlet could be either a single stage outlet system, which comprises a simple pipe or a culvert that restricts the flow for a storm of only one particular selected recurrence interval, or a multi-stage outlet system, which is designed to control the flow for several different recurrence intervals.

Attenuation facilities in the past were designed to control only a single recurrence interval design storm, but current legislation (refer to Section 2.7) in various of South Africa's metropolitan municipalities now obliges developers to implement on-site flood control structures which must control run-off for a full range of design flows (Hotchkiss, 2015:19).

Presently implemented designs of these multi-stage outlet structures are based on empirical, flat-plate weir equations that seldom resemble the outlets that they are intended to represent. Thick-walled concrete orifices and weirs are typically used as discharge control components of multi-stage outlet structures (Barlow and Brandes, 2015). Supplementary research is required to improve the designing of multi-stage outlet structures so that the outlet correctly represents stage-discharge relationships for the flow conditions through a thick-walled orifice-and-weir. Chapter 2 thus provides an overview of the primary literature that had been explored on the topic of the multi-stage outlet structures that function in attenuation facilities.

2.2 Detention and Retention Ponds

2.2.1 Background

Detention ponds are normally dry and provide temporary storage (usually for 24 hours) of stormwater that is released through an outlet that would control the flow to pre-development levels (Laramie County Conservation District, 2001). The detention pond would slow down the water flow, thus flattening the inflow hydrograph.

A retention pond, on the other hand, has a permanent pool of water, the volume of which would fluctuate in response to precipitation and run-off from the contributing areas. The outlet of a retention facility would release water at very slow rates over a prolonged period (Laramie County Conservation District, 2001). Figure 2.2 illustrates the difference between a retention pond (a) and a detention pond (b).

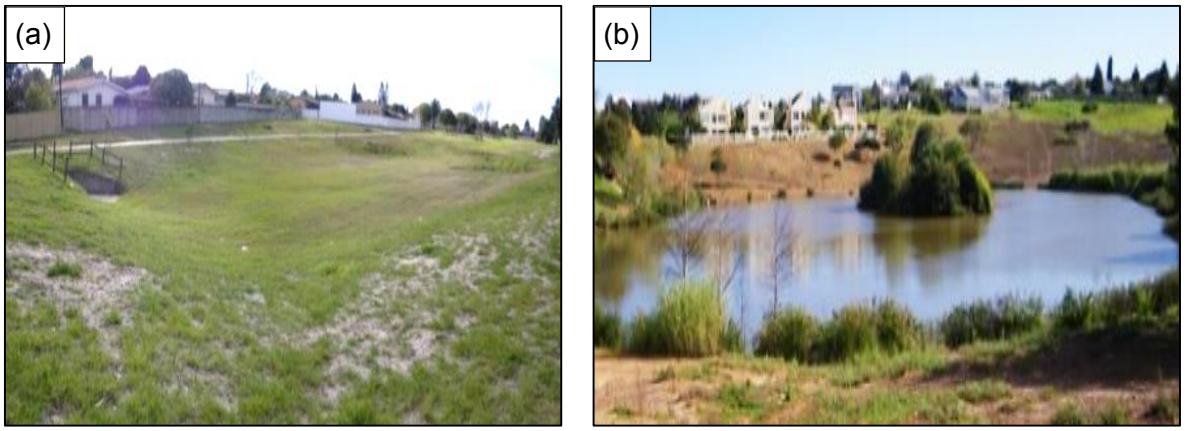

Figure 2.2: Examples of detention (a) and retention (b) ponds (Hotchkiss, 2015:10)

The fundamental requirements of water retention and detention ponds are (McCuen, 1998):

- Adequate capacity to hold the captured stormwater run-off, as it is being released at a slower rate than the inflow rate.
- An outlet structure that restricts the outflow to a rate no greater than the pre-development peak stormwater run-off rate.

The latter requirement is necessary in order for the multi-stage outlet structure to perform as a flood control, or stream-channel erosion control, mechanism. The required volume of the pond is a function of the flow control mechanisms of the outlet structure. Therefore, the simultaneous and complementary sizing of both the storage volume characteristics and the characteristics of the outlet structure are the most important design requirements when planning and designing stormwater detention facilities (McCuen *et al*., 2002:305). The size of the storage facility could be reduced by implementing rainwater harvesting tanks, permeable paving and flowerbed soakaways. Refer to Appendix A for concerns and safety excerpts that require attention when designing a detention or retention pond.

2.3 Multi-Stage Pond Outlet Structures

2.3.1 Background

Multi-stage outlet structures incorporate individual discharge control devices, at different elevations, which restrict the rate of flow from a facility during multiple design storms. According to the Knox County, Tennessee Stormwater Management Manual (Knox County, 2008:1), a multi-stage outlet structure may be used for volume control for purposes of channel protection, water quality control or overbank flood control. Permanent multi-stage outlets are most often constructed of concrete, either precast or cast-in-place, to increase their life expectancy (Virginia Department of Conservations and Recreation, 1999b:5-41). Multi-stage outlets are either housed in a riser, or in several pipes and situated in a single location such as in a retention or detention pond. Figure 2.3 illustrates a typical multi-stage outlet structure which consists of an orifice, weir, riser and culvert.

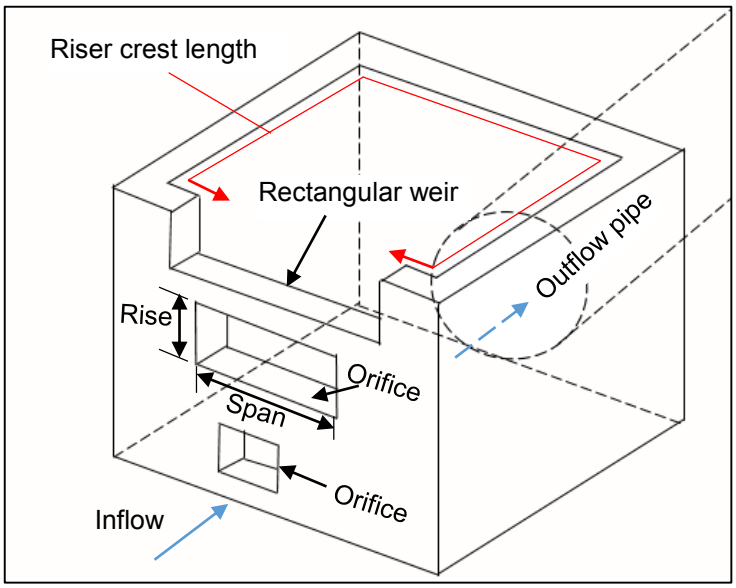

Figure 2.3: Typical layout of a multi-stage outlet structure

The multi-stage outlet structure is of utmost importance in the design of a stormwater management basin, since it controls the relationship between the pond's water surface elevations and the outflow rate (Virginia Department of Conservation and Recreation, 1999b:5-41).

Emerson (2003) surveyed 111 detention basins and emphasised that the most crucial part of the outlet structure was the low-flow orifice, situated at the bottom of the multi-stage outlet structure. The survey also indicated that the low-flow orifices were relatively large, up to 152.4mm in diameter, and were generally unable to restrict the outflow to pre-development peak flows. The general considerations for multi-stage riser sizing is that there are two or more individual design storms that must be designed for, which requires individual estimated storage volumes for each storm event.

General input that is required for sizing a multi-stage outlet structure includes the following (Iowa Stormwater Management Manual, 2009:16):

- The pre- and post-development run-off volume and peak discharges.
- The length and Manning's roughness coefficient of the outlet pipe/culvert.
- Preliminary estimate of the storage volume and area.
- The elevation of the orifice invert level and/or the weir crest height.
- The stage-storage relationship for the proposed storage facility.

2.3.2 Devices used in the Design of Multi-Stage Outlet Structures

Multi-stage outlet structures comprise several discharge control devices that have different depth-discharge relationships, thus each control has different design requirements, which are elaborated in Sections 2.3.2.1 to 2.3.2.5. The multi-stage outlet structure could consist of the following main outlet devices:

- Orifice
- Perforated Riser
- Pipes or culverts
- Broad-crested weir
- Sharp-crested weir
- V-notch weir
- Cipolletti weir
- Proportional weir
- Standpipes and inlet boxes.

Examples of these discharge control devices, as components of a multi-stage outlet structure, are shown in Figure 2.4 and Figure 2.5.

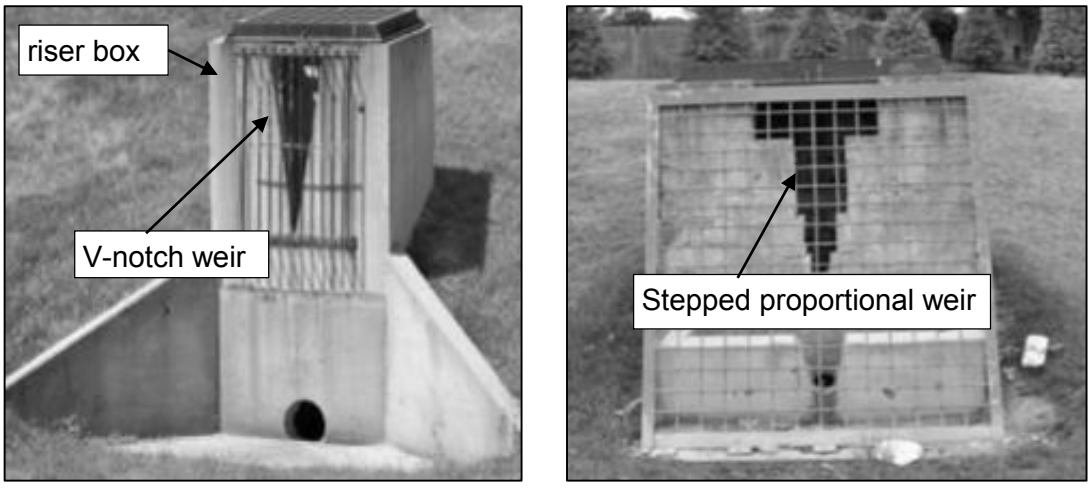

Figure 2.4: Components of a multi-stage outlet structures (adapted from Headley and Wyrick, 2009:5)

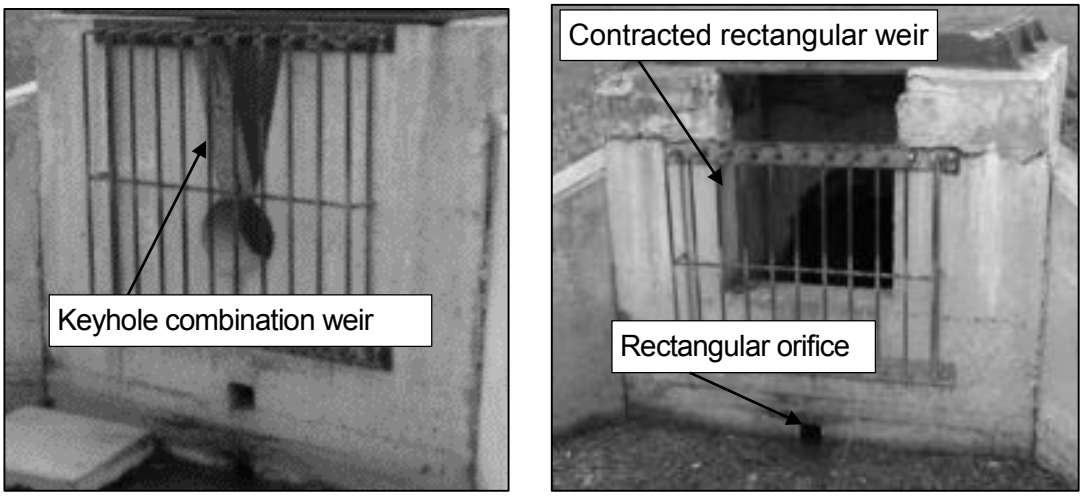

Figure 2.5: Typical components of a multi-stage outlet structures (adapted from Headley and Wyrick, 2009:5)

2.3.2.1 Orifices

An orifice in a multi-stage stage outlet structure consists of an opening, either circular or rectangular, of a recommended size. The discharge through an orifice is influenced by the effective head, measured from the centreline of the orifice to the upstream (inlet) surface elevation (h_o on Figure 2.6), as well as the orifice dimension and edge shape. The size and edge conditions of an orifice have an influence on the overall coefficient of discharge due to the contraction of the water jet and energy losses (Iowa Stormwater Management Manual, 2009:2). Figure 2.6 indicates the effective head when (a) the orifice discharges as a free outfall and (b) when the orifice discharge is submerged.

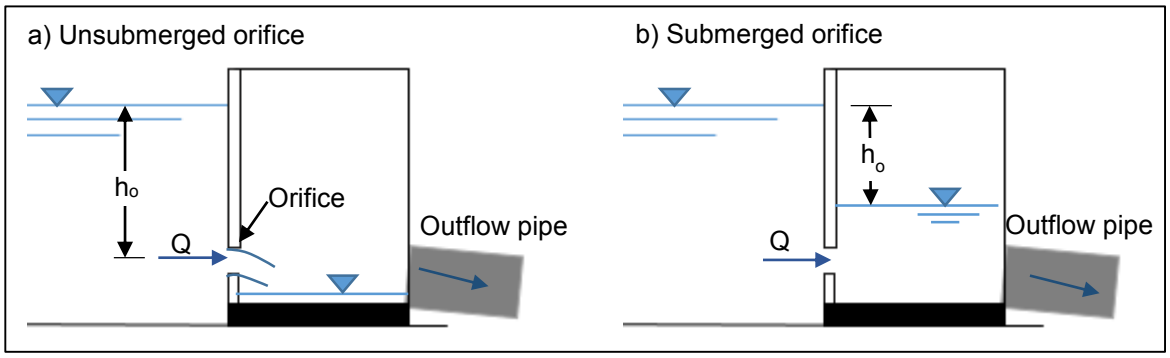

Figure 2.6: Side view of effective head measurement at orifice outlet devices

The Knox County (2008) and the Iowa Stormwater Management Manual (2009) calculates the orifice discharge by using the standard orifice equation defined in Equation 2.1, which is similar to the equation used to determine discharge through a small orifice as recommended by Chadwick, Morfett and Borthwick (2004).

$$Q = C_d A(2gh_o)^{0.5} \quad (2.1)$$

where:

Q = discharge (m^3/s)
C_d = dimensionless coefficient of discharge (typically between 0.4 - 0.6)
A = cross-sectional area of orifice (m^2)
g = gravitational acceleration (9.81 m/s^2)
h_o = effective head, as indicated in Figure 2.6 (m).

Discharge through multiple orifices is determined by the summation of the discharge through each individual orifice. The total discharge of identical sized orifices that operate under the influence of the same effective head is determined by multiplying the discharge for a single orifice by the number of openings.

Values for the discharge coefficient are in the range of 0.5 to 1.0 (McCuen *et al*., 2002:312), with a value of 0.6 for square edge orifice conditions and 0.4 for ragged edge orifice conditions. The most common practice in hydraulic textbooks is to use a single constant discharge coefficient of 0.6 for sharp-edged orifices (Spencer, 2013). An exception is the Ontario Ministry of Environment (2003), whose stormwater guidelines use a single constant value of 0.63. Bos (1989) suggested a range of discharge coefficient values from 0.6 to 0.64, depending on the diameter of the circular sharp-edged orifice.

These particular values for the discharge coefficient for a specific configuration often appear contradictory. A physical model study by Nielsen and Weber (2000) concluded that the discharge coefficient varies from 0.58 to 0.84, for a partially suppressed rectangular orifice, as the ratio of downstream water surface elevation to orifice opening height varied between 2.8 to 1.4, respectively. However, the value of the discharge coefficient for sharp-edged submerged orifices is not greatly affected by submergence (Brater, King, Lindell and Wei, 1996:4.12) and ranged from 0.599 for circular sharp-edged submerged orifices to 0.62 for rectangular sharp-edged submerged orifices.

Thick-walled Concrete Orifice

Reports of experimental work on thin walled orifices and circular weirs are available (Vantankhah, 2010; Barlow and Brandes, 2012), but little literature could be found on the stage-storage relationships for thick-walled circular concrete orifices, which are often used in detention pond outlet structures. However, Barlow and Brandes (2015:3) proposed that for fully submerged flow the discharge coefficient (C_d) for circular thick-walled concrete orifices should vary from 0.55 to 0.65 with increasing head at low values of submergence. This is different for thin-walled orifices, where the discharge coefficient is essentially taken as constant (0.6 for circular orifices and 0.61 for rectangular orifices). Barlow and Brandes (2015:3) concluded that a power-law model, given by Equations 2.1.1 to 2.1.3, provided a good fit to experimental data.

$$\text{for } \frac{h_i}{D} < 1.05, \qquad C_d = 0.55 \tag{2.1.1}$$

$$\text{for } 1.05 \leq \frac{h_i}{D} \leq 2.5, \qquad C_d = 0.6357\,(\frac{h_i}{D} - 1)^{0.0464} \tag{2.1.2}$$

$$\text{for } \frac{h_i}{D} > 2.5, \qquad C_d = 0.65 \tag{2.1.3}$$

where:

h_i = head relative to the orifice invert, see Figure 2.7 (m)

D = orifice diameter (m).

When the orifice is not fully immersed it would behave like a weir (Barlow and Brandes, 2015:1). Barlow and Brandes (2012) proposed an equivalently sized rectangular weir model (Equation 2.2) for thick-walled concrete orifices under partially submerged flow conditions.

$$Q = C_W L_w {h_i}^{3/2} \tag{2.2}$$

where C_W refers to the weir coefficient for the partially full orifice and L_w is the equivalent weir length, which increases as the orifice fills. The equivalent weir length is estimated (refer to Equation 2.2.1) by dividing the cross-sectional area of flow in the circular orifice by the head relative to the orifice invert (h_i). When the submerged fraction (h_i/D) exceeds 0.75, the equivalent weir length begins to decrease with the head relative to the orifice invert, and is then set constant (Equation 2.2.2). The cross-sectional flow area is based on circular geometry (Equation 2.2.3) and the angle of flow, which is indicated on Figure 2.7, is determined by Equation 2.2.4.

$$\text{for } \frac{h_i}{D} < 0.75, \qquad L_w = \frac{A(h_i)}{h_i} \tag{2.2.1}$$

$$\text{for } 0.75 \leq \frac{h_i}{D} \leq 1, \qquad L_w = \frac{A(0.75D)}{0.75D} = 0.84247D \tag{2.2.2}$$

$$A(h_i) = \frac{\pi D^2}{4}\left(\frac{\theta}{360}\right) - \frac{D}{2}\sin(\frac{\theta}{2})(\frac{D}{2} - h_i) \tag{2.2.3}$$

$$\theta = 2\arccos\,(1 - \frac{2h_i}{D}) \tag{2.2.4}$$

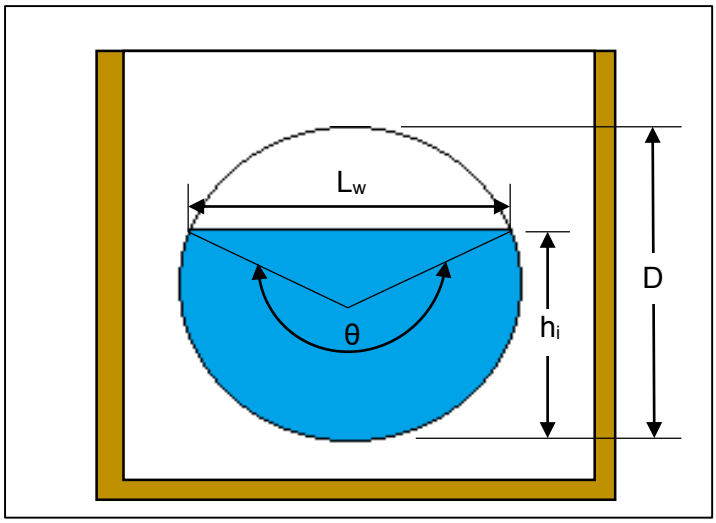

Figure 2.7: Cross-section of circular weir (reproduced from SANRAL, 2013:9-15)

When the orifice is almost fully submerged, the flow behaviour transitions from weir dependence to orifice dependence, and the fully submerged equation must equal the partially submerged equations at $h_i/D = 1$. According to Barlow and Brandes (2015:2), when equating Equation 2.1 and 2.2, the relationship between the weir coefficient (C_W) and the discharge coefficient (C_d) results in $C_W = 2.9199C_d$.

Thin-walled Concrete Orifice

Vatankhah (2010:189) proposed a simple and accurate theoretical discharge equation (Equation 2.3) for circular sharp-crested weirs. Equation 2.3 has a maximum percentage error of less than 0.08% compared to numerical integration results. A suitable discharge coefficient equation (Equation 2.4) was also proposed by Vatankhah (2010:189) for the determination of flow through thin-walled orifices. Barlow and Brandes (2012:925) also proposed a new method for modelling thin-walled orifice flow (Equations 2.5.1 and 2.5.2) and the discharge coefficient is defined by Equation 2.6. Equations 2.3 to 2.6 are summarised in Table 2.1, which also gives their respective limitations.

Table 2.1: Thin-walled orifice flow equations

Vatankhah (2010):	
$for\ \ 0 \le \eta < 1, \quad Q_a = 0.3926 C_d \sqrt{2g} h_w^{\frac{3}{2}} D \eta^{\frac{1}{2}} \times \left(\sqrt{1 - 0.22\,\eta} + \sqrt{1 - 0.773\,\eta}\right)$	(2.3)
$for\ \ 0.1 \le \eta < 1, \quad C_d = \frac{0.728 + 0.24\eta}{1 + 0.668\sqrt{\eta}}$	(2.4)
Brandes and Barlow (2012):	
$for\ \eta < 1, \quad Q = 0.1963\,\eta^2\left(\sqrt{1 - 0.22\,\eta} + \sqrt{1 - 0.773\,\eta}\right) \times \left[C(8gD^5)^{1/2}\right]$	(2.5.1)
$for\ \ \eta \ge 1, \quad Q = 0.2803\left(\sqrt{\eta - 0.3565} + 0.1123\sqrt{\eta - 0.8613}\right) \times \left[C(8gD^5)^{1/2}\right]$	(2.5.2)
$for\ \eta \ge 0.25, \quad C_d = \frac{1.06 + 5.11\eta^{1.8}}{1 + 8.04\eta^{1.8}}$	(2.6)
where: h_i = flow depth above circular orifice invert D = diameter of a circular sharp-crest weir η = h_i / D.	

Comparison of the two proposed models is illustrated in Figure 2.8 for a partially full flow through a thin-walled orifice (D=7.79 cm). Figure 2.8 indicates that Vantankhah's equation (2012) under-predicts the outflow data from Barlow and Brandes (2012). This is due to the discharge coefficient of Vantankhah, which was derived from Greve's data for large orifices (0.076 m ≤ D ≤ 0.76 m), constructed from steel plates, whereas Barlow and Brandes (2012) investigated circular orifices with diameters in a limited range of 5-10 cm, constructed from sheet metal. It is these differences in scale and materials that resulted in differing discharge coefficients under partially full flow.

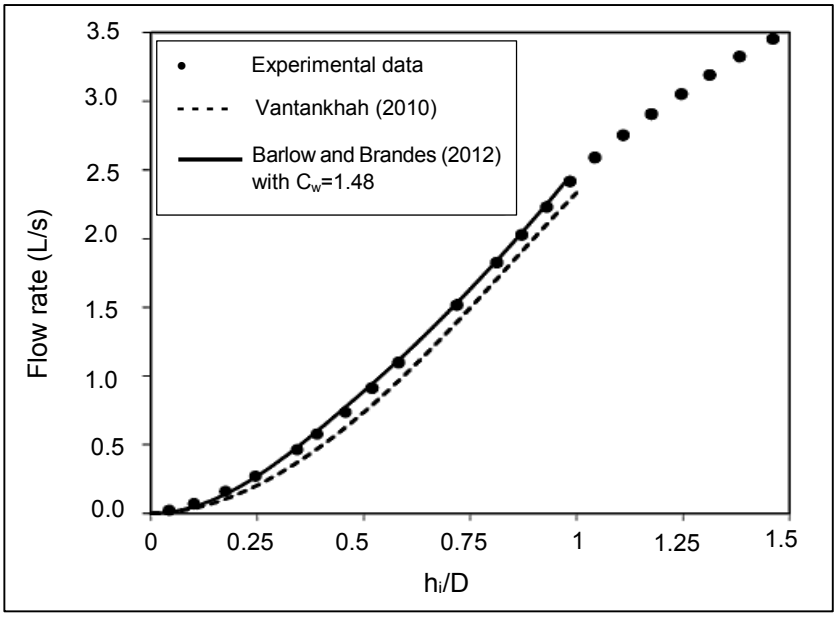

Figure 2.8: Comparison of Vatankhah (2010) with Barlow and Brandes (2012) (adapted from Barlow and Brandes, 2012:925)

2.3.2.2 Perforated Risers

A perforated riser is a unique vertical orifice structure that contains a series of equally sized and spaced round holes, as illustrated in Figure 2.9. The flow in the perforated riser is restricted by an orifice plate situated in the bottom of the riser, or in the outlet pipe downstream from the elbow at the bottom of the riser (Iowa Stormwater Management Manual, 2009:8). The perforations in the riser must convey more flow than the orifice plate in order for the orifice plate to act as the control in the riser (Knox County, 2008:6). The main purpose of the perforated riser is to reduce possible clogging of the bottom orifice plate.

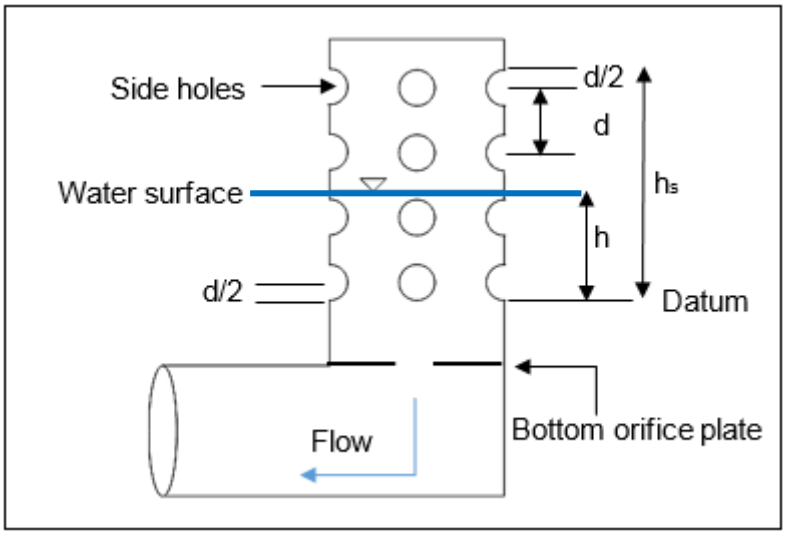

Figure 2.9: Definition sketch of a perforated riser intake (reproduced from Iowa Stormwater Management Manual, 2009:8)

The outflow from a perforated riser is determined by Equation 2.7, a formula by McEnroe (1988), which is recommended by Iowa Stormwater Management Manual (2009) and Knox County (2008). The accepted value of the discharge coefficient (C_s) is 0.61 (McEnroe, Steichen and Schweiger, 1988).

$$Q = C_s \frac{2A_s}{3h_s}\sqrt{2g}h^{3/2} \tag{2.7}$$

where:

C_s = discharge coefficient for perforations (typically 0.611)
A_s = total area of the side holes (m^2)
h = water level with respect to the datum, see Figure 2.9 (m)
h_s = length of the perforated segment of the riser pipe (m)
d_s = length of the perforated segment of the riser pipe (m).

The vertical distance (d) between the centrelines of two side holes, where the side holes are in consecutive horizontal rows, is illustrated on Figure 2.9. Equation 2.7 is only valid when $h < d_s$ and both h and d_s are measured from the same datum. The datum is at a distance d/2 below the centroid of the last row of side holes (Iowa Stormwater Management Manual, 2009:9).

2.3.2.3 Pipes and Culverts

Discharge from culverts are computed and evaluated for both inlet and outlet control. Discharge under inlet control is depended on the culvert shape, cross-sectional area of the pipe and the inlet edge. Discharge under outlet control is depended on the slope, length and Manning roughness of the pipe. Outlet control is exercised when the flow enters the culvert at a faster rate than the exit rate, thus the culvert is flowing full for at least part of its length (Hydrology Studio User's Guide, 2014:122). Under inlet control, the flow passes from subcritical to supercritical flow and it is easier for the water to exit the pipe than enter (SANRAL, 2013:7-7). The relationships for the discharge under inlet control are summarised in Table 2.2.

Table 2.2: Discharge of culverts under inlet control (adapted from SANRAL, 2013)

Rectangular Culverts	Round culverts
$\mathbf{0 < H_1/D \leq 1.2}$	$\mathbf{0 < H_1/D \leq 0.8}$
$Q = \frac{2}{3} C_B B H_1 \sqrt{\frac{2}{3} g H_1}$ (2.8)	$\frac{Q}{D^2\sqrt{gD}} = 0.48\left(\frac{S_o}{0.4}\right)^{0.05}\left(\frac{H_1}{D}\right)^{1.9}$ (2.9)
$\mathbf{H_1/D > 1.2}$	$\mathbf{0.8 < H_1/D \leq 1.2}$
$Q = C_H B D \sqrt{2g\,(H_1 - C_h D)}$ (2.10)	$\frac{Q}{D^2\sqrt{gD}} = 0.44\left(\frac{S_o}{0.4}\right)^{0.05}\left(\frac{H_1}{D}\right)^{1.5}$ (2.11)

where:

D = inside diameter or height (inside) of culvert (m)
B = width (inside) of culvert (m)
H_1 = upstream energy level (m)
H_2 = downstream energy level (m)
R = hydraulic radius (m)
C_B = 1.0 for round inlets and 0.9 for square inlets
C_H = 0.8 for round inlets and 0.9 for square inlets
S_o = slope of culvert bed with slight effect on capacity.

The relationship for the discharge under outlet control is determined by the energy – and continuity equation, sourced from SANRAL's Drainage Manual (SANRAL, 2013), as given by Equation 2.12. The pipe and culvert sizes commercially available should be kept in mind when designing the outlet structure.

$$H_1 - H_2 = \frac{K_{in}\bar{v}_1^{\,2}}{2g} + \frac{K_{out}\bar{v}_2^{\,2}}{2g} + \frac{\bar{v}^2 nL}{R^{\frac{4}{3}}} \quad (2.12)$$

where:

K_{in} = inlet secondary loss coefficients

K_{out} = outlet secondary loss coefficients

$\bar{v}$ = average flow velocity (m/s)

n = Manning roughness coefficient

L = length of culvert (m)

R = hydraulic radius (m).

2.3.2.4 Weirs

A weir could be a depression in the side of a tank, reservoir, channel or it could be an overflow dam. Weirs have been classified in accordance with the shape of the notch which could be either rectangular, triangular, trapezoidal (Cipoletti) or parabolic.

Equation 2.13 (Brater *et al*., 1996:5.4) determines the general formula of rectangular broad-crested weirs, overflow spillways, riser structures and sharp-crested weirs. The weir coefficient becomes a property of a specific weir type when the gravity term is kept in the equation, thus C_w is not dependent on the system of units as presented in Equation 2.13. A dimensionless weir coefficient of 0.37 is generally used for sharp-crested rectangular weirs where more information (i.e. length, thickness, height, approach flow depth) is not available (McCuen *et al*., 2002:8-12).

$$Q = C_w L_w \sqrt{2g}\,(h_1)^{1.5} \tag{2.13}$$

where:

Q = discharge over a horizontal weir (m^3/s)

h_1 = depth of approach flow above the weir (m)

C_w = dimensionless weir coefficient (typically 0.27 to 0.38 for sharp-crested weir)

L_w = length of the weir crest (m).

Broad-Crested Weirs

A broad-crested weir has a nearly horizontal crest and the great breadth (b) of the crest in the direction of the flow produces a supported nappe. Therefore, the hydrostatic pressure would be fully developed for at least a short distance (Brater *et al*., 1996:5.1). A weir is classified as broad-crested under the condition that the breadth of the crest is at least three times greater than the energy head (H), as illustrated in Figure 2.10 (SANRAL, 2013: 4-10). The velocity head ($v^2/2g$) is shown in Figure 2.10.

According to Brater *et al*. (1996:5.24) the broad-crested weir would perform as a sharp-crested weir when the head reaches one to two times the breadth of the weir, since the nappe becomes detached. In such conditions SANRAL's Drainage Manual (SANRAL, 2013:4-11) recommends that one interpolate between the results of the equations for broad-crested and sharp-crest weirs.

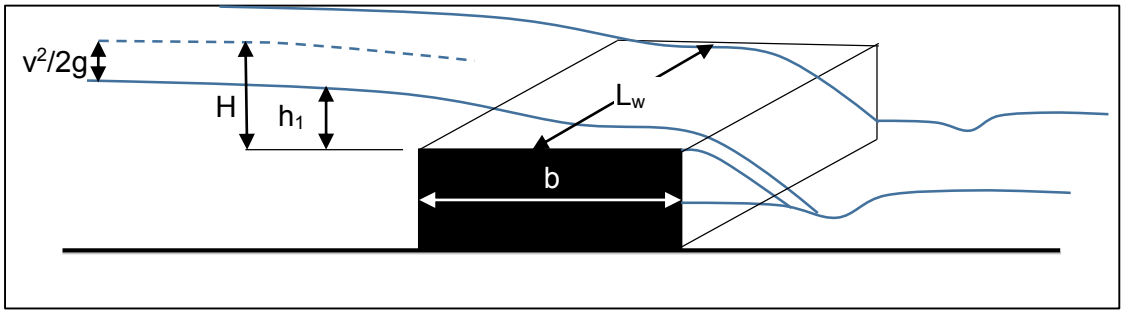

Figure 2.10: Broad-crested weir condition (adapted from SANRAL, 2013: 4-10)

Equation 2.14 present the discharge equation over broad-crested weirs (Brater et al., 1996:5.24).

$$Q = C_W L_w h_1^{1.5} \quad (2.14)$$

where:

C_W = weir coefficient (typically ranging from 1.35 to 1.83)
L_w = length of the weir crest (m)
h_1 = head above weir crest (m).

The recommended broad-crested weir coefficient is 1.71 for SI units (McCuen *et al*., 2002). Table 2.3 encapsulates values of C_W for broad-crested weirs (Brater *et al*., 1996: 5.25). The measured head in Table 2.3 was measured at least 2.5 h_1 upstream of the weir.

Table 2.3: Values of coefficient C_W for Broad-Crested Weirs (Brater et al., 1996:5.25)

Measured head, m	Breadth (b) of crest of weir, m										
	0.15	**0.20**	**0.30**	**0.45**	**0.60**	**0.75**	**0.90**	**1.20**	**1.50**	**3.00**	**4.50**
0.1	1.61	1.55	1.50	1.46	1.44	1.44	1.43	1.40	1.38	1.41	1.49
0.2	1.70	1.60	1.52	1.46	1.44	1.44	1.48	1.49	1.49	1.49	1.49
0.3	1.83	1.73	1.65	1.52	1.47	1.46	1.46	1.48	1.48	1.48	1.45
0.4	1.83	1.8	1.77	1.61	1.53	1.48	1.46	1.46	1.46	1.48	1.46
0.5	1.83	1.82	1.81	1.70	1.60	1.52	1.48	1.47	1.46	1.46	1.45
0.6	1.83	1.83	1.82	1.67	1.57	1.52	1.50	148	1.46	1.46	1.45
0.8	1.83	1.83	1.83	1.81	1.70	1.60	1.55	1.50	1.48	1.46	1.45
0.9	1.83	1.83	1.83	1.83	1.77	1.69	1.61	1.51	1.47	1.46	1.45
1.0	1.83	1.83	1.83	1.83	1.83	1.76	1.64	1.52	1.48	1.46	1.45
1.1	1.83	1.83	1.83	1.83	1.83	1.83	1.70	1.54	1.49	1.46	1.45
1.2	1.83	1.83	1.83	1.83	1.83	1.83	1.83	1.59	1.51	1.46	1.45
1.4	1.83	1.83	1.83	1.83	1.83	1.83	1.83	1.70	1.54	1.46	1.45
1.7	1.83	1.83	1.83	1.83	1.83	1.83	1.83	1.83	1.59	1.46	1.45

The effects of submergence are taken into account by means of a discharge reduction factor as given in Table 2.4. Table 2.4 gives approximated values of discharge reduction factors as a function of the head ratio for a broad-crested weir with a radius of curvature of zero.

Table 2.4: Discharge reduction factor (adapted form Ramamurthy, Tim and Rao, 1998:114)

h_2/h_1	Q_s/Q
0.80	0.95
0.85	0.87
0.90	0.77
0.95	0.48

where:

Q_s = submerge flow (m^3/s)

Q = free discharge corresponding to the upstream depth (h_1) from Equation 2.14 (m^3/s)

h_1 = upstream head above crest elevation (m)

h_2 = downstream head above crest elevation (m).

Rectangular (Sharp-Crested) Weirs

Sharp-crested or thin-plate weirs are overflow structures with a crest length, in the direction of flow, that is equal or less than 2 mm. If the weir plate is thicker than two millimetres, the downstream edge should be bevelled to an angle of not less than 45° to the surface of a rectangular notch (refer to Figure 2.11) and not less than 60° for a non-rectangular notch (Bos, 1989:153). Rectangular weirs can be designed to pass a higher flow for a given head and channel width in comparison to triangular weirs, which are more sensitive in measuring low flows (Chadwick *et al.,* 2004:431).

According to Chadwick *et al*. (2004), Equation 2.15 can be used to determine the discharge over a rectangular weir. For the derivation of Equation 2.15 it was assumed that the water surface level at station 2 above the weir crest was the same as the upstream water surface above the weir crest and there is no contraction. The velocities over the weir crest are assumed almost horizontal and the approach velocity head ($v_1^2/2g$) is neglected (Bos, 1989:46). Where v_1 is defined as the upstream velocity of the water, refer to Figure 2.11.

$$Q_{ideal} = \frac{2}{3} L_w \sqrt{2g}\, h_1^{3/2} \tag{2.15}$$

where:

Q_{ideal} = ideal discharge over weir (m^3/s)

h_1 = upstream head above crest (m)

L_w = width of weir (m).

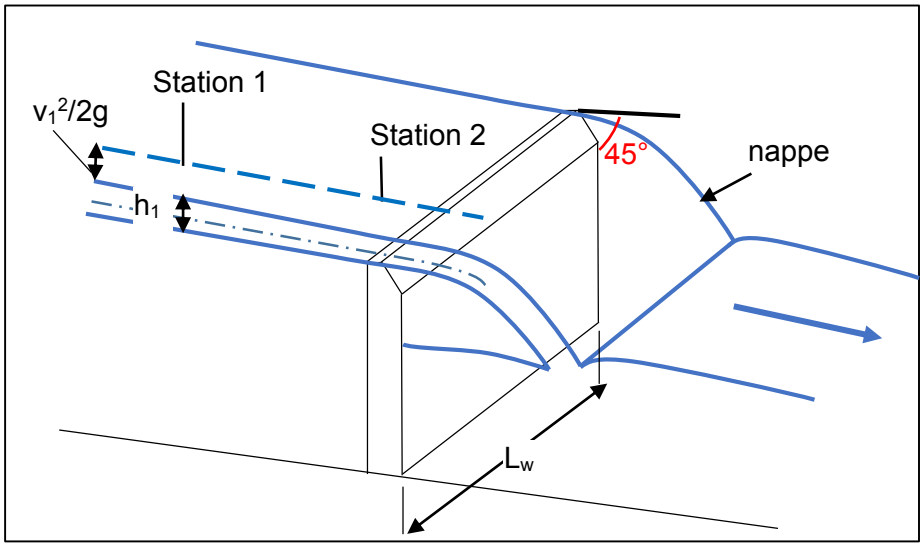

Figure 2.11: Flow over a sharp-crested full-width rectangular weir (adapted form Chadwick et al., 2004:433)

The streamlines converge as they approach the weir, therefore the cross-sectional area of the jet just downstream of the weir would be less than the cross-section of the flow at the weir itself. The contraction of the flow, which causes the actual discharge to be less than the ideal discharge, should be accounted for by means of a discharge coefficient when the discharge is computed (Chadwick *et al*., 2004:434).

Chadwick *et al*. (2004:434) highlighted two further discrepancies in the derivation of the discharge equation over a sharp-crested weir:

- The pressure distribution in the flow that moves over the weir is not atmospheric.
- The approach flow would be subjected to viscous forces, therefore a non-uniform velocity distribution would be present in the channel and there would be a loss of energy between a point upstream of the weir and the weir itself.

It is important to distinguish between contracted sharp-crested weirs and sharp-crested weirs with no end contraction. Contraction of the water flow would occur at the sides of the water jet in the case of a contracted weir, while the jet produced by a weir with no end contractions would cling to the sides of the channel. The nappe for a sharp-crested weir without end contraction would have a tendency to be drawn towards the weir, due to the air that cannot readily gain access to the underside of the nappe (Chadwick *et al*., 2004:435). Definition sketches of sharp-crested weirs without and with end contraction are given in Figure 2.11 and Figure 2.12 respectively.

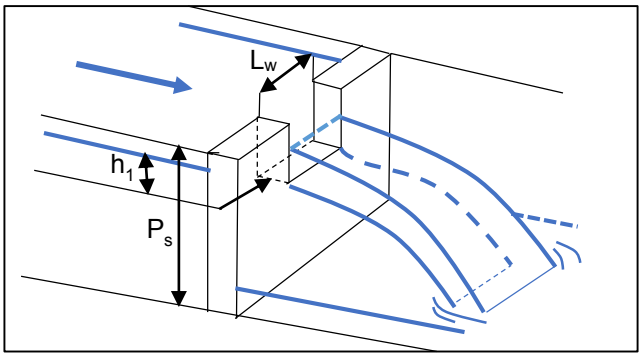

Figure 2.12: Contracted rectangular weir (reproduced from Chadwick et al., 2004:432)

The formulae on the topic of flow over sharp-crested weirs with and without end contraction that were obtained from various sources in the literature consulted are listed below.

a) Rehbock formula (Chadwick *et al*., 2004)

The Rehbock formula (Equation 2.16) and White's formula (Equation 2.17) are two empirical discharge formulae for full-width sharp-crested weirs under free discharge conditions. Both of these formulations took the contraction of the jet into account by the incorporation of the discharge coefficient.

$$Q = \frac{2}{3}\sqrt{2g}(0.602 + 0.083h_1/P_s)L_w(h_1 + 0.0012)^{3/2} \quad (2.16)$$

The Rehbock formula is valid for 30 mm < h_1< 750 mm, L_w > 300 mm, P_s > 100 mm and h_1 < P_s.

b) White's formula (Chadwick *et al*., 2004)

$$Q = 0.562(1 + 0.153h_1/P_s)L_w\sqrt{g}(h_1 + 0.001)^{3/2} \quad (2.17)$$

White's formula is only valid when h_1< 20 mm, P_s > 150 mm and h_1 < 2.2P_s.

c) Francis formula (1852) , as cited in The Bureau of Reclamation (2001)

Equation 2.18 gives the discharge equation for a sharp-crested weir with end contractions. The discharge over a sharp-crested weir without end contractions is defined by Equation 2.19. The discharge coefficient, C_d, is known to vary with the ratio h_1/P_s, however, for a ratio h_1/P_s less than 0.33, a constant discharge coefficient value of 1.84 is recommended.

$$Q = C_d(L_w - 0.2h_1){h_1}^{3/2} \quad (2.18)$$

$$Q = C_d\, L_w\, {h_1}^{3/2} \quad (2.19)$$

where:

h_1 = upstream head above crest (m)

P_s = crest height (m)

L_w = horizontal width of weir (m).

d) Chow (1959)

Equation 2.20 presents the discharge equation for a sharp-crested weir that consist of two end contractions (contracted rectangular weir). The discharge over the weir according to Chow (1959) is formulated in US units.

$$Q = (3.27 + 0.4\,(\frac{h_1}{P_s}))(L_w - 0.2h_1){h_1}^{3/2} \tag{2.20}$$

where:

h_1 = upstream head above crest excluding velocity head (ft)

P_s = height of weir crest above channel bottom (ft)

L_w = horizontal width of weir (ft).

e) Hamilton-Smith formula (Chadwick *et al*., 2004)

Equation 2.15 may be used to determine the discharge over a contracted rectangular weir. However, the actual discharge should be adjusted to account for the contraction of the water jet. The Hamilton-Smith formula (Equation 2.21) was developed to approximate a value for the discharge coefficient (C_d) and is valid for B > (L+ 4h_1), h_1/P_s < 0.5, 75 mm < h_1< 600 mm, P_s > 300 mm and L > 300 mm, where B refers to the width of the channel (m).

$$C_d = 0.616\,(1 - h_1/P_s) \tag{2.21}$$

f) Villemonte formula (1947)

The Villemonte equation, given by Equation 2.22, should be used when the tailwater rises above the weir's crest, thus causing the weir to become submerged, as illustrated by way of Figure 2.13. Submergence would cause a reduction of the discharge over the weir, which would then be less than the free discharge (Chadwick *et al*., 2004:438).

$$Q_s = Q(1 - \left(\frac{h_2}{h_1}\right)^{1.5})^{0.385} \tag{2.22}$$

where:

Q_s = submerge flow (m^3/s)

Q = free discharge, which corresponds to the upstream depth (m^3/s)

h_1 = upstream head above crest (m)

h_2 = downstream head above crest (m).

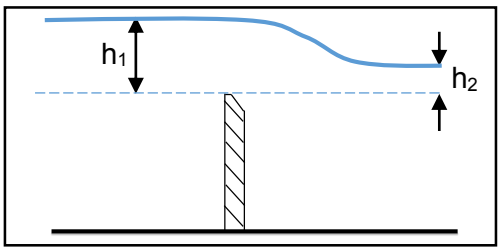

Figure 2.13: Sharp-Crested weir affected by submergence (reproduced from Knox County, 2008:7)

V-notch Weir

The V-notch or triangular weir is also classified as a sharp-crested (or thin plate) weir. The discharge of a notched weir increases more rapidly with the head than a horizontal crested weir does, thus V-notch weirs is more accurate in measuring lower discharge than horizontal crested weirs (Brater *et al*., 1996:5.15). Equation 2.23 is used to determine the discharge over a V-notch weir (Chadwick *et al*., 2004:439).

$$Q = \frac{8}{15} C_d \sqrt{2g} \tan(\frac{\theta}{2}) h_1^{5/2} \quad (2.23)$$

where:

C_d = discharge coefficient (typically taken as 0.59)

θ = angle of the V- notch (degrees)

h_1 = upstream head on apex of V- notch (m).

A general expression for discharge over notched weirs was suggested by Brater *et al.* (1996), which is presented in Equation 2.24.

$$Q = 1.38 \tan(\frac{\theta}{2}) h_1^{5/2} \quad (2.24)$$

When consulting other references for weir equations, the source could report the weir coefficient as a dimensional quantity that varies depending on the applicable unit system. SI units were used in Equations 2.23 and 2.24. Figure 2.14 indicates t he head measured on the apex of the V-notch as well as the angle of the V-notch.

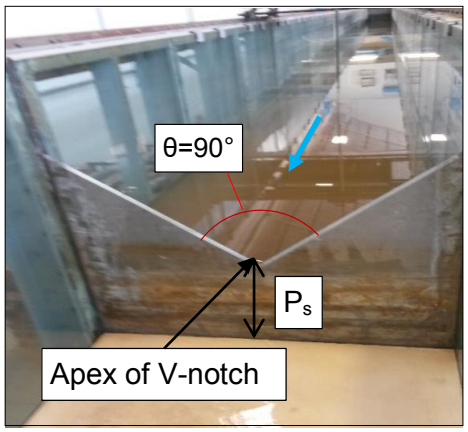

Figure 2.14: V-notch weir definition sketch

Cipolletti Weir

A Cipolletti weir, also a kind of sharp-crested weir, has a trapezoidal shape with a side slope of 1H:4V, as illustrated in Figure 2.15. Equation 2.25 could only be used to determine the discharge over a Cipolletti weir when 0.06096m ≤ h ≤ 0.6096m and h ≤ L/3 (Bengtson, 2011:22).

$$Q = 1.84\, Lh_1^{3/2} \quad (2.25)$$

where:

L_w = length of the weir crest (m)

h_1 = head measured above the weir crest (m).

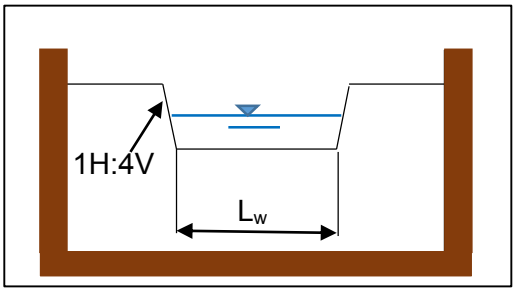

Figure 2.15 : Definition sketch of a Cipoletti Weir (adapted from Bengtson, 2011:23)

Proportional Weir

The design and construction of a proportional weir is more complex than a rectangular weir, but the advantage of the weir is that it could reduce the storage volume required for a specific pond. The proportional weir has a linear head-discharge relationship, which allows the discharge area to vary non-linearly with head (Iowa Stormwater Management Manual, 2009:6). This distinguishes it from other control devices. The discharge equation according to Sandvik (1985) is given as Equation 2.26.

$$Q = C_d\sqrt{2ga}\, b(h_1 - \frac{a}{3}) \quad (2.26)$$

where:

C_d = discharge coefficient (≈ 0.62).

The dimensions of a, b, h, x and y are in metres and are indicated in Figure 2.16. Equation 2.27 is required for the design of the proportional weir.

$$\frac{x}{b} = 1 - (\frac{2}{\pi})(\arctan(\frac{y}{a})^{0.5}) \quad (2.27)$$

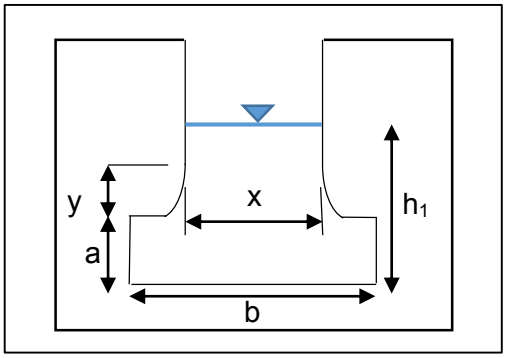

Figure 2.16: Definition sketch of a proportional weir (adapted from CSIR, 2000:6-34)

2.3.2.5 Stand Pipes and Inlet Boxes

The riser outlet is also known as a standpipe or inlet box, depending on the cross-section. A standpipe has a circular cross-section and an inlet box a rectangular cross section. These devices have intake openings that are parallel to the water surface, as indicated in Figure 2.17. Risers discharge into a pipe that must be large enough to prevent surcharge.

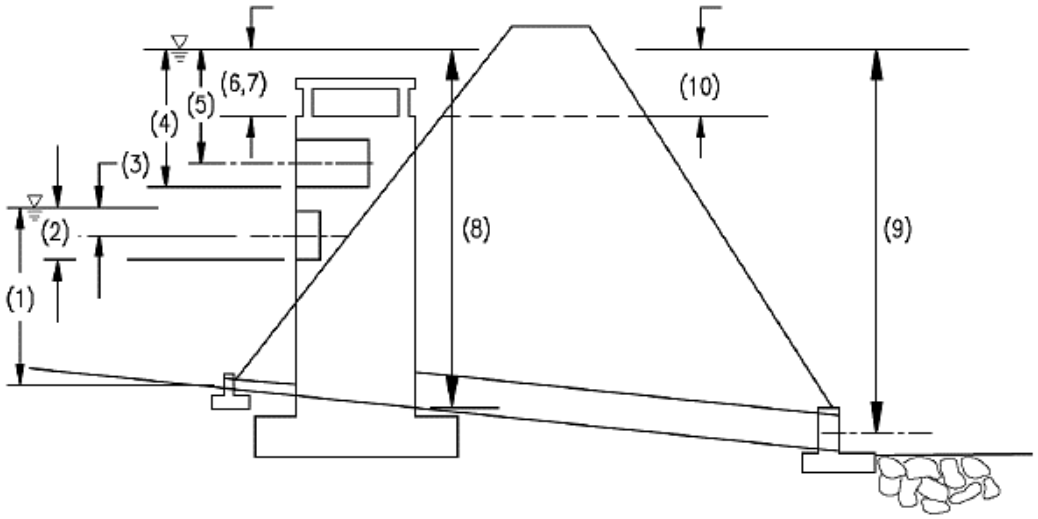

(1) Water quality orifice: head (h) measured from water surface elevation (WSE) to centreline of orifice.
(2) 2-year Control (Weir flow): h measured from WSE to invert of 2-year control weir.
(3) 2-year Control (Orifice flow): h measured from WSE to centreline of opening (fully submerged flow).
(4) 10-year Control (Weir flow): h measured form WSE to crest of opening.
(5) 10-year Control (Orifice flow): h measured form WSE to centreline of opening.
(6) Riser Structure (Weir flow): h measured from WSE to crest of riser top if open.
(7) Riser Structure (Orifice flow): h measured from WSE to crest of riser top, acting as horizontal orifice.
(8) Pipe flow (Inlet control): h measured form WSE to upstream invert of outlet pipe.
(9) Pipe flow (Outlet control): h measured form WSE to centreline of outlet pipe or tailwater, whichever is higher.
(10) Emergency Spillway: h measured from WSE to crest of emergency spillway.

Figure 2.17: Head measurements for multi-stage riser outlet device (adapted from Virginia Department of Conservation and Recreation, 1999b:5-55)

When the head over the stand pipe or inlet box is low it would operate as a weir (see (6) in Figure 2.17), thus Equation 2.13 could be used to determine the discharge over the structure. At higher heads, the standpipe and inlet box function as an orifice (see (7) in Figure 2.17), thus Equation 2.1 is applicable (Iowa Stormwater Management Manual, 2008:7). The transition from weir to orifice control occurs gradually over a transition depth. This transition depth may be defined by Equation 2.28 (Iowa Stormwater management Manual, 2008:7). When the transition depth is greater than the measured head, the orifice equation is recommended, and when the transition depth is less than the head, the weir equation would be used.

$$h_T = \frac{C_o A_o}{C_w L_R} \quad (2.28)$$

where:

h_T = transition head (m)

L_R = circumference of riser (m), $L_R = \pi D$ for stand pipes and $L_R = 2B + 2D$ for inlet boxes

D = stand pipe diameter or side lengths of inlet box (m)

B = side lengths of inlet box (m)

A_o = area of the orifice (m^2)

C_w = dimensionless weir discharge coefficient

C_o = dimensionless orifice discharge coefficient.

Risers that function as an orifice could be subject to vortex flow, which is a circular spiralling of flow immediately above the submerged riser. The occurrence of vortex flow could reduce the flow through an orifice by as much as 75%. Vortex flow could be prevented by an anti-vortex plate or by sizing the riser to have a larger cross-sectional area than the outlet pipe. This would ensure that weir flow is predominant during a storm event.

Cavitation forces, such as surging and vibration, result when the riser is restricting the flow to the outlet pipe. This condition occurs when the riser is flowing full and the outlet pipe is not flowing full. The flow through the riser structure should not transitions from weir flow control to orifice flow control before the outlet pipe controls the flow. This condition could be prevented by checking the flow rates for the riser weir, riser orifice, and the inlet and outlet flow control at each stage of discharge. The lowest discharge would control the flow for any given stage (Virginia Department of Conservation and Recreation, 1999b:5-49).

2.3.3 Summary of Best Practices for Design of Multi-Stage Outlet Structures

Literature recommends that the designer start at the most downstream end of the outlet, thus designing the culvert first. The culvert controls the final outflow and all the other components of the multi-stage outlet would route through the culvert as it facilitates a way for the water to exit the pond. A stepwise design approach is summarised as follows (Stringer, 2013):

1. The culvert is sized to meet or exceed the upper end of the target outflow. A trial route should then be performed to confirm whether the target outflow has been met. If the culvert outflow far exceeded the target outflow, then a secondary structure should be used to satisfy the upper end of the target outflow. Standard, commercially available culvert sizes should be kept in mind when sizing the culvert.

2. The lower return period device (orifice) should then be designed to satisfy the lowest target outflow. The orifice should be set just above the bottom of the pond. Trial routes are then performed to determine the maximum elevation reached.
   This elevation should then be used as the invert for the next structure. However, a minimum distance of 0.03084 m should be added to the maximum water surface elevation that was reached (Virginia Department of Conservation and Recreation, 1999b:5-46).

3. The secondary structure is added next, which could be either a weir or an orifice. These structures should satisfy the intermediate frequencies. Again, trial routes are performed to determine the maximum elevation, which is used as the invert for the next structure. This step is repeated for each intermediate frequency.

4. The riser structure is designed at the end to contain the multi-stage devices. It is not recommended to use a riser as a controlling device. The riser crest elevation should be set just above the maximum elevation reached in step 3. A final trial route should be performed to ensure that the riser is not obstructing the performance of the other devices. If it does obstruct the other devices, the crest length of the riser should be enlarged.

An emergency spillway weir could be added if necessary, but not as a multi-stage structure. Buoyancy calculations should be performed for the outlet structure and footing in order to prevent the structure from becoming buoyant. When the weight of the structure is less than or equal to the buoyant force exerted by the water, the outlet structure would start to float (Knox County, 2008:18).

Hydraulic changes that occur as the depth of storage changes for different design storms must be taken into account in the hydraulic design. The head elevation produced by the culvert should be used as a tailwater elevation against the other devices in the multi-stage device (Hydrology Studio User's Guide, 2014:92). The outflows from the orifice and weir devices would decrease when the head produced by the culvert increased.

When the head produced by the culvert equals the current stage of the pond, then the culvert would become the controlling structure, thus the contributing flow from the orifice and weir devices would diminish (Hydrology Studio User's Guide, 2014:92). Figure 2.18 illustrates the various stage-discharge curves and the controlling curve of the pipe (culvert).

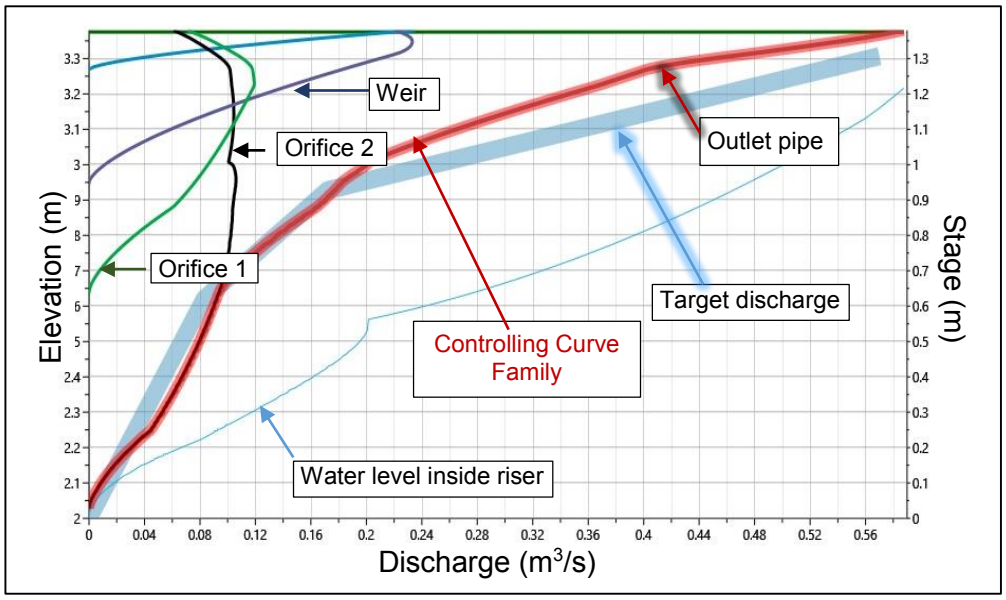

Figure 2.18: Stage-discharge curve of a multi-stage outlet (Output from Hydrology Studio. 2014)

The flow conditions in the pipe could also impact the hydraulic performance of the structure, thus inlet and outlet control should be evaluated. Figure 2.19 illustrates how the flow conditions change from a weir to an orifice as the water surface elevation rises. First, the riser acts as a weir when the water overflows the riser pipe, but as the flow begins to interfere with itself around the circular opening, the flow control transitions to that of orifice flow (Debo and Reese, 2003:617). The designer must compute the elevation at which this transition from riser weir flow control to riser orifice flow control takes place, as different design conditions result in changing water surface elevations.

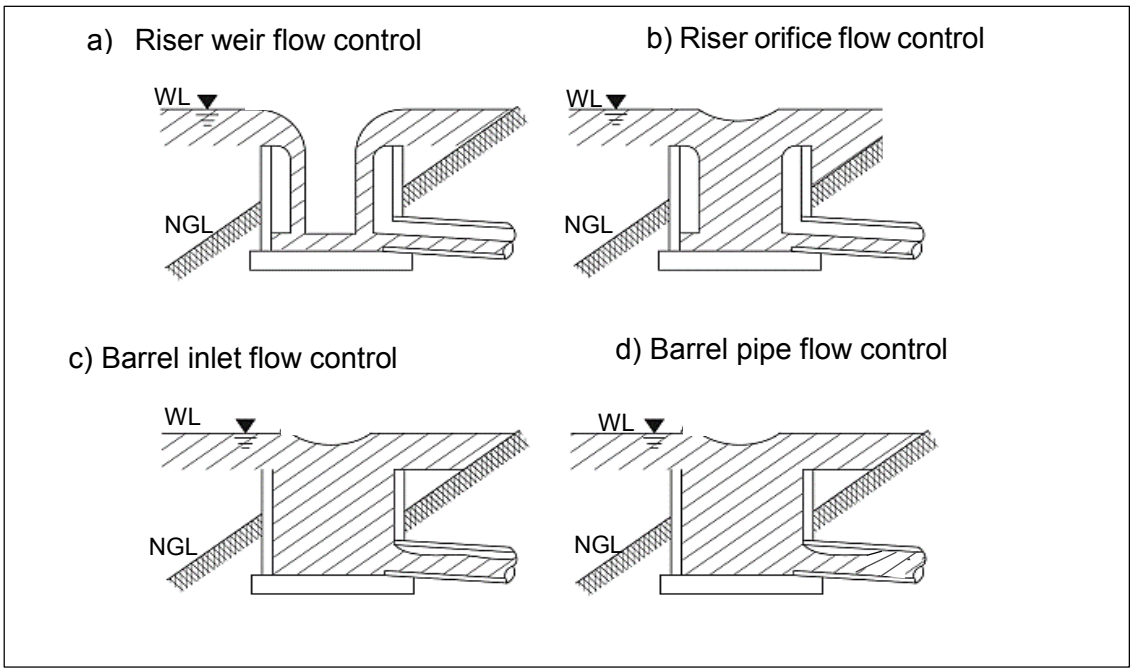

Figure 2.19: Riser flow diagrams (adapted from Virginia Department of Conservation and Recreation, 1999b)

2.4 Trash Racks

2.4.1 Background

Trash racks should be integrated into the outlet structure design as part of Best Management Practices. Although the literature recommends trash racks, field experience has shown that during heavy run-off trash racks could become clogged and the culvert then becomes ineffective (Jones, Guo, Urbonas and Pittinger, 2006:10). A trash rack or safety grate is necessary if one of the following tests is violated (Jones et al, 2006:10):

- The public can clearly, in daylight, see from one side of the culvert to the other side.
- The culvert is of adequate size to pass a 1.2192 m diameter object.
- The outlet would not trap or injure a person.

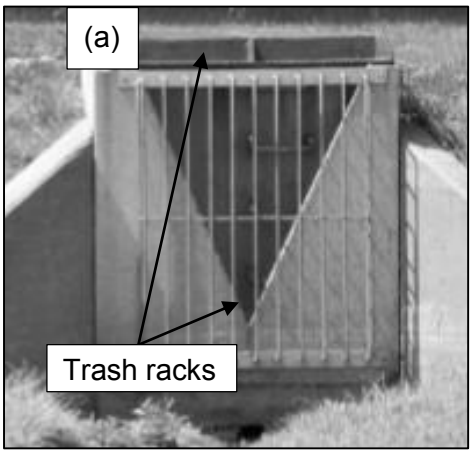

Figure 2.20: Birdcage type trash rack at top inlet (adapted from Headley and Wyrick, 2009:5)

The trash rack in Figure 2.20 prevents trash and people from being conveyed into the riser at high velocity water flows. Anti-vortex devices prevent vortex form forming; thereby the hydraulic efficiency of the outlet structure is maintained (McCuen *et al*., 2002:305). Anti-vortex devices are not required when riser weir flow control is maintained through all flow stages (Virginia Department of Conservation and Recreation, 1999a).

2.4.2 Main Functions of Trash Racks

Trash racks help to keep debris away from the entrance to the outlet and thus to keep the critical components of the structure open. Removal of debris is made easier by trash racks, as they capture the debris. The trash rack also functions as a safety system that prevents people from being drawn into the outlet by keeping them out of confined conveyance area. People could also use the rack to climb to safety if necessary (Iowa Stormwater Management Manual, 2009:25).

The inclined vertical bar rack is effective for lower stage outlets. The inclined vertical bar rack makes it possible for debris to move up the rack when the water level rises. Removal of accumulated debris with a rake is possible when standing on top of the outlet structure (Iowa Stormwater Management Manual, 2009:25).

Sediment has a tendency to accumulate around the lowest stage outlet, therefore it is recommended, for dry basins, to depress the inside of the outlet structure to a depth below the ground surface. According to Knox County (2008:19) this depth should be at least equal to the diameter of the outlet, in order to minimize any clogging caused by sedimentation.

2.4.3 Trash Rack Design Procedure

The Urban Drainage and Flood Control District (2010) estimates the trash rack openings based on the outlet diameter, as demonstrated in Figure 2.21. However, judgement should be exercised in areas with a higher amount of debris, which would require more opening space between bars (Knox County, 2008:19). If the pipe diameter is larger than 600 mm, the net open surface area of the trash rack must be, at the absolute minimum, at least four times larger than the cross-sectional area of the pipe.

In addition, for pipe diameters larger than 600 mm, the average velocities at the rack face should be less than 0.6096 m/s for each stage of flow entering the outlet pipe (UDFCD, 2010:168). As a rule, consulting engineers try to keep approach velocities to about 1 m/s on trash racks, which would determine the necessary gross area for a given flow situation (Law, 2015).

Trash racks that are situated at entrances to the outlet pipe or culvert should be sloped at about 3H:1V to 5H:1V, to permit debris to slide upward as the water level rises. The angle of the trash rack should be adjusted according to the approach flow. In the instance of a slow approach flow, a flatter angle would then recommended (Design and Construction of Urban Stormwater Management Systems, 1992:308).

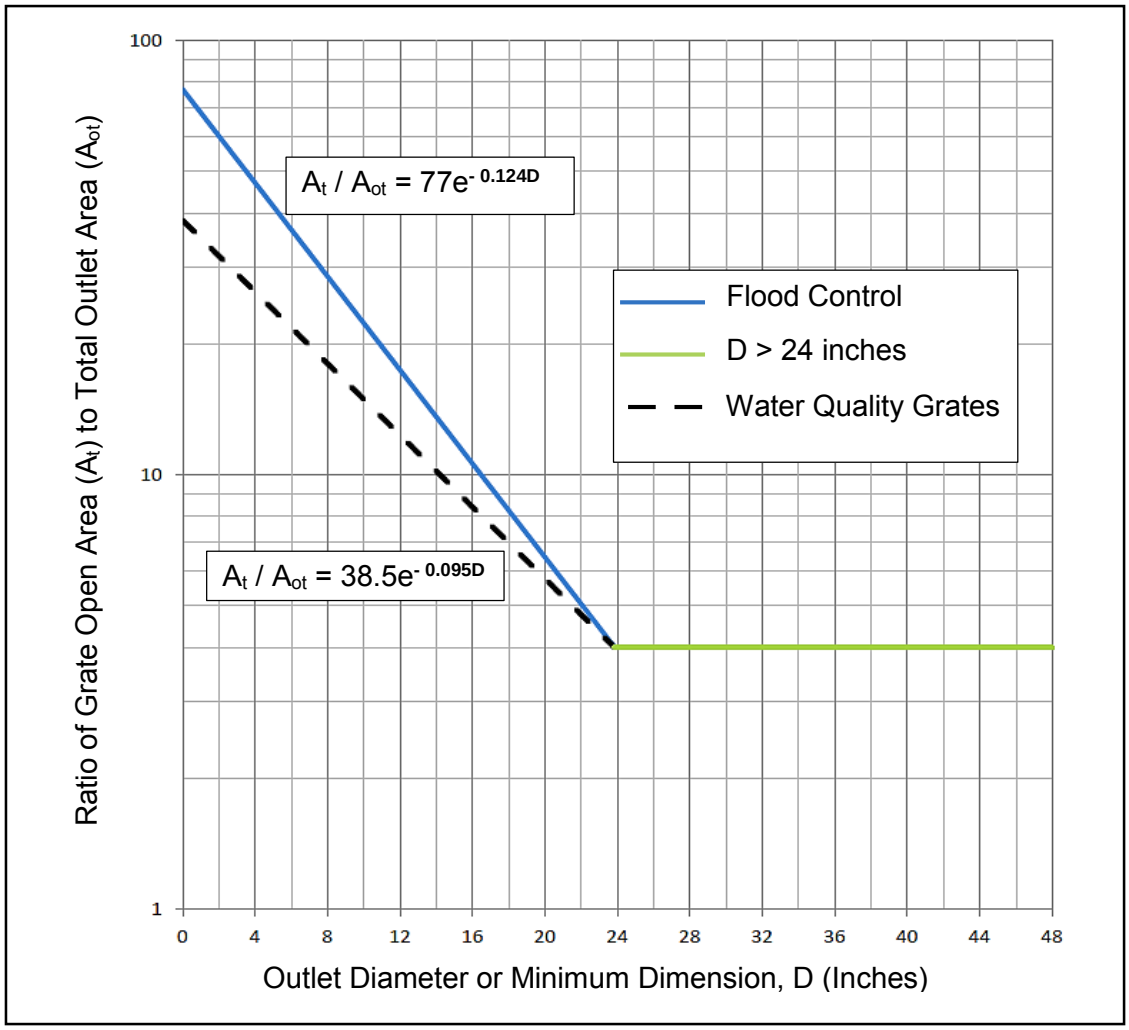

Figure 2.21: Determination of the minimum rack size versus the outlet diameter (UDFCD, 2010:270)

Typically, the minimum clear spacing between the bars is determined by the minimum size of passages on equipment downstream. For pumps or turbines, this is usually not larger than 90 mm, but it could be as small as 20 mm. The clear spacing between trash racks bars at culvert entrances should be restricted to a clear spacing of 152.4 mm in order to prevent children from passing through (Design and Construction of Urban Stormwater Management Systems, 1992:308).

Transverse support bars have to be limited, but sufficient to prevent the rack from collapsing under full hydrostatic loads. The Bureau of Indian Standards (2012) recommended that the laterally unsupported length of the trash rack bars should not be greater than 70 times the thickness of the bar. The minimum thickness of trash rack bars is 8 mm and, for deeply submerged racks, the thickness should be 12 mm, according to the Bureau of Indian Standards (2012). The depth of a trash rack bar should not be more than 12 times the thickness of the bar, nor should it be less than 50 mm (Bureau of Indian Standards, 2012:3). Graham *et al*. (2009) specify other requirements and recommends screen bar dimensions of at least 8 x 75 mm for flat bars with the maximum unsupported length of a bar not exceeding 1.5 m.

Additional width should be provided in the rack for adequate attachment to the outlet structure. It would be more conservative to maximise the width of the trash rack to the geometry of the outlet, which would reduce clogging and extend the interval of regular maintenance (UDFCD, 2010:267). The grate of the trash rack should not control the flow of the outlet and the grate should not cause the headwater to rise above the designed levels.

Head losses through use of the grate should be accounted for when designing a trash rack. Two head loss equations (Equations 2.29 and 2.30) are recommended in order to allow for comparison, which is necessary because of the difficulty of estimating values for variables that are used in empirical head loss equations (Knox County, 2008:21).

Equation 2.29 (Metcalf and Eddy, 1972) could be used to calculate the head loss through a trash rack. It is important to assume a certain percentage of blockage when the design of grate openings is based on Equation 2.29. A blockage of 40% to 50% would be an efficient assumption according to Knox County (2008), which would allow for partial clogging of the racks.

$$H_g = K_{g1}\left(\frac{w}{s}\right)^{4/3}\left(\frac{v^2}{2g}\right)\sin\theta_g \tag{2.29}$$

The United States Army Corps of Engineers (1988) has developed a comparable head loss equation for grates, which is given in Equation 2.30. Equation 2.30 was developed for vertical racks; nevertheless, it could be adjusted through multiplication by the sine of the angle of the grate with respect to the horizontal, which would result in an equation similar to Equation 2.29.

$$H_g = \frac{K_{g2}v^2}{2g} \tag{2.30}$$

where:

H_g = head loss through grate (m)

K_{g1} = bar shape factor (see Table 2.5)

K_{g2} = bar shape factor defined by fit curves (see Table 2.5)

w = maximum cross-sectional bar width facing the flow (mm)

s = minimum clear spacing between bars (mm)

v = approach velocity (m/s)

θ_g = angle of the grate with respect to the horizontal (degrees)

A_r = ratio of the area of the bars to the area of the grate section.

Table 2.5: Bar shape factor, K_{g1} and K_{g2} fit curves (adapted from Iowa Stormwater Management Manual, 2009)

Grate Type	Length/ Thickness	Factor (K_{g1})	Curve
Sharp-edged rectangular	-	2.42	-
Rectangular bars with semi-circular upstream faces	-	1.83	-
Circular bars	-	1.79	-
Rectangular bars with semi-circular up- and downstream faces	-	1.67	-
Sharp-edged rectangular	10	-	$K_{g2} = 0.00158 - 0.03217A_r + 7.1786A_r^2$
Sharp-edged rectangular	5	-	$K_{g2} = -0.00731 + 0.69453A_r + 7.0856A_r^2$
Round edged rectangular	10.9	-	$K_{g2} = -0.00101 + 0.02520A_r + 6A_r^2$
Circular cross-section	N.A	-	$K_{g2} = 0.00866 - 0.13589A_r + 6.0357A_r^2$

The Bureau of Indian Standards (2012) determines the loss of head from Equation 2.31.

$$\text{Head loss} = \frac{KV^2}{2g} \tag{2.31}$$

where:

K = trash rack loss coefficient ($1.45 - 0.45A_n - A_n^2$)

A_n = net area through the rack bars / gross area of the racks and supports

V = approach velocity of flow through trash rack, computed on gross area (m/s).

2.4.4 Hydraulic Capacity of Drop Inlets with Trash Rack

Section 2.3.2.5 discussed the riser intake box component of the multi-stage outlet structure, which acts either as a weir, when the water depth is too shallow to submerge the entire inlet grate, or as an orifice during drowned conditions. Figure 2.22 illustrates both weir flow and orifice flow conditions around drop inlet structures. These riser boxes have intake openings that are parallel to the water surface and, as mentioned, are usually designed with a grid over the openings to make the outlet safe for people and to keep trash out of the riser structure.

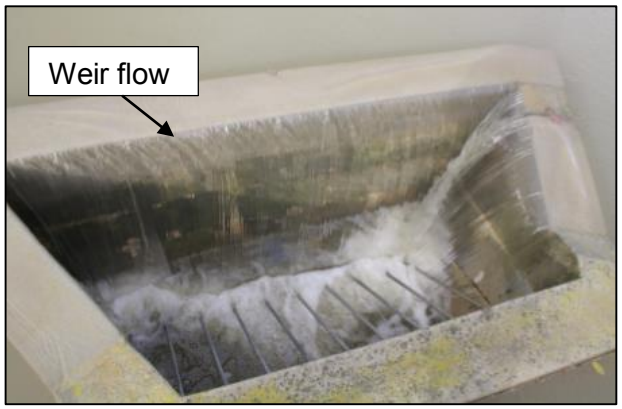

Figure 2.22: Weir flow condition around drop inlet (adapted from Hotchkiss, 2015:29)

Drop outlets, which feed oncoming flows downwards into underground drainage systems (Type 1 outlets), discharge either under free-flow or drowned conditions (SANRAL, 2013:5-8). The riser box thus functions as a type of drop outlet. During subcritical approach flow and free outflow conditions, the outlet may be analysed by applying the broad-crested weir formula (Equation 2.13 in Section 2.3.2.4.1). During critical conditions along the crest of the drop outlet, the contraction coefficient could be taken as 0.6. Then Equation 2.13 becomes Equation 2.32. When considering contraction of oncoming flow, Equation 2.32 becomes Equation 2.33 (SANRAL, 20013:5:10). No blockage factor has been taken into account when using Equations 2.32 or 2.33.

$$Q = 1.7bH^{1.5} \tag{2.32}$$

$$Q = 1.45bH^{1.5} \tag{2.33}$$

where:

b = total flow width

H = energy head, taken as the flow depth for upstream conditions (m).

It is clear from Equations 2.32 and 2.33 that the broad-crested weir is not affected by the bars in the opening of the drop outlet, since during critical conditions, the critical depth is at the edge of the opening.

SANRAL's Drainage Manual (SANRAL, 2013:5-11) recommends that the outflow is calculated by means of the standard orifice equation (Equation 2.1) during subcritical submerged flow conditions. The inlet coefficient is taken as 0.6 for sharp edges and 0.8 for round edges. The area of the drop outlet should be taken as the effective cross-sectional plan area of the opening. Blockage of the drop grid inlet should be taken into account by multiplying Equation 2.1 by a blockage factor, which is typically taken as 0.5. The Urban Drainage Flood Control District (Guo, 2012) determines the flow through the overflow outlet section of the riser box by means of Equations 2.34 and 2.34.1.

$$Q = \frac{2}{3}\, n\, C_d\, (2B + 2L_h)\sqrt{2g}\, h_w^{1.5} \tag{2.34}$$

$$n = (1 - Clog)\frac{L_h - L_b}{L_h} \tag{2.34.1}$$

where:

C_d = discharge coefficient (typically 0.62)

n = open area ratio for the grate (typically between 0.3 and 0.7)

h_1 = headwater depth above weir crest (m)

B = base width of grate (m)

L_h = horizontal grate length (m)

L_b = cumulative width of bars on grate (m)

Clog = clogging factor (ranging from 0 to 1).

Equation 2.34 defines the weir length as the circumference of the riser structure, measured at the crest of the riser, less any support rods or trash rack bars. Equation 2.33 uses the total flow width, making no allowance for a blocking factor.

2.5 Current Practices and Regulatory Requirements in South Africa

Municipalities in South Africa have different requirements for retention and detention facilities, although City of Cape Town, City of Johannesburg and eThekwini Municipality (see Table 2.6) agree upon peak discharge control to ensure a reduction of the post-development flow rate to the pre-development flow rates.

The Johannesburg Metropole requires detention of stormwater for the 5- to 25-year recurrence interval design storm events, as these are the worst scenarios (Townshend n.d). However, the recurrence interval could be increased to 50 years if deemed necessary by the City of Johannesburg. According to the Johannesburg Road Agency (JRA), all developments exceeding 8 500 m^2 are subjected to the above mentioned on-site stormwater attenuation requirements (Aldous, 2007:40).

The Cape Town Metropole is in the process of developing regulations for both attenuation, as well as water quality requirements, which stipulate that the initial run-off of approximately 25 mm depth of rain should be stored for a period of time (48 hours) in order to improve the quality of the stormwater discharged. This requirement would allow pollutants and sediment to settle out, aided by the vegetation in the detention pond, which processes the pollutants naturally (Townshend, n.d).

The City of Cape Town (CCT) also prescribes the protection of the downstream channel by means of 24-hour extended detention of the 1-year recurrence interval, 24-hour storm event. Another requirement of the CCT is to control frequent flood events with a recurrence interval

of up to 10-years. The once in 50-year storm event should also be reduced to the pre-development flow and the once in 100-year storm event must be assessed and managed to ensure that urban properties do not get damaged (City of Cape Town, 2009).

Brownfield and other existing development sites larger than 50 000 m^2 are development scenarios which have to control the quantity and rate of the run-off as mentioned above and stipulated in the Management of Urban Stormwater Impacts Policy (City of Cape Town, 2009). This is also true for all Greenfield developments; however, the policy does not specify a specific area size for Greenfield developments. In addition to requiring on-site attenuation of flows in developments above 50 000 m^2, the Cape Town policy requires shared regional and on-site attenuation for developments between 4000 m^2 and 50 000 m^2 in extent.

The eThekwini Municipality requires engineers to produce a stormwater management plan to control the 10-year storm event at certain critical points, but at all other points in the catchment, design is generally only for the three-year recurrence interval storm. Major disposal systems must be designed for the 20-year recurrence interval design storm. Major disposal systems refers to flows of approximately 10 m^3/s. Special cases require control of the 50- ,or even the 100-year, storm event (eThekwini Municipality, 2008).

The National Water Act (NWA) instructs municipalities to limit new development in townships within flood lines, therefore, it is often required of designers to determine the maximum flood level which would result from a 100-year flood event (Republic of South Africa, 1998). The National Water Act also emphasises the protection of aquatic life and ecosystems, and the prevention of pollution which could lead to the degradation of water resources (Burke and Mayer, 2009:55)

Table 2.6 summarises the different recurrence interval requirements which multi-stage outlet structures are designed, according to various stormwater design manuals. In addition to the design flow, other flows in excess of the design flow, such as the 100-year flood, are usually included in the analysis, as it might be expected to pass through the storage facility.

Table 2.6: Summary of the controlling design criteria

Source	Controlling criteria
City of Cape Town, 2009	24 hr extended detention of 1-year RI, 24 hr storm event, 10- and 50-year RI
eThekwini Municipality, 2008	3- or 10- year and 50-year RI
Townshend, n.d.	5-, 25- and 50-year RI
Debo and Reese, 2003	5- and 10- year RI or 5- and 25-year RI and/or the 100-year storm
Brown, Schall, Morris, Doherty, Stein and Warner, 2009	2-,10-,and 100-year RI

2.6 Laws of Hydraulic Similitudes in Physical Models

The investigation of the relationship between model ($_m$) and prototype ($_p$) performance, which is governed by the laws of hydraulic similarity, is required, as this thesis is centred on the performance of a hydraulic physical model. In order that the physical models reproduce hydraulic conditions in the prototype, the flows must display a similitude to the prototype. Similarity in flow conditions between the prototype and model implies that the model displays similarity of form (geometric similarity), similarity of motion (kinematic similarity) and similarity of forces, also called dynamic similarity (Chanson, 2004).

2.6.1 Implications of the Similarity Laws

The following section highlights the way by which one could achieve similarity of fluid behaviour during a study of physical models. According to Webber (1979), the compressibility property of the prototype fluid is insignificant, and could therefore be omitted. Two similitudes that are generally used when replicating scaled flows in physical models of urban drainage systems are the Reynolds number and the Froude number (Rubinato, 2015).

2.6.1.1 Froude's Law

Froude's Law is applied wherever a free surface gradient exists, that is where gravitational forces prevail. The velocities (v) of the model and prototype must be related in order to comply with Froude's Law ($v/\sqrt{gl}$) as indicated in Equation 2.35 (Webber, 1979:303). The scale factor is referred to as x.

$$\frac{v_p}{v_m} = \frac{(gl_p)^{1/2}}{(gl_m)^{1/2}} = x^{1/2} \tag{2.35}$$

where:

v = velocity (m/s)

g = gravitational acceleration (9.81 m/s^2)

l = characteristic linear dimension (m), e.g. pipe diameter or channel width.

Table 2.7 summarises the scalar relationships for physical models that are scaled based on the Froude Law.

Table 2.7: Scalar relationships for models under Froude similitude (adapted from Webber: 1979:304)

Quantity	Dimensions	Natural scale 1:x
Geometric:		
Length	l	x
Area	l²	x^2
Volume	l³	x^3
Kinematic:		
Time	T	$x^{1/2}$
Velocity	l/T	$x^{1/2}$
Acceleration	l/T²	1
Discharge	l³/T	$x^{5/2}$
Dynamic:		
Pressure	M/lT²	$\rho_r x$
Force	Ml/T²	$\rho_r x^3$
Energy	Ml²/T²	$\rho_r x^4$
Power	Ml²/T³	$\rho_r x^{7/2}$

where:

l = characteristic linear dimension (m) (e.g. pipe diameter or channel width)

T = time interval (sec)

M = mass (kg)

$\rho_r = {}^{\rho_\rho}/_{\rho_m}$ = ratio between the densities of the prototype and the model.

2.6.1.2 Reynolds' Law

A real fluid has viscosity, therefore Reynolds' Law should be considered when viscous shear drag and inertia forces are present. Examples include vortexes and tidal energy converters. Reynolds' Law ($\mathrm{Re} = \mathrm{vl}/\nu$) states that the corresponding velocities of the model and prototype must be related as defined in Equation 2.36 (Webber, 1979:304).

$$\frac{v_p}{v_m} = \frac{\nu_p l_m}{\nu_m l_p} = \frac{\nu_p}{\nu_m}\frac{1}{x} \tag{2.36}$$

where:

l = length of sections in model and prototype respectively (m)

υ = kinematic viscosity ($\approx$1.13 x 10^{-6} m^2/s for water)

2.6.1.3 Euler's Law

The Euler number ($E = v/\sqrt{2\Delta p/\rho}$) is relevant when conducting a physical model study of an enclosed fluid system where turbulence in the system is fully developed, viscous forces are insignificant in comparison to inertial forces, and surface tension and gravity forces are absent (Webber, 1979:302). Euler's Law is therefore applicable when inertial forces are of significance (Webber, 1979:302).

2.6.1.4 Weber's Law

The influences of surface tension are significant only in a structure with small linear dimensions and where an air-water boundary exists. Physical models with very low weir heads, air entrainment, splash or spray should account for the influence of surface tension (Webber, 1979). The Weber number is proportional to the ratio of the inertial force to capillarity force ($W = v/\sqrt{\sigma/l\rho}$). Model velocities must be scaled to $x^{1/2}$ times the velocities in the prototype in order to conform to Weber's Law when the fluid in the model and prototype is identical.

2.6.2 Similarity Requirements for Multi-Stage Outlets

The multi-stage outlet structure is modelled in an open glass flume and the model has a free surface. Thus, the effects of gravity are dominant and model-prototype similarity is performed with a Froude similitude. However, the outlet pipe of the multi-stage outlet functions as a fully enclosed system. A main concern for such flow situations is the potential for scale effects induced by viscous forces (Chanson, 2004:262). If the same fluid is used in the model and prototype, it would be impossible to satisfy both the Froude's and Reynolds' law simultaneously. It is therefore elementary to show that a Froude similitude implies $Re_r = L_r^{3/2}$, where Re_r refers to the Reynolds number of the prototype-to-model and L_r refers to the geometric scale. This relation indicates that the Reynolds number becomes much smaller in the model than in nature (Kobus, 1980:14).

These discrepancies between the performance of the model and that of the prototype are known as the "scale effect" (Webber, 1971:298). According to Kobus (1980:15), the requirement to limit scale effects, is that the Reynolds number in the model remain large enough to ensure turbulent flow conditions in the model, when the flow in the prototype is turbulent. In general, for a Froude model, high Reynolds and Weber numbers are required to mitigate the potential scale effects due to viscosity and surface tension (Webber, 1979:305).

The relevant question is whether scale effects could be neglected. Thus, the following section gives an overview of the minimum Reynolds and Weber numbers, as recommended by various authors, that would be required to reduce scale effects due to viscosity and surface tension for physical models based on the Froude law scaling. These minimum Reynolds and Weber numbers refer specifically to those at either sharp-crested weirs or outlet pipe

systems, since the multi-stage outlet structure comprises these flow control devices, which form part of a whole system.

- Ghetti (1966; cited in the E-proceedings of the 36th IAHR World Congress, 2015) concluded that the head on a sharp-crested notch should be at least 50 mm to exclude scale effects, while Ghetti and D'Alpaos (1977; cited in Heller, 2011) noted that the parabolic nappe profile applies only for a head of at least 45 mm. This condition gives a minimum Reynolds number of 2100. The Weber number should also be at least equal to 120.
- Sarginson (1972:444) concluded that surface tension has negligible effect on the profiles of the lower nappe surface, for flow over sharp-crested weirs, at heads exceeding 50 mm.
- Webber (1979:310) recommend that the head on a model weir should be at least 6 mm, otherwise surface tension forces could cause false clinging of the nappe flow profile.
- According to Chason (2004; cited in Wood, 1991) the effects of gravity are predominant in free-surface flows, but surface tension scale effects could take place for L_r > 10-20, where L_r refers to the geometric scale.
- Novak and Cábelka (1981:41) stated that the same regime of flow must be conserved in a scale model and in the prototype, because the energy loss in laminar and turbulent flow differ. For fully turbulent flow in the prototype, the Reynolds number in the model should be larger than $1x10^6$. For transitional turbulent flow in the prototype, the Reynolds number in the model should be larger than 2300.
- Chanson (2004:268) indicated that for free surface flows (overflow weirs, or open channels), the Reynolds number in the model, defined in terms of the hydraulic diameter, should be larger than 5000 to reduce viscous forces.
- The USBR (1980:48) states that when the Reynolds number of the model is greater than $1x10^4$, where the depth of flow is substituted for L in the Reynolds number ($R = VL/v$), then the viscous forces are comparatively unimportant.

Based on the above limitations, it is recommended that the minimum Reynolds number should be 5000 for open channel flows and most importantly for the pipe outlet, the flow regime (laminar, smooth turbulence, transitional turbulence, or rough turbulence) in the model and prototype must be similar. For transitional turbulent flow in the prototype, the Reynolds number in the model should be larger than 2300. The minimum head above a thin-crested weir (h) should at least be 45 mm to exclude scale effect. Often the model does not reproduce the flow patterns in the prototype, since the model is to smooth or too rough. A recommended solution is to adjust the resistance coefficient (Chanson, 2004:267). However, Webb, Barfuss and Johnson (2010:264) concluded that roughness scaling methods are limited to conditions where the prototype and the model operate in the fully rough flow regime.

2.7 Summary of Literature Review

The main objective of the study was to evaluate the hydraulic performance of different outlet device configurations to control a full range of storm events. The design of multi-stage outlet structures is based on theoretical equations as summarised in Table 2.8. Lastly, current practices and regulations from municipalities within South Africa have indicated that stormwater outlets are designed to attenuate only three recurrence interval storm events (refer to Section 2.5). The question is, however, whether the post-development flood peaks for a full range (2-, 5-, 10-, 20-, 50- and 100-year) of storm events could be restricted to the pre-development flood peaks.

Table 2.8: Equations to determine discharge for multi-stage outlet structures

Discharge control device	Equation	Source
Circular orifice (partially submerged upstream)	Equation 2.2 and Equations 2.2.1 to 2.2.4	Barlow and Brandes, 2012
Circular orifice (fully submerged upstream)	Equation 2.1 and Equations 2.1.3 to 2.1.5	Chadwick *et al.* , 2004 and Barlow and Brandes, 2015
Rectangular orifice (partially submerged upstream stream)	Equation 2.13, with C_d= 0.37	McCuen *et al*., 2002
Rectangular orifice (fully submerged upstream)	Equation 2.1, with C_d=0.61	Barlow and Brandes, 2015
Rectangular sharp-crested weir	Equation 2.19 or Equation 2.18 to make allowance for end contractions	The Bureau of Reclamation, 2001
V-notch weir	Equation 2.24	Brater *et al.*, 1996
100-year outlet pipe	Check Equation 2.1, 2.9, 2.11 for inlet control and Equation 2.12 for outlet control	SANRAL, 2003
Submerged orifice	Equation 2.1 with C_d= 0.6 for circular and 0.61 for rectangular orifice. Effective head equals the difference between upstream and downstream water surface elevations.	Knox County, 2008 and Iowa Stormwater Management Manual, 2009
Submergence of sharp-crested weir	Villemonte Equation 2.22	Chadwick *et al*., 2004
Riser structure without trash rack (Inlet boxes)	Check both weir flow conditions (Equation 2.19) and orifice flow conditions (Equation 2.1)	The Bureau of Reclamation, 2001 and Virginia Department of Conservation and Recreation, 1999b
Riser structure with trash rack	Equation 2.33 for weir flow and Equation 2.1 for orifice flow, with the riser dimensions determined by means of Figure 2.24.	SANRAL, 2003 and UDFCD, 2010
Water Surface Elevation inside riser	Head produced by 100-year pipe, thus rearrange Equations 2.1, 2.9, 2.11, or 2.12, depending on controlling condition	SANRAL, 2003
Level-Pool Routing	**Equation**	**Source**
To verify maximum water surface and outflow from multi-stage outlet for various RI storms	Refer to Section 10.4.2 of SANRAL, 2013	SANRAL, 2003

3. Model Development: Pre- and Post-Development Hydrographs

3.1 Introduction

Chapter 2 focused on the general input requirements for designing multi-stage outlet structures for flood attenuation facilities, which, by means of several discharge devices, control the rate of outflow during multiple design storms. Urban development drives much of the need for performing pre- and post-development analysis. Thus, following from the literature review, Chapter 3 focuses on the development of the pre- and post-development hydrographs for a hypothetical medium to high income residential development, which are situated in either a coastal or inland region of South Africa. These hydrographs were then used as input parameters for the design of multi-stage outlet structures.

Different flood hydrology methods such as the unit hydrograph-, rational- and SCS- methods could be used to generate the design hydrographs that are required to design an attenuation facility. Currently in practice, when the catchment area is less than 1 km^2, the modified rational method is used to determine the time of concentration (T_c) and the peak run-off rate, which results in a simplified triangle hydrograph (Townshend, n.d.). Available software packages, such as SWMM, use the rational method for small urban catchments, which also makes it possible to route the run-off through the storage facility using fixed outlets (Townshend, n.d.).

The hypothetical catchment area under consideration was assumed to be less than 1 km^2 (refer to Section 3.2) and municipal guidelines requires at least a rational method of determination (eThekwini Municipality, 2008:10). The use of the rational method has been adapted as a theoretically acceptable approach to developing triangular pre- and post-design hydrographs, as demonstrated in Figure 3.1 (Van Vuuren, 2012:24).

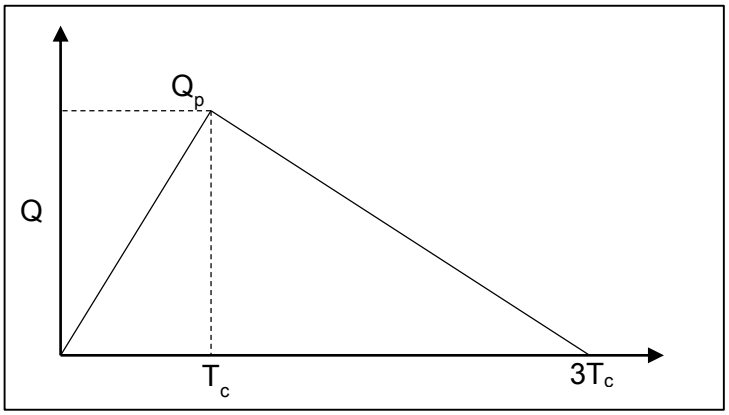

Figure 3.1: Simplified triangular hydrograph for the rational method (adapted from SANRAL, 2013:3-30)

The main aims of Chapter 3 are to:

- Estimate the input requirements (catchment area, mean annual rainfall, longest watercourse, run-off coefficient etc.) of the rational method for both inland and coastal regions.
- Calculate the peak discharge for the 2-, 5-, 10-, 20-, 50- and 100- year storm event by means of the rational method for both inland and coastal regions.
- Generate the synthetic design hydrographs based on the results of the rational method for both inland and coastal regions.

The main assumption regarding the input requirements for the rational method are discussed in Section 3.2 and parameter sensitivity assessments elaborated in Section 3.3.

3.2 Selection of Catchment Area

In order to understand the literature, it should be clear that brownfield refers to an area of land that was previously occupied by a permanent structure, which may have become under-used or abandoned, and has the potential for redevelopment, whereas greenfields refer to land such as parkland, open space, or agricultural land which has not previously been developed. Greenfield development would require a change of land use or zoning (City of Cape Town, 2009).

Brownfield and existing development sites larger than 50 000 m^2 are development sites which have to control the quantity and rate of the run-off as stipulated in the Management of Urban Stormwater Impacts Policy, which was elaborated in Section 2.7 (City of Cape Town, 2009). This is also true for all greenfield developments; however, the policy does not specify a specific area size for these developments. In addition to requiring on-site attenuation of flows in developments above 50 000 m^2, the Cape Town municipal policy requires shared regional and on-site attenuation for developments between 4 000 m^2 and 50 000 m^2 in extent. On the other hand, in order to comply with the Johannesburg Road Agency (JRA) requirement, all developments exceeding 8 500 m^2 are subject to storm water attenuation on site (Aldous, 2007:40).

The maximum available pump capacity of 700 l/s at the Stellenbosch University hydraulic laboratory limited the peak flow for model tests. The maximum peak inflow was limited to approximately 10.9 m^3/s, for a model scale of 1:3. Thus, the catchment area had to be smaller than 230 000 m^2, in order not to exceed the limit of 10.9 m^3/s, according to the Rational method.

The Association for Residential Communities (ARC), which represents the residential estate industry in South Africa, published figures in the Residential Industry Journal (ARC, 2014) with respect to community's size, type (ecological, golf, retirement, lifestyle, and nature), and region. Figure 3.2 indicates that communities covering fifty hectares or less comprise the predominant portion of the total number of communities. The hypothetical catchment area for

the study was taken as 50 000 m^2 in order to meet the City of Cape Town's requirement of on-site attenuation, while keeping in mind the laboratory pump's capacity of 700 l/s. The catchment area was considered large enough to also be applicable to a wide range of future developments, see Figure 3.2.

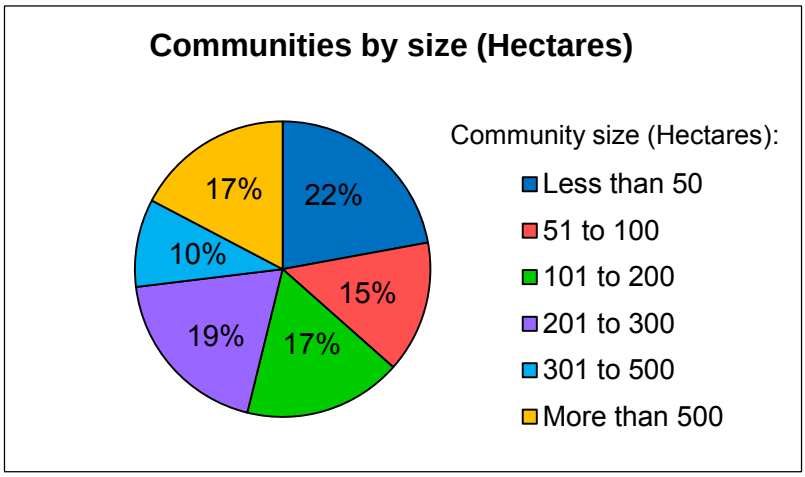

Figure 3.2: Typical size of communities in hectares (reproduced from ARC, 2014)

3.2.1 Physical Characteristics of the Case Study Area

3.2.1.1 Slope and Area

An assumption was made that the site had been filled and levelled to an average slope of 1%. The latter assumption was also made by Hotchkiss (2015), who assumed that bulk earthworks were often undertaken to level the ground surface in order to facilitate infrastructure and building development. The catchment area was taken as only the area of the development site (50 000 m^2), since it was assumed that only the flow on the developed site had to be attenuated. The multi-stage outlet structures that were designed for hydrographs based on either inland rainfall data or coastal rainfall data, could then be compared, since the catchment size was similar. The area reduction factor could be ignored, as the catchment area was less than 1km^2.

3.2.1.2 Mean Annual Rainfall

Mean annual rainfall (MAP) is know to effect catchment run-off. Table D.1, enclosed in Appendix D, gives the run-off factors for different classes of mean annual rainfall, namely, less than 600 mm, 600 mm to 900 mm, and greater than 900 mm (SANRAL, 2013:3-19). The peak discharge should, therefore, be calculated for three mean annual rainfall conditions, which would result in three different values for the run-off coefficient (C_1) for the pre-development (rural) scenario. Figure D.1, enclosed in Appendix D, illustrates the mean annual precipitation distribution in South- Africa.

Based on Table D.1 and Figure D.1, it was decided to calculate the peak discharge for coastal and inland regions with mean annual precipitations of 400 mm, 700 mm and 1000 mm, respectively. The latter was done in order to compute hydrographs for a wider range of rainfall conditions, which would provide valuable insight with respect to the design of multi-stage outlet structures for peak discharge of different magnitude.

3.2.1.3 Time of Concentration (T_c)

Clearing of vegetation and levelling of the hypothetical development site would change the natural meandering watercourse. The longest watercourse of the hypothetical site was approximated as the diagonal path taken from the point at the site boundary with the highest elevation to an outlet at the opposite end of the site boundary with the lowest elevation. A surface slope of 1% was taken into account, as mentioned previously. The diagonal path would decrease the meandering watercourses and the time run-off takes to reach the outlet. Thus, the multi-stage outlet would be exposed to greater peak flows because of the decreased time of concentration (T_c). Therefore, the simplified assumption is justified for the worst case scenario. Figure 3.3 demonstrates the approximation of the longest watercourse for a hypothetical development site. A site with a layout of 250 m x 200 m resulted in a watercourse length of 0.32 km.

The time of concentration was determined by using Equation 3.1. This resulted in a time of concentration less than 15 minutes, due to the relatively small catchment. A time of concentration of less than 15 minutes is generally not significant (SANRAL, 2013) and thus the rainfall intensity is based on the assumption that the duration of a storm is at least 15 minutes for undeveloped, rural or residential sites, and at least 10 minutes for industrial, commercial or fully developed sites, where the site is predominantly impermeable (eThekwini, 2008:7).

$$T_C = \left(\frac{0.87L^2}{1000S_{av}}\right)^{0.365} \quad (3.1)$$

where:

L = longest watercourse (km)

S_{av} = average watercourse slope (0.01 m/m).

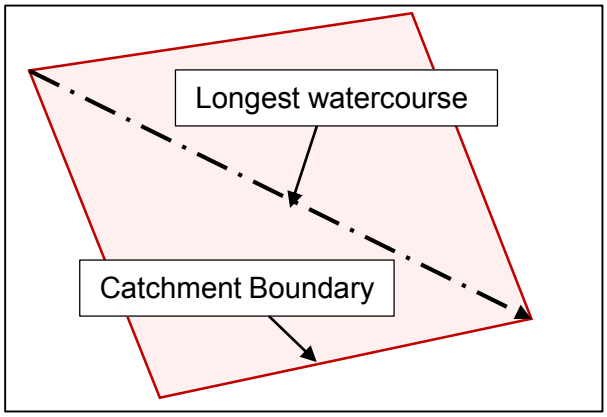

Figure 3.3 Approximation of the longest watercourse

Point rainfall was determined for both inland and coastal regions by using the SANRAL Drainage Manual's (2013) Depth-Duration-Frequency Diagram. The point rainfall was converted to rainfall intensity by dividing the point rainfall by the time of concentration. The rainfall intensities were also increased by a climate change factor of 1.15, which agreed with the Standard Requirements for a Stormwater Master Plan (City of Cape Town, 2011).

Table 3.1 summarises the catchment parameters that were required to determine the peak discharge and the simplified triangular hydrographs for the hypothetical residential site by means of the rational method.

Table 3.1: Summary of input parameters for hypothetical residential site

Input parameters	Value
Catchment area (km)	0.05
Longest watercourse (km)	0.32
Average watercourse slope (m/m)	0.01
Area reduction factor	1
Mean annual precipitation	400 mm, 700 mm and 1000 mm

3.2.1.4 Physical Characteristics of the Pre-Development Scenario

The pre-development scenario refers to the natural catchment prior to any development and comprising of 100% rural conditions. The surface slope was taken as 1% as discussed in Section 3.2.1.1, thus the catchment was classified as a flat surface. The permeability of the soil had to be assumed as 50% permeable and 50% semi-permeable, since the residential development was hypothetical and site-specific soil information was unobtainable. This assumption gave a comprehensive classification of the permeability of the site.

Literature repeatedly indicated that residential estates were often developed on land which had previously been used as farmland (Dennis Moss Partnership Project Portfolio, 2014). Thus, the vegetation of the pre-development scenario was classified as 100% light bush and farmlands. The above physical characteristics determined the rural run-off coefficient (C_1). The calculation procedure for C_1 may be seen in Appendix D, Tables D.2 and D.4.

3.2.1.5 Physical Characteristics of the Post-Development Scenario

The post-development scenario refers to the catchment area covered with impervious surfaces and 100% urban conditions. Layout plans of proposed residential developments (Whittemore, 2015) were investigated, as well as zoning schemes (City of Cape Town, 2012), and residential density and spatial development planning (City of Cape Town, 2010). This was done in order to approximate the typical proportions of the site that would be used for roads, houses, lawns, and open spaces in a residential estate.

Land utilisation percentages were based on data published by the CSIR (CSIR, 2000), which are summarised in Table 3.2. The data obtained from the Guidelines for Human Settlement Planning and Design (CSIR, 2000:5-6), agreed with the data obtained from existing locality maps of proposed residential developments (Whittemore, 2015) as indicated in Table 3.2. Therefore, the data obtained from the Guidelines for Human Settlement Planning and Design (CSIR, 2000) was used as typical input percentages for the urban area classification, which were then used to determine the value of the urban run-off coefficient (C_2). The calculation procedure of the maximum urban run-off coefficient, for use in the rational method of the post-development scenario, may be seen in Appendix D, Tables D.3 and D.5.

Table 3.2: Urban land use distribution for hypothetical site

Land use (%)	Estate A (Residential Estate)	Estate B (Country Estate)	CSIR,
Lawns (open space, public facilities etc.)	25	31	25
Residential area (houses)	57	54	55
Roads	18	15	20

3.2.1.6 Flood Hydrology (Rational Method) Results

The calculated pre- and post development peak discharge for the 2-, 5-, 10-, 20-, 50- and 100-year storm event, by means of the rational method, for both inland and coastal regions are summarised in Table 3.3. Detailed discussion of the peak flow results and calculations by means of the rational method are provided in Appendix D for both coastal and inland regions.

Table 3.3: Summary of pre- and post-development peak discharges

Return Period	Target Discharge* (m^3/s)					
	Coastal Region					
	400 mm MAP		700 mm MAP		1000 mm MAP	
	Pre	Post	Pre	Post	Pre	Post
2	0.049	0.269	0.11	0.427	0.2	0.585
5	0.074	0.366	0.165	0.581	0.299	0.796
10	0.102	0.463	0.228	0.736	0.413	1.008
20	0.141	0.572	0.314	0.908	0.57	1.244
50	0.226	0.744	0.506	1.181	0.918	1.617
100	0.336	0.915	0.75	1.453	1.361	1.991
Return Period	**Inland Region**					
	400 mm MAP		700 mm MAP		1000 mm MAP	
	Pre	Post	Pre	Post	Pre	Post
2	0.083	0.461	0.186	0.732	0.337	1.003
5	0.125	0.628	0.279	0.997	0.505	1.366
10	0.172	0.795	0.385	1.261	0.697	1.728
20	0.237	0.981	0.53	1.557	0.961	2.134
50	0.382	1.275	0.854	2.025	1.547	2.774
100	0.566	1.569	1.266	2.492	2.294	3.414

*Note: Target discharges include 15% increase due to climate change

The pre- and post- triangular hydrographs that resulted from the rational method for the coastal region, 400 mm MAP category, are illustrated in Figure D.2 in Appendix D. These hydrographs were used to estimate the preliminary storage volume of the pond, as described in Section 4.2. The 2-, 5-, 10-, 20-, 50- and 100-year hydrographs were also used to route through the storage facility, as discussed in Appendix E. The calculations of the peak flows (rational method) are enclosed in Appendix D for both coastal and inland regions, 400 mm MAP category. Detailed calculations of the pre- and post-development flood peaks for the 700 mm and 1000 mm MAP category scenarios, are included on the CD-ROM.

3.3 Sensitivity Analysis of Input Parameters

A sensitivity analysis was conducted to test the effect of one input parameter on the peak discharge, while keeping the other input parameters constant. The parameters that were evaluated in the sensitivity analysis were the urban run-off coefficient, the mean annual precipitation, and the average slope of the catchment.

3.3.1 Urban Run-Off Coefficient (C_2)

The influence of the minimum (C_2=0.338) and maximum (C_2=0.518) urban run-off coefficient on the peak flow of the post-development scenario was evaluated by comparing the resultant peak flow with the post-development peak flow scenario, obtained when using an average

urban run-off coefficient of C_2=0.423. These urban run-off coefficients were computed by using the minimum, maximum and average urban run-off factors, respectively, obtained from Table D.1 in Appendix D. Each urban run-off factor was then multiplied by the corresponding percentage of urban land used, as discussed in Table 3.2 of Section 3.2.1.5 to compute the urban run-off coefficient for that specific use of urban land. The urban run-off coefficient was then taken as the sum of the above mentioned urban run-off coefficients computed for each urban land use, by using the minimum, maximum and average urban run-off factors, respectively.

The average urban run-off coefficient (C_2=0.423) was increased with 22.45%, resulting in the maximum urban run-off coefficient (C_2=0.518). The average urban run-off coefficient (C_2=0.423) was decreased with 20.09%, resulting in the minimum urban run-off coefficient (C_2= 0.338). Tests were conducted to determine the sensitivity of the flood peaks to changes in the urban run-off coefficient, and may be seen in Appendix C, Table C.1 and Table C.2. The maximum difference in the flood peaks due to the 22.45% increase and 20.09% decrease, respectively, in the urban run-off coefficient are summarised in Table 3.4, for both coastal and inland regions. Another point to highlight is that the urban run-off factor has a moderately large impact (24.39%) on the peak flows. Therefore, it is necessary to design for the maximum urban run-off coefficient instead of the average urban run-off coefficient.

Table 3.4: Maximum difference in flood peaks due to change in C_2

Region	MAP (mm)	Recurrence interval (years)	Flood peak (m^3/s) (% change)	
			Ave. Post-development C_2 =0.423	22.45% increase in C_2
Coastal	700	5	0.41	0.51
				(24.39)
Inland	400	10	0.56	0.69
				(23.21)
Region	**MAP (mm)**	**Recurrence interval (years)**	**Flood peak (m^3/s) (% change)**	
			Ave. Post-development C_2 =0.423	**20.09% decrease in C_2**
Coastal	400	20	0.41	0.32
				(-21.95)
Inland	400	2	0.33	0.26
				(-21.21)

3.3.2 Rural Run-Off Coefficient (C_1)

The rural run-off coefficient is affected by the mean annual precipitation (MAP) and there are recommended values of C_1 for the different classes of MAP, as discussed in Table D.1,

enclosed in Appendix D. A MAP of 400 mm was increased by 75% and 150% to the subsequent MAP classes of 700 mm and 1000 mm, respectively. The sensitivity of the mean annual precipitation on the flood peak was tested for the pre-developed scenario. The change in the flood peaks are provided in Table 3.5 and Table 3.6 for the coastal and inland regions respectively.

Table 3.5: Test for sensitivity of MAP, pre-development scenario, coastal region

Recurrence interval (years)	MAP (400 mm)	Flood peak (m^3/s) (% change)	
		75% increase in MAP (700 mm)	150% increase in MAP (1000 mm)
2	0.04	0.10	0.17
		(150.00)	(325.00)
5	0.06	0.14	0.26
		(133.33)	(333.33)
10	0.09	0.20	0.36
		(122.22)	(300.00)
20	0.12	0.27	0.50
		(125.00)	(316.67)
50	0.2	0.44	0.80
		(120.00)	(300.00)
100	0.29	0.65	1.18
		(124.14)	(306.90)

Table 3.6: Test for sensitivity of MAP, pre-development scenario, inland region

Recurrence interval (years)	MAP (400 mm)	Flood peak (m^3/s) (% change)	
		75% increase in MAP (700 mm)	150% increase in MAP (1000 mm)
2	0.07	0.16	0.29
		(128.57)	(314.29)
5	0.11	0.24	0.44
		(118.18)	(300.00)
10	0.15	0.33	0.61
		(120.00)	(306.67)
20	0.21	0.46	0.84
		(119.05)	(300.00)
50	0.33	0.74	1.35
		(124.24)	(309.09)
100	0.49	1.10	2.00
		(124.49)	(308.16)

From Table 3.5 and Table 3.6 it can be concluded that the flood peak of the pre-development scenario is relatively sensitive to a change in the rural run-off coefficient, which is dependent

on the MAP. The peak flood increases with the increase of the MAP for both coastal and inland regions. The 150% increase in the pre-development MAP parameter (from 400 mm to 1000 mm), results in significant changes to the peak flow rates parameter. For the 5-year recurrence interval event of the coastal region, the peak flow rate increased by 333.33%. It is therefore necessary to design for all three MAP categories as discussed in Section 3.2.1.

3.3.3 Average catchment slope

A sensitivity study was also undertaken to test the effect of different average catchment slopes on the pre- and post-development peak flows. The average slope of the catchment changes the time of concentration, but for the assumed catchment area the time of concentration remained less than 15 min, even though the slope was varied between 0.5%, 1% and 2%. Since the literature recommends a minimum time of concentration of 15 min for the pre-development scenario, the influence of the catchment slope was regarded as insignificant for the pre-development scenario.

For the post-development scenario, the literature recommends a minimum time of concentration of 10min. Although slopes of 1% and 2% result in a time of concentration less than 10min, a slope of 0.5% results in a time of concentration longer than 10 min. Therefore, the change in the peak flows for the post-development scenario needed to be evaluated.

Following from Table C.3 and Table C.4 in Appendix C, it was noted that a 50% decrease in the average catchment slope results in a maximum change in the peak flow of 9.8% and 9.4% for the coastal and inland post-development scenario respectively. The post-development flood peak is not considered sensitive to a change in the catchment slope, when compared to the MAP and C_2. The average slope of 1% was assumed, as discussed in Section 3.2.1.

3.3.4 Summary of Sensitivity Analyses

In conclusion, the peak flow was the most sensitive to the mean annual precipitation, which influenced the rural run-off coefficient value, and to the rainfall intensity. This had been the prediction prior to the analysis, since the peak flow is directly dependent on the run-off coefficient and rainfall intensity. Therefore, the proposal to generate the synthetic design hydrographs for coastal and inland regions with 400 mm, 700 mm, and 1000 mm MAP, respectively, was substantiated. This would provide valuable insight with respect to the design of multi-stage outlet structures for peak discharges of different magnitude. Lastly, the maximum urban run-off coefficient has a moderately large impact (24.39%) on the peak flows. Therefore, it is required to design for the maximum urban run-off coefficient and not the average or minimum urban run-off coefficient.

4. Preliminary Design Calculations

4.1 Introduction

The final design of multi-stage outlet structures, which are to function in a storage facility, requires an inflow (post-development) hydrograph and outflow (pre-development) hydrograph as determined in Section 3.4. The other two inputs are the stage-storage curve and a stage-discharge curve. However, a preliminary estimate of the required storage volume and the shape of the storage facility are required for the development of these curves. This entails trial calculations in order to determine whether the estimated storage volume has the capacity to provide the desired outflow (pre-development) hydrograph. For multiple design storms, the attenuation facility must be capable of providing adequate storage for the design storm that required the greatest storage volume.

Using the estimated volume and knowing the stage-storage curve of the basin, the maximum value of the stage corresponding to the storage requirement could then be determined. The maximum value of the stage, and the maximum allowable release rate for each recurrence interval storm, were used to design the geometry of the multi-stage outlet structure.

4.2 Storage Volume Estimation

Estimates of the storage volume and required shape of the storage facility were needed in order to achieve the allowable outflow hydrograph for each recurrence interval storm. The Rational Formula Hydrograph method uses the difference between the triangular shaped hydrographs to estimate the required storage volume (V_s), as shown in Figure 4.1. From the area above the outflow hydrograph, and inside the inflow hydrograph, the storage volume may be estimated as defined by Equation 4.1 (Debo and Reese, 2003:653).

$$V_s = 0.5\,(Q_i - Q_o)t_i \qquad (4.1)$$

where:

V_s = storage volume estimate (m^3)

t_i = duration of storage facility inflow (s)

t_{ci} = time to peak of the inflow hydrograph (s)

t_{co} = time to peak of the outflow hydrograph (s)

Q_i = peak inflow rate into the basin, namely post-development peak discharge (m^3/s)

Q_o = peak outflow rate out of pond, namely pre-development peak discharge (m^3/s).

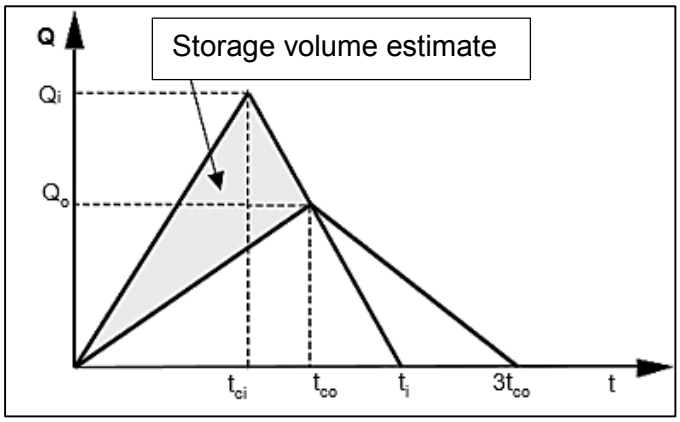

Figure 4.1: Estimation of preliminary storage volume (adapted from McCuen et al., 2002:308)

4.3 Stage-Storage Relationship

After the storage volume has been approximated, the geometric shape of the storage basin must be determined in order to establish a stage-storage curve. The stage-storage relationship refers to the relationship between the depth of water in the storage facility and the storage volume. Rectangular, trapezoidal, or circular conic geometric shapes could be used for computing the storage volume at specific depths in a detention facility.

A trapezoidal basin shape was chosen for the estimation of the storage volume, since the case study area is not site-specific. An example of the storage estimation is enclosed in Appendix E. Therefore, the double-end area or frustum of a pyramid formulas, which estimate the storage volume for a natural basin in irregular terrain, could not be used. An additional ten to fifteen percent storage is required when multiple levels of detention are provided (Stormwater Design Example, n.d.). Therefore, for preliminary sizing purposes, 10% to 15% storage should be added to the required volume.

4.4 Sizing Calculations of the Multi-Stage Outlet Structure

Based on the literature review study, an Excel spreadsheet-based model was compiled that could be used to determine the configuration and hydraulic performance of multi-stage outlets. The Excel spreadsheet-based model is also referred to as the theoretical model in this report. The target discharges are already known (pre-developed hydrographs), as determined in Chapter 3, and the corresponding maximum heads can be read off the stage-storage curve. Thus, the principal unknowns are the dimensions of the various components of the multi-stage outlet works. The unknowns include the orifice area, crest length of the weir, pipe size, and invert levels. The stage-discharge curves, resulting from using the Excel spreadsheet-based model, is based on the standard theoretical equations as discussed in Section 2.3.2. The Excel spreadsheet set-up is described with the aid of Figure 4.2, which illustrates the modelling methodology as a hierarchical process. The mathematical procedure of the spreadsheet is enclosed in Appendix E.

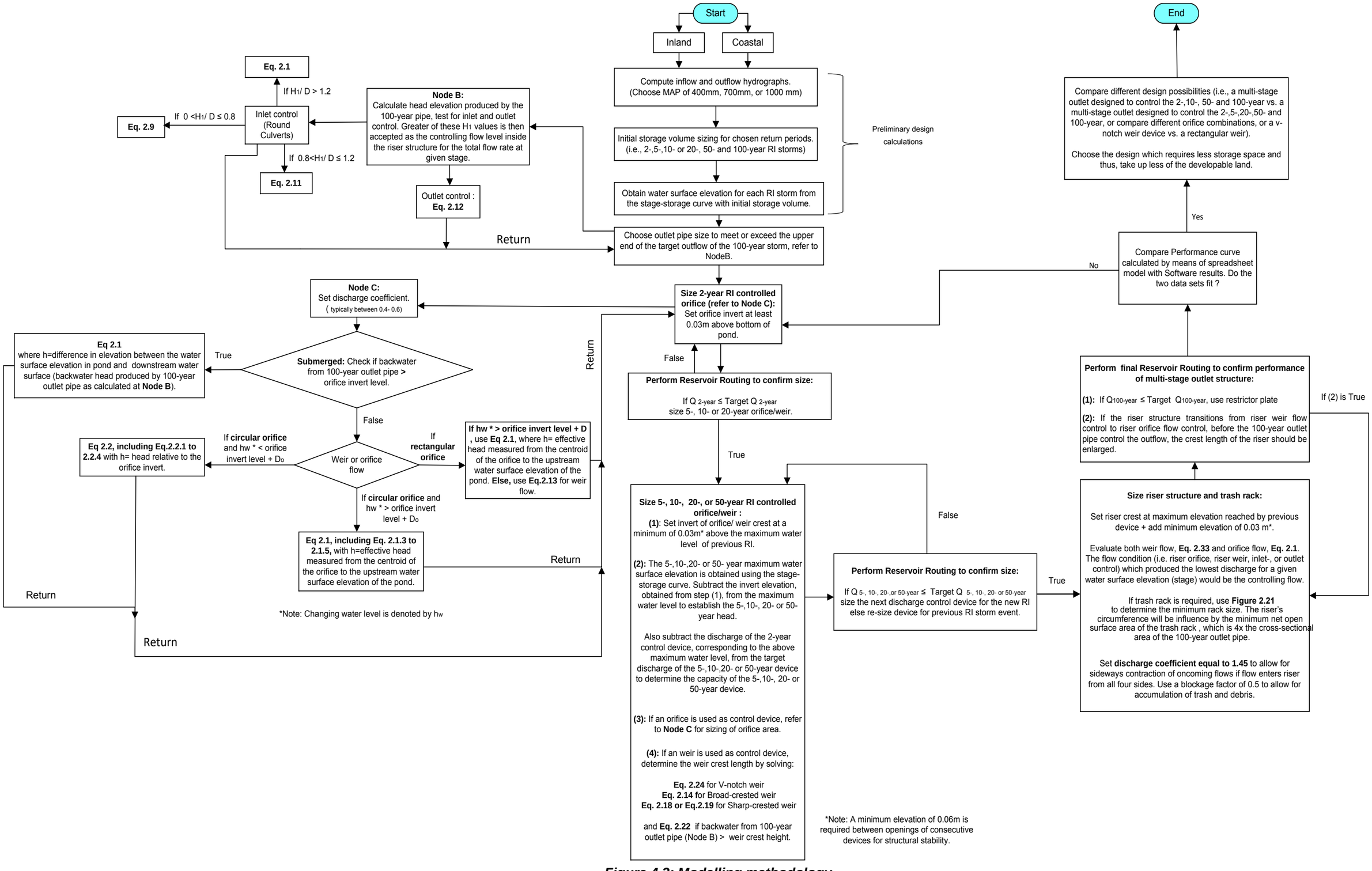

Figure 4.2: Modelling methodology

The spreadsheet (refer to Appendix E) was then used to size the control devices of twenty-two different multi-stage outlet configurations for both coastal and inland regions, where after routing calculations were carried out to verify the hydraulic performance of each outlet. The dimensions and stages of the control components which comprise the multi-stage outlet structures, were then verified by a hydrology software package called Hydrology Studio (Hydrology Studio, 2015), which is used to model urban and rural watersheds. The software modelling was conducted in order to establish confidence in the preliminary design calculations and to see whether there was sufficient correlation between the two sets of results. The different design possibilities for each MAP category and region are described with the aid of Figure 4.3. Figure 4.3 also elaborates the preliminary design section of the flow diagram illustrated in Figure 4.2.

The configurations that best met the design criteria, namely attenuation of the 2-, 5-, 10-, 20-, 50- and 100-year storm events, for each region (coastal or inland) and mean annual precipitation class (400 mm, 700 mm, and 1000 mm MAP), were then selected to be scaled, constructed, and tested in the hydraulic laboratory at Stellenbosch University. The physical model study was required to validate the hydraulic performance of these structures and to recommend some improvements related to the multi-stage outlet design that would better fulfil the objectives of the design of stormwater detention ponds.

From Figure 4.3 it is clear that the multi-stage outlet was sized to meet at least four of the six peak pre-development flow rates (2-, 10-, 50- and 100-year storm events, or 2-, 20-, 50- and 100-year storm events). This was done to evaluate whether it would be necessary to design multi-stage outlet structures consisting of six control devices or if only four devices would be sufficient to control all six recurrence interval storms.

Thus, it was necessary to verify whether a multi-stage outlet, which had been designed based on the 10-year design storm event, would exceed the 20-year requirement, or whether designing for the 20-year storm event would provide sufficient constriction to reduce the 5- and 10-year storms to the pre-development conditions (Lafleur and McBean, 1981). If the capacity of the outlet device more than meets the flow criteria, the discharge rate corresponding to this storm event would be less than the allowable peak pre-development rate, and would still be a viable option.

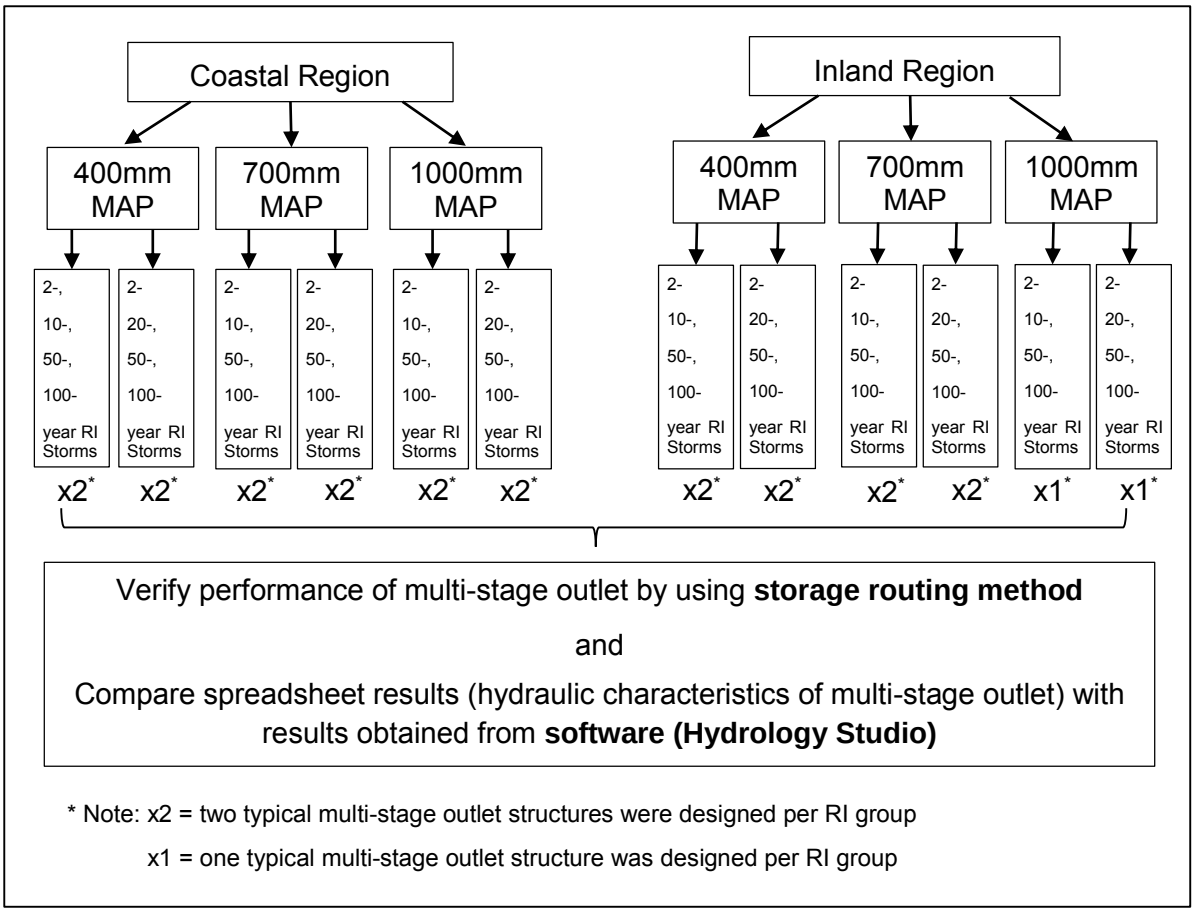

Figure 4.3: Design criteria of the multi-stage outlets

4.4.1 Layout and Dimensions of Prototype Multi-Stage Outlet Structures

The different configurations of each of the twenty-two prototype multi-stage outlet designs that were sized to attenuate either the 2-,10-,50- and 100-year RI storm events or the 2-, 20-, 50- and 100-year RI storm events for both coastal and inland regions, are summarised in Table F.1 to Table F.6 (see Appendix F).

The size, elevation and shape of the control devices (i.e. rectangular, circular, or triangular weirs and orifices) differ among the designs given in Appendix F, Tables F.1 to F.6. The size of the control devices was changed to control different RI storm events, as set out in the line diagram in Figure 4.3, whereas the shape of the typical control devices were changed to compare the stage-discharge relationship of the multi-stage outlets.

4.5 Design Results

4.5.1 Background

The computed outflow from each of the multi-stage outlet configurations presented in Table F.1 to Table F.6, obtained by routing the post-development inflow hydrograph through the pond, were compared to the respective target discharge. The maximum allowable pre-development flow, as determined in Section 3.2.1.6, is the target discharge at which the multi-stage outlet should release the flow. The target discharge was compared to the computed outflow in Table 4.1 to Table 4.3, and Table 4.4 to Table 4.6, for coastal and inland regions, with 400 mm, 700 mm, and 1000 mm MAP respectively.

The multi-stage outlet was ineffective in controlling a specific design storm event when the peak outflow exceeded the target discharge, as indicated in red in Table 4.1 to Table 4.6. The latter occurs when the outlet is designed to discharge at a high rate of release under a very low head (for instance that of the 5-year storm). The same discharge control device, when subjected to a significantly higher head (for instance that of the 20-year storm), would then discharge at a much higher rate. The outflow would then be in excess of the total design flow.

Corrections were made to designs that exceeded the target discharge, by re-designing a smaller opening or weir. However, the corrections increased the maximum head level, which would require a larger storage volume, increase the cost to the developer, and reduce the area of developable land. By keeping the surface area of the ponds constant for all multi-stage outlet designs per MAP category, the storage volume is directly related to the water elevation (stage) reached after routing the post-development hydrograph through the pond. Thus, if a design exceeded the target discharge, and after re-sizing the device to meet the target discharge, exceeded the maximum elevation reached by one of the alternative designs, the design process was stopped, which indicated that one of the other designs would be more effective.

The absolute difference was calculated in Table 4.1 to Table 4.6, by subtracting the target discharge value from the theoretical spreadsheet-based peak outflow rate. The percent difference between the target discharge and theoretical outflow was determined by dividing the absolute difference by the target discharge value and multiplying by 100. The percentage differences between the target discharge and the peak outflow obtained from the software were also calculated. These percentage differences were then used to decide which of the multi-stage outlet designs were more capable of meeting the target discharges.

4.5.2 Computed Outflow of Multi-Stage Outlets in Coastal Regions

This section compares the maximum computed outflows of each of the twelve multi-stage outlet configurations, sized for coastal regions with a MAP of 400 mm, 700 mm, and 1000 mm, respectively, with the target discharges of various RI storm events. Refer to Table F.1, Table F.3, and Table F.5 in Appendix F for the geometry of each of the multi-stage outlet structures, which were evaluated in this section in terms of their hydraulic performance.

Design C.3 (refer to Table 4.1), which consists of a circular orifice to control the 2-year RI storm, a rectangular orifice to control the 20-year RI storm, and a contracted rectangular weir to control the 50-year RI storm, exceeded the target discharge of the 100-year RI storm by 3.57%. This is due to the 20-year device (rectangular orifice), which has a larger outflow capacity at the corresponding 100-year head, than design C.1 and design C.2, which are designed with a rectangular orifice that controls the 10-year recurrence storm. In addition, the 50-year rectangular weir of design C.3 has a larger discharge capacity than the V-notch weir used in the configuration of designs C.2 and C.4 at the corresponding 100-year head.

Design C.2 (see Table 4.1), which consists of a 2-year RI control circular orifice, a 10-year RI control rectangular orifice, and a V-notch weir to control the 50-year RI storm, restricted the outflow to the pre-development peaks for all the recurrence intervals. Although design C.1 and design C.4 also met the pre-development outflow peaks for all the design storms, design C.2 required less storage volume than designs C.1 and C.4, when comparing the volume of the pond, as computed with Hydrology Studio. Thus, design C.2 was, therefore, chosen to restrict the outflow from the multi-stage outlet, which design was based on the 400 mm MAP class.

Design C.5 (refer to Table 4.2), which consists of a rectangular orifice at the base to control the 2-year RI, a 10-year RI control rectangular orifice, and a contracted rectangular weir to control the 50-year RI storm, restricted the outflow to the pre-development peaks for all the recurrence intervals. Design C.6 (820 m^3) and design C.7 (780 m^3) also met the target discharge of all the design storms, but required a larger storage volume than Design C.5 (772 m^3).

The peak outflow values ranged from -21.15% to 0.44% different from the target discharge for the different recurrence intervals, and multi-stage outlet designs, as indicated in Table 4.2. The reason for the large deviation from the target discharge (-21.15%) for design C.6 is that the discharge capacity of the V-notch weir is much smaller than that of the rectangular weir of Design C.5 when operating under the same head. The multi-stage outlet is forced to operate under low heads, thus, using a rectangular weir instead of a V-notch weir is recommended in order to limit the depth of water in the pond along with the storage volume.

Design C.8, designed with a rectangular orifice at an elevation which controls the 20-year RI storm, was ineffective in restricting the outflow to the pre-development peak flow (target

discharge) for the 10-year RI storm and required a storage volume (809 m^3) that is larger than designs C.5 and C.6. Thus, based on the results summarised in Table 4.2, it is evident that out of the four designs (C.5 to C.8), design C.5 is best design, for the 700 mm MAP class, to restrict the outflow from the pond, since design C.8 exceeded the 10-year RI storm, and designs C.6 and C7 required a larger pond volume.

Designs C.9 to C.12 (refer to Table 4.3) restricted the outflow to the pre-development peaks for all the recurrence intervals. Designs C.10 and C.12 consisted of a rectangular orifice at the base to control the 2-year RI, two rectangular orifices to control the 10-year RI storm, and two contracted rectangular weirs to control the 50-year RI storm. Design C.9 and C.11 have similar configurations to designs C.10 and C.12, with the exception of the 50-RI storm being controlled by one contracted rectangular weir and not two, as for designs C.10 and C.12. From Table 4.3, it was clear that design C.10 was the most promising multi-stage outlet, which was designed for the 1000 mm MAP class, since it restricted the outflow for all RI storms and required the least amount of storage volume.

Table 4.1: Summary of peak outflow results – Coastal Region, 400 mm MAP

Coastal Region, 400 mm MAP Category													
Design I.D	**Design criteria**	**RI**	**Peak outflow after routing calculations (m^3/s)**	**Maximum elevation (m)**	**Volume of pond (m^3)**	**Exceeding peak (0=No, 1=Yes)**	**Percentage difference between Target and Actual outflow (%)**	**Target outflow (m^3/s)**	**Percentage difference between Target and Hydrology Studio's outflow (%)**	**Hydrology Studio's peak outflow (m^3/s)**	**Hydrology Studio's maximum elevation (m)**	**Hydrology Studio's pond volume (m^3)**	**Percentage difference between spreadsheet results and Hydrology Studio's solution (%)**
C.1	2-,10-,50- and 100-year	2	0.042	0.62		0	-14.29	0.049	-8.16	0.045	0.612	193	-6.67
C.3	2-,20-,50- and 100-year		0.042	0.62		0	-14.29		-8.16	0.045	0.612	193	-6.67
C.1	2-,10-,50- and 100-year	5	0.065	0.79		0	-12.16	0.074	-9.46	0.067	0.778	265	-2.99
C.3	2-,20-,50- and 100-year		0.062	0.79		0	-16.22		-13.51	0.064	0.78	266	-3.13
C.1	2-,10-,50- and 100-year	10	0.091	0.9		0	-10.78	0.102	-6.86	0.095	0.91	329	-4.21
C.3	2-,20-,50- and 100-year		0.100	0.91		0	-1.96		3.92	0.106	0.904	326	-5.66
C.1	2-,10-,50- and 100-year	20	0.111	1.05		0	-21.28	0.141	-20.57	0.112	1.052	406	-0.89
C.3	2-,20-,50- and 100-year		0.126	1.03		0	-10.64		-9.93	0.127	1.039	398	-0.79
C.1	2-,10-,50- and 100-year	50	0.191	1.22		0	-15.49	0.226	-12.39	0.198	1.226	509	-3.54
C.3	2-,20-,50- and 100-year		0.214	1.2		0	-5.31		-3.98	0.217	1.206	497	-1.38
C.1	2-,10-,50- and 100-year	100	0.334	1.33	584	0	-0.60	0.336	2.38	0.344	1.332	579	-2.91
C.3	2-,20-,50- and 100-year		0.348	1.33	572	1	3.57		2.98	0.346	1.311	564	0.58
C.2	2-,10-,50- and 100-year	2	0.042	0.62		0	-14.29	0.049	-8.16	0.045	0.612	193	-6.67
C.4	2-,20-,50- and 100-year		0.042	0.61		0	-14.29		-8.16	0.045	0.612	193	-6.67
C.2	2-,10-,50- and 100-year	5	0.065	0.79		0	-12.16	0.074	-9.46	0.067	0.778	265	-2.99
C.4	2-,20-,50- and 100-year		0.062	0.79		0	-16.22		-13.51	0.064	0.781	267	-3.13
C.2	2-,10-,50- and 100-year	10	0.091	0.9		0	-10.78	0.102	-6.86	0.095	0.91	329	-4.21
C.4	2-,20-,50- and 100-year		0.101	0.9		0	-0.98		3.92	0.106	0.904	326	-4.72
C.2	2-,10-,50- and 100-year	20	0.116	1.05		0	-17.73	0.141	-14.18	0.121	1.049	404	-4.13
C.4	2-,20-,50- and 100-year		0.134	1.03		0	-4.96		-4.26	0.135	1.033	395	-0.74
C.2	2-,10-,50- and 100-year	50	0.185	1.22		0	-18.14	0.226	-3.54*	0.218	1.209	498	-15.14
C.4	2-,20-,50- and 100-year		0.178	1.21		0	-21.24		-15.49*	0.191	1.216	503	-6.81
C.2	2-,10-,50- and 100-year	100	0.332	1.33	584	0	-1.79	0.336	4.76*	0.352	1.313	566	-6.25
C.4	2-,20-,50- and 100-year		0.326	1.33	584	0	-2.98		1.79*	0.342	1.327	575	-4.68

Notes: Design I.D = Refer to Table F.1 (enclosed in Appendix F)

C = Coastal

* = Hydrology Studio used a different discharge coefficient to determine the discharge from the V-notch weir than the spreadsheet based model.

Table 4.2: Summary of peak outflow results – Coastal Region, 700 mm MAP

Coastal Region, 700 mm MAP Category													
Design I.D	**Design criteria**	**RI**	**Peak outflow after routing calculations (m^3/s)**	**Maximum elevation (m)**	**Volume of pond (m^3)**	**Exceeding peak (0=No, 1=Yes)**	**Percentage difference between Target and Actual outflow (%)**	**Target outflow (m^3/s)**	**Percentage difference between Target outflow and Hydrology Studio's outflow (%)**	**Hydrology Studio's peak outflow (m^3/s)**	**Hydrology Studio's maximum elevation (m)**	**Hydrology Studio's pond volume (m^3)**	**Percentage difference between spreadsheet results and Hydrology Studio's solution (%)**
C.5	2-,10-,50- and 100-year	2	0.096	0.64		0	-12.73	0.11	-6.36	0.103	0.628	277	-6.80
C.7	2-,20-,50- and 100-year		0.096	0.65		0	-12.73		-6.36	0.103	0.63	277	-6.80
C.5	2-,10-,50- and 100-year	5	0.147	0.81		0	-10.91	0.165	-6.67	0.154	0.803	379	-4.55
C.7	2-,20-,50- and 100-year		0.149	0.85		0	-9.70		-6.06	0.155	0.802	378	-3.87
C.5	2-,10-,50- and 100-year	10	0.228	0.94		0	0.00	0.228	-2.19	0.223	0.935	464	2.24
C.7	2-,20-,50- and 100-year		0.228	0.98		0	0.00		2.63	0.234	1.058	461	-2.56
C.5	2-,10-,50- and 100-year	20	0.310	1.07		0	-1.27	0.314	-3.18	0.304	1.068	558	1.97
C.7	2-,20-,50- and 100-year		0.310	1.06		0	-1.27		-2.23	0.307	1.06	550	0.98
C.5	2-,10-,50- and 100-year	50	0.494	1.22		0	-2.37	0.506	-5.53	0.478	2.22	674	3.35
C.7	2-,20-,50- and 100-year		0.472	1.23		0	-6.72		-9.09	0.46	2.227	680	2.61
C.5	2-,10-,50- and 100-year	100	0.694	1.34	773	0	-7.47	0.75	-10.00	0.675	1.342	775	2.81
C.7	2-,20-,50- and 100-year		0.701	1.34	780	0	-6.53		-10.27	0.673	1.34	781	4.16
C.6	2-,10-,50- and 100-year	2	0.096	0.64		0	-12.73	0.11	-6.36	0.103	0.62	277	-6.80
C.8	2-,20-,50- and 100-year		0.096	0.65		0	-12.73		-6.36	0.103	0.63	277	-6.80
C.6	2-,10-,50- and 100-year	5	0.151	0.81		0	-8.48	0.165	-4.85	0.157	0.8	377	-3.82
C.8	2-,20-,50- and 100-year		0.150	0.82		0	-9.09		-5.45	0.156	0.801	378	-3.85
C.6	2-,10-,50- and 100-year	10	0.224	0.94		0	-1.75	0.228	-1.75	0.224	0.93	462	0.00
C.8	2-,20-,50- and 100-year		0.229	0.93		1	0.44		3.07	0.235	0.928	460	-2.55
C.6	2-,10-,50- and 100-year	20	0.274	1.08		0	-12.74	0.314	-12.10	0.276	1.077	564	-0.72
C.8	2-,20-,50- and 100-year		0.314	1.06		0	0.00		-1.27	0.31	1.056	549	1.29
C.6	2-,10-,50- and 100-year	50	0.399	1.27		0	-21.15	0.506	-16.21*	0.424	1.256	703	-5.9
C.8	2-,20-,50- and 100-year		0.414	1.25		0	-18.18		-17.39*	0.418	1.245	694	0.96
C.6	2-,10-,50- and 100-year	100	0.645	1.39	820	0	-14.00	0.75	-13.47*	0.649	1.379	807	0.62
C.8	2-,20-,50- and 100-year		0.627	1.37	809	0	-16.4		-14.27*	0.643	1.375	803	-2.49

Notes: Design I.D = Refer to Table F.3 (enclosed in Appendix F)

C = Coastal

* = Hydrology Studio used a different discharge coefficient to determine the discharge from the V-notch weir than the spreadsheet based model.

Table 4.3: Summary of peak outflow results – Coastal Region, 1000 mm MAP

Coastal Region, 1000 mm MAP Category													
Design I.D	**Design criteria**	**RI**	**Peak outflow after routing calculations (m^3/s)**	**Maximum elevation (m)**	**Volume of pond (m^3)**	**Exceeding peak (0=No, 1=Yes)**	**Percentage difference between Target and Actual outflow (%)**	**Target outflow (m^3/s)**	**Percentage difference between Target outflow and Hydrology Studio's outflow (%)**	**Hydrology Studio Peak outflow (m^3/s)**	**Hydrology Studio's maximum elevation (m)**	**Hydrology Studio's pond volume (m^3)**	**Percentage difference between Spreadsheet results and Hydrology Studio's solution (%)**
C.9	2-,10-,50- and 100-year	2	0.195	0.66		0	-2.50	0.2	-2.00	0.196	0.659	329	-0.51
C.11	2-,20-,50- and 100-year		0.195	0.66		0	-2.50		-2.00	0.196	0.659	329	-0.51
C.9	2-,10-,50- and 100-year	5	0.299	0.84		0	0.00	0.299	-0.67	0.297	0.836	445	0.67
C.11	2-,20-,50- and 100-year		0.264	0.85		0	-11.71		-10.03	0.269	0.856	459	-1.86
C.9	2-,10-,50- and 100-year	10	0.411	0.96		0	-0.48	0.413	-3.15	0.4	0.975	547	2.75
C.11	2-,20-,50- and 100-year		0.405	0.98		0	-1.94		0.24	0.414	0.986	554	-2.17
C.9	2-,10-,50- and 100-year	20	0.570	1.09		0	0.00	0.57	-4.21	0.546	1.107	651	4.40
C.11	2-,20-,50- and 100-year		0.567	1.1		0	-0.53		-6.14	0.535	1.113	655	5.98
C.9	2-,10-,50- and 100-year	50	0.869	1.23		0	-5.34	0.918	-19.83	0.736	1.294	811	18.07
C.11	2-,20-,50- and 100-year		0.848	1.25		0	-7.63		-22.11	0.715	1.305	821	18.60
C.9	2-,10-,50- and 100-year	100	1.162	1.37	880	0	-14.62	1.361	-8.96	1.239	1.371	883	-6.21
C.11	2-,20-,50- and 100-year		1.212	1.38	891	0	-10.95		-9.77	1.228	1.385	895	-1.30
C.10	2-,10-,50- and 100-year	2	0.195	0.66		0	-2.50	0.2	-2.00	0.196	0.659	329	-0.51
C.12	2-,20-,50- and 100-year		0.195	0.66		0	-2.50		-2.00	0.196	0.659	329	-0.51
C.10	2-,10-,50- and 100-year	5	0.296	0.84		0	-1.00	0.299	-9.03	0.272	0.849	455	8.82
C.12	2-,20-,50- and 100-year		0.267	0.85		0	-10.70		-9.70	0.27	0.854	458	-1.11
C.10	2-,10-,50- and 100-year	10	0.410	0.97		0	-0.73	0.413	-4.12	0.396	0.978	549	3.54
C.12	2-,20-,50- and 100-year		0.404	0.98		0	-2.18		-0.48	0.411	0.985	554	-1.70
C.10	2-,10-,50- and 100-year	20	0.569	1.09		0	-0.18	0.57	-7.02	0.53	1.138	676	7.36
C.12	2-,20-,50- and 100-year		0.566	1.09		0	-0.70		-5.09	0.541	1.11	653	4.62
C.10	2-,10-,50- and 100-year	50	0.887	1.22		0	-3.38	0.918	-12.20	0.806	1.299	816	10.05
C.12	2-,20-,50- and 100-year		0.905	1.23		0	-1.42		-13.94	0.79	1.286	804	14.56
C.10	2-,10-,50- and 100-year	100	1.181	1.35	867	0	-13.23	1.361	-8.23	1.249	1.36	872	-5.44
C.12	2-,20-,50- and 100-year		1.263	1.36	872	0	-7.20		-8.01	1.252	1.36	872	0.88

Notes: Design I.D = Refer to Table F.5 (enclosed in Appendix F)
C = Coastal

4.5.3 Computed Outflow of Multi-Stage Outlets in Inland Regions

This section compares the maximum computed outflow of each of the ten multi-stage outlet configurations, sized for inland regions with a MAP of 400 mm, 700 mm, and 1000 mm, respectively, with the target discharge for various RI storm events. The various configurations of the multi-stage outlets are defined in Tables F.2, F.4 and F.6 (see Appendix F).

Design I.1 (refer to Table 4.4), which consist of a rectangular orifice to control the 2-year RI storm, a rectangular orifice to control the 10-year RI storm, and a contracted rectangular weir to control the 50-year RI storm, best met the design criteria. The latter is true, since the outlet's outflow was at a rate equal to, or slightly less than the pre-development peak stormwater run-off for all RI storm events and required less storage volume than designs I.2, I.3, and I.4. Designs I.3 and I.4 (refer to Table 4.4), both designed with a rectangular orifice that was sized to control the 20-year RI storm at the corresponding 20-year head, were insufficient in limiting the outflow to the maximum allowable 10-year pre-development flow for the corresponding 10-year head. Design I.2 also restricted the outflow to a discharge equal or less than the target discharge, but required a larger storage facility than design I.1. Since designs I.3 and I.4 exceeded the target discharge for the 10-year RI storm, design I.1 was chosen to restrict the outflow from the pond for inland regions with 400 mm of MAP.

Designs I.5 to I.8, as indicated in Table 4.5, were sufficient in restricting the outflow to the target outflow for all RI storm events. Design I.6 was chosen as the more efficient design, for inland regions with 700 mm of MAP, since it would use a smaller amount of the developable land as a storage facility than the other three multi-stage outlet designs. The peak outflow values ranged from -14.52% to 0.0% different from the target discharge. The 2-year control device, which was similar for all four designs, more than meets the target outflow by -14.52% as tabulated in Table 4.5. However, by over controlling the 2-year design storm, one is able to limit the 5-year flood to the maximum allowable pre-development flow without having an additional orifice to control the 5-year flood.

Designs I.9 and I.10, designed for the inland regions receiving 1000 mm of MAP, as indicated in Table 4.6, were sufficient in restricting the outflow to the target outflow for all RI storm events. However, design I.9 was chosen as the more efficient design, since it necessitates a smaller amount of the developable land for use as a storage facility. Both multi-stage outlets controls the 100-year RI storm by means of two 900 mm, nominal diameter (DN) outlet pipes, prototype dimension, as illustrated in Section 4.4.1. A single commercially available pipe with a nominal diameter of 1200 mm would have over controlled the 100-year outflow and produce a head, which submerged the 2-, 10- or 20- year, and 50-year discharge devices downstream. A larger pipe (nominal diameter of 1350 mm, 1500 mm, and 1800 mm) is usually only available on request, thus two outlet pipes with nominal diameters of 900 mm were chosen.

Table 4.4: Summary of peak outflow results – Inland Region, 400 mm MAP

Inland Region, 400 mm MAP													
Design I.D	Design criteria	RI	Peak outflow after routing (m^3/s)	Maximum elevation (m)	Exceeding peak (0=No, 1=Yes)	Pond volume (m^3)	Percentage difference between Target and Actual outflow (%)	Target outflow (m^3/s)	Percentage difference between Target outflow and Hydrology Studio's outflow (%)	Hydrology Studio's peak outflow (m^3/s)	Hydrology Studio's maximum elevation (m)	Hydrology Studio's pond volume (m^3)	Percentage difference between Spreadsheet results and Software solution (%)
I.1	2-,10-,50- and 100-year	2	0.083	0.60	0		0.00	0.083	7.23	0.089	0.594	322	-6.74
I.3	2-,20-,50- and 100-year		0.083	0.6	0		0.00		7.23	0.089	0.594	322	-6.74
I.1	2-,10-,50- and 100-year	5	0.117	0.77	0		-6.40	0.125	0.00	0.125	0.768	443	-6.40
I.3	2-,20-,50- and 100-year		0.119	0.77	0		-4.80		1.60	0.127	0.767	442	-6.30
I.1	2-,10-,50- and 100-year	10	0.171	0.91	0		-0.58	0.172	1.16	0.174	0.916	556	-1.72
I.3	2-,20-,50- and 100-year		0.179	0.91	1		4.07		4.65	0.18	0.912	553	-0.56
I.1	2-,10-,50- and 100-year	20	0.236	1.06	0		-0.42	0.237	-1.27	0.234	1.058	674	0.85
I.3	2-,20-,50- and 100-year		0.217	1.06	0		-8.44		-9.28	0.215	1.061	677	0.93
I.1	2-,10-,50- and 100-year	50	0.370	1.24	0		-3.14	0.382	-1.57	0.376	1.236	836	-1.60
I.3	2-,20-,50- and 100-year		0.354	1.26	0		-7.33		-8.64	0.349	1.255	854	1.43
I.1	2-,10-,50- and 100-year	100	0.564	1.37	0	976	-0.35	0.566	1.77	0.576	1.371	969	-2.08
I.3	2-,20-,50- and 100-year		0.562	1.38	0	988	-0.71		1.41	0.574	1.385	983	-2.09
I.2	2-,10-,50- and 100-year	2	0.083	0.60	0		0.00	0.083	7.23	0.089	0.594	322	-6.74
I.4	2-,20-,50- and 100-year		0.083	0.61	0		0.00		7.23	0.089	0.594	322	-6.74
I.2	2-,10-,50- and 100-year	5	0.117	0.77	0		-6.40	0.125	-0.80	0.124	0.769	443	-5.65
I.4	2-,20-,50- and 100-year		0.121	0.77	0		-3.20		3.20	0.129	0.765	442	-6.20
I.2	2-,10-,50- and 100-year	10	0.170	0.91	0		-1.16	0.172	0.00	0.172	0.913	554	-1.16
I.4	2-,20-,50- and 100-year		0.187	0.91	1		8.72		8.14	0.186	0.909	551	0.54
I.2	2-,10-,50- and 100-year	20	0.210	1.07	0		-11.39	0.237	-10.13	0.213	1.066	681	-1.41
I.4	2-,20-,50- and 100-year		0.227	1.05	0		-4.22		-4.22	0.227	1.044	671	0.00
I.2	2-,10-,50- and 100-year	50	0.319	1.27	0		-16.49	0.382	-6.54*	0.357	1.253	853	-10.64
I.4	2-,20-,50- and 100-year		0.299	1.26	0		-21.73		-17.54*	0.315	1.255	863	-5.08
I.2	2-,10-,50- and 100-year	100	0.552	1.40	0	1004	-2.47	0.566	1.94	0.572	1.384	980	-4.33
I.4	2-,20-,50- and 100-year		0.559	1.41	0	1007	-1.24		-0.88	0.561	1.397	996	-0.36

Notes: Design I.D = Refer to Table F.2 (see Appendix F)

I = Inland

* = Hydrology Studio used a different discharge coefficient to determine the discharge from the V-notch weir than the spreadsheet based model.

Table 4.5: Summary of peak outflow results – Inland Region, 700 mm MAP

Inland Region, 700 mm MAP													
Design I.D	**Design criteria**	**RI**	**Peak outflow after routing (m^3/s)**	**Maximum elevation (m)**	**Exceeding peak (0=No, 1=Yes)**	**Pond volume (m^3)**	**Percentage difference between Target and Actual outflow (%)**	**Target outflow (m^3/s)**	**Percentage difference between Target outflow and Hydrology Studio's outflow (%)**	**Hydrology Studio's peak outflow (m^3/s)**	**Hydrology Studio's maximum elevation (m)**	**Hydrology Studio's pond volume (m^3)**	**Percentage difference between Spreadsheet results and Software solution (%)**
I.5	2-,10-,50- and 100-year	2	0.159	0.65	0		-14.52	0.186	-9.68	0.168	0.642	489	-5.36
I.7	2-,20-,50- and 100-year		0.159	0.65	0		-14.52		-9.68	0.168	0.642	489	-5.36
I.5	2-,10-,50- and 100-year	5	0.241	0.83	0		-13.62	0.279	-10.04	0.251	0.826	665	-3.98
I.7	2-,20-,50- and 100-year		0.247	0.83	0		-11.47		-8.24	0.256	0.824	663	-3.52
I.5	2-,10-,50- and 100-year	10	0.383	0.98	0		-0.52	0.385	-4.68	0.367	0.971	816	4.36
I.7	2-,20-,50- and 100-year		0.368	0.97	0		-4.42		-1.56	0.379	0.966	810	-2.90
I.5	2-,10-,50- and 100-year	20	0.518	1.11	0		-2.26	0.53	-6.79	0.494	1.117	979	4.86
I.7	2-,20-,50- and 100-year		0.528	1.1	0		-0.38		-6.23	0.497	1.107	967	6.24
I.5	2-,10-,50- and 100-year	50	0.788	1.29	0		-7.73	0.854	-6.67	0.797	1.294	1192	-1.13
I.7	2-,20-,50- and 100-year		0.776	1.3	0		-9.13		-10.19	0.767	1.3	1200	1.17
I.5	2-,10-,50- and 100-year	100	1.226	1.41	0	1346	-3.16	1.266	-4.34	1.211	1.41	1343	1.24
I.7	2-,20-,50- and 100-year		1.219	1.42	0	1356	-3.71		-5.85	1.192	1.42	1356	2.27
I.6	2-,10-,50- and 100-year	2	0.159	0.65	0		-14.52	0.186	-9.68	0.168	0.642	489	-5.36
I.8	2-,20-,50- and 100-year		0.159	0.65	0		-14.52		-9.68	0.168	0.642	489	-5.36
I.6	2-,10-,50- and 100-year	5	0.239	0.83	0		-14.34	0.279	-10.75	0.249	0.827	666	-4.02
I.8	2-,20-,50- and 100-year		0.246	0.83	0		-11.83		-8.60	0.255	0.825	665	-3.53
I.6	2-,10-,50- and 100-year	10	0.385	0.97	0		0.00	0.385	-2.34	0.376	0.969	814	2.39
I.8	2-,20-,50- and 100-year		0.381	0.97	0		-1.04		1.04	0.389	0.963	807	-2.06
I.6	2-,10-,50- and 100-year	20	0.530	1.09	0		0.00	0.53	-3.58	0.511	1.108	969	3.72
I.8	2-,20-,50- and 100-year		0.529	1.09	0		-0.19		-5.47	0.501	1.103	963	5.59
I.6	2-,10-,50- and 100-year	50	0.831	1.28	0		-2.69	0.854	-3.28	0.826	1.278	1173	0.61
I.8	2-,20-,50- and 100-year		0.772	1.29	0		-9.60		-9.13	0.776	1.296	1195	-0.52
I.6	2-,10-,50- and 100-year	100	1.178	1.40	0	1338	-6.95	1.266	-6.24	1.187	1.406	1337	-0.76
I.8	2-,20-,50- and 100-year		1.230	1.41	0	1346	-2.84		-5.06	1.202	1.414	1348	2.33

Notes: Design I.D = Refer to Table F.4 (see Appendix F)
I = Inland.

Table 4.6: Summary of peak outflow results – Inland Region, 1000 mm MAP

Inland Region, 1000 mm MAP													
Design I.D	**Design criteria**	**RI**	**Peak outflow after routing (m^3/s)**	**Maximum elevation (m)**	**Exceeding peak (0=No, 1=Yes)**	**Pond volume (m^3)**	**Percentage difference between target and actual outflow (%)**	**Target outflow (m^3/s)**	**Percentage difference between Target outflow and Hydrology Studio's outflow (%)**	**Hydrology Studio Peak outflow (m^3/s)**	**Hydrology Studio's maximum elevation (m)**	**Hydrology Studio's pond volume (m^3)**	**Percentage difference between spreadsheet results and Software solution (%)**
I.9	2-,10-,50- and 100-year	2	0.336	0.62	0		-0.30	0.337	5.64	0.356	0.612	569	-5.62
I.10	2-,20-,50- and 100-year		0.336	0.62	0		-0.30		5.64	0.356	0.612	569	-5.62
I.9	2-,10-,50- and 100-year	5	0.505	0.80	0		0.00	0.505	1.39	0.512	0.788	769	-1.37
I.10	2-,20-,50- and 100-year		0.454	0.82	0		-10.10		-9.70	0.456	0.807	792	-0.44
I.9	2-,10-,50- and 100-year	10	0.689	0.93	0		-1.15	0.697	-2.01	0.683	0.932	945	0.88
I.10	2-,20-,50- and 100-year		0.678	0.95	0		-2.73		-0.29	0.695	0.947	964	-2.45
I.9	2-,10-,50- and 100-year	20	0.954	1.07	0		-0.73	0.961	-3.64	0.926	1.078	1136	3.02
I.10	2-,20-,50- and 100-year		0.956	1.07	0		-0.52		-5.10	0.912	1.078	1135	4.82
I.9	2-,10-,50- and 100-year	50	1.547	1.22	0		0.00	1.547	-0.71	1.536	1.218	1330	0.72
I.10	2-,20-,50- and 100-year		1.484	1.23	0		-4.07		-3.36	1.495	1.234	1352	-0.74
I.9	2-,10-,50- and 100-year	100	2.118	1.31	0	1471	-7.67	2.294	-7.76	2.116	1.313	1469	0.09
I.10	2-,20-,50- and 100-year		2.135	1.32	0	1491	-6.93		-7.54	2.121	1.324	1484	0.66

Notes*: Design I.D= Refer to Table F.6 (see Appendix F)
I = Inland

4.5.4 Findings and Discussion of Design Results

From Table 4.1 to Table 4.6, the following should be noted:

- The stage-discharge relationship of the multi-stage outlet structures, as determined by the theoretical spreadsheet-based model, were in good agreement with the software results. The two data sets had a multiple-correlations coefficient (R^2) of 0.99, which indicates that the theoretical spreadsheet-based model and the software output were in close agreement. The maximum percentage difference between the results of the theoretical spreadsheet-based model and the software results was 18.6% (indicated as an outlier on Figure 4.4), but did not influence the correlation of the two data sets.

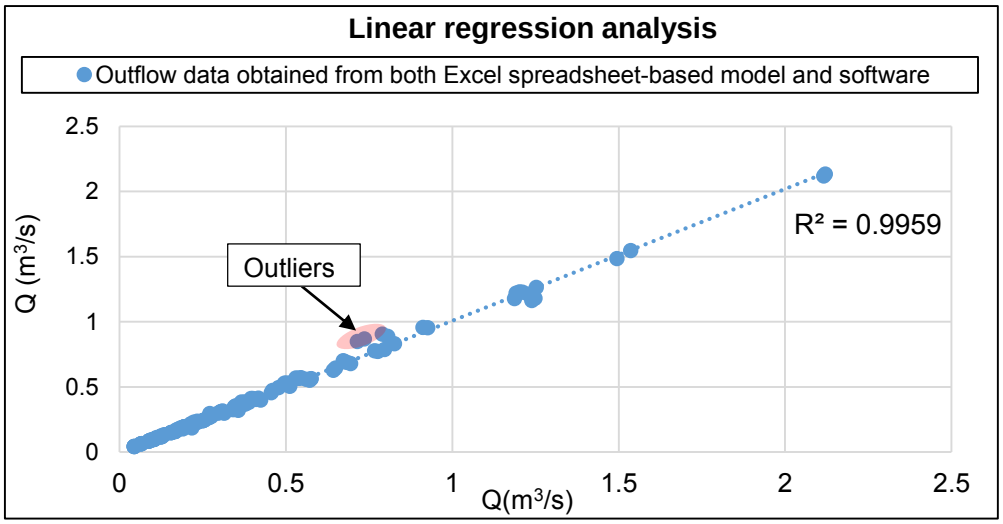

Figure 4.4: Outflow results obtained from spreadsheet-based model and software

- All the multi-stage outlets designed with a 90° V-notch weir over-controlled the target discharge for the 50-year recurrence interval storms. The crest length of a rectangular weir could easily be increased, whereas a V-notch weir requires a higher riser structure. This is significant since discharge control devices in stormwater detention ponds are frequently flowing under low heads (Spencer, 2013). The 50-year sized rectangular weirs discharged closer to the target discharge, which limits the depth of the pond, along with the storage volume.

- It was also found that three multi-stage outlets (design C.8, I.3 and I.4), that were sized with openings to control the 20-year RI storm, were ineffective in restricting the 10-year RI storm, while having a storage volume less than the alternative design. The maximum deviation of 8.72% occurred with design I.4. In order for these designs to attenuate all design storms, the storage volume would have to be increased. Thus, re-designing the 20-year RI control device would not be a feasible solution, since the alternative designs, which were designed with an opening to control the 10-year RI storm, were effective in restricting the 20-year RI to an outflow equal to or less than the pre-development peak flow.

- Eight of the eleven multi-stage outlets that were designed to control the 20-year recurrence interval storm, over-controlled the 50-year design storm more than the multi-stage outlets with a rectangular orifice, sized to control the 10-year design storm. This is because the 10-year orifice has a larger head during the 50-year recurrence interval storm than the 20-year orifice, since the 20-year orifice is designed at a higher stage. The 20-year rectangular orifice then has a smaller discharge capacity than the 10-year orifice at the corresponding 50-year head.

- Another reason for the deviation from the target outflow for the 50-year recurrence interval was in the case where the required size outlet pipe was not commercially available to control the 100-year design storm, and the 50-year contracted rectangular weir was made smaller to restrict the 100-year outflow. Another solution would be to construct a restrictor plate at the entrance to the 100-year outlet pipe (UDFCD, 2010).

- Both the 2-year, and 10- or 20-year discharge devices controlled the 5-year storm event, which resulted in the 5-year design storm being over-controlled, since there was no individual discharge device to control the 5-year storm event. Thus, for the 5-year return period, the outflow from all the multi-stage outlet designs had large percentage differences between the computed outflow and the target outflow.

- Designs C.2 (Table 4.8), C.5 (Table 4.9), and C.9 (Table 4.10) were determined as being the most effective designs for MAP classes of 400 mm, 700 mm, and 1000 mm respectively, in coastal regions. Designs I.1 (Table 4.11), I.6 (Table 4.12), and I.9 (Table 4.13) were determined to be the most effective designs for MAP classes of 400 mm, 700 mm, and 1000 mm respectively, in inland regions.

It could be concluded that multi-stage outlets that are designed to control 2-, 10-, 50- and 100-year RI storms, would also be able to control the 5-year and 20-year RI storms and require less storage volume in the detention pond. Thus, multi-stage outlet structures consisting of four discharge devices would be sufficient to control storms at all six recurrence intervals. Also, when designing for the 2-, 20-, 50- and 100-year RI storms, the multi-stage outlet would not restrict the outflow for a 10-year RI storm sufficiently.

5. Physical Model Study

5.1 Physical Model Layout

The six multi-stage outlet structures discussed in Section 4.5, that best met the design criteria, namely the attenuation of the 2-, 5-, 10-, 20-, 50- and 100- year storm events, for each region (coastal and inland) and MAP class (400 mm, 700 mm, and 1000 mm), were selected to be scaled, constructed, and tested in the hydraulic laboratory of Stellenbosch University. The physical models were built on a 1:3 scale, according to Froude similitude, to avoid significant scale effects (see Section 5.6). The physical model study was required in order to conduct performance tests of the multi-stage outlet's ability to control the outflow to no more than the pre-development peak flows.

The six different model configurations were termed 'Model 1' to 'Model 6' for the purposes of this thesis, as defined in Table 5.1. The experimental models applied in this study were, however, not of an existing multi-stage outlet, but based on hypothetical conditions and components of prototype multi-stage outlets which are typically used in South Africa. Since the multi-stage outlet structure consists of several discharge devices, each device was designed according to the relevant theoretical guidelines as discussed in Section 2.3.2.

Table 5.1: Summary of model identification

Name	I.D	Region	MAP Class
Model 1	C.2	Coastal	400 mm
Model 2	I.1	Inland	400 mm
Model 3	I.6	Inland	700 mm
Model 4	C.5	Coastal	700 mm
Model 5	C.9	Coastal	1000 mm
Model 6	I.9	Inland	1000 mm

Detailed as-built drawings of the six multi-stage outlets models that best met the pre-development peak flows (refer to Section 4.5), are provided in Table G.1 to Table G.3 in Appendix G. The models consisted of low flow orifice(s) to control a 2-year RI storm, rectangular orifice(s) to control a 10-year RI storm, rectangular weir(s) with end-contractions to control a 50-year RI storm, and outlet pipe(s) to control a 100-year RI storm. Trash racks were designed according to Section 2.4 and 50% blockage was accounted for by placing Perspex sheets over 50% of the grate openings. Photographs of the as-built models are shown in Figures G.1 to G.6 in Appendix G.

5.1.1 Experimental Set-up

Water was pumped via a steel pipe with nominal diameter 300 mm, connected to a PVC pipe with nominal diameter 100 mm, with a gate valve that controls the flow into the glass flume. A photograph of the glass flume and flow straightener are shown in Figure 5.1. The PVC pipe with nominal diameter 100 mm could deliver a maximum flow of 32 l/s. For larger discharge requirements, the steel pipe, with nominal diameter 300 mm, supplied up to 200 l/s. The flow into the glass flume was monitored by using a SAFMAG magnetic flow meter for flows above 4 l/s. Two 45 mm pipes released flow into a box fixed with V-notch weir and a point gauge, to measure flows below 4 l/s.

The glass flume was 2 m wide, 0.62 m high and 12.38 m long, which is large enough to ensure near hydrostatic conditions, as for detention basins in the field. Within the glass flume, water was directed through a flow straightener (a row of hollow bricks) upstream of the multi-stage outlet model, in order to ensure a stable approaching flow. Each multi-stage outlet model was constructed form clear Perspex to allow visualisation of flow patterns and tail water levels inside the multi-stage model.

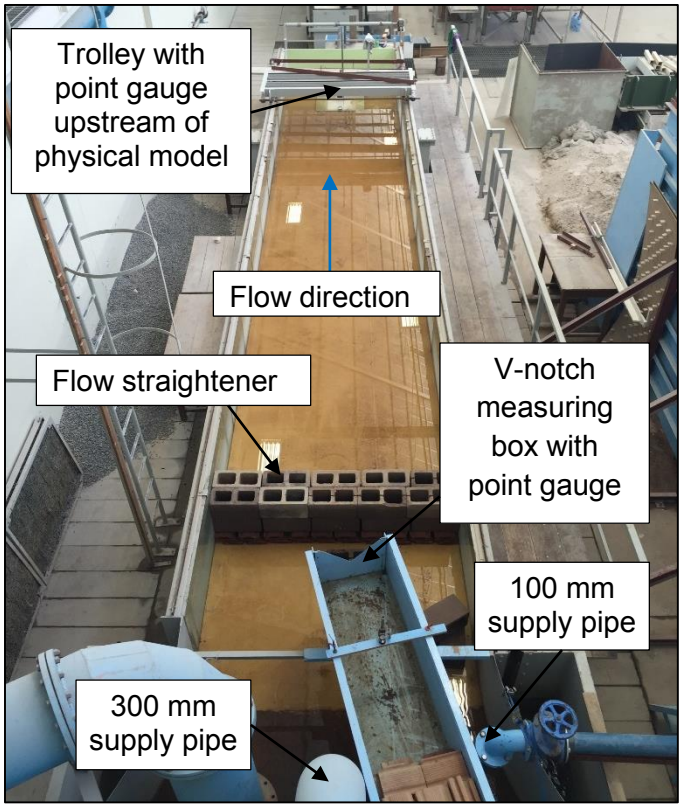

Figure 5.1: Glass flume and flow straightener bricks

Downstream of the multi-stage outlet model, the water exited the glass flume via the 100-year storm sized outlet pipe and entered a second V-notched box, which was a second control to measure the outflow. The water then flowed into a drainage channel and was then recirculated. The plan view of the laboratory set-up is illustrated in Figure 5.2.

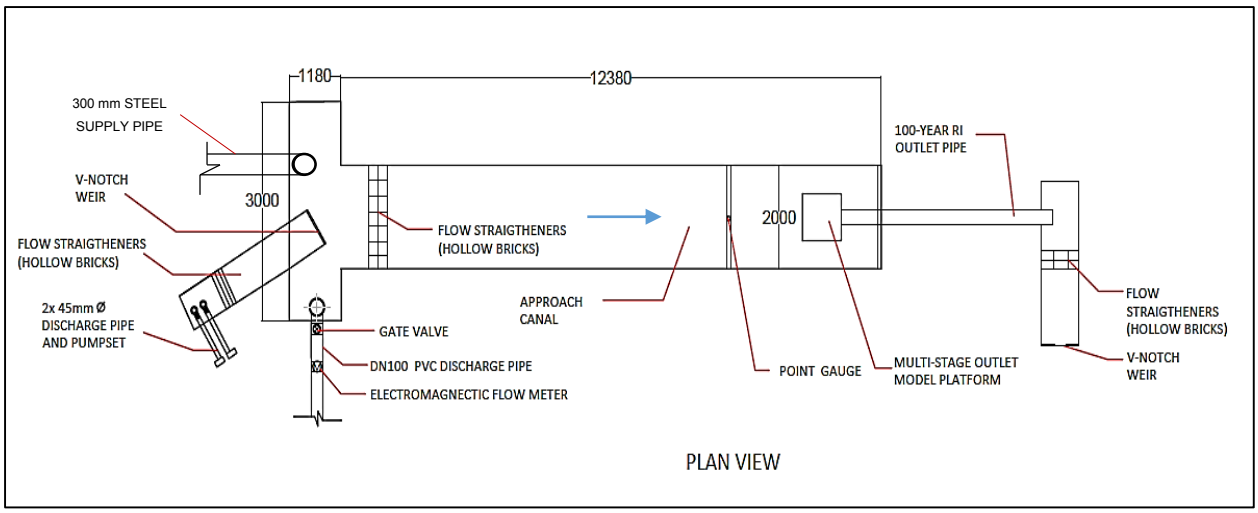

Figure 5.2: Plan view of laboratory set-up

5.2 Laboratory Apparatus

5.2.1 Discharge Measurement

Electromagnetic SAFMAG flow meters, installed on both the 100 mm and 300 mm nominal diameter pipes, were used to measure the flow in l/s into the glass flume and a valve was manually adjusted to ensure that the required discharge was delivered. The flow readings were recorded manually from the display face of the flow meter, as shown in Figure 5.3. The flow meter had a stated accuracy of ± 0.5% of the flow rate, which is equivalent to a maximum error of ±0.735 l/s at 147 l/s, which was the maximum tested flow rate. By applying the similitude of Froude for the free surface flow, this value corresponds 0.011 m^3/s in a real scale system.

The second device was a sharp-crested V-notch weir (Figure 5.4) to measure model flows of less than 4l/s. The theoretical V-notch weir discharge formula, as discussed in Section 2.3.2, was used to calculate the expected discharged for each recorded water level. The variation in the water levels measured upstream of the V-notch weir with a point gauge, at a distance which was at least four times the maximum head on the V-notch weir, was found to be ±0.65% for all discharges tested.

Figure 5.3: SAFMAG electromagnetic flow meter

Figure 5.4: Measuring needle in V-notch box

5.2.2 Pressure Measurement

The total pressure was measured by means of a piezometer, as illustrated in Figure 5.5 and Figure 5.6, to facilitate flow depth measurement inside the multi-stage outlet model. The piezometer measured the hydrostatic pressure that results from a change in elevation (P), dynamic pressure ($\frac{\rho v^2}{2}$) due to fluid motion, and the static pressure due to the fluid weight (γz). All tubing connected to the multi-stage outlet model was thoroughly bled to expel air bubbles prior to taking pressure readings.

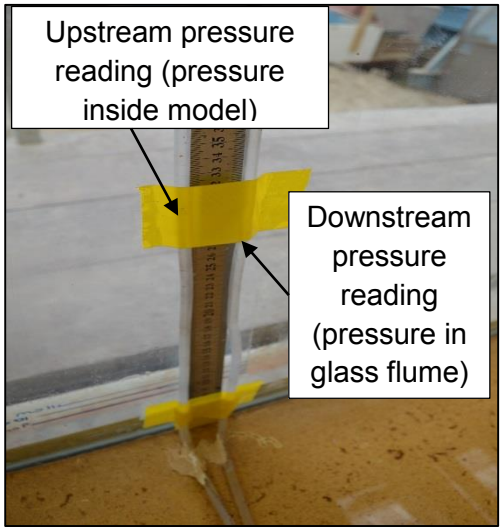

Figure 5.5: Piezometer reading

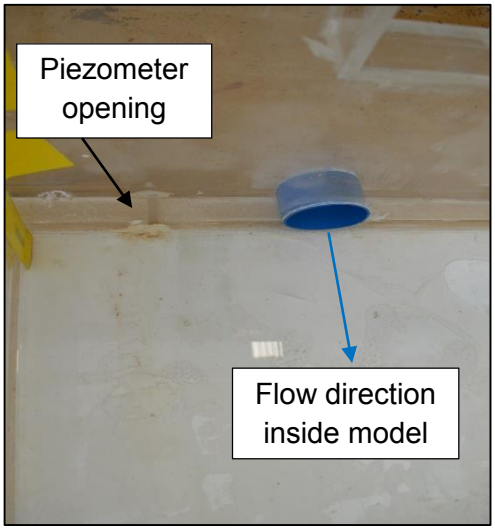

Figure 5.6: Opening of piezometer inside multi-stage outlet model

The pressure reading was reworked to determine the water surface elevation. In addition, the water elevation in the model is equal to the head produced by the outlet pipe on the downstream side of the multi-stage model, which is typically lower than the water surface in the glass flume. This backwater produced by the 100-year storm outlet pipe would submerge the other discharge devices, such as the orifice and weir, and reduce the discharge through these devices. Thus, the tailwater elevation is required to determine this reduction in discharge (Hydrology Studio User's Guide, 2014:124) and to determine the differential head on the low-flow orifice situated on the upstream side of the multi-stage outlet model, as described with the aid of Figure 5.3.

The piezometer also diminished the impeding effect of the fluctuating water surface elevation inside the multi-stage outlet model on the level of tailwater measured. The fluctuations in water surface elevations occurred because of the water accelerating though the orifice and the plunging of the water when overflowing the weir component of the model. When water surface fluctuations were present, a visual averaging of the piezometric reading on the piezometer was required.

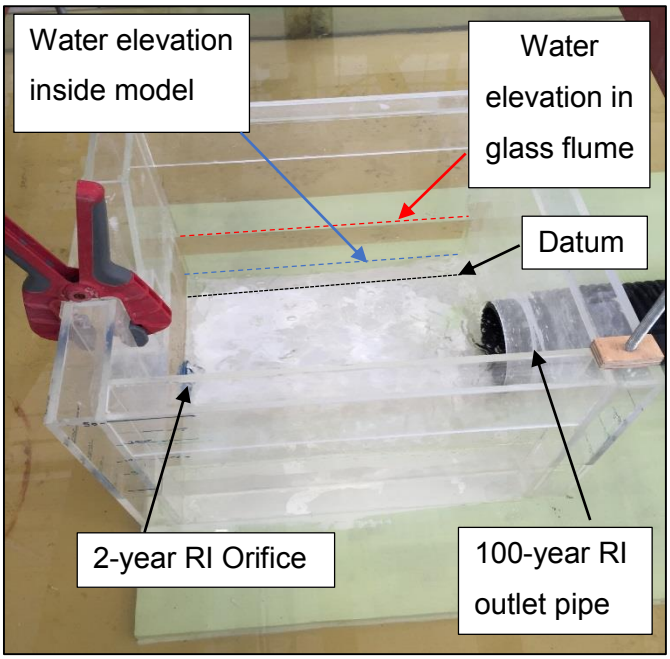

Figure 5.3: Tailwater produced by 100-year RI outlet pipe

5.2.3 Water Level Measurement

The water level in the glass flume was measured with a point gauge (Figure 5.4), at a distance of at least three times the maximum head on the model, upstream of the model. This latter requirement is necessary to ensure that the water level measurement is not influenced by the drawdown of the water surface as the flow approach the model.

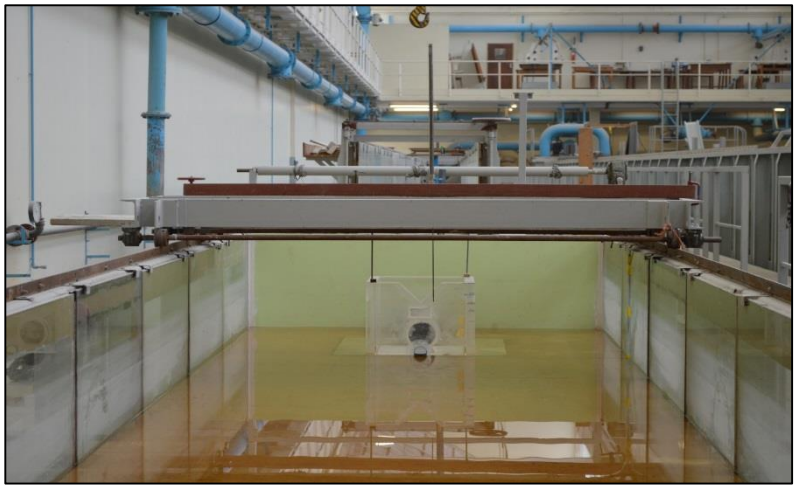

Figure 5.4: Point gauge fixed in glass flume upstream of model

5.3 Test Procedure

Each of the six physical models was tested by carrying out the following steps:

1. The specific flow rate into the glass flume was measured (firstly the maximum allowable 2-year pre-development storm event) by means of the electromagnetic flow meter. The flow was verified by measuring the outflow from the outlet pipe with a sharp-crested V-notch weir, since the inflow is equal to the outflow.
2. The flow was allowed to stabilise for the required amount of time, i.e. until there has been no change in the level of the water surface in the glass flume for at least 5- to 10-minutes. Then steady state was assumed to have been achieved.
3. The upstream water surface elevation measurements were taken with a point gauge upstream from the weir and orifice devices, at a distance of four times the maximum head on the discharge control device (The Bureau of Reclamation, 2001). Redundant measurements (every 10 minutes until the water surface level stabilised) were therefore necessary for consistency. By using the equation, $\Delta Q=\Delta h \times$horizontal area of glass flume/Δt, the current researcher could confirm that the discharge from the model was equal to the flow into the glass flume.
4. The tailwater elevation inside the multi-stage outlet model was obtained by means of a piezometer tube.
5. Repeat steps 1-5 for the other flood events (5-, 10-, 20-, 50- and 100-year RI) in order to set up a complete rating curve.

The maximum velocity head, corresponding to the approach velocity in the flume at the location of the point gauge, was less than 1.1 mm. Thus, it was decided that the approach velocities were negligible, as would be the field condition of a detention facility. The inflow and stage were recorded to 0.01 l/s (1 x 10^{-5} m^3/s) and 0.5 mm respectively, and plotted to generate stage-discharge curves for each configuration. The experimental data were then compared to the compound rating curves determined by means of the known theoretical equations, as discussed in the literature study.

Repetition of tests, in order to eliminate random error in the physical model tests, was unnecessary, since water-level readings were taken every ten minutes until the water level stabilised. Therefore, for each of the six models an average of 80 water levels were manually measured to establish stage-discharge curves. In addition, the inflow discharge readings of the electromagnetic flow meter was verified by means of a V-notch weir at the downstream side. Tests were repeated only when data varied significantly from the theoretical data set.

5.4 Limitations

The discharge coefficient for each 2-year control orifice was determined by inserting the measured experimental data into Equation 2.1 to compute the empirically-derived discharge coefficient. First, only the 10-year orifices were tested while the other components of the multi-stage outlet were sealed to determine the discharge coefficient for the 10-year control orifice experimentally. The same procedure was repeated, to determine only the weir coefficient of the 50-year control rectangular weirs.

With the total inflow, the capacity of the 10-year storm sized orifices and the 50-year storm sized weirs known, only the discharge coefficient for the low-flow orifice of the multi-stage outlet model was altered, since the upper components of the multi-stage outlet model were already calibrated. However, it was possible to take only three to five head-discharge reading when the 10-year orifice and 50-year weir were calibrated individually, as the available head on the 10-year orifices and 50-year weirs was limited. Any head of less than 50 mm would lead to possible scaled viscosity and surface tension effects (Hager, 1994).

5.5 Modelling Criteria Considering Scale Effects

As recognised in Section 2.6.2, the choice of scales is subjected to certain limits to account for the effects of viscous and surface tension forces. The choice is further limited by the prevailing possibilities of the hydraulic laboratory, such as space and pumping capacity. A previous physical model study by the Bureau of Reclamation (2014) used a scale of 1:3 to build and test the flow passing through the overflow outlet portion of the multi-stage outlet structure to determine the head-discharge rating of the structure. Multi-stage outlet structures discharges at low heads, thus a scale of 1:5 would result in a head of less than 50 mm on the physical model. Ghetti and D'Alpaos (Heller, 2011) recommended that the head on a sharp-crested notch should be at least 50 mm to exclude scale effects, as mentioned in Section 2.6.2. This section therefore investigates scale effects for a proposed scale of 1:3.

A scale of 1:3 would allow the author to ignore the effects of surface tension on scale, since for free surface flows, surface tension effects arise only at geometric scales from 1:10 to 1:20, according to Chason (2004; cited in Wood, 1991), as discussed in Section 2.6.2. Thus, it was not necessary to evaluate the minimum Weber number.

It was, however, necessary to evaluate the minimum Reynolds number for the outlet pipe, which in return would be used to determine the flow regime in the pipe. Tables B.1 to B.6, enclosed in Appendix B, summarises the prototype information and evaluates the similarity requirements (mentioned in Section 2.6.2) for the outlet pipe, based on a scale of 1:3. The velocities and flows were scaled in accordance with Table 2.7 in Section 2.6.1. It is evident from the Moody diagram (Figure 5.5) that a scale of 1:3 would satisfy similar flow regimes (transitional turbulent) in the prototype and model outlet pipe

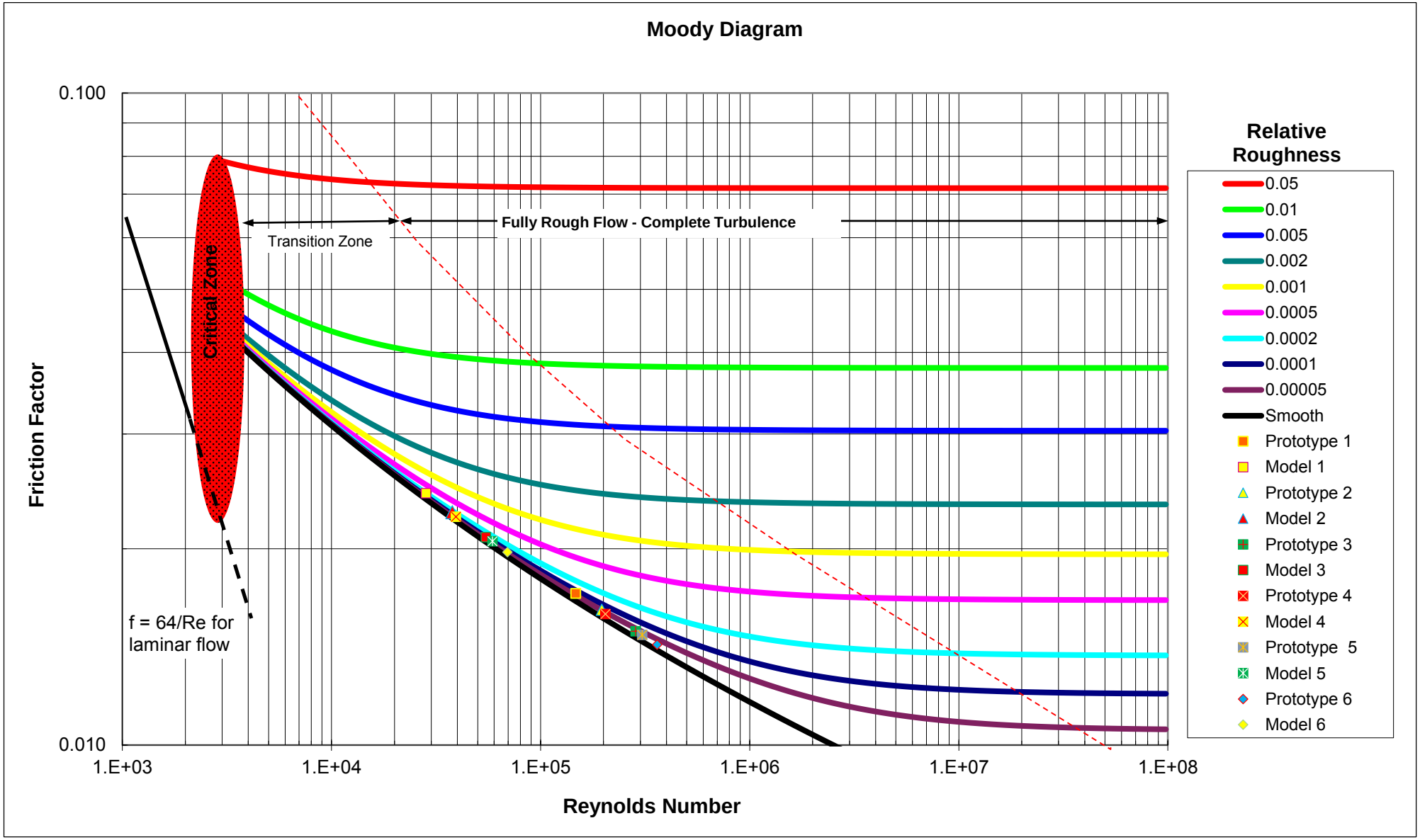

Figure 5.5: Moody Diagram indicating flow regime in outlet pipe (calculations included in Appendix B)

6. Experimental Model Test Results and Analysis

By using a physical model, it is possible to evaluate the validity of the developed Excel spreadsheet-based model (the theoretical model) and to evaluate which parameters, for instance the tailwater height or discharge coefficient, would strongly affect the performance rating curve of the multi-stage outlet structure. To cover these subjects a detailed explanation of the performance rating curve is given for Model 3. The performance rating curves were created for each of the six model configurations, but only Model 3 is elaborated in Chapter 6 to give a representative sample of the data comparisons.

In Appendix H, each physical model was compared to the spreadsheet-based model, which consist of the theoretical equations provided in Section 2.3.2 to determine if any of the standard theoretical equations generated rating curves consistent with the physical model data. Minor differences between generated plots occurred as discussed in Appendix H. Inconsistencies existing between the experimental and theoretical data are summarised in Section 6.2 for all six models. Results in this section are reported and tabulated in prototype dimensions, unless otherwise stated. Computations were carried out to the nearest three significant figures. The experimental water level was collected to the nearest mm (0.001 m) and the discharge to the nearest 0.1 l/s (0.0001 m^3/s). As a rule, discharges from experimental data are computed to the same number of significant figures as is contained in the experimental data having the fewest significant figures (Bureau of Reclamation, 2001).

The pre-development peak flows (target discharges) for each recurrence interval have been marked in red, enabling a comparison of the effectiveness of the each discharge component of the multi-stage model in meeting their design criteria. A trash rack was only installed after testing the 2- to 50-year peak flow to allow clear visual observations of the downstream water profile inside the riser.

The exact target flow could not be supplied in the hydraulic laboratory due to fluctuating electromagnetic flow meter readings of approximately ±0.69% at low flows. In addition, a valve had to be manually operated until the electromagnetic flow meter gave a discharge reading in close approximation of the target discharge.

The fractional change of discharge of the discharge control devices, due to the difference between the differential heads theoretically calculated and experimentally measured, was determined by means of Equation 6.1 (Bos, 1989:95).

$$S = \frac{u}{h}\Delta h \times 100 \tag{6.1}$$

where:

S = sensitivity (%)

u = the power of h in the head-discharge equation (0.5 for an orifice, 1.5 for rectangular control and 2.5 for triangular control)

h = head or differential head on discharge control device (m)

Δ h = change in head or differential head (error between theoretical and physical data).

Visual observations of the physical model tests (Figure 6.1 and Figure 6.2) indicated that once the riser structure overflowed, the 50-year storm control weirs no longer discharge under true weir flow conditions due to the trash rack. As a result, the stage-discharge relationships for the 50-year storm control weirs were only plot to the stage before the riser overflowed. The graphs of the individual 2-year orifices were also only plotted up to the maximum 50-year surface elevation, since the discharge from the 2-year storm control orifices were empirically derived from experimental data collected from the 10- and 50-year discharge control components.

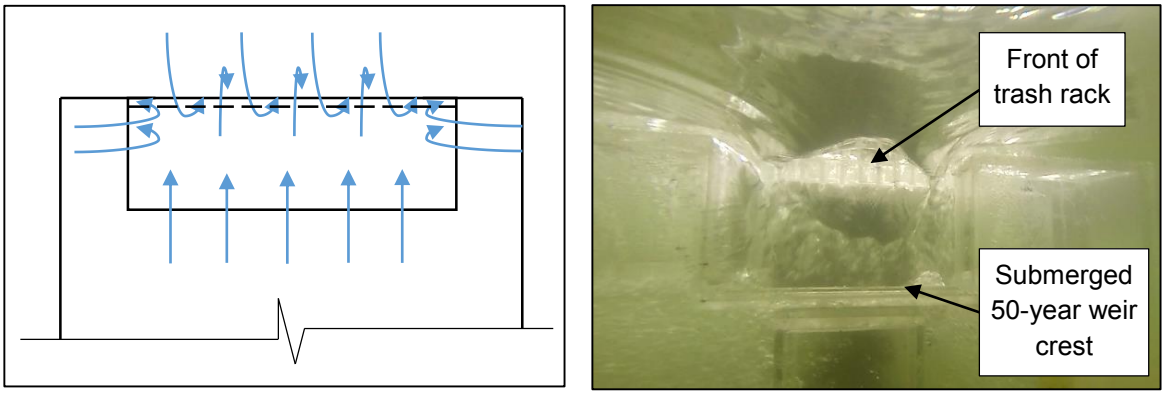

Figure 6.1: (a) Front view of flow patterns when riser overflows (b) Front view of Model 2, discharging at the 100-year water surface elevation

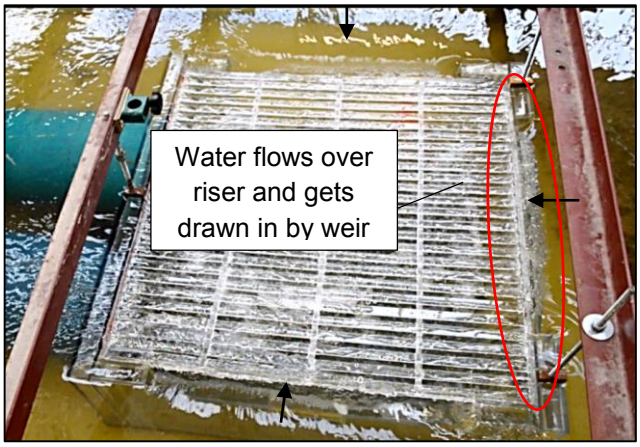

Figure 6.2: Model 6 discharging at the 100-year water surface elevation

Discharge calculations from the multi-stage outlet would transfer to using the 100-year outlet pipe before utilizing the overflow outlet as an orifice under large heads. The 100-year control outlet pipe was designed to restrict the 100-year RI storm, and not the overflow riser. The riser operated under weir flow conditions for all tested models at the 100-year target discharge. Thus, the theoretical discharge equation of the riser structure did not require verification.

6.1 Results of Model 3

The measured outflow of Model 3 (I.6) was plotted against the stage to determine if the outlet discharged at a rate equal to the pre-development peak flow levels, or if the target flow was exceeded. Model 3 (I.6) was designed to control the 2-, 10-, 50-, and 100-year RI storm events for inland regions receiving 700 mm MAP. Figure 6.3 illustrates that the stage-discharge curve of the physical model plots below the red target stage-discharge markers. Thus, the physical model controlled the outflow effectively, but released the flow at higher stages than initially estimated.

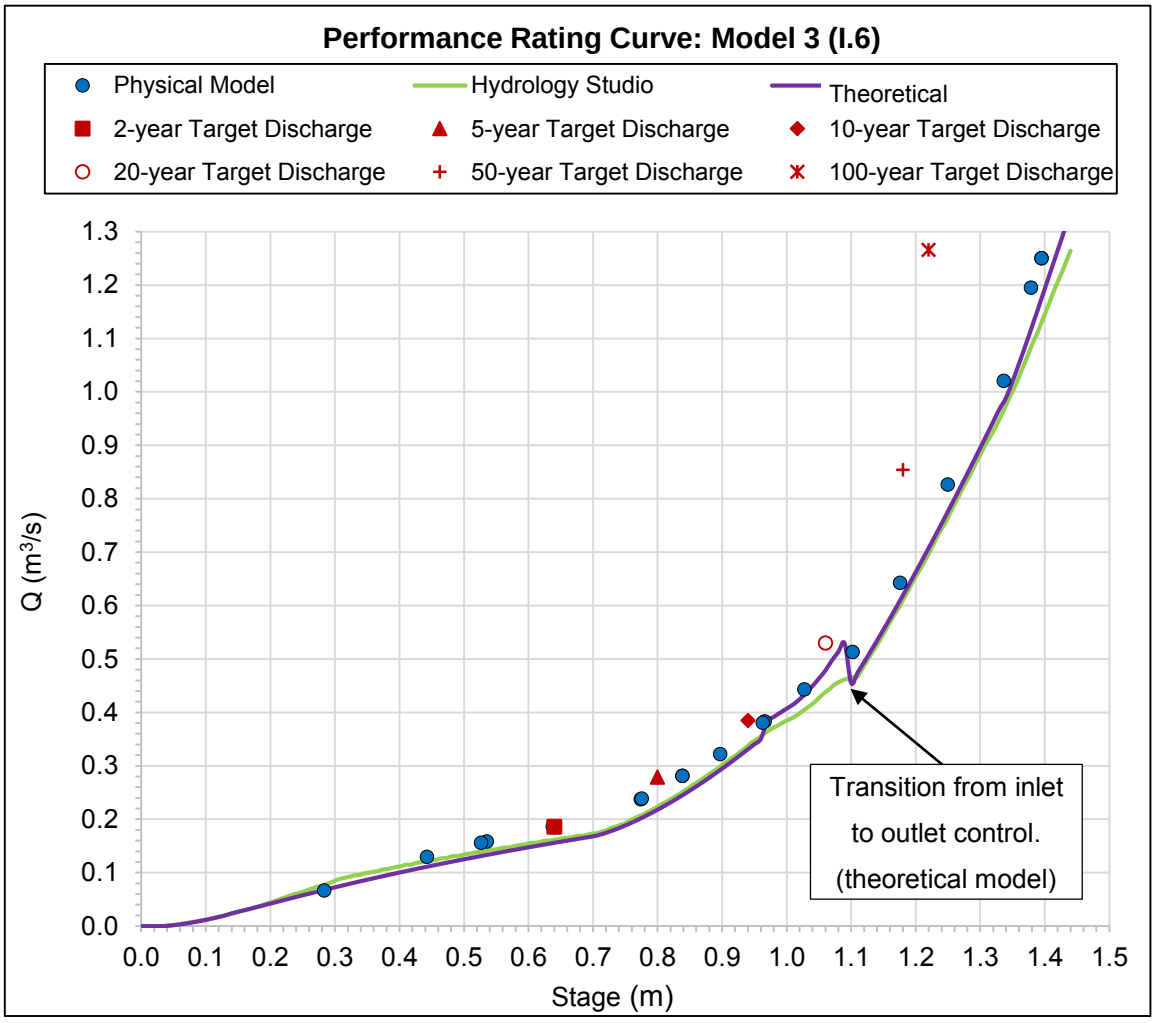

Figure 6.3: Calculated and physically modelled stage-discharge relationship of Model 3 (prototype dimensions)

It is evident from Figure 6.3 that although Model 3 was designed with outlet devices to control the 2-, 10-, 50- and 100-year RI storm events, the physical model still restricted the outflow at the 5- and 20-year maximum water surface elevation to meet or more than meet the pre-development target discharge.

The discharge released by the multi-stage outlet model in the hydraulic laboratory was compared with the theoretical discharge in Table 6.1. From Table 6.1 it is clear that the hydraulic performance of the 2-year storm control component of the multi-stage model deviates the most from the theoretical model. The ratio of flow contributed by the 2-year orifice to the total flow, at consecutive stages, decreased as the other control components start to function since the other components had larger discharge capacities at higher stages. Thus, the effect of the 2-year orifice on the percentage difference between the theoretical and measured discharge decreased at higher stages.

Table 6.1: Difference between theoretical discharge and physically measured discharge of Model 3

RI (years)	Stage (m)	Actual discharge of physical model(1) (m^3/s)	Theoretical discharge (m^3/s)	Absolute difference (m^3/s)	Percentage difference (%)
2	0.527	0.156	0.131	-0.025	-15.75
5	0.776	0.239	0.203	-0.036	-15.16
10	0.963	0.381	0.353	-0.028	-7.27
20	1.089	0.493	0.528	0.035	7.03
50	1.251	0.832	0.778	-0.053	-6.41
100	1.395	1.255	1.174	-0.081	-6.42

(1) The actual discharge equals the average of the discharge measurements, taken every 10 minutes until water surface elevation stabilised

Each component of the multi-stage outlet was further investigated in Sections 6.1.1 to 6.1.3, at different water surface elevations, to identify the parameters that contributed to the differences between the design guidelines (theoretical model) and the collect data of the physical model.

6.1.1 Discharge Component of Model 3 Controlling the 2-year Storm Event

The differential head measured in the hydraulic laboratory increased from stage 0 m to stage 0.897 m, which increased the discharge of the 2-year storm control orifice (refer to Figure 6.4). After stage 0.897 m, the 10-year component of the multi-stage model discharged at full capacity, which increased the water surface elevation inside the riser and decreased the differential head acting on the 2-year storm control. Thus, the outflow from the 2-year storm control orifice decreased. In addition, the 50-year storm control weir also started to contribute to the total discharge of Model 3 around stage 1.03 m.

The 100-year outlet pipe of the physical model transitioned from inlet control to outlet control as the upstream water level approached stage 1.2 m. Thus, the measured discharge of the 2-year control orifice at stage 1.251 m (50-year water level) fitted the stage-discharge curve of the theoretical model closer as both models were operating under outlet control conditions.

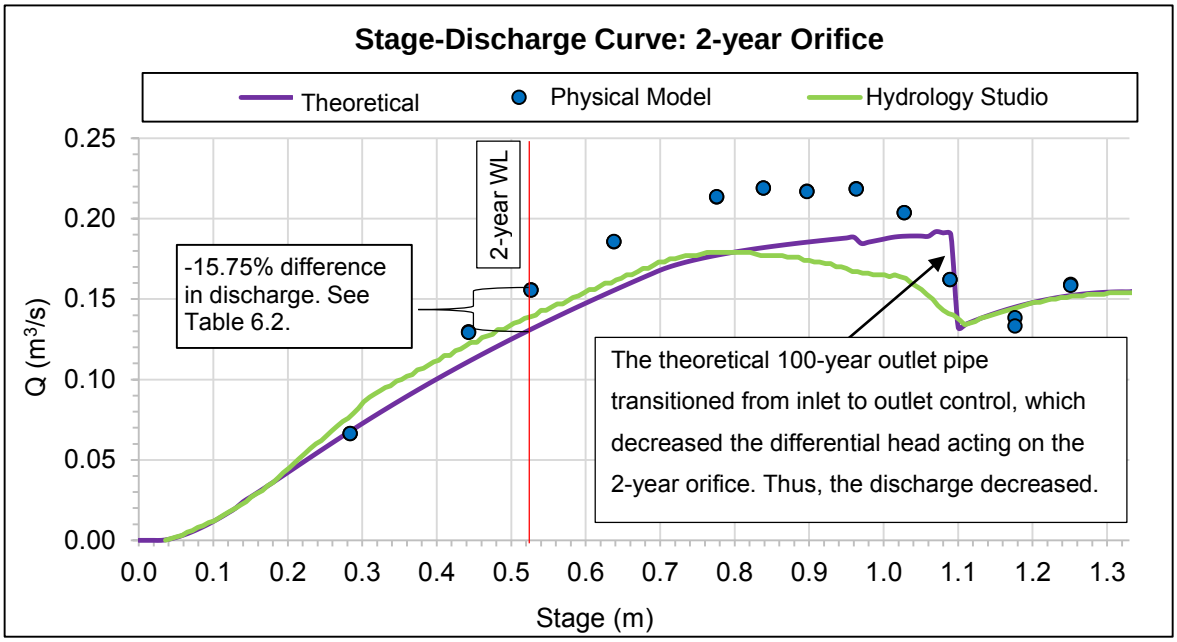

Figure 6.4: Stage-discharge curve for the 2-year control component of Model 3

The fractional change in the discharge of the 2-year storm control orifice, due to the difference between the differential head calculated and experimentally measured, was determined to be -9.2% (see Table 6.2). The mean value of the empirically derived discharge coefficient, for the modelled 2-year storm control orifice, varied from 0.63 at stage 0.776 m to 0.645 at stage 0.963 m. Thus, the discharge coefficient empirically derived from the experimental data was larger than the constant equation discharge coefficient of 0.61, which was recommended in Section 2.3.2.1. After stage 0.963 m the empirically derived discharge coefficient of the 2-year storm control orifice, based on experimentally collected data, decreased from 0.65 to 0.54, as the differential head and discharged decreased, with increase in the stage.

Section 7 elaborates on the variation in the discharge coefficient. The mean of the discharge coefficients was determined to be 0.6 (refer to Table I.3 in Appendix I) and is the most probable equation coefficient based on 24 readings.

Table 6.2: Fractional change in the discharge at the 2-year water level (stage 0.527 m)

Parameter	2-year control orifice		Fractional change in discharge (%)	Total fractional change in discharge (%)	Percentage difference from Table 6.1 (%)	Error (%)
	Theoretical	Physical				
C_d	0.61	0.654	-6.73	-15.93	**-15.75**	0.18
Δh (Eq. 6.1)	0.201	0.246	-9.20			

The 0.18% error, as summarised in Table 6.2, is due to experimental error and the assumption that the theoretical approach velocity of the 100-year pipe is negligible.

6.1.2 Discharge Component of Model 3 Controlling the 10-year Storm Event

Figure 6.5 indicates that the slope of the stage-discharge curve of the physical model flattens from stage 1.176 m to 1.251 m as the orifices were partially submerged downstream. From stage 1.337 m to 1.395 m, the 10-year storm control orifices were fully submerged downstream. Thus, the slope of the stage-discharge curve of the physical model declined. After stage 1.337 m, the 10-year storm control orifices released less water owing the reduction in the differential head as the modelled 100-year outlet pipe operated under outlet control conditions.

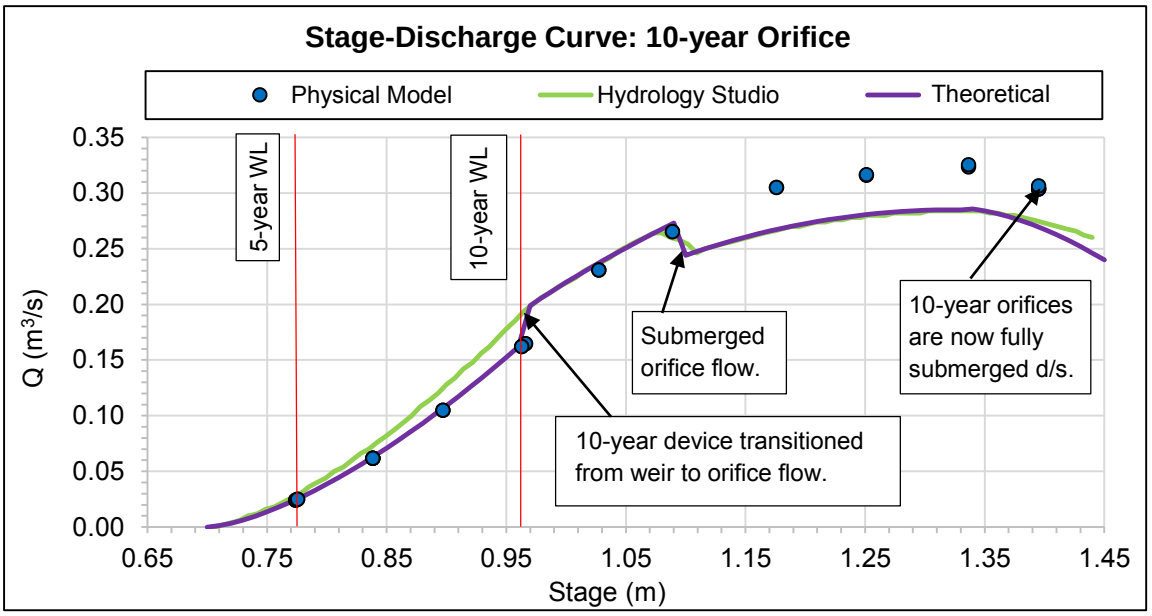

Figure 6.5: Stage-discharge curve for the two 10-year control components of Model 3

The fractional change in the discharge of the 2-year storm control orifice is the main cause for the difference between the actual and theoretical discharge at stage 0.776 m (5-year water level) and stage 0.963 m (10-year water level) respectively (see Table 6.4 and Table 6.6).

The mean value of the discharge coefficient of the modelled 10-year storm control orifices were determined to be 0.365 for weir flow conditions (before stage 0.963 m) and 0.6 for orifice flow conditions (after stage 0.963 m), which is in good agreement with the typical discharge coefficients found in literature. Therefore, Figure 6.5 illustrates that the 10-year storm control orifice, evaluated in the hydraulic laboratory, operated as designed at the 5- and 10-year water surface elevations but the 2-year storm control orifice differed from the theoretical model.

At stage 1.1 m, the theoretical outlet pipe transitioned from inlet to outlet control. Therefore, the backwater head produced by the theoretical outlet pipe increased, which decreased the differential head acting on the 2-year storm control orifice. Thus, the discharge suddenly decreased at stage 1.1 m, as illustrated on Figure 6.5. However, at stage 1.1 m, the 100-year outlet pipe of the physical model was still operating under inlet control conditions.

Table 6.3: Percentage difference between theoretical and actual discharge at the 5-year water level (stage 0.776 m)

Individual components of multi-stage outlet	Stage (m)	Actual discharge of individual component, physical model (1) (m^3/s)	Theoretical discharge of individual component (m^3/s)	Percentage difference between theoretical and physical discharge (%)
2-year component	0.776	0.2137	0.1772	-17.07
10-year component	0.776	0.0250	0.0253	1.35
Total		0.2387	0.2025	**-15.15**

(1) The actual discharge equals the average of the discharge measurements, taken every 10 minutes until water surface elevation stabilised

Table 6.4: Fractional change in discharge at the 5-year water level (stage 0.776 m)

Parameter	Theoretical	Physical	Fractional change in discharge (%)	Total fractional change in discharge (Compare to Table 6.3) (%)
2-year control orifice				
C_d	0.61	0.63	-3.17	-17.00
Δh (Eq. 6.1)	0.3663	0.5064	-13.83	
2x 10-year control orifice				
C_d	0.37	0.365	1.37	1.37

Table 6.5: Percentage difference between empirical and actual discharge at 10-year water level (stage 0.963 m)

Individual components of multi-stage outlet	Stage (m)	Actual discharge of individual component, physical model (1) (m^3/s)	Theoretical discharge of individual component (m^3/s)	Percentage difference between theoretical and physical discharge (%)
2-year component	0.963	0.2186	0.1886	-13.73
10-year component	0.963	0.1621	0.1645	1.47
Total		0.381	0.3531	**-7.27**

(1) The actual discharge equals the average of the discharge measurements, taken every 10 minutes until water surface elevation stabilised

Table 6.6: Fractional change in discharge at 10-year water level (stage 0.963 m)

Parameter	Theoretical	Physical	Fractional change in discharge (%)	Total fractional change in discharge (Compare to Table 6.5) (%)
2-year control orifice				
C_d	0.61	0.645	-4.69	-13.91
Δh (Eq. 6.1)	0.4149	0.4996	-8.48	
2x 10-year control orifice				
C_d	0.37	0.365	1.37	1.37

The total percentage difference between the theoretical and physical discharge, summarised in Table 6.3 and Table 6.5, varied by a maximum of -0.2% from the total fractional change in discharge, as determined in Table 6.4 and Table 6.6. However, an experimental error of at least $\pm$ 0.5% was expected, as mentioned in Section 5.3.1. The length scale of the physical model also contributed to the variance, since the physical model could only be constructed to the nearest millimetre.

6.1.3 Discharge Component of Model 3 Controlling the 50-year Storm Event

The modelled 50-year storm control weir had a weir discharge coefficient that ranged from 1.79 to 1.88 when calibrated as a broad-crested weir (Equation 2.14). Equation 2.14 incorporates a varying discharge coefficient for different head values, as summarised in Table 2.3. Whereas the theoretical, spreadsheet-based model, used a constant weir coefficient of 1.84 for sharp-crested weirs (Equation 2.19).

Figure 6.6 illustrates the stage-discharge curves of the 50-year storm control weir, determined by means of different theoretical equations, software output (Hydrology Studio), and data from the physical model. The yellow stage-discharge curve in Figure 6.6, empirically derived from the broad-crested weir equation (Equation 2.14), only fitted the stage-discharge curve of the physical model when the 50-year weir discharged at low stages.

Figure 6.6 further illustrates that the stage-discharge curve, empirically derived from the sharp-crested weir equation without end contractions (Equation 2.19), fit the experimental data better than Equation 2.18, which allows for end contractions. The reason being that Model 3 had an almost full width weir and could be classified as only partially contracted.

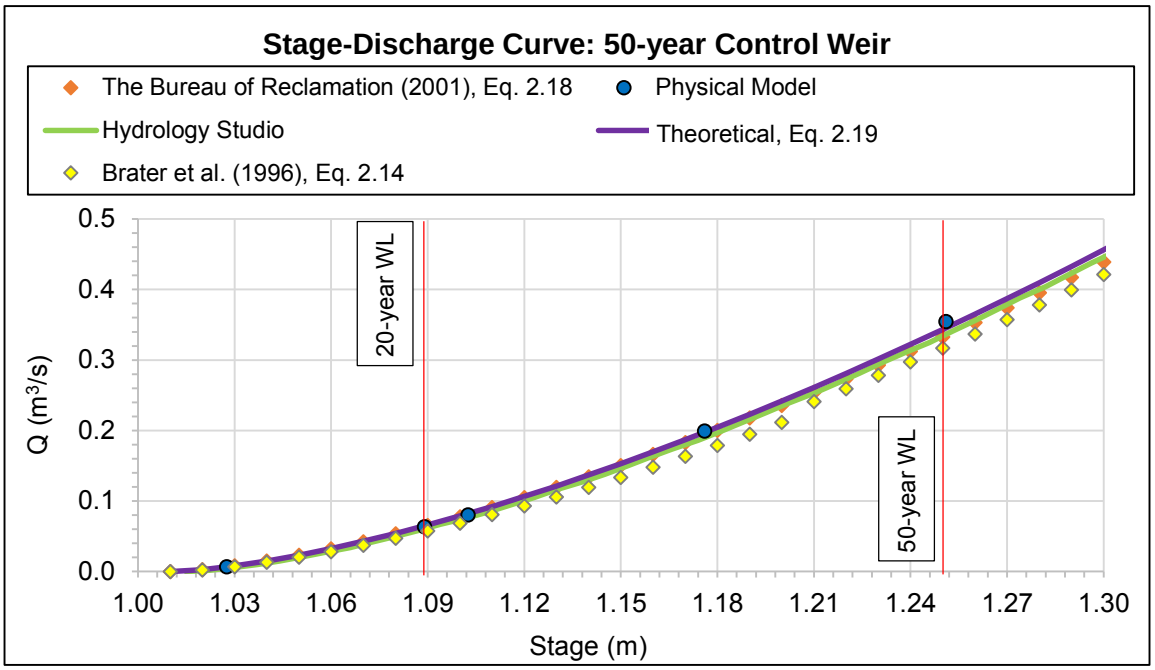

Figure 6.6: Relationship between the discharge and stage for the 50-year control component of Model 3

Figure 6.7 indicates that at the 20-year water level (stage 1.089 m), the 2-year storm control orifice was fully submerged up- and downstream. The 10-year storm control orifices were fully submerged upstream, but discharged freely downstream, where the water inside the riser was just below the bottom edge of the 10-year orifices. Figure 6.7 also indicates that the 50-year storm control weir also discharged at the 20-year maximum water surface elevation, but under a low head of 0.08 m (prototype dimension).

At stage 1.251 m, the 50-year water level, the 10-year storm control orifices of the multi-stage model were partially submerged downstream to an elevation just above the centre of the 10-year storm control orifices. Stage 1.251 m is illustrated by the aid of Figure 6.8, where the 10-year storm control orifices had a submergence ratio of only 34.5%.

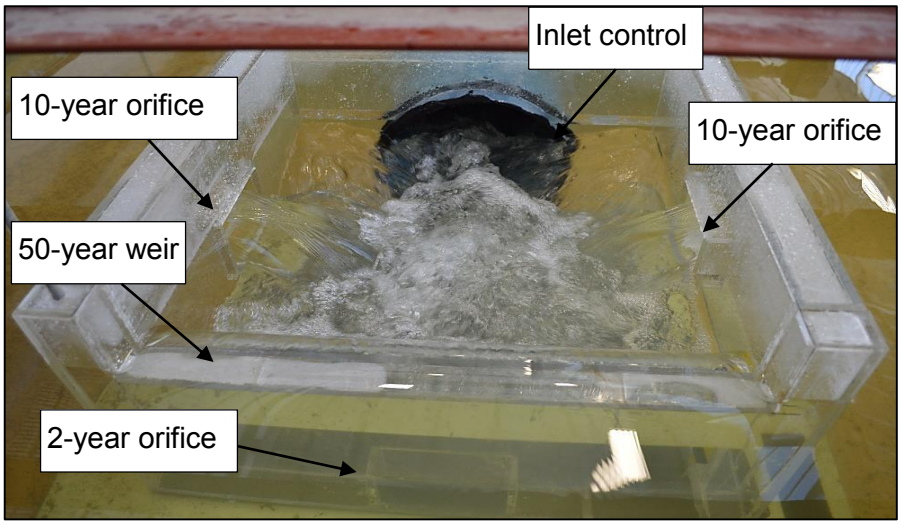

Figure 6.7: Model 3 operating at the 20-year water level (stage 1.089 m)

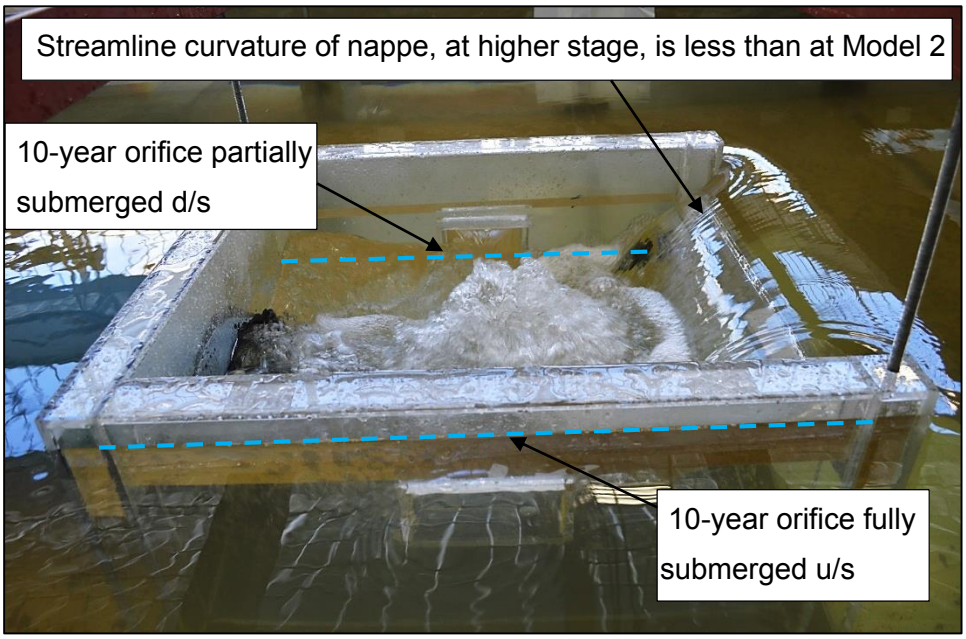

Figure 6.8: 10-year orifices partially submerged d/s at stage 1.251 m

Table 6.7 and Table 6.9 encapsulate the differences between the theoretical and physical measured discharge of each individual control component of the multi-stage outlet. Table 6.8 and Table 6.10 indicates the differences between the theoretical and physical discharge coefficient, and differential head of each component. The measured 50-year outflow deviated from the theoretical discharge due to the differential head acting on the submerged orifices, as summarised in Table 6.10.

Table 6.7: Percentage difference between theoretical and physical measured discharge at the 20-year water level, stage 1.089m

Individual components of multi-stage outlet	Stage (m)	Actual discharge of individual component, physical model (1) (m^3/s)	Theoretical discharge of individual component (m^3/s)	Percentage difference between theoretical and physical discharge (%)
2-year component	1.089	0.1623	0.1903	17.27
10-year component	1.089	0.2655	0.2724	2.61
50-year component	1.089	0.0638	0.0649	1.68
Total		0.493	0.528	**7.03**

(1) The actual discharge equals the average of the discharge measurements, taken every 10 minutes until water surface elevation stabilised

The total percentage difference between the theoretical and physical discharge, determined in Table 6.7 and Table 6.9, varied slightly from the total change in fractional discharge, determined in Table 6.8 and Table 6.10, as a result of experimental error.

Table 6.8: Contribution of discharge coefficient and differential head measurements to the percentage difference between theoretical and physical measured discharge at the 20-year water level (stage 1.089 m)

Parameter	Theoretical	Physical	Fractional change in discharge (%)	Total fractional change in discharge (Compare to Table 6.7) (%)
2-year control orifice				
C_d	0.61	0.54	12.96	16.36
Δh (Eq. 6.1)	0.423	0.396	3.39	
2x 10-year control orifice				
C_d	0.61	0.60	1.67	1.67
50-year control weir				
C_d	1.84	1.794	2.56	1.62
Head (Eq. 6.1)	0.0790	0.0795	-0.94	

Table 6.9: Percentage difference between theoretical and actual discharge at the 50-year water level (stage 1.251 m)

Individual component of multi-stage outlet	Stage (m)	Actual discharge of individual component, physical model (1) (m^3/s)	Theoretical discharge of individual component (m^3/s)	Percentage difference (%)
2- year component	1.251	0.159	0.152	-4.03
10-year component	1.251	0.317	0.281	-11.40
50-year component	1.251	0.355	0.345	-2.58
Total		**0.832**	**0.778**	**-6.41**

(1) The actual discharge equals the average of the discharge measurements, taken every 10 minutes until water surface elevation stabilised

Table 6.10: Contribution of discharge coefficient and differential head to the percentage difference between theoretical and actual discharge at the 50-year water level (stage 1.251 m)

Parameter	Theoretical	Physical	Fractional change in discharge (%)	Total fractional change in discharge (Compare to Table 6.9) (%)
2-year control orifice				
C_d	0.61	0.553	10.31	-2.11
Δh (Eq. 6.1)	0.270	0.360	-12.42	
2x 10-year control orifice				
C_d	0.61	0.60	1.67	-10.75
Δh (Eq. 6.1)	0.270	0.360	-12.42	
50-year control weir				
C_d	1.84	1.883	-2.28	-2.59
Head (Eq. 6.1)	0.241	0.2415	-0.31	

6.2 Summary of Experimental Results

If the physically modelled multi-stage outlets released the target discharge at a stage lower than the approximated maximum water surface, as determined in Section 4.2, the model would be releasing too much water to meet the specific design storm when it operates under the approximated maximum head. When the multi-stage outlet model released the target discharge at a higher stage than the approximated maximum water surface, it would be able to restrict the outflow to the target discharge when it operates under the approximated maximum head.

Data comparison between the theoretical estimated target stage and the stage measured in the hydraulic laboratory, corresponding to the 2-year RI target discharge, indicated that Models 2, 3 and 5, were ineffective in restricting the outflow to meet the target discharge of the 2-year RI storm (indicated in red in Table 6.11). However, four of the multi-stage outlet models, which were physically modelled, restricted the flow to meet, or to be less than, the target discharge for the 10-, 20-, 50- and 100-year RI storms. Models 1 and 3 restricted the flow to meet, or be less than, the target discharge for the full range of RI storms, as tabulated in Table 6.11.

Table 6.11: Percentage difference between the theoretically estimated target stage and physical recorded stage

RI	Percentage difference (Model 1) (%)	Percentage difference (Model 2) (%)	Percentage difference (Model 3) (%)	Percentage difference (Model 4) (%)	Percentage difference (Model 5) (%)	Percentage difference (Model 6) (%)
2	-8.15	25.25	0.16	3.06	20.25	11.41
5	-2.78	7.44	-10.36	-4.24	5.2	3.27
10	-2.44	4.31	-2.69	-0.76	4.07	0.28
20	-8.36	1.45	-3.85	-1.48	-2.23	-5.43
50	-8.95	-1.84	-5.68	-5.6	-11.22	-11.17
100	-4.98	-2.07	-12.54	-13.59	-24.33	-24.90

The maximum water level measured in the hydraulic laboratory, corresponding to the 100-year target discharge, was less than the estimated maximum water level (target stage) for Models 5 and 6 (indicated in green in Table 6.11). The estimated maximum water level was obtained from the theoretical stage-storage curve. The Rational Formula Hydrograph method used the difference between the triangular shaped pre- and post-development hydrographs to estimate the required storage volume. The initial approximation of the pre- and post-development hydrographs as a triangular shaped outflow hydrographs was required, since the development site was hypothetical and actual flood data was not available.

The estimation of the storage volume, based on the triangular pre- and post-development hydrographs, caused the target stage to be underestimated; hence, the maximum head level was underestimated (see Figure 6.9). In return, the underestimation of the maximum head

level caused the 100-year design storm to be over-controlled, especially for Models 5 and 6, which had larger pre- and post-development flood peaks than the other models. Thus, more storage volume was required than initially estimated. To determine if the multi-stage outlet models could hydraulically perform as the design guidelines predict the experimental data should rather be compared to the theoretical stage-discharge curve than to the target stage-discharge curve, due to the above approximation of the storage volume.

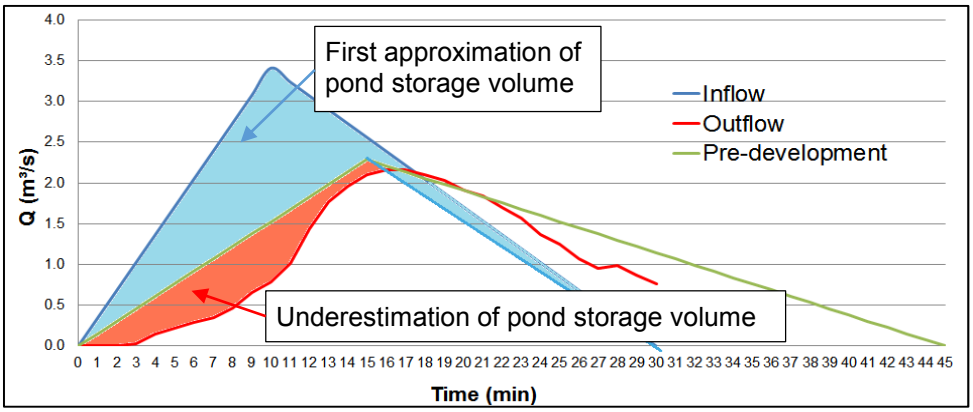

Figure 6.9: Inflow (post-development) and outflow hydrographs used to estimate storage volume

A multiple correlation coefficient R^2 has been calculated (see Table 6.12) to determine the overall accuracy of the physical model and spreadsheet-based model data for each multi-stage outlet model using Equation 7.5 (Young *et al.*, 1980). Equation 6.2 measure how well the variables could have been predicted using a linear function of a set of other variables. The closer R^2 is to one, the stronger the linear association is, and the data are represented perfectly by the model, while a R^2 value of zero indicates that the model has failed to represent any of the data.

$$R_t^2 = 1 - \left[\frac{\sum_{t=1}^{n_o}(m_t - p_t)^2}{\sum_{t=1}^{n_o} m_t^2}\right] \quad (6.2)$$

where:

R_t^2 = multiple correlation coefficient

m_t = value measured in the physical model

p_t = value obtained from spreadsheet-based computer model

n_o = the total number of samples in the dataset

Table 6.12: Multiple correlation coefficient values for each multi-stage model test

R^2 Model 1	R^2 Model 2	R^2 Model 3	R^2 Model 4	R^2 Model 5	R^2 Model 6
0.998	0.993	0.993	0.997	0.952	0.990

Analysing the multiple correlation coefficient given in Table 7.3 it is possible to conclude that the physical and spreadsheet-based model were in close agreement and provides confidence that the multi-stages models can reproduce full scale systems.

7. Discussion and Findings of Test Results

7.1 Discharge Coefficient of the 2-year Storm Control Orifice

Oscillations occurred inside the riser at different head and discharge relationships for each model. The flow entering the multi-stage outlet models became turbulent between the 2-year storm control orifice and the 100-year storm control outlet pipe. Figure 7.1 illustrates this phenomenon, which was present with all configurations of the multi-stage outlet models. These oscillations were smaller for the larger riser structures of Model 5 and Model 6, which had 100-year outlet pipes with larger nominal diameters.

The noise in the dataset and the variation in discharge coefficient among experiments was likely to have been due to the fluctuation in the water surface elevation inside the riser. However, this is typically how the multi-stage outlet structure would perform in the field. It was, therefore, questioned whether using the typical orifice discharge coefficient of 0.61 would yield accurate discharge calculations for the 2-year storm control orifice.

The experimental discharge coefficient for the 2-year storm control orifice of Model 1 was discarded from this analysis, as the individual discharge control types (circular orifice) of Model 1 differed from the other physical models (rectangular orifice).

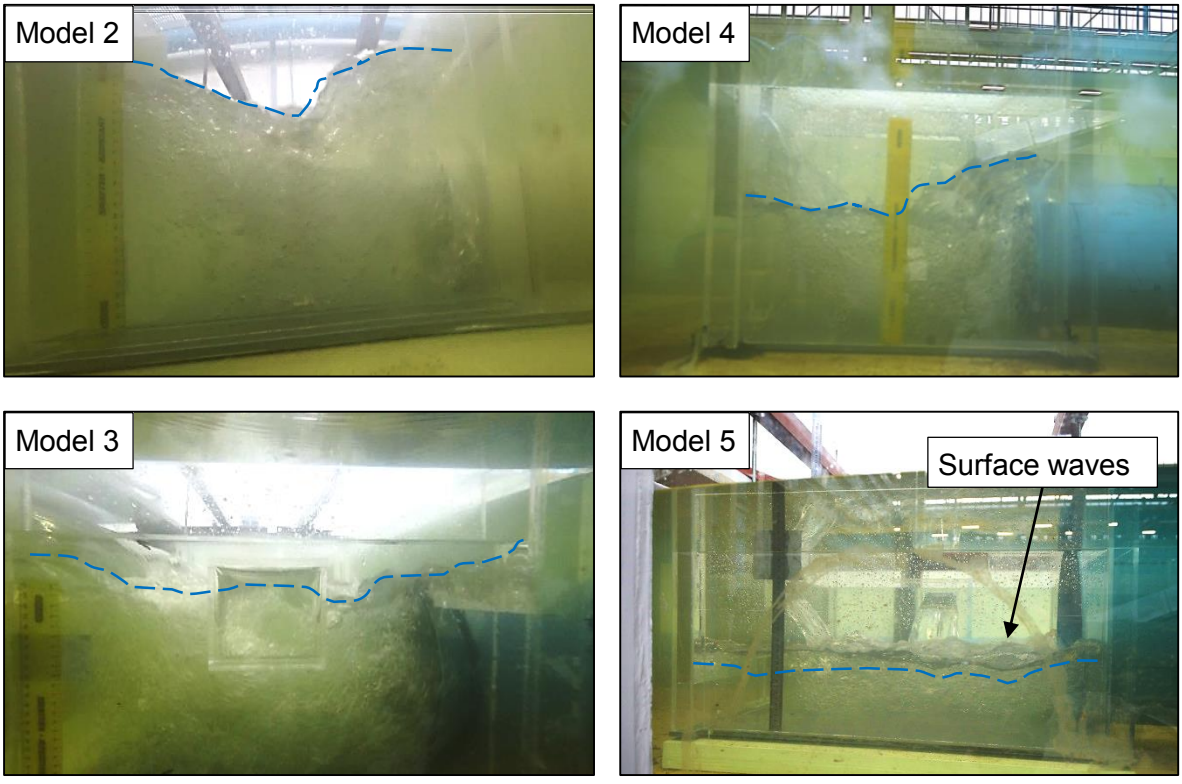

Figure 7.1: Section views of water surface elevation inside riser of different models

No literature was found that reported having investigated the effect of submergence on the discharge coefficient of a fully contracted rectangular orifice. However, for a partially suppressed rectangular orifice, a model study showed that the discharge coefficient varied from 0.58 to 0.84, as the ratio of downstream water surface elevation to orifice opening height varied between 2.8 to 1.4 (Nielsen and Weber, 2000). The operating conditions were such that the submergence ratio (Y_3/Y_1) was 0.96 to 0.99. Chapter 2 indicated that numerous physical model studies have been performed to determine the discharge coefficient for free-outflow orifices. The most common discharge coefficient used in the design of a rectangular orifice for multi-stage outlet structures is 0.61 (Brandes and Barlow, 2015).

The experimental results from Models 2 to 6 in demonstrated that the discharge coefficient, for different sizes of 2-year control orifices, varied from 0.58 to 0.68 at different stages and total discharges. This excludes the variation in the discharge coefficient when the 2-year orifice was more than 60% submerged. The variation in the discharge coefficient when the 2-year orifice was less than 60% submerged is plotted on the left-hand side of the red line in Figure 7.2.

The discharge coefficient varied from 0.46 to 0.76 when the 2-year orifice was submerged more than 60%, as illustrated right of the red line in Figure 7.2, which differs from Brater *et al*. (1996). Brater suggested that submergence does not affect the discharge coefficient value. However, the discharge coefficient values cited in Brater *et al*. (1996) did not apply to orifices with interaction effects from the other nearby discharge control devices, as was the case of this physical model study.

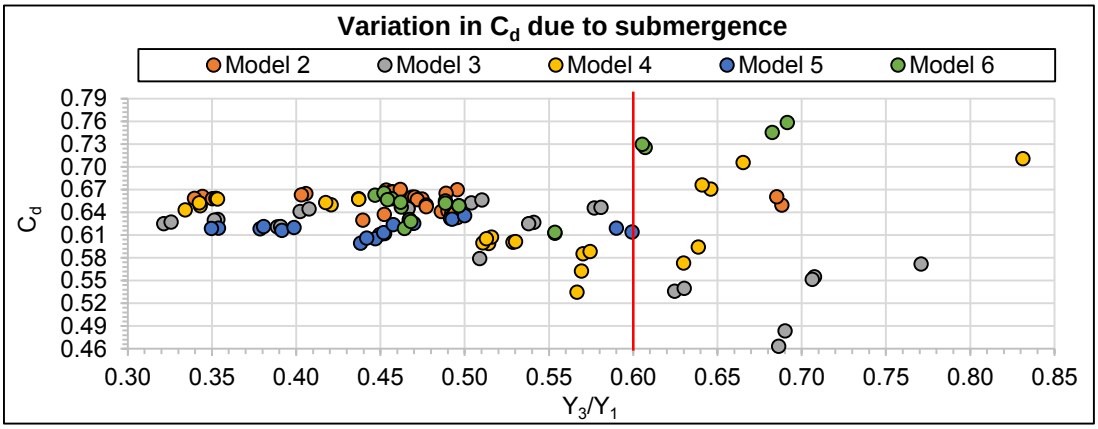

Figure 7.2: Empirically derived discharge coefficient versus the submergence ratio of the 2-year storm control orifice

Submergence greater than 60% occurred at upstream depths where the water level was either less than the maximum 2-year storm water surface elevation and, or, at the maximum 50-year storm water surface elevation. One of two conditions occurred at stages less than the maximum 2-year water level.

First, the 2-year release orifice was fully submerged upstream and partially submerged downstream, where the differential head that was acting on the orifice was small, relative to the vertical height of the orifice. The pressure profile was not uniform throughout the orifice's cross-section, as the upstream flow depth above the upper edge of the modelled orifice was very low.

A difference between the true discharge and the discharge given by the small-orifice equation (Equation 2.1) would occur, when the head acting on a vertical orifice is small compared to the height of the orifice. In deriving Equation 2.1, the head producing discharge was assumed to be the head on the centre of the orifice. However, the deviation from the theoretical form of the small-orifice equation being corrected for in the discharge coefficient. The second situation occurred when the differential head was large in comparison to the amount of water discharged, and the discharge coefficient decreased.

At the maximum 50-year water surface elevation, two scenarios occurred that influenced the discharge coefficient. The discharge coefficient increased when there was a large decrease in the differential head. This occurred as the water level inside the riser increased when the total discharge of the multi-stage outlet increased. The second scenario occurred when a small decrease in the differential head caused a large decrease in the discharge through the 2-year control orifice, which resulted in a decrease in the discharge coefficient, although the total discharge of the multi-stage outlet structure increased.

The differential head increased and decreased differently for each model. This was because the 100-year storm control pipe, that influenced the water surface elevation inside the riser, was of different size in each model. Each pipe transitioned from inlet to outlet control flow at a different stage. Therefore, the variation in the discharge coefficient could not be related directly to the downstream depth (Y_3), as had been the case with Nielsen and Weber (2000). In addition, the fluctuation in the downstream depth was also influenced by the jet of the 10-year storm control orifice, and the nappe of the 50-year storm control weir that plunged into the riser. The latter caused fluctuations of different magnitude in the water surface elevations downstream of the 2-year control orifice, which affected the discharge coefficient. Figure 7.3 illustrates this phenomenon.

It is interesting to note that those models which had similar orifice configurations and 100-year storm pipe sizes, had similar trend lines, as illustrated in Figure 7.3. Models 3 and 6 had two 10-year orifices that discharged directly opposite each other (on either side of the multi-stage outlet structure), whereas Model 2 and Model 4 had one 10-year storm control orifice on the front face of the multi-stage outlet model. Model 5 was the only model with one 10-year storm control orifice on the front and one on the side of the multi-stage outlet structure.

Model 2 and Model 4 had 100-year storm control outlet pipes with internal diameters of approximately 200 mm. Model 3 had one outlet pipe with internal diameter of approximately 298 mm and Model 6 had two of these 298 mm pipes. Model 5 consisted of a 100-year storm control outlet pipe with a large internal diameter of approximately 380 mm.

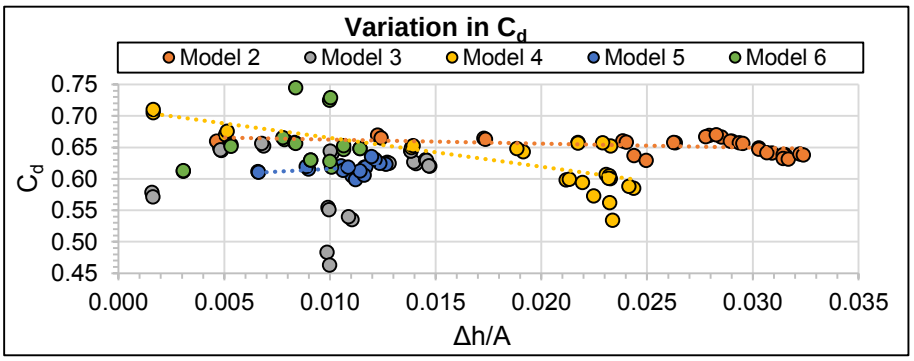

Figure 7.3: Effect of the multi-stage outlet's configuration on C_d

In order to compare the head-discharge relationships between the various orifice sizes, the head-discharge relationship had to be normalised. Refer to Appendix K for the development of Equations 7.1 and 7.2. Equation 7.2 is the physical function relation between the unit discharge and different parameters of channel and orifice size. The differential head was normalised by the vertical length of the orifice (D), as presented in Equation 7.1. The non-dimensionalised discharge and differential head are defined as Q* and H* respectively.

$$H^* = \frac{\Delta h}{D} \tag{7.1}$$

$$Q^* = \frac{q}{D^{1.5}\sqrt{2g}} \tag{7.2}$$

The non-dimensionalised head-discharge curve was determined for all 2-year storm control orifices of Models 2 to 6, which had rectangular orifices, and is presented in Figure 7.4. The data was analysed to determine whether a single new equation of consistent form could be generated that would describe the discharge through the rectangular 2-year storm control orifice for all multi-stage outlet model configurations.

It was difficult to determine a single discharge coefficient for the 2-year storm control orifice of all the models, due to the differences in the configuration of the multi-stage outlet models, which influenced the submergence of the 2-year storm control orifice. The data points that were recorded where the submergence was above 60% were disregarded, since the main purpose of the 2-year orifice was to restrict the outflow from the multi-stage outlet at the maximum 2-year water level. As mentioned, submergence greater than 60% occurred only at upstream depths where the water level was either less than the maximum 2-year storm water level, or, at the maximum 50-year storm water level.

Although the data points, which were recorded where the submergence was greater than 60%, were disregarded, the new proposed discharge coefficient model (Equation 7.3) could still improve the discharge accuracy of the 2-year orifice at the 2-, 5-, 10-, and 20-year water levels.

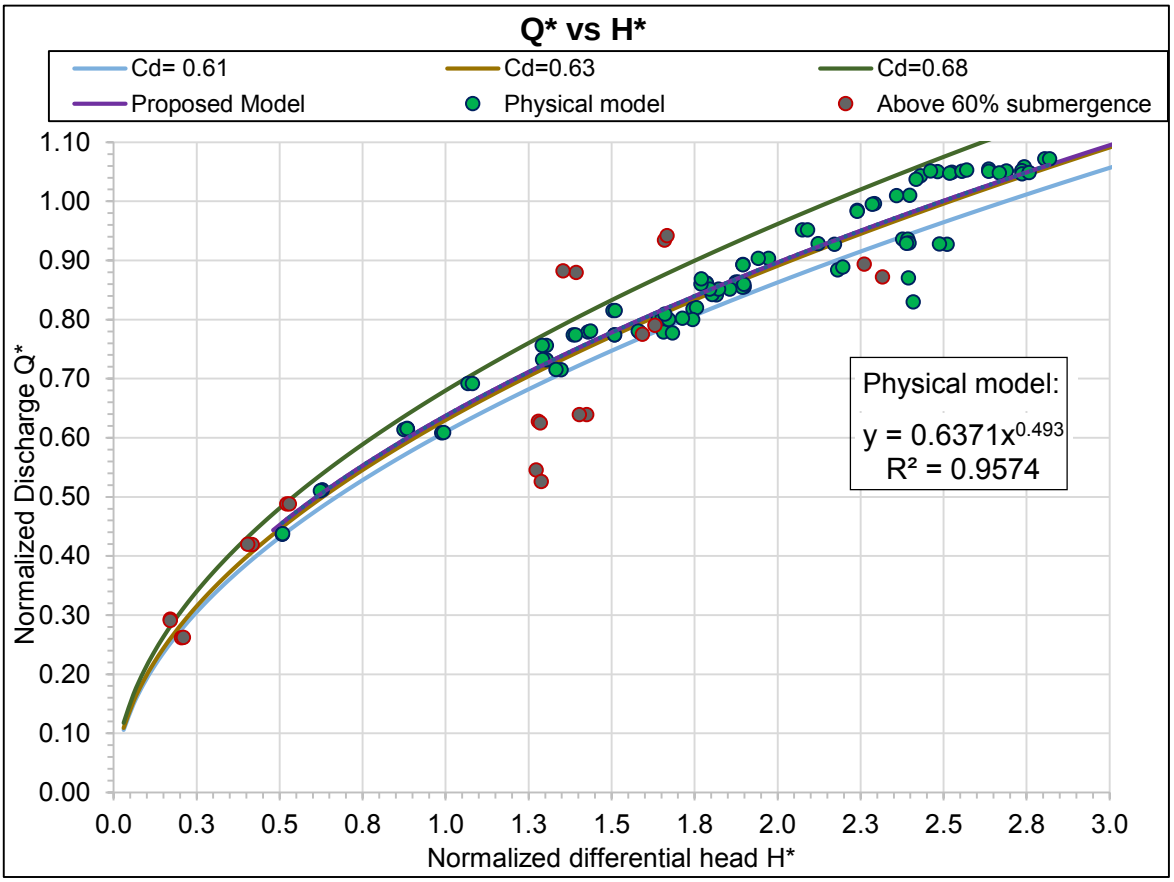

Figure 7.4: Normalised head-discharge curve for all 2-year control orifices

Shown on Figure 6.4 are the results determined with the standard orifice equation, with C_d=0.61, as typically used in multi-stage outlet design, and then with C_d=0.68, which was the highest theoretically derived discharge coefficient when the orifice was less than 60% submerged. The average discharge coefficient of 0.633 fits the proposed model. The proposed model was obtained by using a power-law model for the discharge coefficient. The power-law model for C_d was obtained by fitting the normalised discharge against the normalised differential head and since the dimensionless discharge coefficient is equal to the normalised discharge divided by the square of the normalised differential head, the following model for C_d was obtained for $H^* \geq 0.5$ and less than 60% submergence:

$$C_d = \frac{Q^*}{\sqrt{H^*}} = 0.6371 \left(\frac{\Delta h}{D}\right)^{-0.007} \tag{7.3}$$

It is evident from Figure 6.4 that a single-valued discharge coefficient of 0.61 did not fit the experimental data. The higher average discharge coefficient (0.633) for all the data points were expected, since the literature had indicated that the low flow orifice was affected by the

height at which the orifice is situated above the flume floor or detention basin. The streamlines on the sides of the flume floor gradually become parallel to the floor boundary. The streamlines thus become more suppressed and the jet experience less contraction. This means the contraction decreases, which increases the discharge coefficient (Prohaska *et al.,* 2010).

Prohaska concluded that at heights of 457 mm and 559 mm, the discharge coefficient for a circular free outflow orifice was unaffected by the floor of the tank. When using Equation 7.3 it should be noted that the orifices were tested in the hydraulic laboratory at a height of 9 mm to 108 mm above the flume floor. The height is significant since sedimentation in a detention basin would also decrease the distance between the invert of the orifice and detention floor, increasing the discharge coefficient. Equation 7.3 provides an usable prediction of the discharge coefficient for fully contracted rectangular orifices discharging under submerged conditions.

7.2 Discharge Coefficient of the 10-year Storm Control Orifice

The head on the 10-year storm control orifices during calibration in the hydraulic laboratory was limited. In the standard orifice equation (Equation 2.1), the head is taken as the height of water above the orifice centreline, as the hydrostatic pressure difference between the bottom and top of the orifice is assumed negligible. However, at low head conditions and when the orifice is large, i.e. when the head acting on the orifice is small compared to the size of the orifice, there will be a significant difference between the head acting on the top and bottom of the orifice. Thus, the assumption of Equation 2.1 (for small orifices) would no longer be valid and the discharge through a large rectangular orifice in a flat plate is then defined by Equation 7.4 (Chadwick et al., 2004:47).

$$Q = \frac{2}{3} b_o \sqrt{2g} \left(h_2^{3/2} - h_1^{3/2} \right) \quad \textbf{(7.4)}$$

where:

b_o = width of rectangular orifice (m)

h_1 = head on the upper edge of the orifice (m)

h_2 = head on the lower edge of the orifice (m).

Figure 7.5 evaluate the use of the large-orifice equation instead of the small-orifice equation. From Figure 7.5 it is evident that the large-orifice equation yielded only slightly larger discharge coefficient values at low heads. Thus, the variation in the discharge coefficient (C_d) between the six physical models is independent of the equations used to calculate the discharge from the 10-year storm control orifice. Prohaska *et al.* (2010) also proposed that the large-orifice equation is insignificant for orifices used in riser structures, even at low heads.

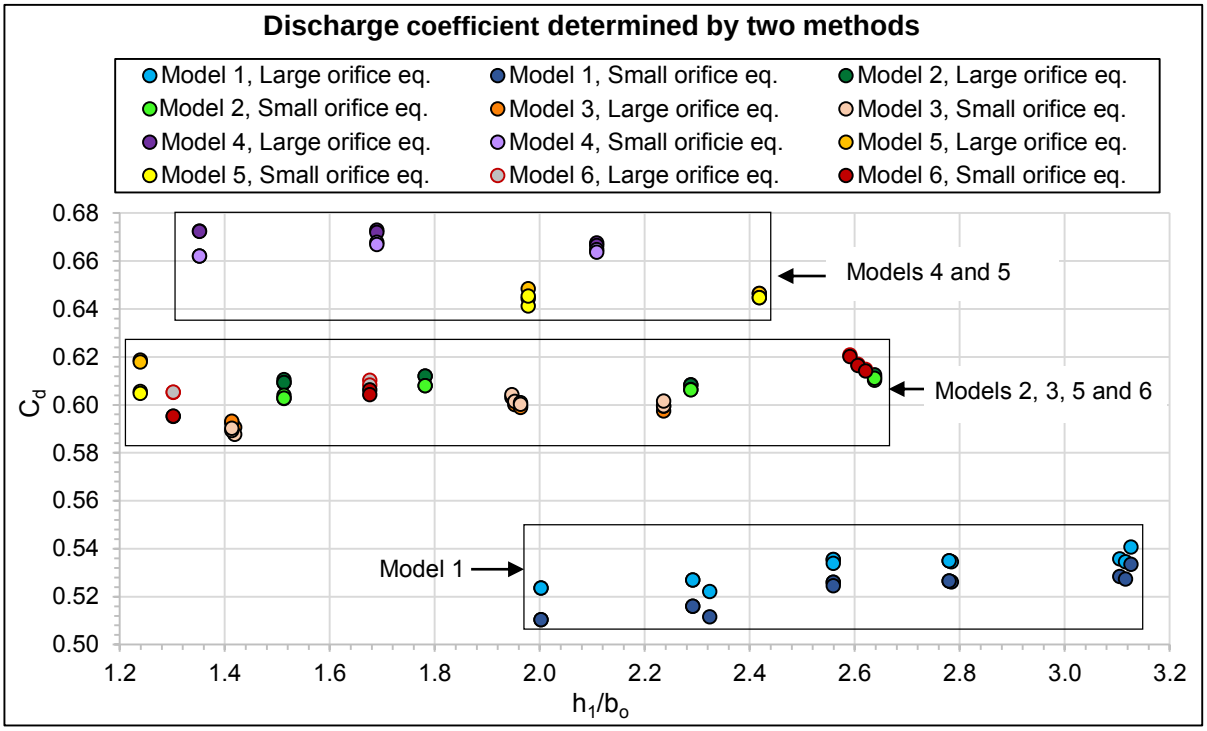

Figure 7.5: Comparison of C_d with the large and small orifice equation

The formation of a vortex at the opening of the 10-year control orifice of Model 1 was observed during calibration of the orifice at very low head values, refer to Figure 7.6. True orifice flow would not occur during the formation of an air-entraining vortex at low heads (Bos, 1989).

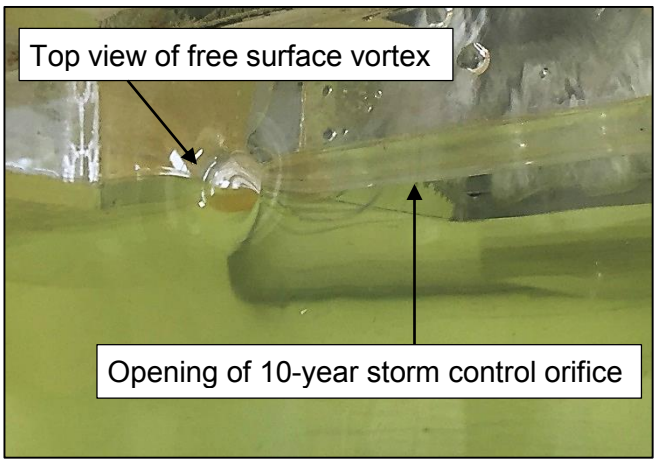

Figure 7.6: Formation of vortex at orifice opening

Thus, the variation in the discharge coefficient between the different physical models could be attributed to many factors, such as the differences in the size of the orifices, the sharpness of the edge of the orifice, interference of boundaries with the contraction of the jet, and the presence of vortices (*Brater et al.,*1996). Similar variation in the characteristics of the orifice is also to be expected under field conditions.

Brandes *et al.* (2015) proposed a model where the discharge coefficient increased non-linearly from 0.55 to 0.65 for thick-walled circular concrete orifice, as the submergence

upstream increased (refer to Section 2.3.2.1). However, the experimentally derived discharge coefficients of the 10-year storm control orifice of each model could not be directly compared to other experimental studies found in literature, because of the lack of the experimental data for thick-walled rectangular orifices at low head.

The equation discharge coefficient of 0.61, as found in literature for rectangular sharp-edged orifices, should therefore be used when sizing the 10-year storm control orifice, since three of the six models had a single value, empirically derived, discharge coefficient of approximately 0.61. Further testing is needed on concrete thick-walled (150 mm) rectangular orifices, before applying greater discharge coefficient values to thick-walled orifices.

7.3 50-year Storm Control Rectangular Weir

The results of the 50-year storm control rectangular weir of Models 2 to 6 indicated that no single theoretical relationship had been found that accurately calculated the discharge over the weir for all configurations. The reason being that the crests of the weirs fell between sharp and broad crested. A broad-crested or thick-walled weir could discharge as a sharp-crested weir when the head reaches one to two times the breadth of the weir (crest length in the direction of flow), according to Brater *et al*. (1996). Under these conditions, the nappe becomes detached from the weir crest. Each theoretical weir discharge equation had different limits of application and determined the flow regime over the weir for different conditions (see Appendix L).

To ensure reasonable accuracy, once these limits had been reached, the spreadsheet-based model was adjusted accordingly. Thus, for every different upstream head (h_1) to weir crest breadth (b_c) ratio, the theoretical equation was classified as either broad-crested or sharp-crested. Fourteen theoretical equations with different limitations and ranges were compared to the experimental data from the 50-year storm control rectangular weir (see Appendix L).

The theoretical equation that differed the least when compared to the experimental data, for all model configurations under similar limits, were then used in the spreadsheet-based model to ensure that the spreadsheet calculations would be applicable to a wide range of limits and conditions. Based on the laboratory results and observations, Table 7.1 summarises the theoretical equations for use in the spreadsheet-based model.

After applying these theoretical equation changes presented in Table 7.1 to the spreadsheet model, the theoretical data fit more closely to the physical model data (see Figure 7.7) than did Equation 2.19. Equation 2.19 was generally recommended by most of the stormwater drainage manuals, such as Knox County, Tennessee-Stormwater Management Manual (2008), Iowa Stormwater Management Manual (2009) and Hydrology Studio (2014), to name a few. The percentage difference between the discharges determined by the spreadsheet-based model and the experimental data, for the 2-year RI storm, decreased by 1.42% for Model 2 and decreased by 3.14% for Model 6 after applying Equation 7.1.

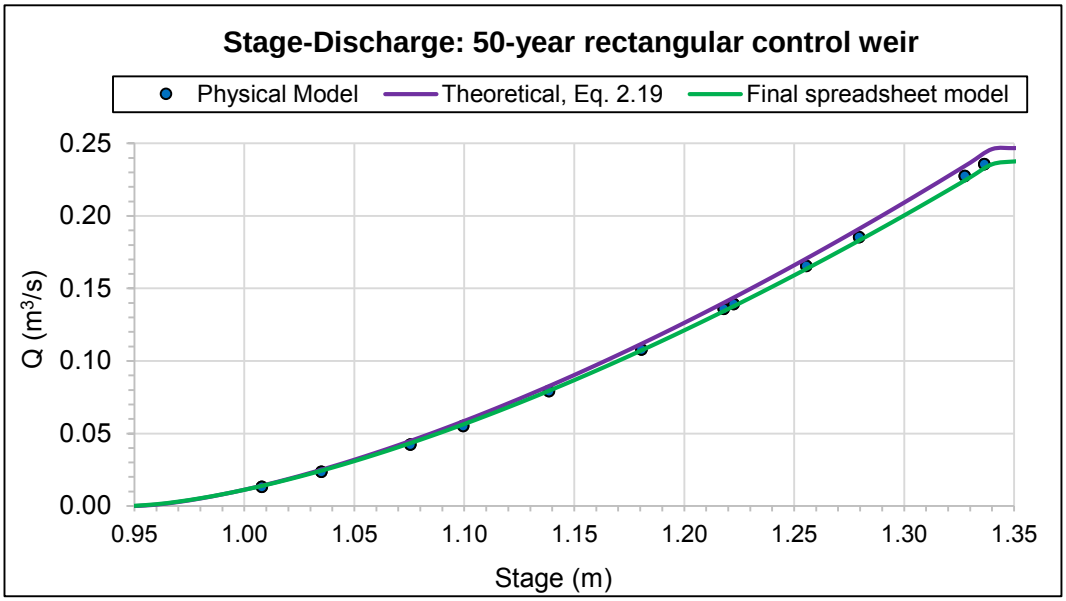

Figure 7.7: Stage-discharge relationship for the 50-year weir component of Model 3

From visual observations, fluctuation in the water surface elevation inside the riser caused surface waves periodically to fill the under-nappe cavity of the 50-year storm control weir. Because of this, the nappe was not fully ventilated at the 10-year maximum water surface elevation. An underpressure beneath the nappe deflects the nappe downwards, increasing the curvature of the overfalling jet, which leads to an increase in the discharge (Bos, 1989). This occurrence was not taken into account in the spreadsheet-based model.

Table 7.1: Theoretical equations to be used for calculations of multi-stage outlets

Reference	Flow type	Equation	Discharge coefficient	Remarks/Range
Physical Model Study (Section 7.1), or Ontario Ministry of Environment, 2003	Rectangular orifice	$Q = C_d A\sqrt{2g\Delta h}$	$C_d = 0.6371\,(\frac{\Delta h}{D})^{-0.007}$ or a constant coefficient of 0.63	If at a distance of 9 mm to 108 mm from detention basin floor. Submergence ratio < 60%
Kindsvater and Carter, 1957	Fully contracted, full-width, and partially contracted sharp-edged rectangular weir	$Q = C_e L_e {h_e}^{1.5}$ L_e equals $L+K_L$, where: for $0 \le L_w/B \le 0.35$: $K_L = 0.002298 + 0.00048\,(\frac{L}{B})$ for $0.35 < L/B \le 1$: $K_L = -0.10609(\frac{L_w}{B})^4 + 0.1922(\frac{L_w}{B})^3 - 0.11417(\frac{L_w}{B})^2 + 0.028182\,(\frac{L_w}{B}) - 0.00006$ h_e equals $h_1 + K_h$, where: K_h=0.001 m Let B equal the width of the riser structure	$C_e = \alpha_{ce}\frac{h_w}{P_s} + \beta_{ce}$, with $\beta ce = 1.724 + 0.04789\,(L_w/B)$, and $\alpha_{ce} = \frac{-0.00470432 + 0.030365(\frac{L_w}{B})}{1 - 1.76542\,(\frac{L_w}{B}) + 0.8779917(\frac{L_w}{B})^2}$	h_1> 30mm, L_w >150mm, P_s >100mm. Tailwater should remain at least 0.05 m below the crest of weir
Henderson, 1966, as cited in SANRAL, 2013	Sharp-edged rectangular weir	$q = C_d\frac{2}{3}\sqrt{2g}{h_w}^{1.5}$	$C_d = 0.611 + 0.08\frac{h_w}{P_s}$	For a model where the weir length (L_w) is equal to the inside width of the riser, refer to Model 3.Thus for, $B-L_w < 4h_1$
Bureau of Reclamation, 2001 and Brater *et al*., 1996	Broad-crested rectangular weir	$Q = C_d L_w {h_w}^{1.5}$	Varying discharge coefficient, refer to Table 2.3	Only valid if $1/20\ b_c < h_1 < 1/2\ b_c$
Chanson, 2004		$q = C_d\frac{2}{3}\sqrt{\frac{2}{3}g{h_w}^3}$	$C_d = 0.95$ if $0.15 < h_1/P_s < 0.6$	

7.4 100-year Outlet Pipe

Figure 7.8 indicates that the stage-discharge curve of Model 6, determined by the data collected during the physical model tests, fit more closely to the stage-discharge curve of the spreadsheet-based model, when the 100-year storm control outlet pipe was calculated theoretically under inlet conditions. This was true for all tested models. The outflow of the 100-year pipe that was physically modelled indicated that inlet control governed, producing higher outflows than expected. The velocity head of the physical data was added to the water elevation inside the riser, but this made very little difference, as shown in Figure 7.9 (b).

It could also be that the roughness of the outlet pipe differed from the assumed Manning value of 0.009 for PVC pipes, since under outlet control, the discharge depends on the

manning roughness of the pipe. The investigation of the pipe's manning value was outside the scope of the physical model study.

The stage increased sharply at 1.01 m, since the three rectangular weirs, sized to control the 50-year storm, then started to contribute to the outflow of the multi-stage outlet. At stage 1.136 m, the 10-year sized orifices of the physically modelled multi-stage outlet were submerged. Thus, as the head produced by the pipe increased, the outflow from the 2-year storm control orifice components and 10-year sized orifice components decreased, as illustrated in Figure 7.8. When the head produced by the 100-year storm control pipe, which acted as a tailwater elevation against the other multi-stage components, was at almost the same stage as the current upstream water surface elevation, the pipe would become the controlling component of the multi-stage outlet.

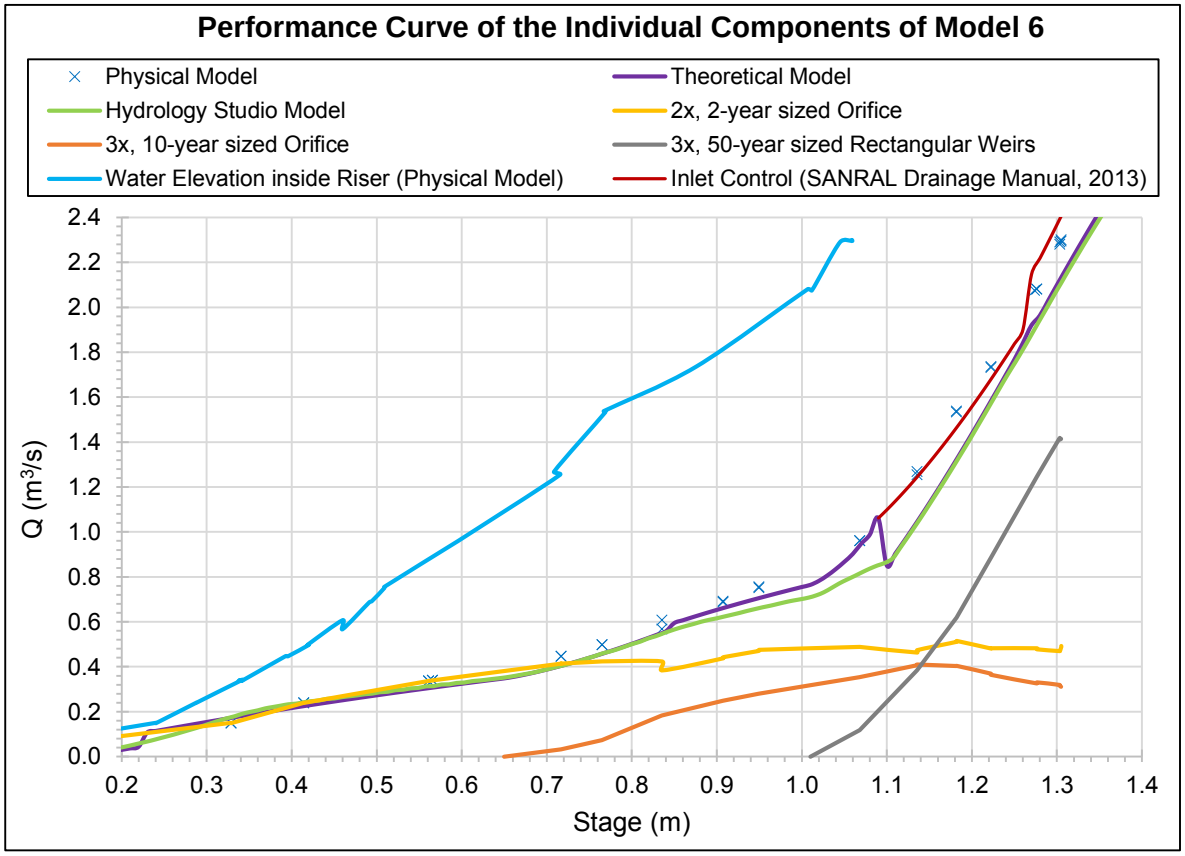

Figure 7.8: Stage-discharge relationship of individual components of Model 6

When the discharge from the 100-year outlet pipe was calculated theoretically under inlet control conditions, the theoretically calculated head of the 100-year pipe (water elevation inside the riser) and the experimental head plot closer together, as illustrated by Figure 7.9. This explains why the 50- and 100-year target discharges of the aforementioned physical models were exceeded. From Figure 7.9 it is evident that, at the lower stages, the water inside the riser was lower than theoretically calculated.

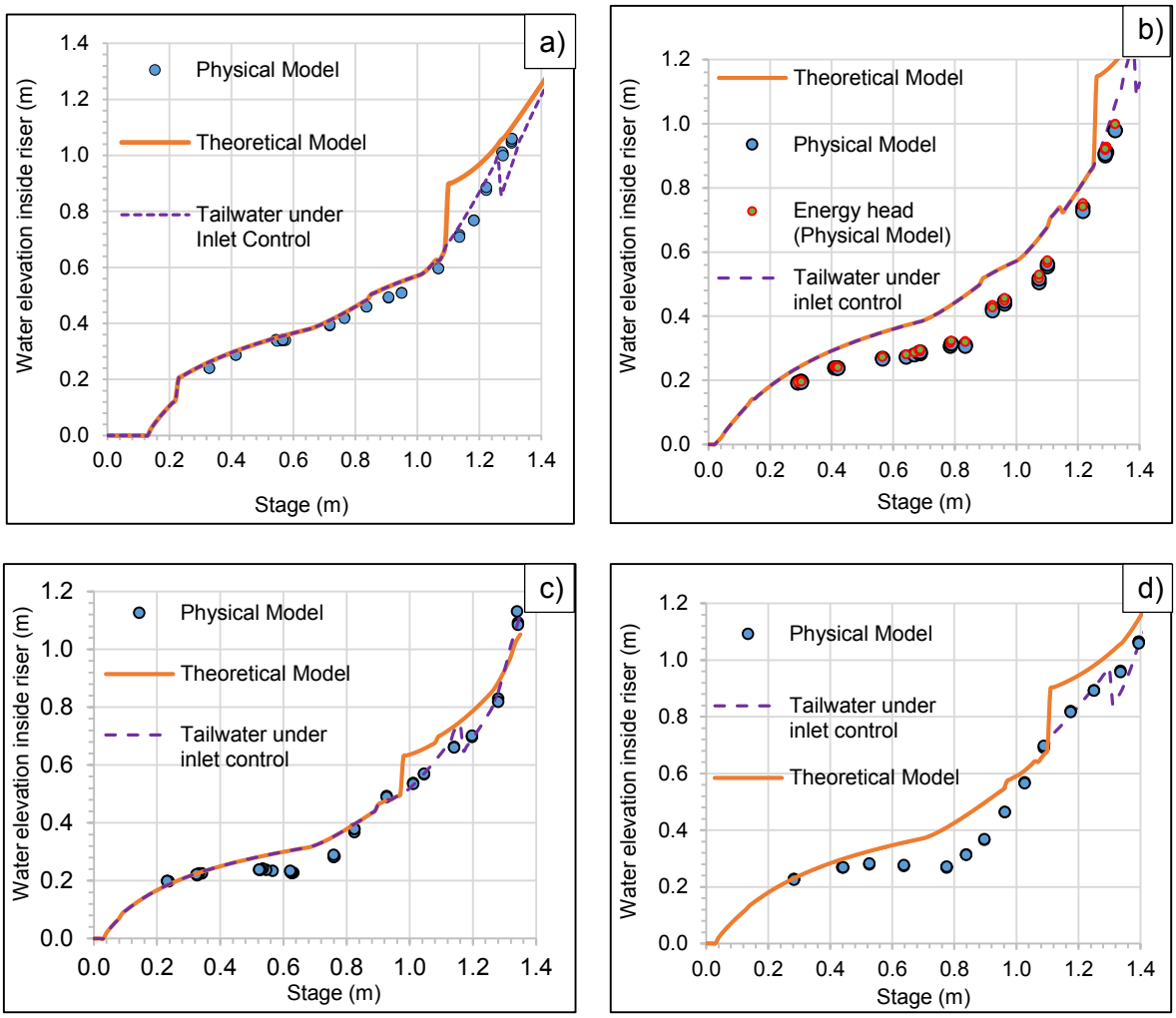

Figure 7.9: Water elevation inside riser for (a) Model 6, (b) Model 5, (c) Model 4, and (d) Model 3

When water surface fluctuations were present, a visual averaging of the pressure reading on the piezometer was required. When the maximum pressure reading was used to determine the water surface elevation inside the riser, instead of the average reading, it equalled the energy grade line. The piezometer was installed just downstream of the low flow orifice, whereas the water elevation further downstream, at the entrance of the 100-year storm control outlet pipe, was higher, due to the contraction of the flow at the pipe inlet. This explains why the water surface inside the riser was lower, when compared to the theoretical model. Figure 7.9 (c) indicates that when the flow in the 100-year outlet pipe converts from partially-full to full-pipe flow after stage 1.2 m, the water levels in the pipe rise significantly.

In addition, the irregular flow patterns inside the riser increase the energy losses. The resulting turbulence and energy dissipation within the riser box from the free outfalls of the 10-year storm control orifice and 50-year storm control weir have an effect on the head loss for the low flow orifice, whose flow is not plunging. An adjusted minor loss coefficient is therefore required to account for the additional energy losses inside the riser of the multi-stage outlet structure.

In conclusion, the backwater head produced by the 100-year modelled pipe affected the measured differential head, which differed from the theoretical differential head. To improve the spreadsheet-based (theoretical) model, further investigation with regard to the energy and pressure losses inside the box-shaped riser of the multi-stage outlet is required, in order to determine the discharge from the submerged orifices and weirs as accurately as possible. This emphasise the effect that the selection of the 100-year outlet pipe could have on the discharge of the other components of the multi-stage outlet structure.

8. Conclusions and Recommendations

8.1 Conclusions

Physical models of detention basin multi-stage outlet structures are rare in hydraulic structure research experiments. Insight into the variable stage-discharge relationship of the multi-stage outlet structure was required to verify whether it would be suitable for the control of multiple storm events. Experimental data was required for the development of a spreadsheet program for practitioners to use when determining the discharge from multi-stage outlet structures. Therefore, a 1:3 scaled physical model study was undertaken in order to verify that the theoretical equations and design guidelines recommended in the literature accurately reflected the flow through multi-stage outlet structures.

Six different configurations of multi-stage outlet structures were tested in the hydraulic laboratory to evaluate the control of discharge for a wide range of scenarios. Six models were designed to control the flow to pre-development peak rates, which had been determined for scenarios where the catchments were situated in either coastal or inland regions, receiving either 400 mm, 700 mm, or 1000 mm of MAP. Thus, each of the six models was designed to control different peak discharges.

The following conclusions resulted from the data collected by means of the physical model study and the associated literature review:

- From the preliminary designs, eight of the eleven multi-stage outlets that had been designed to control the 20-year RI storms, over-controlled the 50-year design storm, and more so than the multi-stage outlets with a rectangular orifice, which were sized to control a 10-year design storm. The 10-year storm control orifice had a greater head during a 50-year RI storm than the 20-year storm control orifice did. The 20-year storm control orifice was designed at a higher stage (20-year water level compared to the 10-year water level). Therefore, the 20-year storm control orifice had a smaller discharge capacity than the 10-year storm control orifice at the corresponding 50-year head.

- Preliminary design calculations indicated that the three multi-stage outlets (designs C.8, I.3 and I.4), that had been sized with openings to control a 20-year RI storm, were ineffective in restricting the 10-year RI storm, while having a storage volume less than the alternative designs. In order for these designs to attenuate all design storms, the storage volume would have to be increased. Therefore, re-designing the 20-year RI control device would not be a feasible solution, since the alternative designs, which had been designed with an opening suitable to control the 10-year RI storm, were effective in restricting the 20-year RI to an outflow equal to or less than the pre-development peak flow.

- It was concluded in Section 4.5.8 that multi-stage outlets that are designed to control 2-, 10-, 50- and 100-year RI storms, would also be able to control the 5-year and 20-year RI storms and require less storage volume for the detention pond. When designing for the 2-, 20-, 50- and 100-year RI storms, the multi-stage outlet is more likely to provide insufficient constriction of the 10-year RI storm event. The physical model study verified that a multi-stage outlet comprising discharge devices sized to control four of the RI storm types, was sufficient to control all six RI storms. This shortens the design process of the multi-stage outlet.

- Preliminary calculations of the multi-stage outlets designed with a 90° V-notch weir, over-controlled the target discharge for the 50-year RI storm. The crest length of a rectangular weir can easily be increased, whereas a V-notch weir requires a higher riser structure. This is significant, since discharge control devices in stormwater detention ponds are frequently flowing under low heads (Spencer, 2013). Therefore, it is recommended that a rectangular weir, instead of a 90° V-notch weir, be used to control the 50-year RI storm. The discharge from the 50-year storm control rectangular weirs was closer to the target discharge than that of the V-notch weir, which minimises the depth of the pond along with the storage volume.

- Riser structures should be over-sized to ensure that the water inside the riser is less turbulent, as turbulence greatly affected the discharge of the low flow orifice during the physical model tests.

- The discharge from the 2-year storm control orifice was influenced by the flume floor (or detention basin). The short distance between the invert of the low flow orifice and the flume floor reduced the contraction of the water jet, thus the discharge and contraction coefficients were higher. Knowing the extent and effect of suppression could be valuable when determining a minimum height an orifice should be placed above the ground level.

- The standard orifice equation with a single-valued discharge coefficient of 0.61 does not fit the experimental data. The empirically derived discharge coefficient varied with different heads. It was concluded that a power-law model (C_d= 0.6371 $(\Delta h/D)^{-0.007}$) provided an usable prediction of the discharge coefficient for submerged, fully contracted rectangular orifices, which discharge at heights of 9 mm to 108 mm above ground level.

- The results of the 50-year storm control rectangular weir component of Models 2 to 6 indicated that no single theoretical relationship was found that accurately calculates the discharge over the weir for all configurations. The spreadsheet-based model determined the discharge over the 50-year control weir as being broad-crested overflow, when the

head (h_1) to crest breadth (b_c) ratio was within the limits ($b_c/20 < h_1 < b_c/2$). As the head increases, the flow is determined by means of the sharp-crested weir formula.

- The final compiled spreadsheet-based model (theoretical) and coded Visual Basic program showed good agreement with the experimental data and would assist practitioners in the design of multi-stage outlet structures.

8.2 Recommended Multi-Stage Outlet Structure Design Guidelines

The researcher recommends using the Excel spreadsheet-based model, or Visual Studio code (refer to Appendix E and Appendix M) created in conjunction with this physical model study to calculate the discharge through a multi-stage outlet structures. The overall experimental results are in good agreement with the literature reviewed (from which the spreadsheet was compiled) and the visual studio output for all configurations tested. Refer to Figure 8.1, where the final spreadsheet stage-discharge plot is showing the rating calculated from the spreadsheet-based model (purple), the output from the Visual Studio code (green) and the physical model data (blue) of Model 2.

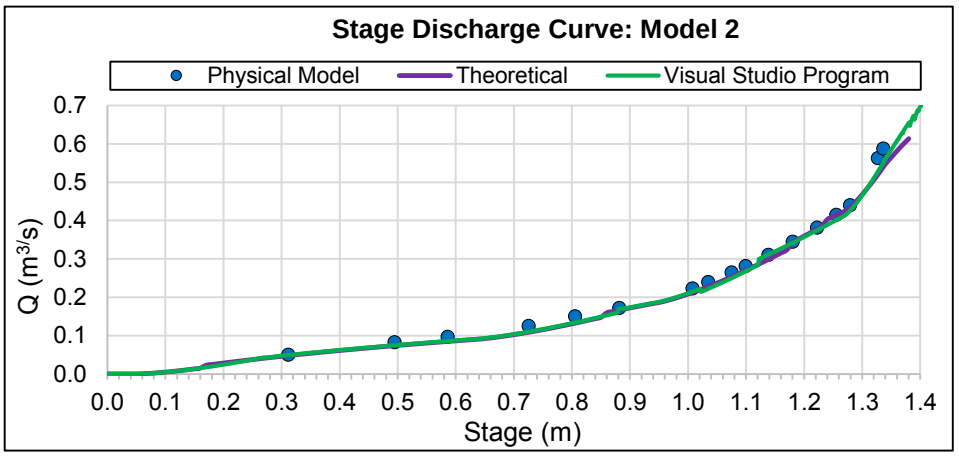

Figure 8.1: Stage-discharge plot showing the rating calculated and measured for Model 2

The spreadsheet has some limitations:

- Only horizontal, flat weir riser structures and trash racks were constructed.
- The spreadsheet determines the quantity of stormwater released by the multi-stage outlet only, and does not calculate the flow through an extended, water quality orifice at the front of the outlet structure. The necessary calculations could be added if required.
- The theoretical equation used to determine the discharge over the riser (overflow structure of the multi-stage outlet) and trash rack could not be verified against the experimental data, since the riser and 50-year control weir operated simultaneously, which would require a combined discharge coefficient. Therefore, it is recommended that the discharge over the riser should be verified by a separate physical model study.

- Further investigation is required regarding the energy and pressure losses inside the box-shaped riser of the multi-stage outlet in order to determine the discharge from the submerged orifices and weirs as accurately as possible.

Literature recommends a minimum distance of 0.0348m (1 ft) between the maximum water surface elevation of one control device and the invert of the next discharge control device (Virginia Department of Conservation and Recreation, 1999). However, there are instances where this maximum water surface is just above the upper edge of the 10-year control orifice, since the orifice restricts the flow by operating first as a weir. The crest of the 50-year control weir cannot be placed at only 0.0348 m above the upper edge of the 10-year control orifice because of construction constraints. As a result of these concerns, it is recommended that a model configuration similar to Model 3 be used when the distance between consecutive discharge control components is limited, or a minimum spacing of 0.06 m is recommended to allow for construction limitations.

9. Future Research on the Design of Multi-Stage Outlet Structures

The preliminary design of multi-stage outlet structures relies on the estimation of the required storage volume of the pond in order to determine the maximum elevation of the water surface, and hence also the head on the discharge control device, for different recurrence interval storms. The current research study used the Rational Formula Hydrograph method (Equation 4.1) to estimate the required storage volume, which approximates the outflow as a triangular shaped outflow hydrograph. Rational method triangular design inflow and outflow hydrographs were used to perform level-pool routing calculations, which determine whether the control devices of the multi-stage outlet structure would restrict the outflow.

It is recommended that further investigation be undertaken to compare the effect of different design hydrographs, for instance, triangular hydrographs compared to unit hydrographs, on the design of multi-stage outlet structures. If real-time (historical run-off data) are available it should rather be used instead of the deterministic or empirical methods to determine the design floods.

The physical model study indicated that the placement of multiple orifices in the same vertical plane (Models 2 and 4) instead of the placement of orifices in opposite vertical planes of the multi-stage outlet model (Models 3, 5 and 6) affects the flow profile inside the riser which, in effect, influences the discharge of the low flow orifice. However, the outlet pipe sizes of the models differed, which also influenced the discharge of the low flow orifice. Thus, further in-depth investigation is required, which analyses only the interaction of multiple orifices and evaluates the changes in discharge when orifices are spaced close together.

The current models that were tested had orifices spaced as closely as 25 mm (75 mm prototype dimension) to the 50-year weir, and it may be questioned whether the discharge of the 10-year orifice was affected by the flow drawdown of the 50-year control weir. Therefore, a physical model study is required, which investigate the interaction of the discharge control devices at different spacing. When designing a multi-stage outlet structure, the designer is forced to space the discharge control devices as close to the consecutive device in order to limit both the amount of storage space required and the depth of the detention pond.

Future research is required to verify the hydraulic performance of the multi-stage outlet under unsteady stage conditions, since the effects of a falling head on the discharge of both the thick-plate rectangular orifice and weir are largely unstudied (Spencer, 2013). The consideration of time scaling may also be important for future physical model test, as the turbulence created inside the riser box of the multi-stage outlet may be different if the flow rise or fall at different flow rates and in return affect local energy losses (Rubinato, 2015).

The results of the investigation of multi-stage outlet structures indicated that some uncertainty exists as to the performance of the submerged 2-year storm control orifice, as the components of the multi-stage models tested in the hydraulic laboratory operated under circumstances of low hydraulic head. The discharge coefficient of the 2-year storm control orifice was empirically derived from data collected experimentally for the 10-year storm control orifice and 50-year storm control weir. It was only possible to take three to five head-discharge readings when the 10-year storm control orifice and 50-year storm control weir were calibrated individually, as the available head on the orifices and weirs was limited. It is therefore recommended that a model study should be conducted on a thick-plate rectangular orifice of at least 150 mm under submerged conditions to verify that the discharge coefficient does not vary greatly and is greater than 0.61.

Further investigation of both pressure and energy changes inside multi-stage outlet risers, and energy losses due to pipe friction, should be conducted in a hydraulic laboratory. The effects on the energy and pressure changes as a result of varying riser (box-shaped pit) sizes, the ratio of outlet pipe diameters to inlet orifice opening sizes, and inflows from the top of the riser, should be investigated. The theoretical equations used to determine the head produced by the outlet pipe should account for the friction between the fluid and the walls of the riser box and the turbulence caused whenever the flow in the riser box is redirected of affected by the other devices of the multi-stage outlet structure.

10. References

ARC. 2014. Estate Global Standards. *The Residential Industry Journal*, **1**. South Africa: Estate Living.

Aldous, M.G. 2007. The Perceived Economic Impact of the City of Johannesburg's Storm Water Attenuation Policy on Private Property Developers. Johannesburg: Nelson Mandela Metropolitan University.

Barlow, W.T. and Brandes, D. 2015. Stage-Discharge Models for Concrete Orifices: Impact on Estimating Detention Basin Drawdown Time. *Journal of Irrigation and Drainage Engineering,* **141** (12):1-7.

Barlow, W.T. and Brandes, D. 2012. New Method for Modelling Thin-walled Orifice Flow under Partially Submerged Conditions. *Journal of Irrigation and Drainage Engineering,* **131** (10): 924-928.

Bos, M.G. 1989. *Discharge Measurement Structures, 3rd ed.* Wageningen, The Netherlands: International Institute for Land Reclamation and Improvement.

Bengtson, H.H. 2011. *Sharp-Crested Weirs for Open Channel Flow measurement*. [Online]. Available: http://www.pdhsite.com/courses/ [2015, Mei 18].

Brater, E.F, King, H.W., Lindell, J.E. and Wei, C.Y. 1996. *Handbook of Hydraulic*, 7th ed. United States of America: McGraw-Hill Inc.

Brown, S.A., Schall, J.D., Morris, J.L., Doherty, C.L., Stein, S.M. and Warner, J.C. 2009. Urban Drainage Design Manual. *Hydraulic Engineering Circular 22, 3rd ed.* Washington, D.C: Federal Highway Administration.

Bureau of Indian Standards. 2012. *Recommendations for Design of Trash Racks for Intakes*. New Delhi: BIS.

Burke, J. and Mayer, X. 2009. *Strategic Guidance towards Prioritising Stormwater Management Research in Human Settlements*. Report No. 1670/1/09. Gezina: Water Research Commission.

Chanson, H. 2004. *The Hydraulics of Open Channel Flow: An Introduction- Basic principles, Sediment Motion, Hydraulic Modeling, Design of Hydraulic Structures, 2nded*. Oxford: Elsevier Butterworth-Heinemann.

City of Cape Town. 2009. *Management of Urban Stormwater Impacts Policy.*

City of Cape Town. 2010. Evaluation of Developable Land within Urban Edge. *Metropolitan Spatial Planning and Urban Design.*

City of Cape Town. 2011. Standard Requirements for a Stromwater Master Plan.

City of Cape Town. 2012. Zoning Scheme Regulation. *A Component of the Policy-Driven Land Use Management System.*

Chadwick, A., Morfett, J. and Borthwick, M. 2004. *Hydraulics in Civil and Environmental Engineering*. Oxon: Spon Press.

CSIR. 2000. *Guidelines for Human Settlement Planning and Design, The Red Book, 2nd ed*. Vol. 1. Pretoria.

Chow, V.T. 1959. *Open Channel Hydraulics*. New York: McGraw-Hill Inc.

Debo, T.N., Reese, A.J. 2003. *Municipal Stormwater Management*. United States of America: CRC Press LLC.

Dennis Moss Partnership Project Portfolio. 2014. [Online]. Available: http://www.dmp.co.za/portfolio/urban-design/ [2015, June 12].

***Design and Construction of Urban Stormwater Management Systems*.** 1992. New York: American Society of Civil Engineers, Alexandria: Water Environment Federation.

eThekwini Municipality. 2008. *Design Manual: Guidelines and Policy for the Design of Stormwater Drainage and Stormwater Management Systems*. Durban: Coastal Stormwater and Catchment Management Department.

Emerson, C.H. 2003. Evaluation of the Additive Effects of Stormwater Detention Basins at the Watershed Scale. Philadelphia: Drexel University

Graham, M., Magenis, D., Ramsbottom, D., Rickard, C., Robinson, P., Whiting, M. and Wicks, H. 2009. *Trash and Security Screen Guide*. Bristol: Environment Agency.

Guo, C.Y. 2012. *Hydraulic Capacity of CDOT TYPE C and D Area Inlets.* Denver: Urban Drainage and Flood Control District.

Hager, W.H. 1994. Breitkroniger U¨ berfall (Broad-crested weir). [in German].

Headley, R.R, Wyrick, J.R. 2009. Modeling Stormwater Basins for Potential Retrofit Designs. Glassboro: Rowan University.

Heller, V. 2011. Scale effects in physical hydraulic engineering models. *Journal of Hydraulic Research*, **49** (3): 293-306.

Henderson, F.M. *Open Channel Flow*. New York: Macmillan Publishing Co., Inc.

Hotchkiss, T.S. 2015. Evaluation of the use of Flood Attenuation Controls for the Management of Urban Stormwater Impacts in Cape Town, South Africa. Stellenbosch: University of Stellenbosch.

Hydrology Studio (computer software). 2015. [Online]. Available: https://www.hydrologystudio.com/ [2015, June 20].

***Hydrology Studio User's Guide*. 2014.** [Online]. Available: http://www.hydrologystudio.com [2015, February 26].

Institute for Agricultural Engineering. 2003. *Irrigation Design Manual*. ARC.

Iowa Stormwater Management Manual. 2009. [Online]. Available: http://www.iowadnr.gov/Environment/WaterQuality/WatershedImprovement/WatershedBasics/Stormwater/StormwaterManual.aspx [2015, March 23].

Jones, J.E., Guo, J., Urbonas, B. and Pittinger, R. 2006. *Essential Safety Consideration for Urban Stormwater Retention and Detention Ponds.* [Online]. Available: http://www.udfcd.org [2015, April 15].

Kindsvater, C.E. and Carter, R.W.C. 1957. Discharge characteristics of rectangular thin-plate weirs. *Journal of the Hydraulic Division*, **83**(6).

Knox County. 2008. *Know County, Tennessee-Stormwater Management Manual, Vol.2.* 2008. Knoxville: AMEC Earth and Environmental Inc.

Kobus, H. 1980. *Hydraulic Modelling*. Hamburg, Berlin: Verlag Paul Parey

Lafleur, D.W and McBean, E.A. 1981. Multi-Stage Outlet Design of Stormwater Retention Facilities. *Canadian Water Resources Journal,* **6**(1):25-47.

Laramie County Conservation District. 2011. *Best Management Practices for Stormwater Runoff*. [Online]. Available: http://www.lccdnet.org/wp-content/uploads/2011/04/Ponds.pdf [2015, April 23].

Law, D. 2015. Trash rack design at multi-stage outlet structures, E-mail to M. Myburgh [Online], 10 Oct. Available E-mail: David.Law@entura.com.au.

McCuen, R.H. 1998. *Hydrologic Analysis and Design*, 2nd ed. Upper Saddle River: Pearson Education.

McCuen, R.H., Johnson, P.A. and Ragan, R.M. 2002. Highway Hydrology. *Hydraulic Design Series Number 2, 2nd ed*. Washington, D.C: Federal Highway Administration.

McEnroe, B.M., Steichen, J.M. and Schweiger, R.M. 1988. Hydraulics of Perforated Riser Inlets for Underground Outlet Terraces. *Transactions of the American Society of Agricultural Engineers*, **31**(4):1082-1085.

Metcalf and Eddy. 1972. *Wastewater Engineering*. New York: McGraw-Hill Inc.

Nielsen, K.D.and Weber, I.J. 2000. *Submergence Effects on Discharge Coefficients for Rectangular Orifices*. United States: American Society of Civil Engineers

Normann, J.M., Houghtalen, R.J. and Johnston, W.J. 2001. *Hydraulic Design of Highway Culverts, 2nd ed.* Washington, D.C: Federal Highway Administration.

Novak, P. and Cábelka, J. 1981. *Models in Hydraulic Engineering – Physical Principles and Design Applications*. London: Pitman.

Novak, P., Guinot, V., Jeffrey A. and Reeve, D.E. 2010. *Hydraulic Modelling: An Introduction.* Oxon: Spon Press.

Ontario Ministry of the Environment. 2003. *Stormwater Management Planning and Design Manual*.

Prohaska, P.D., Khan, A. A. and Kaye, N.B. 2010. Investigation of flow through orifices in riser pipes. *Journal of Irrigation and Drainage Engineering,* **136**(5), 340-347.

***Pennsylvania Stormwater Best Management Practices Manual*.** 2006. Harrisburg: Department of Environmental Protection, Bureau of Watershed Management.

Ramamurthy, A.S., Tim, U.S and Rao, M.V.J.1988. Characteristics of square-edged and round-nosed broad-crested weirs. *Journal of Irrigation and Drainage Engineering. ASCE* **1**:114.

Ramamurthy, A.S. and Vo, N.D. 1993. Characteristics of Circular-Crested Weir. *Journal of Hydraulic Engineering,* **119**:1055.

Rubinato, M. 2015. Physical scale modelling of urban flood systems. Department of Civil and Structural Engineering: University of Sheffield.

SANRAL. 2013. *Drainage Manual, 6th ed*. Pretoria: The South African National Roads Agency SOC Ltd.

Sandvik, A. 1985. Proportional weirs for stormwater pond outlets. *Civil Engineering*. ASCE, March: 54-56.

Sarginson, E.J. 1972. The influence of surface on weir flow. *Journal of Hydraulic Research*, **10**(4):431-446.

Sivanathan, S., Martens, S., Sivapalan, M. and Davies, J. 2000. *Multi Stage Outlet Compensating Basins for Multi ARI Design.* Australia: Institution of Engineers Australia.

Shand, M. 2013. Factors affecting lifetime costs of water supply pipelines. Unpublished paper delivered at the IMESA Conference. South Africa.

Spencer, P.R. 2013. Investigation of Discharge Behaviour from a Sharp-Edged Circular Orifice in Both Weir and Orifice Flow Regimes Using and Unsteady Experimental Procedure. Ontario: University of Western Ontario.

Stringer, T. 2013. No-Fail Detention Pond Design. *Hydrology Studio blog.* [Web log post]. Available: https://www.hydrologystudio.com/no-fail-detention-pond-design/ [2015, April 12].

***Stormwater Design Example**: Pond.* n.d. [Online]. Available: http://www.stormwatercenter.net/Manual_Builder/pond_design_example.htm [2015, June 7].

Townshend, P.D., *Automatic Control Equipment to reduce the size of retention facilities in urban areas.* [Online]. Available: http://amanziflow.co.za/index.php?option=com_contentandview=articleandid=106andItemid=71 [2015, May 18].

Tullis, B.P., Olsen, E.C. and Gardener, K. 2008. Reducing Detention Volumes with Improved Outlet Structures. *Journal of Irrigation and Drainage Engineering*, **134**:824-830.

Urban Drainage and Flood Control District (UDFCD). 2010. *Urban Storm Drainage Criteria Manual*, *Best Management Practices,* Vol. 3, Denver: Water Resources Publication, LLC.

U.S. Department of the Interior, Bureau of Reclamation. 2001. *Water Measurement Manual.* [Online]. Available: http://www.usbr.gov/pmts/hydraulics_lab/pubs/wmm/index.htm, [2015, June 19].

U.S Department of the Interior, Bureau of Reclamation. 2014. *Physical Modeling of Overflow Outlets for Extended Detention Stormwater Basins.* [Online]. Available: http://www.usbr.gov/pmts/hydraulics_lab/pubs/, [2015, September 9].

Van Vuuren, S.J. 2012. *Influence of Catchment Development on Peak Urban Runoff*. Report No. 1752/1/12. Gezina: Water Research Commisson.

Vatankhah, A.R. 2010. Flow Measurements using Circular Sharp-Crested Weirs. *Flow measurement and Instrumentation,* **21**(2): 118-122.

Virginia Department of Conservations and Recreation. 1999a. *Virginia Stormwater Manangement Handbook, 1st ed.*, Vol. 1. Richmond: NOAA.

Virginia Department of Conservations and Recreation. 1999b. *Virginia Stormwater Manangement Handbook, 1st ed.*, Vol. 2. Richmond: NOAA.

Villemonte, J.R. 1947. Submerged-Weir Discharge Studies. *Engineering News Records*.

Webber, N.B. 1979. *Fluid Mechanics for Civil Engineers.* London: Chapman and Hall.

Whittemore, C. 2015. Stormwater Attenuation, E-mail to C. Whittemore [Online], 16 June. Available E-mail: Colin.Whittemore@aurecongroup.com.

Young P.C., Jakeman A.J., McMurtie R. 1980. An instrumental variable method for model order identification. *Automatica*, **16**: 281-294.

APPENDIX A: Concerns Related to Stormwater Quantity Control Facilities

Release time, maintenance and safety are the three main issues associated with the design of a storage facility. The reason for downstream problems is the shifting of flows to a later time due to the detention pond. Although the pond does reduce the peak flow from the site, the total combined detained peak flow could be higher than the original total flow, due to the delaying of the peak discharge (Brown *et al.*, 2009:305).

Likewise, increased recession time due to the detention pond could result in a higher peak on the main channel. By comparing the hydrograph recession limbs from the pre-development and routed post-development outflow hydrographs (see Figure A.1), one is able to estimate these downstream effects. According to Debo and Reese (2003), if the maximum difference between the recessions limbs of the pre-development and routed post-development outflow hydrographs is less than 20%, the downstream effects may be considered negligible and downstream flood routing omitted.

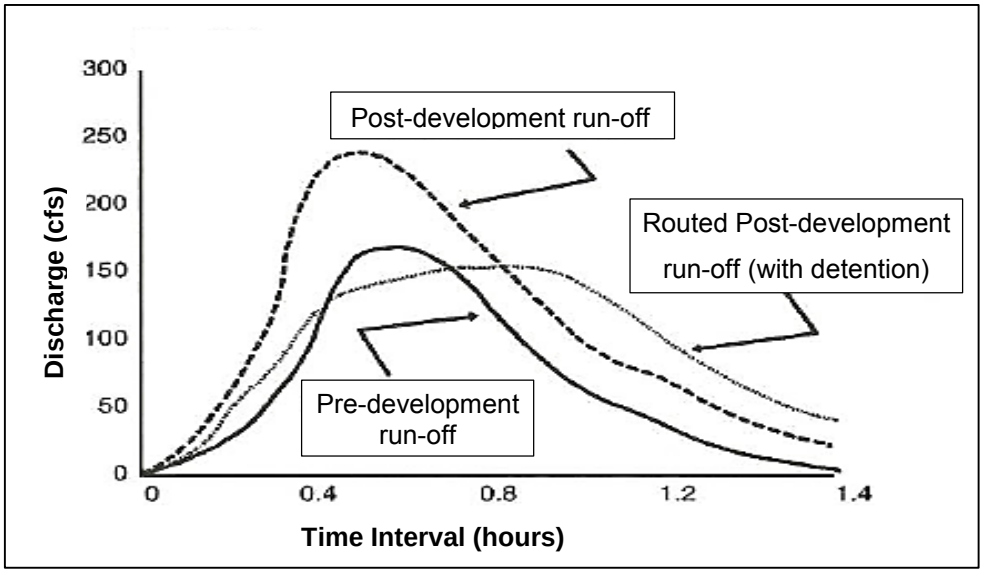

Figure A.1: Run-off hydrograph (adapted from Debo & Reese, 2003:660)

Maintenance refers to the inspection, control of sediment, debris and litter, and structural repairs of the storage facility, which must be properly maintained if the facility is to function as intended over a long period of time (Brown, *et al.*, 2009:306).

Many municipalities around the United States have significant safety requirements for attenuation facilities in place, which are outlined in their stormwater management manuals. Table A.1 summarised safety extracts from some of these stormwater guidance manuals that specifically focus on the outlet structures, and the trash racks built in conjunction with them, in these storage facilities.

Table A.1: Safety excerpts from various Stormwater Manuals

Title of Storm Drainage Regulation	Safety Measure Description/ Quotation
Maryland Stormwater Design Manual, Volume 2, 2000	*All pipe inlet structures should have a trash rack. Openings for trash racks should be limited to half of the pipe diameter, but in no case should the openings be less than 150 mm.*
Public Facilities Manual Fairfax County, Virginia, 2001	*Trash racks and other debris control structures shall be sized as to prevent children from entering the control structure. Bar spacing of the debris control structure should be no greater than 300 mm in any direction with the preferred spacing being 150 mm.* *Fencing or other barriers shall be required around spillway structures having open or accessible drops in excess of 900 mm.*
Construction and Materials Specifications Kansas City Metropolitan Chapter, American Water Works Association, 2003	*All openings shall be protected by trash racks, grates, stone filters, or other approved devices to insure that the outlet works will remain functional.* *No orifice should be less than 0.0762 m (3 inches). Smaller orifices are more susceptible to clogging.*
Design and Construction of Urban Stormwater Management Systems, Water Environment Federation American Society of Civil Engineers, 1992	*Outlet safety considerations include both the safety of the structure and safety of the public at the facility. Low entrance velocities at the trash rack are recommended.* *Fencing or other effective measures should be provided to exclude people from potentially hazardous areas. Alternative measures include education, site grading, signing, planting of thorny scrubs, and grading for safety ledges along the pond perimeter.*

APPENDIX B: Scale Effects

Table B.1: Evaluation of scale effects for the pre-development 2-year RI storm event

Description	MAP = 400 mm				MAP = 700mm				MAP = 1000 mm			
	Coastal		Inland		Coastal		Inland		Coastal		Inland	
	Prototype D=0.419 m		Prototype D=0.538 m		Prototype D= 0.614 m		Prototype D=0.898 m		Prototype D=1.17 m		Prototype D=0.898m	
	Multi-Stage Outlet 1		Multi-Stage Outlet 2		Multi-Stage Outlet 4		Multi-Stage Outlet 3		Multi-Stage Outlet 5		Multi-Stage Outlet 6	
	P	M	P	M	P	M	P	M	P	M	P	M
Flow (P = m^3/s) (M = ℓ/s)	0.05	3.2	0.083	5.32	0.11	7.06	0.186	11.93	0.2	12.83	0.17	10.91
Pipe inlet velocity (m/s)	0.363	0.209	0.365	0.211	0.372	0.214	0.294	0.198	0.186	0.107	0.268	0.155
Froude number	0.179	0.179	0.159	0.159	0.151	0.151	0.099	0.099	0.055	0.055	0.09	0.009
Reynolds number	1.519.E+05	2.92.E+04	1.96.E+05	3.78.E+04	2.28.E+05	4.39.E+04	2.64.E+05	5.08.E+04	2.18.E+05	4.19.E+04	2.41.E+05	4.64.E+04
Flow Regime	Transitional Turbulence	Transitional Turbulence	Transitional Turbulence	Transitional Turbulence	Transitional Turbulence	Transitional Turbulence	Transitional Turbulence	Transitional Turbulence	Transitional Turbulence	Transitional Turbulence	Transitional Turbulence	Transitional Turbulence
Relative Roughness (*e/D*)	0.0007	0.00021	0.00006	0.00017	0.00005	0.00015	0.00003	0.0001	0.00003	0.00008	0.00003	0.0001
Friction Factor (*f*)	0.017	0.024	0.016	0.023	0.016	0.022	0.015	0.021	0.016	0.022	0.015	0.022
$L_r^{3/2}$	3	-	3	-	3	-	3	-	3	-	3	-

P = prototype

M = model

D = inside diameter

f = friction factor, as determined by Colebrook-White-Darcy-Weissbach equation. Also called the Colebrook-White Transition Formula (Chadwick et al., 2004)

e = absolute wall roughness taken as 0.03 mm for uPVC pipes according to Shand (2013).

Table B.2: Evaluation of scale effects for the pre-development 5-year RI storm event

Description	Prototype D=0.419 m		Prototype D=0.538 m		Prototype D= 0.614 m		Prototype D=0.898 m		Prototype D=1.17 m		Prototype D=0.898m	
	Prototype pipe inlet velocity =		**Prototype pipe inlet velocity =**		**Prototype pipe inlet velocity =**		**Prototype pipe inlet velocity =**		**Prototype pipe inlet velocity =**		**Prototype pipe inlet velocity =**	
	0.477 m/s		**0.55 m/s**		**0.461 m/s**		**0.442 m/s**		**0.279 m/s**		**0.395m/s**	
	P	M	P	M	P	M	P	M	P	M	P	M
Flow (P = m^3/s) (M = ℓ/s)	0.07	4.49	0.125	8.02	0.17	10.91	0.28	17.96	0.3	19.25	0.25	16.04
Pipe inlet velocity (m/s)	0.508	0.293	0.550	0.317	0.461	0.266	0.442	0.255	0.279	0.161	0.395	0.228
Froude number	0.250	0.250	0.239	0.239	0.178	0.178	0.149	0.149	0.082	0.082	0.133	0.133
Reynolds number	2.13.E+05	4.09.E+04	2.96.E+05	5.69.E+04	3.16.E+05	6.08.E+04	3.97.E+05	7.64.E+04	3.26.E+05	6.28.E+04	3.54.E+05	6.82.E+04
Flow Regime	Transitional Turbulence	Transitional Turbulence	Transitional Turbulence	Transitional Turbulence	Transitional Turbulence	Transitional Turbulence	Transitional Turbulence	Transitional Turbulence	Transitional Turbulence	Transitional Turbulence	Transitional Turbulence	Transitional Turbulence
Relative Roughness (*e/D*)	0.00007	0.00021	0.00006	0.00017	0.00004	0.00013	0.00003	0.00010	0.00003	0.00008	0.00003	0.00010
Friction Factor (*f*)	0.01603	0.02253	0.0151	0.0209	0.014	0.0205	0.014	0.0195	0.01451	0.0202	0.0114	0.01994
$L_r^{3/2}$	3	-	3	-	3	-	3	-	3	-	3	-

where:

P = prototype

M = model

D = inside diameter

f = friction factor, as determined by Colebrook-White-Darcy-Weissbach equation. Also called the Colebrook-White Transition Formula (Chadwick et al., 2004)

e = absolute wall roughness taken as 0.03 mm for uPVC pipes according to Shand (2013).

Table B.3: Evaluation of scale effects for the pre-development 10-year RI storm event

Description	Prototype D=0.419 m		Prototype D=0.538 m		Prototype D= 0.614 m		Prototype D=0.898 m		Prototype D=1.17 m		Prototype D=0.898m	
	Prototype pipe inlet velocity =		Prototype pipe inlet velocity =		Prototype pipe inlet velocity =		Prototype pipe inlet velocity =		Prototype pipe inlet velocity =		Prototype pipe inlet velocity =	
	0.725 m/s		0.757 m/s		0.777 m/s		0.6 m/s		0.44 m/s		0.35 m/s	
	P	M	P	M	P	M	P	M	P	M	P	M
Flow (P = m^3/s) (M = ℓ/s)	0.1	6.41	0.172	11.03	0.23	14.75	0.38	24.38	0.41	26.30	0.35	22.45
Pipe inlet velocity (m/s)	0.725	0.419	0.757	0.437	0.777	0.448	0.600	0.346	0.381	0.220	0.553	0.319
Froude number	0.358	0.358	0.329	0.329	0.317	0.317	0.202	0.202	0.113	0.113	0.186	0.186
Reynolds number	3.04.E+05	5.85.E+04	4.07.E+05	7.83.E+04	4.77.E+05	9.18.E+04	5.39.E+05	1.04.E+05	4.46.E+05	8.59.E+04	4.96.E+05	9.55.E+04
Flow Regime	Transitional Turbulence	Transitional Turbulence	Transitional Turbulence	Transitional Turbulence	Transitional Turbulence	Transitional Turbulence	Transitional Turbulence	Transitional Turbulence	Transitional Turbulence	Transitional Turbulence	Transitional Turbulence	Transitional Turbulence
Relative Roughness (*e/D*)	0.00007	0.00021	0.00006	0.00017	0.00004	0.00013	0.00003	0.00010	0.00003	0.00008	0.00003	0.00010
Friction Factor (*f*)	0.0154	0.021	0.0144	0.0197	0.0139	0.019	0.0135	0.0184	0.0138	0.019	0.0136	0.0187
$L_r^{3/2}$	3	-	3	-	3	-	3	-	3	-	3	-

where:

P = prototype

M = model

D = inside diameter

f = friction factor, as determined by Colebrook-White-Darcy-Weissbach equation. Also called the Colebrook-White Transition Formula (Chadwick et al., 2004)

e = absolute wall roughness taken as 0.03 mm for uPVC pipes according to Shand (2013).

Table B.4: Evaluation of scale effects for the pre-development 20-year RI storm event

Description	Prototype D=0.419 m		Prototype D=0.538 m		Prototype D= 0.614 m		Prototype D=0.898 m		Prototype D=1.17 m		Prototype D=0.898m	
	Prototype pipe inlet velocity =		Prototype pipe inlet velocity =		Prototype pipe inlet velocity =		Prototype pipe inlet velocity =		Prototype pipe inlet velocity =		Prototype pipe inlet velocity =	
	1.015 m/s		1.043 m/s		1.047 m/s		0.837 m/s		0.5 m/s		0.758 m/s	
	P	M	P	M	P	M	P	M	P	M	P	M
Flow (P = m^3/s) (M = ℓ/s)	0.14	8.98	0.237	15.20	0.31	19.89	0.53	34.0	0.57	36.57	0.48	30.79
Pipe inlet velocity (m/s)	1.015	0.586	1.043	0.602	1.047	0.604	0.837	0.483	0.530	0.306	0.758	0.438
Froude number	0.501	0.501	0.454	0.454	0.427	0.427	0.282	0.282	0.156	0.156	0.255	0.255
Reynolds number	4.25.E+05	8.19.E+04	5.61.E+05	1.08.E+05	6.43.E+05	1.24.E+05	7.51.E+05	1.45.E+05	6.20.E+05	1.19.E+05	6.81.E+05	1.31.E+05
Flow Regime	Transitional Turbulence	Transitional Turbulence	Transitional Turbulence	Transitional Turbulence	Transitional Turbulence	Transitional Turbulence	Transitional Turbulence	Transitional Turbulence	Transitional Turbulence	Transitional Turbulence	Transitional Turbulence	Transitional Turbulence
Relative Roughness (*e/D*)	0.00007	0.00021	0.00006	0.00017	0.00004	0.00013	0.00003	0.00010	0.00003	0.00008	0.00003	0.00010
Friction Factor (*f*)	0.0144	0.0197	0.0137	0.0186	0.0133	0.018	0.0128	0.0173	0.0131	0.0178	0.013	0.0176
$L_r^{3/2}$	3	-	3	-	3	-	3	-	3	-	3	-

where:

P = prototype

M = model

D = inside diameter

f = friction factor, as determined by Colebrook-White-Darcy-Weissbach equation. Also called the Colebrook-White Transition Formula (Chadwick et al., 2004)

e = absolute wall roughness taken as 0.03 mm for uPVC pipes according to Shand (2013).

Table B.5: Evaluation of scale effects for the pre-development 50-year RI storm event

Description	Prototype D=0.419 m		Prototype D=0.538 m		Prototype D= 0.614 m		Prototype D=0.898 m		Prototype D=1.17 m		Prototype D=0.898m	
	Prototype pipe inlet velocity =		**Prototype pipe inlet velocity =**		**Prototype pipe inlet velocity =**		**Prototype pipe inlet velocity =**		**Prototype pipe inlet velocity =**		**Prototype pipe inlet velocity =**	
	1.668 m/s		**1.672 m/s**		**1.722 m/s**		**1.342 m/s**		**0.856 m/s**		**0.775 m/s**	
	P	M	P	M	P	M	P	M	P	M	P	M
Flow (P = m^3/s) (M = ℓ/s)	0.23	0.0148	0.38	0.0244	0.51	0.0327	0.85	0.0545	0.92	0.0590	0.775	0.0497
Pipe inlet velocity (m/s)	1.668	0.963	1.672	0.965	1.722	0.994	1.342	0.775	0.856	0.494	1.224	0.706
Froude number	0.823	0.823	0.728	0.728	0.702	0.702	0.452	0.452	0.253	0.253	0.412	0.412
Reynolds number	6.99.E+05	1.35.E+05	8.99.E+05	1.73.E+05	1.06.E+06	2.04.E+05	1.21.E+06	2.32.E+05	1.00.E+06	1.93.E+05	1.10.E+06	2.11.E+05
Flow Regime	Transitional Turbulence	Transitional Turbulence	Transitional Turbulence	Transitional Turbulence	Transitional Turbulence	Transitional Turbulence	Transitional Turbulence	Transitional Turbulence	Transitional Turbulence	Transitional Turbulence	Transitional Turbulence	Transitional Turbulence
Relative Roughness (*e/D*)	0.00007	0.00021	0.00006	0.00017	0.00004	0.00013	0.00003	0.00010	0.00003	0.00008	0.00003	0.00010
Friction Factor (*f*)	0.0135	0.0182	0.013	0.0173	0.0125	0.0166	0.0121	0.016	0.0122	0.0158	0.0122	0.0163
$L_r^{3/2}$	3	-	3	-	3	-	3	-	3	-	3	-

where:

P = prototype

M = model

D = inside diameter

f = friction factor, as determined by Colebrook-White-Darcy-Weissbach equation. Also called the Colebrook-White Transition Formula (Chadwick et al., 2004)

e = absolute wall roughness taken as 0.03 mm for uPVC pipes according to Shand (2013).

Table B.6: Evaluation of scale effects for the pre-development 100-year RI storm event

Description	Prototype D=0.419 m		Prototype D=0.538 m		Prototype D= 0.614 m		Prototype D=0.898 m		Prototype D=1.17 m		Prototype D=0.898m	
	Prototype pipe inlet velocity =		Prototype pipe inlet velocity =		Prototype pipe inlet velocity =		Prototype pipe inlet velocity =		Prototype pipe inlet velocity =		Prototype pipe inlet velocity =	
	2.466 m/s		2.507 m/s		2.533 m/s		2.0 m/s		1.265 m/s		1.808m/s	
	P	M	P	M	P	M	P	M	P	M	P	M
Flow (P = m^3/s) (M = ℓ/s)	0.34	21.81	0.57	36.57	0.75	48.11	1.27	81.47	1.36	87.24	1.145	73.457
Pipe inlet velocity (m/s)	2.466	1.424	2.507	1.448	2.533	1.462	2.005	1.158	1.265	0.730	1.808	1.044
Froude number	1.216	1.216	1.091	1.091	1.032	1.032	0.676	0.676	0.373	0.373	0.609	0.609
Reynolds number	1.03.E+06	1.99.E+05	1.35.E+06	2.60.E+05	1.56.E+06	2.99.E+05	1.80.E+06	3.47.E+05	1.48.E+06	2.85.E+05	1.62.E+06	3.12.E+05
Flow Regime	Transitional Turbulence	Transitional Turbulence	Transitional Turbulence	Transitional Turbulence	Transitional Turbulence	Transitional Turbulence	Transitional Turbulence	Transitional Turbulence	Transitional Turbulence	Transitional Turbulence	Transitional Turbulence	Transitional Turbulence
Relative Roughness (*e/D*)	0.00007	0.00021	0.00006	0.00017	0.00004	0.00013	0.00003	0.00010	0.00003	0.00008	0.00003	0.00010
Friction Factor (*f*)	0.013	0.0172	0.0124	0.0163	0.0112	0.016	0.0115	0.015	0.0116	0.0153	0.0117	0.0153
$L_r^{3/2}$	3	-	3	-	3	-	3	-	3	-	3	-

where:

P = prototype

M = model

D = inside diameter

f = friction factor, as determined by Colebrook-White-Darcy-Weissbach equation. Also called the Colebrook-White Transition Formula (Chadwick et al., 2004)

e = absolute wall roughness taken as 0.03 mm for uPVC pipes according to Shand (2013).

APPENDIX C: Sensitivity Assessment

A sensitivity analysis was conducted to test the effect of one input parameter on the peak discharge, while keeping the other input parameters constant. The parameters that were evaluated in the sensitivity analysis are the urban run-off coefficient (C_2), the mean annual precipitation (MAP), and the average slope of the catchment (S_{av}). The sensitivity analysis was conducted before the flood peaks was increased by 15% to compensate for future climate change effects. Results are tabulated in Tables C.1 to C.4, which indicate the change in flood peaks due to a change in C_2 and catchment slope, respectively.

The 22.45% increase in the urban run-off coefficient resulted in a maximum difference of 24.39% in the flood peak, for the coastal region, which occurred for the 5-year recurrence interval and a MAP of 700 mm. A 23.21% increase in the peak flow resulted form a 22.45% increase in the urban run-off factor for the inland region, for the 10-year recurrence interval event, and a MAP of 400 mm.

Table C.1: Test for sensitivity of urban run-of factor– Coastal post-development scenario

MAP (mm)	RI (years)	Average post-development scenario, C_2 =0.423	Flood peak m^3/s (% change)	
			20.09% decrease in C_2	22.45% increase in C_2
400	2	0.19	0.15	0.23
			(-21.05)	(21.05)
	5	0.26	0.21	0.32
			(-19.23)	(23.08)
	10	0.33	0.26	0.40
			(-21.21)	(21.21)
	20	0.41	0.32	0.50
			(-21.95)	(21.95)
	50	0.53	0.42	0.65
			(-20.75)	(22.64)
	100	0.65	0.52	0.80
			(-20.00)	(23.08)
700	2	0.30	0.24	0.37
			(-20.00)	(23.33)
	5	0.41	0.33	0.51
			(-19.51)	(24.39)
	10	0.52	0.42	0.64
			(-19.23)	(23.08)
	20	0.64	0.51	0.79
			(-20.31)	(23.44)
	50	0.84	0.67	1.03
			(-20.24)	(22.62)
	100	1.03	0.82	1.26
			(-20.39)	(22.33)
1000	2	0.42	0.33	0.51
			(-21.43)	(21.43)
	5	0.57	0.45	0.69
			(-21.05)	(21.05)
	10	0.72	0.57	0.88
			(-20.83)	(22.22)
	20	0.88	0.71	1.08
			(-19.32)	(22.73)
	50	1.15	0.92	1.41
			(-20.00)	(22.61)
	100	1.41	1.13	1.73
			(-19.86)	(22.70)

Table C.2: Test for sensitivity of urban run-off factor– Inland post-development scenario

MAP (mm)	RI (years)	Average post-development scenario, C_2 =0.423	Flood peak m^3/s (% change)	
			20.09% decrease in C_2	22.45% increase in C_2
400	2	0.33	0.26	0.40
			(-21.21)	**(21.21)**
	5	0.45	0.36	0.55
			(-20.00)	**(22.22)**
	10	0.56	0.45	0.69
			(-19.64)	**(23.21)**
	20	0.70	0.56	0.85
			(-20.00)	**(21.43)**
	50	0.91	0.72	1.11
			(-20.88)	**(21.98)**
	100	1.11	0.89	1.36
			(-19.82)	**(22.52)**
700	2	0.52	0.42	0.64
			(-19.23)	**(23.08)**
	5	0.71	0.57	0.87
			(-19.72)	**(22.54)**
	10	0.90	0.72	1.10
			(-20.00)	**(22.22)**
	20	1.11	0.88	1.35
			(-20.72)	**(21.62)**
	50	1.44	1.15	1.76
			(-20.14)	**(22.22)**
	100	1.77	1.41	2.17
			(-20.34)	**(22.60)**
1000	2	0.71	0.57	0.87
			(-19.72)	**(22.54)**
	5	0.97	0.77	1.19
			(-20.62)	**(22.68)**
	10	1.23	0.98	1.50
			(-20.33)	**(21.95)**
	20	1.51	1.21	1.85
			(-19.87)	**(22.52)**
	50	1.97	1.57	2.41
			(-20.30)	**(22.34)**
	100	2.42	1.94	2.97
			(-19.83)	**(22.73)**

Table C.3: Test for sensitivity of average catchment slope – Coastal post-development scenario

MAP (mm)	RI (years)	1% Catchment slope	Flood peak m^3/s (% change)
			0.5% Catchment slope
400	2	0.23	0.21
			(-8.70)
	5	0.32	0.29
			(-9.38)
	10	0.40	0.37
			(-7.50)
	20	0.50	0.46
			(-8.00)
	50	0.65	0.59
			(-9.23)
	100	0.80	0.73
			(-8.75)
700	2	0.37	0.34
			(-8.11)
	5	0.51	0.46
			(-9.80)
	10	0.64	0.59
			(-7.81)
	20	0.79	0.73
			(-7.59)
	50	1.03	0.94
			(-8.74)
	100	1.26	1.16
			(-7.94)
1000	2	0.51	0.47
			(-7.84)
	5	0.69	0.64
			(-7.25)
	10	0.88	0.81
			(-7.95)
	20	1.08	0.99
			(-8.33)
	50	1.41	1.29
			(-8.51)
	100	1.73	1.59
			(-8.09)

Table C.4: Test for sensitivity of average catchment slope –Inland post-development scenario

MAP (mm)	RI (years)	1% Catchment slope	Flood peak m^3/s (% change)
			0.5% Catchment slope
400	2	0.40	0.37
			(-7.50)
	5	0.55	0.50
			(-9.09)
	10	0.69	0.63
			(-8.70)
	20	0.85	0.78
			(-8.24)
	50	1.11	1.01
			(-9.01)
	100	1.36	1.24
			(-8.82)
700	2	0.64	0.58
			(-9.38)
	5	0.87	0.79
			(-9.20)
	10	1.10	1.00
			(-9.09)
	20	1.35	1.23
			(-8.89)
	50	1.76	1.60
			(-9.09)
	100	2.17	1.97
			(-9.22)
1000	2	0.87	0.79
			(-9.20)
	5	1.19	1.08
			(-9.24)
	10	1.50	1.37
			(-8.67)
	20	1.85	1.69
			(-8.65)
	50	2.41	2.20
			(-8.71)
	100	2.97	2.70
			(-9.09)

APPENDIX D: Flood Hydrology Results and Calculations

Table D.1: Recommended values of run-off factor for use in the rational method (SANRAL, 2013:3-18)

Rural (C1)					Urban (C2)	
Component	Classification	Mean annual rainfall (mm)			Use	Factor (Min. - Max.)
		< 600	600-900	> 900		
Surface slope (Cs)	Vleis and pans (< 3%) Flat areas (3 to 10%) Hilly (10 to 30%) Steep areas (>30%)	0.01 0.06 0.12 0.22	0.03 0.08 0.16 0.26	0.05 0.11 0.20 0.30	*Lawns* -Sandy, flat (<2%) -Sandy, steep (>7%) -Heavy soil, flat (<2%) -Heavy soil, steep (>7%)	 0.05 - 0.10 0.15 - 0.20 0.13 - 0.17 0.25 - 0.35
Permeability (Cp)	Very permeable Permeable Semi-Permeable Impermeable	0.03 0.06 0.12 0.21	0.04 0.08 0.16 0.26	0.05 0.10 0.20 0.30	*Residential areas* -Houses -Flats	 0.03 - 0.50 0.50 - 0.70
Vegetation (Cv)	Thick bush and plantation Light bush and farm lands Grasslands No vegetation	0.03 0.07 0.17 0.26	0.04 0.11 0.21 0.28	0.05 0.15 0.25 0.3	*Industry* -Light industry -Heavy industry *Business* -City centre -Suburban -Streets -Maximum flood	 0.50 - 0.80 0.50 - 0.70 0.70 - 0.95 0.50-0.70 0.70-0.95 1.00

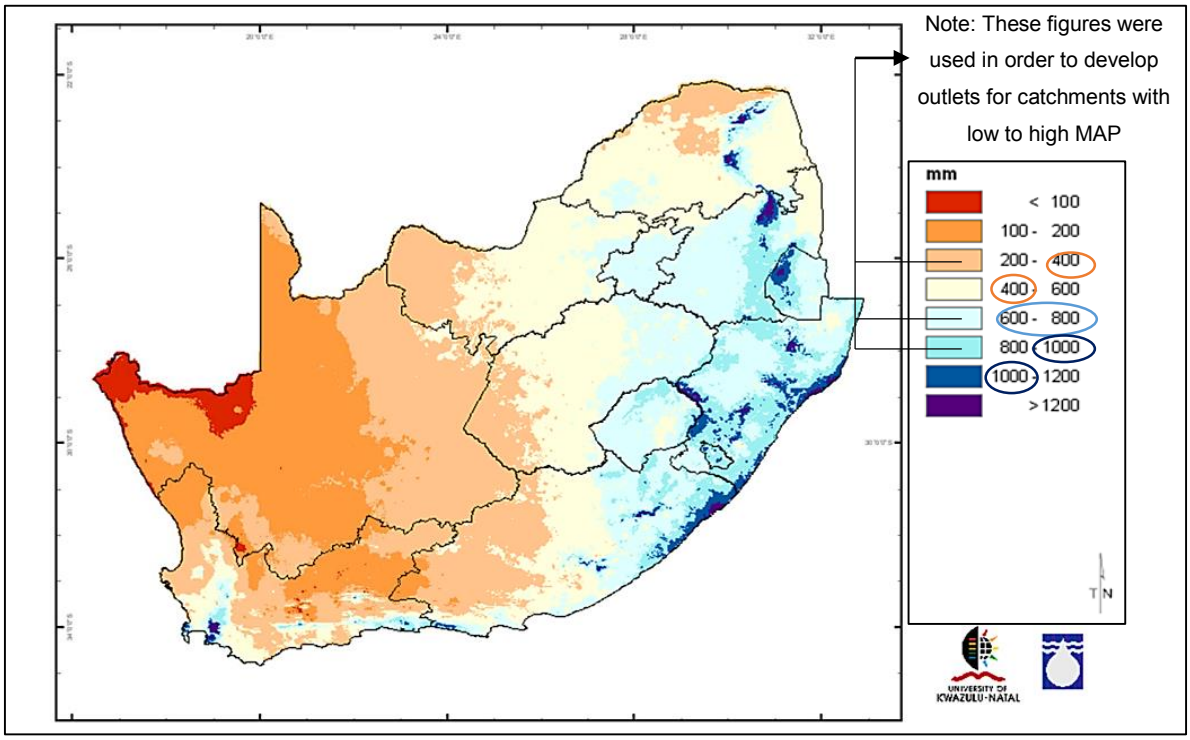

Figure D.1: Mean Annual Precipitation in South Africa (SANRAL, 2013:3-21)

Table D.2: Pre-development Scenario for Coastal Regions with 400 mm of MAP

RATIONAL METHOD (ALTERNATIVE 1):								
Description of the catchment				**Pre-development / Natural scenario**				
Calculated by				Marisa Myburgh		Date	24/06/2015	
Physical characteristics								
Size of the catchment (A)		0.05	km^2			Rainfall region		Coastal
Longest watercourse (L)		0.32	km			**Area distribution factors**		
Average slope (S_{av})		0.01	m/m			Rural (α)		1
Dolomite area ($D_{\%}$)		0	%			Urban (β)		0
Mean annual rainfall (MAP)		400	mm			Lakes (γ)		0
Rural				**Urban**				
Surface slope	%	Factor	C_s	**Description**	%	Factor	C_2	
Vleis and pans	0	0.01	0.000	**Lawns**				
Flat areas	100	0.06	0.060	Sandy, flat (<2%)				
Hilly	0	0.12	0.000	Sandy, steep (>7%)				
Steep areas	0	0.22	0.000	Heavy soil, flat (<2%)				
Total	100		**0.060**	Heavy soil,steep (>7%)				
Permeability	%	Factor	C_p	**Residential area**				
Very permeable	0	0.03	0.000	Houses				
Permeable	50	0.06	0.030	Flats				
Semi-permeable	50	0.12	0.060	**Industry**				
Impermeable	0	0.21	0.000	Light industry				
Total	100		**0.090**	Heavy industry				
Vegetation	%	Factor	C_v	**Business**				
Thick bush & plantation	0	0.03	0.000	City centre				
Light busch and farmlands	100	0.07	0.070	Suburban				
Grasslands	0	0.17	0.000	Streets				
No vegetation	0	0.26	0.000	Maximum flood				
Total	100		**0.070**	Total				
Time of concentration (T_c)				**Notes**				
Overland flow		**Defined watercourse**						
$\left(\frac{\quad}{\sqrt{\quad}}\right)$		$\left(\frac{\quad}{\quad}\right)$						
Tc =	hours	Tc =	0.250 hours	Tc =9.75 min ,thus use Tc of at least 15 min				

Run-off coefficient							
Return period (years), T	2	5	10	20	50	100	Max
Run-off coefficient C_1 ($C_1 = C_s + C_p + C_v$)	0.220	0.220	0.220	0.220	0.220	0.220	
Adjusted for dolomitic areas, C_{1D} ($=C_1 (1 - D_{\%}) + C1\ D_{\%}(\sum(D_{factor} \times C_{S\%})$)	0.220	0.220	0.220	0.220	0.220	0.220	
Adjustment factor for initial saturation, F_t	0.5	0.55	0.6	0.67	0.83	1	
Adjusted run-off coefficient, C_{1T} ($= C_{1D} \times F_t$)	0.110	0.121	0.132	0.147	0.183	0.220	
Combined run-off coefficient C_t ($= \alpha C_{1T} + \beta_{C2} + \gamma_{C3}$)	0.110	0.121	0.132	0.147	0.183	0.220	
Rainfall							
Return period (years), T	2	5	10	20	50	100	Max
Point rainfall (mm), P_T	7.02	9.55	12.09	14.93	19.40	23.88	
Point intensity (mm/hour), P_{iT} (= P_T / T_C)	28.06	38.21	48.36	59.70	77.61	95.53	
Area reduction factor (%), ARF_T	100	100	100	100	100	100	
Average intensity (mm/hour), I_T (= P_{IT}xARF_T)	28.06	38.21	48.36	59.70	77.61	95.53	
Peak flow							
Return period (years), T	2	5	10	20	50	100	Max
Peak flow (m3/s) ———	**0.04**	**0.06**	**0.09**	**0.12**	**0.20**	**0.29**	
Peak flow (m3/s) ——— x1.15	**0.05**	**0.07**	**0.10**	**0.14**	**0.23**	**0.34**	

Table D.3: Post-development Scenario for Coastal Regions with 400 mm of MAP

RATIONAL METHOD: ALTERNATIVE 1								
Description of the catchment			**Urban/ Post-development scenario (Max urban factor)**					
Calculated by			Marisa Myburgh		Date	24/06/2015		
Physical characteristics								
Size of the catchment (A)	0.05	km^2			Rainfall region	Coastal		
Longest watercourse (L)	0.32	km			**Area distribution factors**			
Average slope (S_{av})	0.01	m/m			Rural (α)	0		
Dolomite area ($D_{\%}$)	0	%			Urban (β)	1		
Mean annual rainfall (MAP)	400	mm			Lakes (γ)	0		
Rural				**Urban**				
Surface slope	%	Factor	C_s	**Description**	%	Factor	C_2	
Vleis and pans				**Lawns**				
Flat areas				Sandy, flat (<2%)	0	0.1	0.000	
Hilly				Sandy, steep (>7%)	0	0.2	0.000	
Steep areas				Heavy soil, flat (<2%)	25	0.17	0.043	
Total				Heavy soil,steep (>7%)	0	0.35	0.000	
Permeability	%	Factor	C_p	**Residential area**				
Very permeable				Houses	55	0.5	0.275	
Permeable				Flats	0	0.7	0.000	
Semi-permeable				**Industry**				
Impermeable				Light industry	0	0.8	0.000	
Total				Heavy industry	0	0.9	0.000	
Vegetation				**Business**				
Thick bush & plantation				City centre	0	0.95	0.000	
Light busch and farmlands				Suburban	0	0.7	0.000	
Grasslands				Streets	20	1	0.200	
No vegetation				Maximum flood		1		
Total				Total	100		**0.518**	
Time of concentration (T_c)				**Notes**				
Overland flow		**Defined watercourse**						
Tc =	hours	Tc =	0.167	hours	Tc =9.746 min ,thus use Tc of at least 10 min			

Run-off coefficient							
Return period (years), T	2	5	10	20	50	100	Max
Run-off coefficient C_1 ($C_1 = C_s + C_p + C_v$)	0.000	0.000	0.000	0.000	0.000	0.000	
Adjusted for dolomitic areas, C_{1D} ($=C_1 (1 - D_{\%}) + C1\ D_{\%}(\sum(D_{factor} \times C_{S\%}))$)	0.000	0.000	0.000	0.000	0.000	0.000	
Adjustment factor for initial saturation, F_t	0.5	0.55	0.6	0.67	0.83	1	
Adjusted run-off coefficient, C_{1T} ($= C_{1D} \times F_t$)	0.000	0.000	0.000	0.000	0.000	0.000	
Combined run-off coefficient C_t ($= \alpha C_{1T} + \beta_{C2} + \gamma_{C3}$)	0.518	0.518	0.518	0.518	0.518	0.518	
Rainfall							
Return period (years), T	2	5	10	20	50	100	Max
Point rainfall (mm), P_T	5.42	7.38	9.34	11.53	14.99	18.45	
Point intensity (mm/hour), P_{iT} (= P_T / T_C)	32.52	44.29	56.05	69.20	89.96	110.72	
Area reduction factor (%), ARF_T	100	100	100	100	100	100	
Average intensity (mm/hour), I_T (= P_{iT}xARF_T)	32.52	44.29	56.05	69.20	89.96	110.72	
Peak flow							
Return period (years), T	2	5	10	20	50	100	Max
Peak flow (m3/s) ——	**0.23**	**0.32**	**0.40**	**0.50**	**0.65**	**0.80**	
Peak flow (m3/s) —— x 1.15	**0.27**	**0.37**	**0.46**	**0.57**	**0.74**	**0.92**	

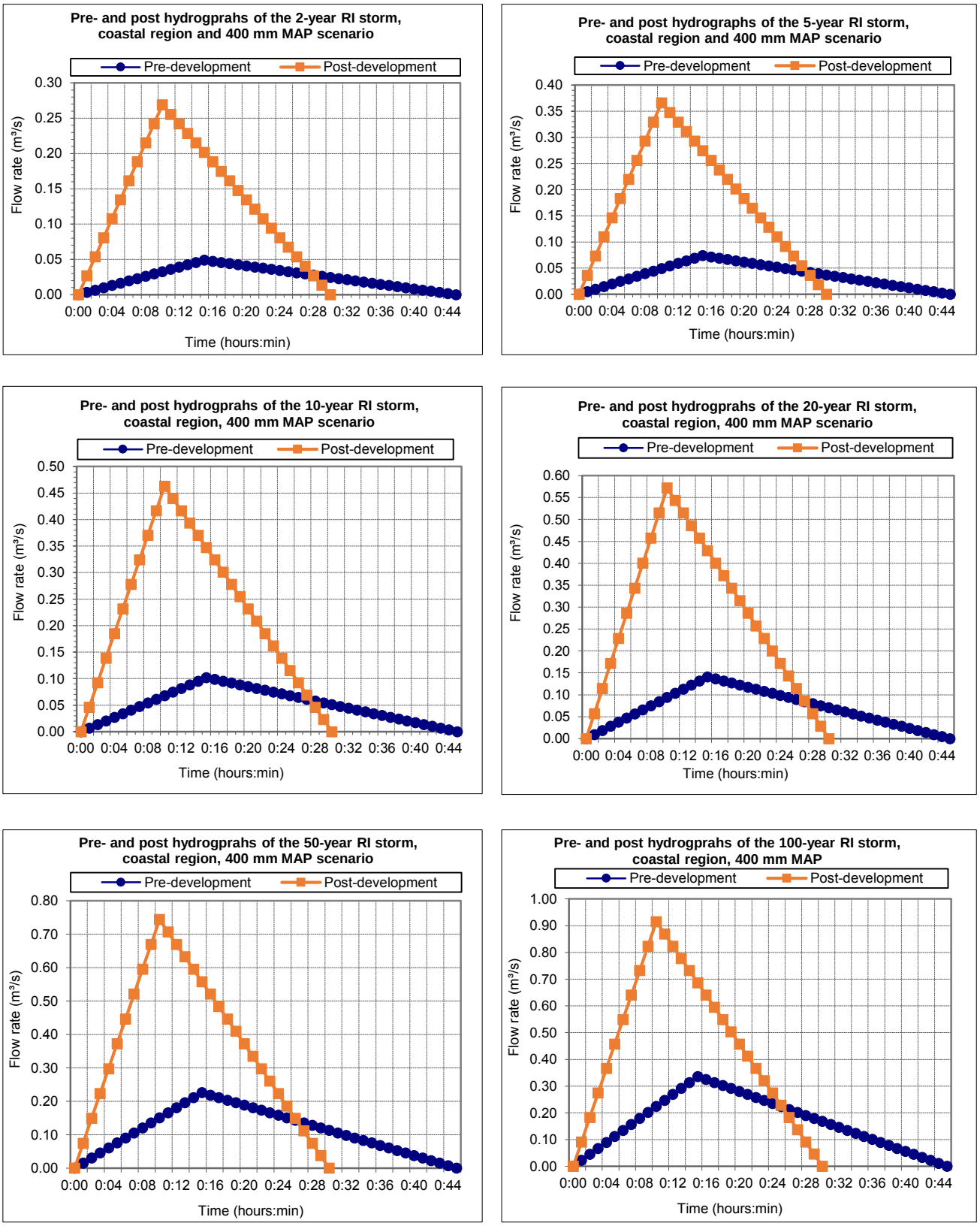

Figure D.2: Pre- and post-hydrographs for 2-, 5-, 10-, 20-, 50- and 100-year RI storm events of the coastal region and MAP of 400 mm

Table D.4: Pre-development scenario for inland regions with 400 mm of MAP

RATIONAL METHOD: ALTERNATIVE 1												
Description of the catchment				Pre-development / Natural scenario								
Calculated by				Marisa Myburgh				Date	6/24/2015			
Physical characteristics												
Size of the catchment (A)	0.05	km^2						Rainfall region	Inland			
Longest watercourse (L)	0.32	km						**Area distribution factors**				
Average slope (S_{av})	0.01	m/m						Rural (α)	1			
Dolomite area ($D_{\%}$)	0	%						Urban (β)	0			
Mean annual rainfall (MAP)	400	mm						Lakes (γ)	0			
Rural					**Urban**							
Surface slope	%	Factor	C_s		**Description**	%	Factor	C_s				
Vleis and pans	0	0.01	0.000		**Lawns**							
Flat areas	100	0.06	0.060		Sandy, flat (<2%)							
Hilly	0	0.12	0.000		Sandy, steep (>7%)							
Steep areas	0	0.22	0.000		Heavy soil, flat (<2%)							
Total	100		**0.060**		Heavy soil,steep (>7%)							
Permeability	%	Factor	C_p		**Residential area**							
Very permeable	0	0.03	0.000		Houses							
Permeable	50	0.06	0.030		Flats							
Semi-permeable	50	0.12	0.060		**Industry**							
Impermeable	0	0.21	0.000		Light industry							
Total	100		**0.090**		Heavy industry							
Vegetation	%	Factor	C_v		**Business**							
Thick bush & plantation	0	0.03	0.000		City centre							
Light bush and farmlands	100	0.07	0.070		Suburban							
Grasslands	0	0.17	0.000		Streets							
No vegetation	0	0.26	0.000		Maximum flood							
Total	100		**0.070**		Total							
Time of concentration (T_c)					**Notes**							
Overland flow		**Defined watercourse**			Tc =9.75 min < 15 min, therefore use minimum of 15 min							
$\left(\frac{\quad}{\sqrt{\quad}}\right)$		$\left(\frac{\quad}{\quad}\right)$										
Tc =	hours	Tc =	0.250	hours								
Run-off coefficient												
Return period (years), T	2	5	10	20	50	100	Max					
Run-off coefficient C_1 ($C_1 = C_s + C_p + C_v$)	0.220	0.220	0.220	0.220	0.220	0.220						
Adjusted for dolomitic areas, C_{1D} ($=C_1 (1 - D_{\%}) + C1\ D_{\%}(\sum(D_{factor} \times C_{S\%})$)	0.220	0.220	0.220	0.220	0.220	0.220						
Adjustment factor for initial saturation, F_t	0.5	0.55	0.6	0.67	0.83	1						
Adjusted run-off coefficient, C_{1T} ($= C_{1D} \times F_t$)	0.110	0.121	0.132	0.147	0.183	0.220						
Combined run-off coefficient C_t ($= \alpha C_{1T} + \beta_{C2} + \gamma_{C3}$)	0.110	0.121	0.132	0.147	0.183	0.220						
Rainfall												
Return period (years), T	2	5	10	20	50	100	Max					
Point rainfall (mm), P_T	11.83	16.11	20.38	25.17	32.72	40.27						
Point intensity (mm/hour), P_{iT} (= P_T / T_C)	47.31	64.42	81.54	100.66	130.86	161.06						
Area reduction factor (%), ARF_T	100	100	100	100	100	100						
Average intensity (mm/hour), I_T (= P_{iT}xARF_T)	47.31	64.42	81.54	100.66	130.86	161.06						
Peak flow												
Return period (years), T	2	5	10	20	50	100	Max					
Peak flow (m3/s) ——	**0.072**	**0.11**	**0.15**	**0.21**	**0.33**	**0.49**						
Peak flow (m3/s) —— x 1.15	**0.083**	**0.125**	**0.172**	**0.237**	**0.382**	**0.566**						

Table D.5: Post-development scenario for inland regions with 400 mm of MAP

RATIONAL METHOD: ALTERNATIVE 1							
Description of the catchment	Urban / Post-development (Maximum urban factor)						
Calculated by	Marisa Myburgh			Date	6/8/2015		
Physical characteristics							
Size of the catchment (A)	0.05	km^2		Rainfall region	Inland		
Longest watercourse (L)	0.32	km		**Area distribution factors**			
Average slope (S_{av})	0.01	m/m		Rural (α)	0		
Dolomite area ($D_{\%}$)	0	%		Urban (β)	1		
Mean annual rainfall (MAP)	400	mm		Lakes (γ)	0		

Rural				**Urban**			
Surface slope	%	Factor	C_s	**Description**	%	Factor	C_s
Vleis and pans				**Lawns**			
Flat areas				Sandy, flat (<2%)	0	0.1	0.000
Hilly				Sandy, steep (>7%)	0	0.2	0.000
Steep areas				Heavy soil, flat (<2%)	25	0.17	0.043
Total				Heavy soil,steep (>7%)	0	0.35	0.000
Permeability	%	Factor	C_p	**Residential area**			
Very permeable				Houses	55	0.5	0.275
Permeable				Flats	0	0.7	0.000
Semi-permeable				**Industry**			
Impermeable				Light industry	0	0.8	0.000
Total				Heavy industry	0	0.9	0.000
Vegetation				**Business**			
Thick bush & plantation				City centre	0	0.95	0.000
Light busch and farmlands				Suburban	0	0.7	0.000
Grasslands				Streets	20	1	0.200
No vegetation				Maximum flood		1	
Total				Total	100		**0.518**

Time of concentration (T_c)					**Notes**
Overland flow		**Defined watercourse**			
$\left(\frac{}{\sqrt{}}\right)$		$\left(\frac{}{}\right)$			Tc =9.75 min ,thus use Tc of at least 10 min
Tc =	hours	Tc =	0.167	hours	

Run-off coefficient							
Return period (years), T	2	5	10	20	50	100	Max
Run-off coefficient C_1 ($C_1 = C_s + C_p + C_v$)	0	0	0	0	0	0	
Adjusted for dolomitic areas, C_{1D} ($=C_1 (1 - D_{\%}) + C1\ D_{\%}(\sum(D_{factor} \times C_{S\%}))$)	0	0	0	0	0	0	
Adjustment factor for initial saturation, F_t	0.5	0.55	0.6	0.67	0.83	1	
Adjusted run-off coefficient, C_{1T} ($= C_{1D} \times F_t$)	0	0	0	0	0	0	
Combined run-off coefficient C_t ($= \alpha C_{1T} + \beta_{C2} + \gamma_{C3}$)	0.518	0.518	0.518	0.518	0.518	0.518	

Rainfall							
Return period (years), T	2	5	10	20	50	100	Max
Point rainfall (mm), P_T	9.30	12.66	16.02	19.78	25.71	31.65	
Point intensity (mm/hour), P_{iT} (= P_T / T_C)	55.78	75.95	96.12	118.67	154.27	189.88	
Area reduction factor (%), ARF_T	100	100	100	100	100	100	
Average intensity (mm/hour), I_T (= P_{iT}xARF_T)	55.78	75.95	96.12	118.67	154.27	189.88	

Peak flow							
Return period (years), T	2	5	10	20	50	100	Max
Peak flow (m3/s) ———	**0.40**	**0.55**	**0.69**	**0.85**	**1.11**	**1.36**	
Peak flow (m3/s) ——— x 1.15	**0.461**	**0.628**	**0.795**	**0.981**	**1.275**	**1.569**	

Peak Flow Results using the Deterministic Rational Method

The peak flows expected at various recurrence intervals, obtained by the rational method, are plotted on Figures D.3 to D.5 for the coastal region and for various different MAP values. The flood peaks are those before the peaks were increased by 15% to compensate for future climate change effects. Figures D.3 to D.5 indicate the percentage reduction in peak flow that the multi-stage outlet structure would have to reduce in order to meet the pre-development design requirements.

For a MAP of 400 mm, the maximum post-development peak flows are typically in the order of three times greater than the pre-development peak flow for less frequently occurring events. For the more frequent events, this ratio increase to almost six times greater than the pre-development peak flow (refer to Figure D.3). The maximum post-development peak flows refer to the scenario where maximum urban run-off factors were used and average post-development peak flow refer to the scenario where average urban run-off factors were used. Both C_2 factors were obtained from Table D.1.

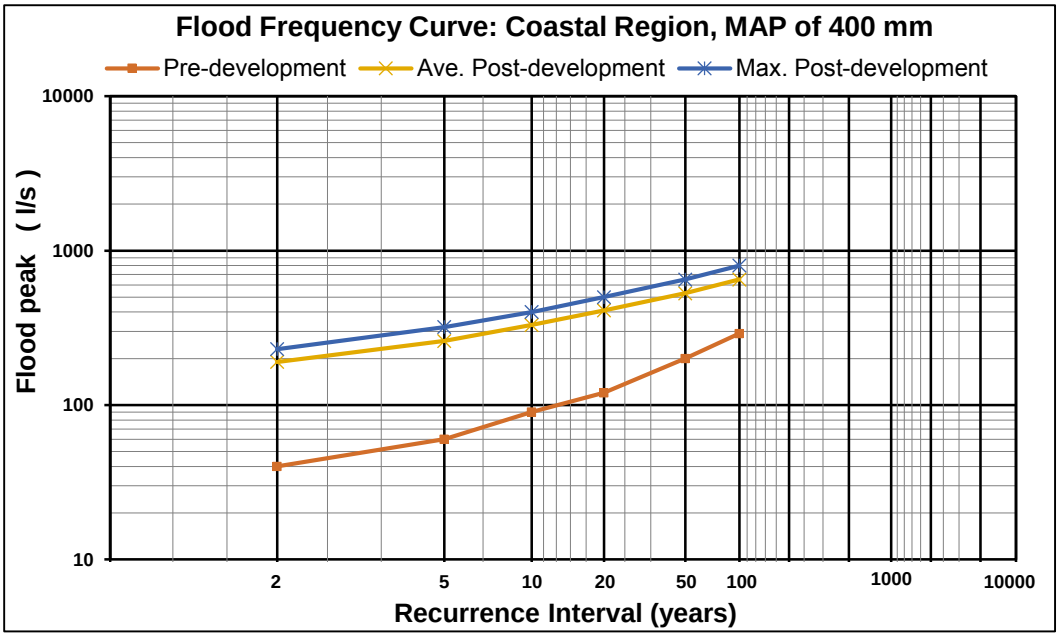

Figure D.3: Flood frequency curve of the coastal region with a MAP of 400 mm

For a MAP of 700 mm, the maximum post-development peak flows are typically in the order of two times greater than the pre-development peak flow for less frequently occurring events. For more frequent events, this ratio increase to four times greater than the pre-development peak flow (see Figure D.4). However, for a MAP of 1000 mm (see Figure D.5), the maximum post-development peak flows are typically in the order of only one and a half times greater than the pre-development peak flow for less frequently occurring events, and three times greater than the pre-development peak for more frequent storm events. The aforementioned results underline the effects of urbanisation on less frequent events (50- and 100-year storm events), which are significantly less than they are on more frequent events (2-,5- year storm events).

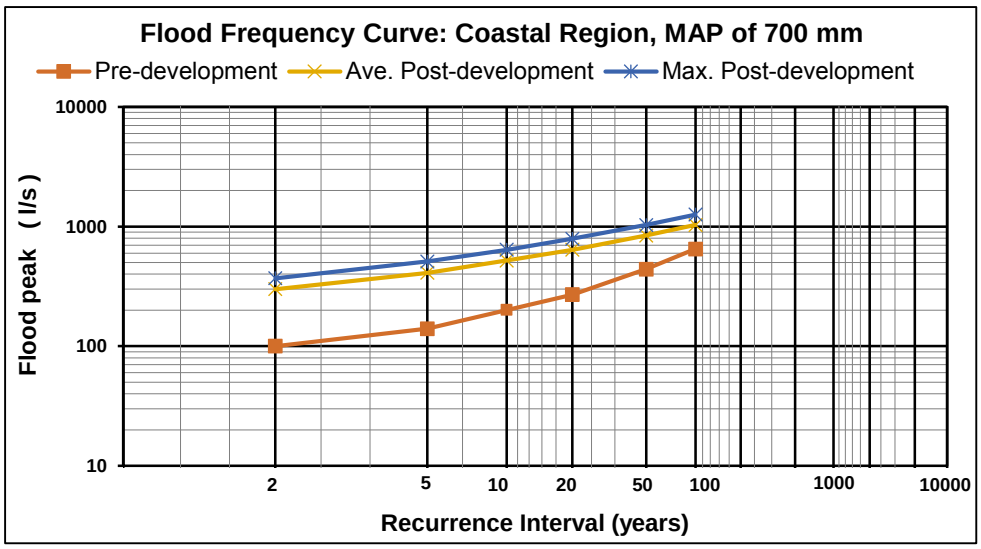

Figure D.4: Flood frequency curve of the coastal region for a MAP of 700 mm

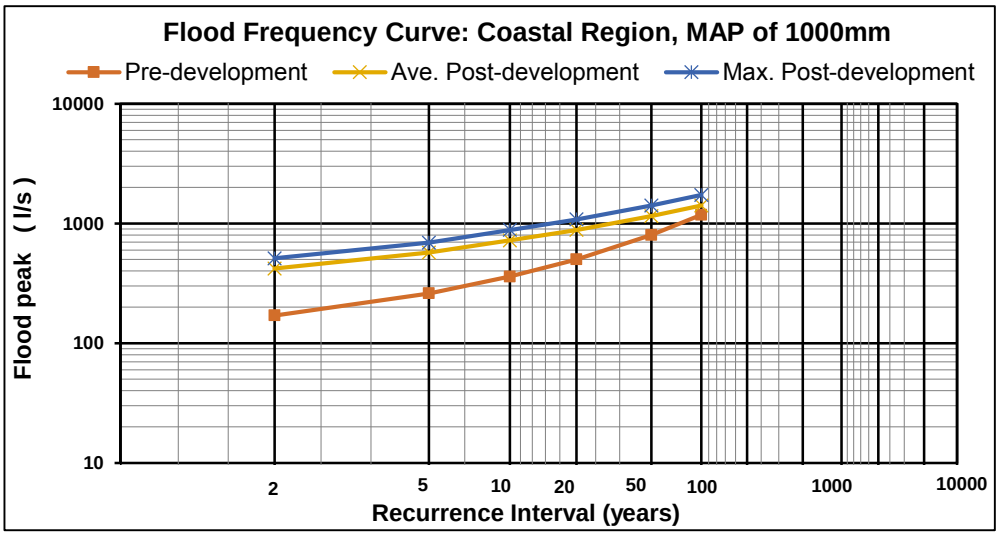

Figure D.5: Flood frequency curve of the coastal region for a MAP of 1000 mm

The inland scenario had similar results, which are illustrated in Figures D.6 to D.8. The only difference between the coastal and inland scenarios is that the inland scenario produced higher peak flows. However, the percentage difference of the post-development peak flow in comparison to pre-development peak flow, for both coastal and inland scenarios, were within the same range. These observations are tabularised in Table D.6 and Table D.7.

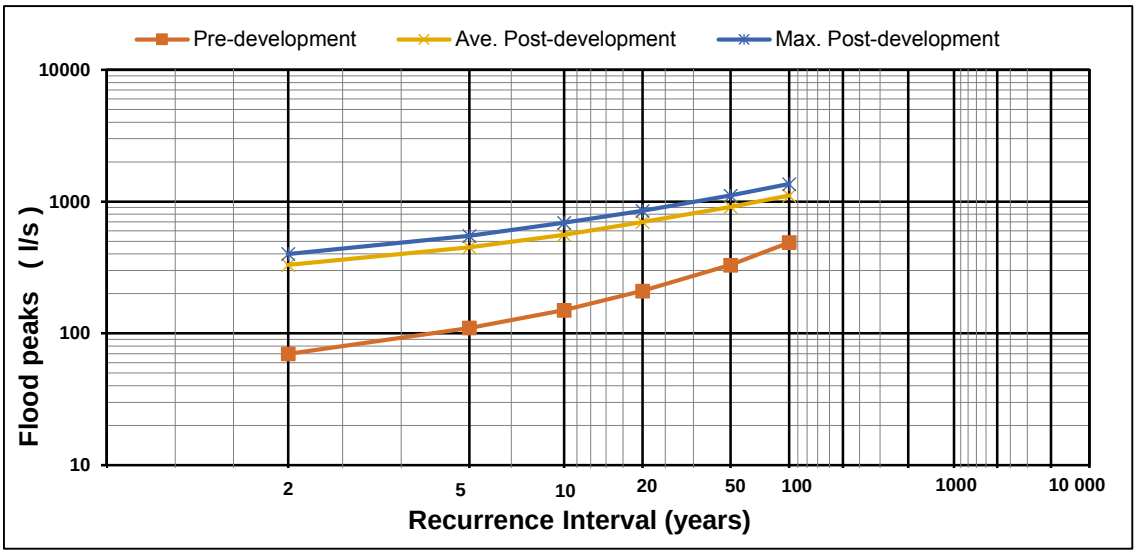

Figure D.6: Flood Frequency Curve for the Inland region and a MAP of 400mm

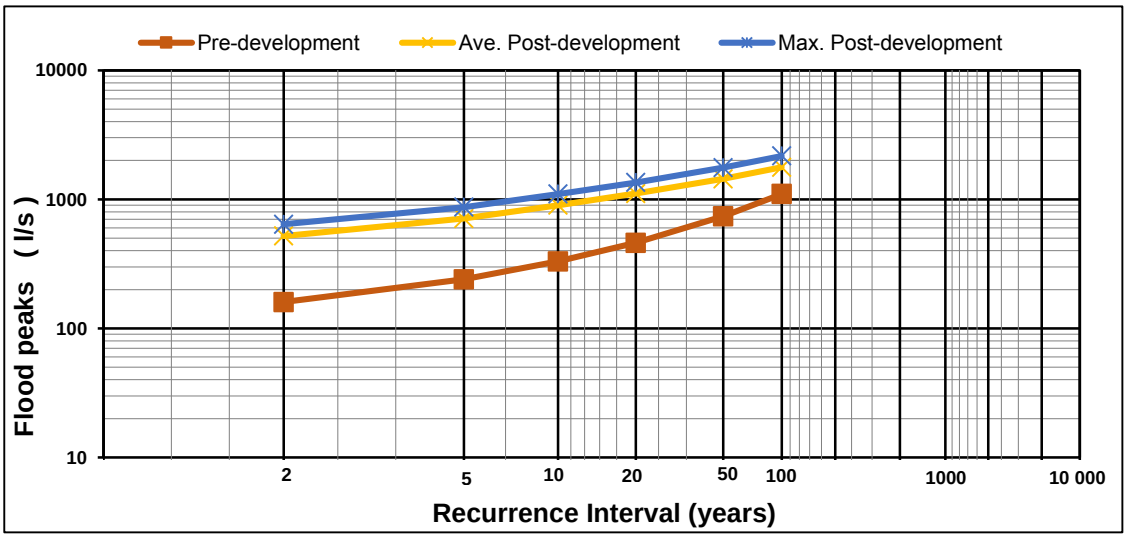

Figure D.7: Flood Frequency Curve for the Inland region and a MAP of 700 mm

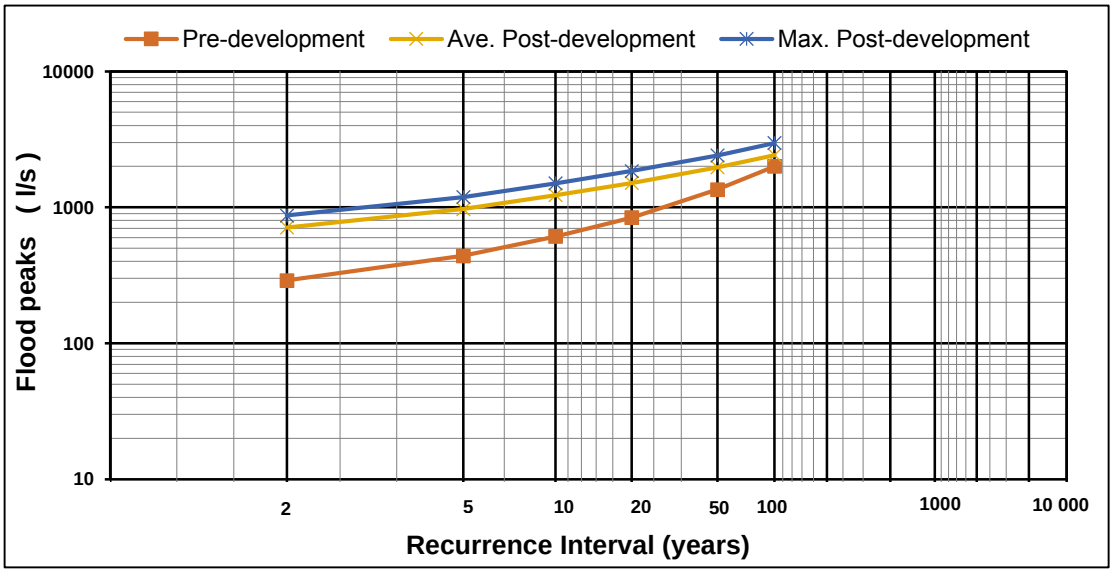

Figure D.8: Flood Frequency Curve for the Inland region and a MAP of 1000 mm

Table D.6: Flood peak comparison between pre- and post-development flood peaks presented in percent difference – Coastal region

MAP (mm)	RI (years)	Default Pre-development Scenario, C_2=0	Flood peak m^3/s (% change)	
			Average Post-development Scenario, C_2= 0.423	Maximum Post-development Scenario,C_2=0.518
400	2	0.04	0.19	0.23
			(375.00)	**(475.00)**
	5	0.06	0.26	0.32
			(333.33)	**(433.33)**
	10	0.09	0.33	0.40
			(266.67)	**(344.44)**
	20	0.12	0.41	0.50
			(241.67)	**(316.67)**
	50	0.2	0.53	0.65
			(165.00)	**(225.00)**
	100	0.29	0.65	0.80
			(124.14)	**(175.86)**
700	2	0.1	0.30	0.37
			(200.00)	**(270.00)**
	5	0.14	0.41	0.51
			(192.86)	**(264.29)**
	10	0.2	0.52	0.64
			(160.00)	**(220.00)**
	20	0.27	0.64	0.79
			(137.04)	**(192.59)**
	50	0.44	0.84	1.03
			(90.91)	**(134.09)**
	100	0.65	1.03	1.26
			(58.46)	**(93.85)**
1000	2	0.17	0.42	0.51
			(147.06)	**(200.00)**
	5	0.26	0.57	0.69
			(119.23)	**(165.38)**
	10	0.36	0.72	0.88
			(100.00)	**(144.44)**
	20	0.5	0.88	1.08
			(76.00)	**(116.00)**
	50	0.8	1.15	1.41
			(43.75)	**(76.25)**
	100	1.18	1.41	1.73
			(19.49)	**(46.61)**

Table D.7: Flood peak comparison between pre- and post-development flood peaks presented in percent difference–Inland region

MAP (mm)	RI (years)	Default Pre-development Scenario, C_2=0	Flood peak m^3/s (% difference)	
			Average Post-development Scenario, C_2= 0.423	Maximum Post-development Scenario,C_2=0.518
400	2	0.07	0.33	0.40
			(371.43)	**(471.43)**
	5	0.11	0.45	0.55
			(309.09)	**(400.00)**
	10	0.15	0.56	0.69
			(273.33)	**(360.00)**
	20	0.21	0.70	0.85
			(233.33)	**(304.76)**
	50	0.33	0.91	1.11
			(175.76)	**(236.36)**
	100	0.49	1.11	1.36
			(126.53)	**(177.55)**
700	2	0.16	0.52	0.64
			(225.00)	**(300.00)**
	5	0.24	0.71	0.87
			(195.83)	**(262.50)**
	10	0.33	0.90	1.10
			(172.73)	**(233.33)**
	20	0.46	1.11	1.35
			(141.30)	**(193.48)**
	50	0.74	1.44	1.76
			(94.59)	**(137.84)**
	100	1.1	1.77	2.17
			(60.91)	**(97.27)**
1000	2	0.29	0.71	0.87
			(144.83)	**(200.00)**
	5	0.44	0.97	1.19
			(120.45)	**(170.45)**
	10	0.61	1.23	1.50
			(101.64)	**(145.90)**
	20	0.84	1.51	1.85
			(79.76)	**(120.24)**
	50	1.35	1.97	2.41
			(45.93)	**(78.52)**
	100	2	2.42	2.97
			(21.00)	**(48.50)**

APPENDIX E: Multi-Stage Outlet Design Sizing Calculations

Chapter 4 discussed the preliminary design calculations and computed the outflow of the designed multi-stage outlets by utilising the Excel spreadsheet model. The calculated outflow was compared to the outflow computed by the watershed modelling software (Hydrology Studio, 2014) in Table 4.1 to Table 4.6. Table E.1 summarises the procedure to determine the outflow (stage-discharge relationship) of a multi-stage outlet structure, designed for coastal regions with a MAP of 400 mm (Design C.2). Design C.2 (refer to Table G.1 in Appendix G), which consists of a 2-year RI control circular orifice, a 10-year RI control rectangular orifice, and a V-notch weir to control the 50-year RI storm, restricted the outflow to the pre-development peaks for all the recurrence intervals.

The following steps were implemented to compile Table E.1:

First, the 100-year outlet pipe was sized to meet or exceed the upper end of the target outflow of the 100-year storm. A trial route should then be performed to confirm if the target outflow was met. Standard, commercially available culvert sizes should be kept in mind when selecting a pipe to control the 100-year storm event.

Step 1: Approximate the 2-, 5-, 10-, 20-, 50-, and 100-year maximum water surface elevation, respectively.

Enter the stage-storage curve, Figure E.1, with the estimated storage volume, for example the 2-year estimated storage was 217.8 m^3, calculated with Equation E.1. Then, h_{2max}= 0.67m and the procedure is repeated for each design storm. The maximum approximated head for each RI storm is indicated in blue in column 1 of Table E.1. When the orifice size is selected, the maximum head value was adjusted, since the head it measured from the centreline of the orifice to the maximum surface elevation when calculating the discharge for a free outflow orifice.

An additional ten to fifteen percent storage is required when multiple levels of detention are provided (Stormwater Design Example, n.d.). Therefore, for preliminary sizing purposes, ten percent storage was added to the estimated storage volume.

$$V_s \quad .5\,(Q_i - Q_o)t_i \qquad \text{(E.1)}$$

where:

V_s = storage volume estimate (m^3)

t_i = duration of storage facility inflow (s)

t_p = time to peak of the inflow hydrograph (s)

Q_i = peak inflow rate into the basin (m^3/s)

Q_o = peak outflow rate out of the pond (m^3/s).

The storage volume at each elevation interval is indicated in column 2 of Table E.1. The storage volume of the trapezoidal basin was calculated with Equation E.2. A trapezoidal basin with a length of 18.5 m, a base width of 12.5 m, and a side slope factor (Z) of four, were required to provide a storage volume equal to the maximum estimated volume of 574 m^3 for the 100-year RI storm, at a storage depth less than or equal to 1.5 m. Since the depth of the pond is a safety concern, a limiting depth of 1.5 m was selected for all storage facility designs. Figure E.2 illustrates the geometry of the trapezoidal basin.

$$V = (L \times W \times D) + ((L + W)ZD^2) + ((4/3)Z^2D^3) \quad \text{(E.2)}$$

where:

V = volume at a specific depth (m^3)
D = depth of basin (m)
L = length of basin at base (m)
W = width of basin at base (m)
R = ratio of width to length of basin at the base
Z = side slope factor (ratio of horizontal to vertical components of side slope).

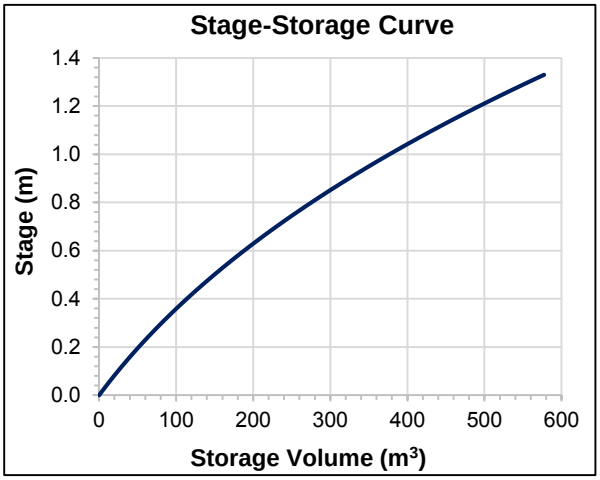

Figure E.1: Stage-Storage Curve for Design C.2

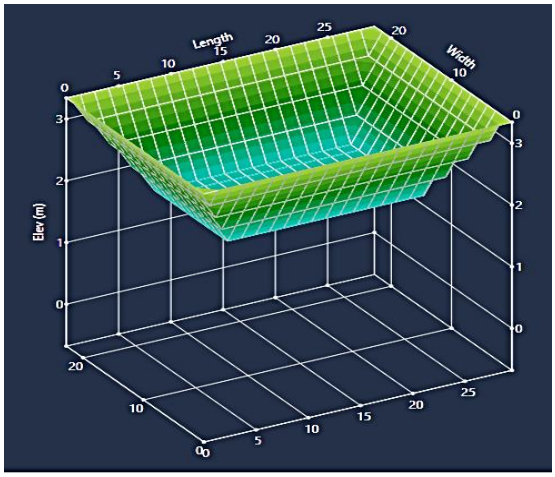

Figure E.2: Dimensions of storage pond (Hydrology Studio, 2015)

Step 2: Calculate the size of the 2-year control orifice (Column 3 of Table E.1).

Since the maximum allowable 2-year discharge rate was found to be 0.05 m^3/s, refer to Section 3.4, and the maximum 2-year head is known from Step 1, the size of the 2-year control device was determined by rearranging the standard orifice equation, Equation E.3.

$$\frac{Q}{C_d\sqrt{2gh}} \quad A \quad \text{(E.3)}$$

where:

Q = discharge (m^3/s)
C_D = dimensionless coefficient of discharge (≈0.6)
A = cross-sectional area of orifice (m^2)
h = head, measured from the centreline of the orifice to the maximum water level (m).

The orifice would initially act as a weir until the top of the orifice is submerged. Thus, as indicated in column 3, the transition from weir flow to orifice flow is taken into consideration by using partially submerged flow equations, Equations 2.2.1 to 2.2.4 in Section 2.3.2.1, until the water elevation in the pond reached the top of the circular orifice, at an elevation of 0.21 m, where after it acts as a fully submerged orifice. The orifice has a diameter of 0.18 m and the bottom of the opening is located at a pond elevation of 0.03 m.

At a certain stage, the head produced by the 100-year outlet pipe would submerge the 2-year control orifice, and then the head was taken as the difference between the upstream water elevation in the pond and the head produced by the 100-year outlet pipe. The standard orifice equation, Equation 2.1 in Section 2.3.2.1, was used to determine the discharge for submerged conditions, with the discharge coefficient equal to 0.6, and the head taken as the differential head as discussed above.

The head produced by the 100-year outlet pipe (column 6) was determined by means of inlet and outlet control calculations (refer to Section 2.3.2.3). The head corresponding to the smaller of the two discharges (i.e. inlet control discharge or outlet flow control discharge) was the controlling head at any given discharge, and therefore, used as the tailwater (column 12) of the submerged orifice.

Step 3: Perform routing calculations.

The routing procedure was accomplished by utilizing another spreadsheet enclosed on the CD-ROM. Figure E.3 indicates how the inflow hydrograph was routed through the basin and 2-year control orifice to check the geometry of the multi-stage outlet. If the routed post-development peak discharge from the 2-year design storm exceeds the pre-development peak discharge, then the storage volume and outlet device was re-sized and Step 1 to Step 3 repeated. The maximum water surface elevation reached after routing the 2-year (post-development) storm through the basin is indicated in green in column 1 of Table E.1.

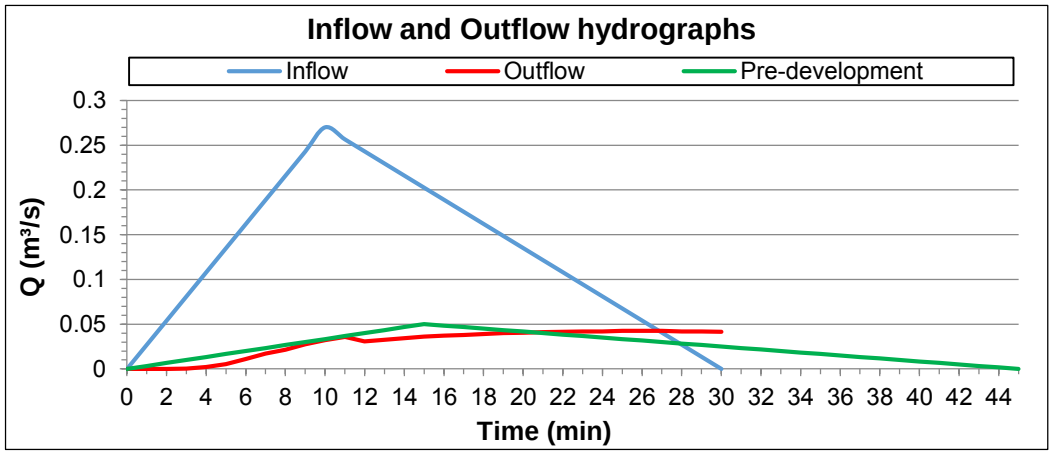

Figure E.3: Outflow hydrograph after routing calculations for the 2-year control device of the multi-stage outlet

Step 4: Size the 10-year Control Opening (Column 4 of Table E.1).

The 10-year control invert was set just above the minimum distance of 0.03 m above the 2-year maximum water surface elevation reached during the routing calculations (Virginia Department of Conservation and Recreation, 1999b:5-49). The maximum head, corresponding to the 10-year storm, was determined by subtracting the invert elevation of the 10-year control component from the estimated 10-year maximum water surface elevation. The 10-year maximum water surface elevation was read off from the stage-storage curve. With the maximum allowable 10-year discharge rate known, refer to Section 3.4, the required area of the 10-year release component could be determined.

The 2-year control orifice operates simultaneously with the other components of the multi-stage outlet. Thus, the discharge of the 2-year control orifice, corresponding to the estimated 10-year maximum water surface elevation, should be subtracted from the target discharge of the 10-year control device in order to determine the capacity of the 10-year device.

A rectangular orifice was chosen to control the 10-year storm. Again, Equation E.3 was used to determine the required area of the rectangular orifice. Equation 2.13, refer to Section 2.3.2.1, was used to determine the flow through the rectangular opening as the flow transitions from weir flow to orifice flow, with a weir coefficient equal to 0.37. Equations 2.2.1 to 2.2.4, which was used for the 2-year orifice control, couldn't be used for the 10-year rectangular orifice, since these equations are only true for thick-walled circular orifices. The standard orifice equation, Equation 2.1 in Section 2.3.2.1, was used to determine the discharge through the orifice for fully submerged conditions, with the discharge coefficient equal to 0.61 for a rectangular orifice.

For the multi-stage outlet under consideration, the head produced by the 100-year control outlet pipe (column 6) during the 100-year storm event, submerged the 10-year control orifice so that it no longer performed as a free-outfall orifice during the 100-year storm event. Thus, at stage 1.31m, the head used in the standard orifice equation, was taken as the differential head (i.e. the difference between the upstream water elevation and the head produced by the 100-year outlet pipe). This is illustrated in column 4 of Table E.1.

The hydraulic performance of the 10-year device was verified by routing the 2-year, 5-year, and 10-year inflow hydrograph through the basin. If the 10-year release rate exceeded the pre-development peak discharge, the orifice opening was resized or additional storage was added.

Step 5: Size the 50-year Control Opening (Column 5 of Table E.1)

The 50-year control invert was set just above the minimum distance of 0.03 m above the 2-year maximum water surface elevation reached during the routing calculations (Virginia Department of Conservation and Recreation, 1999b:5-49). The maximum head, corresponding to the 50-year storm, was determined by subtracting the invert elevation of the

50-year control from the estimated 50-year maximum water surface elevation. With the maximum allowable 50-year discharge rate known, refer to Section 3.4, the required size of the 50-year release opening could be determined. However, subtract the discharge of the 2- and 10-year control component of the multi-stage outlet, corresponding to the 50-year maximum surface elevation, from the target discharge of the 50-year device to determine the capacity of the 50-year device.

The multi-stage outlet under consideration, used a 90° V-notch weir to limited the 50-year storm to meet the pre-development peak flow. The head on the apex of the V-notch was determined by means of Equation 2.23, with the discharge coefficient taken as 0.59. For the multi-stage outlet under consideration, the 50-year control V-notch weir was affected by submergence, that is when the tailwater raised above the weir's crest. Thus, at stage 1.32 m, the Villemonte equation, Equation 2.22, was used to account for the reduction in discharge. This is indicated in column 5 of Table E.1. Lastly, verify the hydraulic performance of the 50-year device by routing the 2-, 5-, 10-, 20- and 50-year inflow hydrograph through the basin. If the 50-year release rate exceeds the pre-development peak discharge, reduce the size of the device or provide additional storage volume.

Step 6: Size the riser (Column 7 of Table E.1)

The riser structure was designed at the end to contain the multi-stage devices. The riser crest elevation was set just above the maximum elevation reached in Step 5. The size of the riser was selected so that the riser would not perform as a controlling device. The crest length of the riser should be enlarged if the riser structure transitions from riser weir flow control to riser orifice flow control, before the 100-year outlet pipe control the outflow (Virginia Department of Conservation and Recreation, 1999b).

Since the riser box functions as both a weir and an orifice, depending on the water surface elevation in the pond, both situations were evaluated in column 7 of Table E.1. The flow condition (i.e. riser orifice, riser weir, inlet-, or outlet control) which produced the lowest discharge for a given water surface elevation (stage) would be the controlling flow.

The standard orifice equation, with a discharge coefficient of 0.6 was used to determine the discharge for orifice flow conditions. The inside dimensions of the riser structure were used as the area of the orifice. Equation 2.13 was used to determine the flow over the riser crest for weir flow conditions, where the circumference of the riser box was taken as the weir length. The analysis indicates in column 7 of Table E.1 that the riser does not transition from riser weir flow to riser orifice flow within the range of water surface elevations. The thickness of the riser was taken as 150 mm (6ft) (Virginia Department of Conservation and Recreation, 1999b).

If a trash rack is required, use Figure 2.21 to determine the minimum rack size. The riser's circumference would then be influence by the minimum net open surface area of the trash rack, which is four times the cross-sectional area of the 100-year outlet pipe. Lastly, the discharge coefficient, used in Equation 2.14, is set equal to 1.45, to allow for sideways contraction of oncoming flows if water overflow riser from all four sides. Use a blockage factor of 0.5 to allow for accumulation of trash and debris. It is best to oversize the weir length of the riser box after reducing its length by the trash rack bars so as not to become the primary control when the trash rack becomes clogged by trash or debris. The latter would also ensure that weir flow is predominant during the storm event.

Figure E.4 plots the final outflow (column 10) from the multi-stage outlet (refer to Figure E.5) against the water elevation of the pond (column 1). From Figure E.4 it is evident that there was a good agreement between the stage-discharge curve obtained from the software (Hydrology Studio, 2015) and the theoretical calculations.

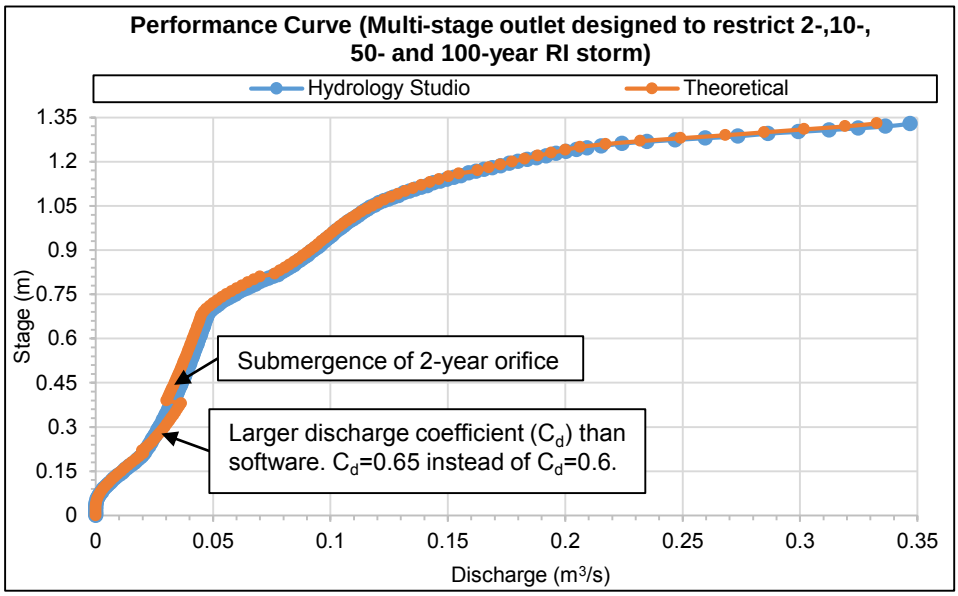

Figure E.4: Stage-discharge curve of multi-stage outlet structure

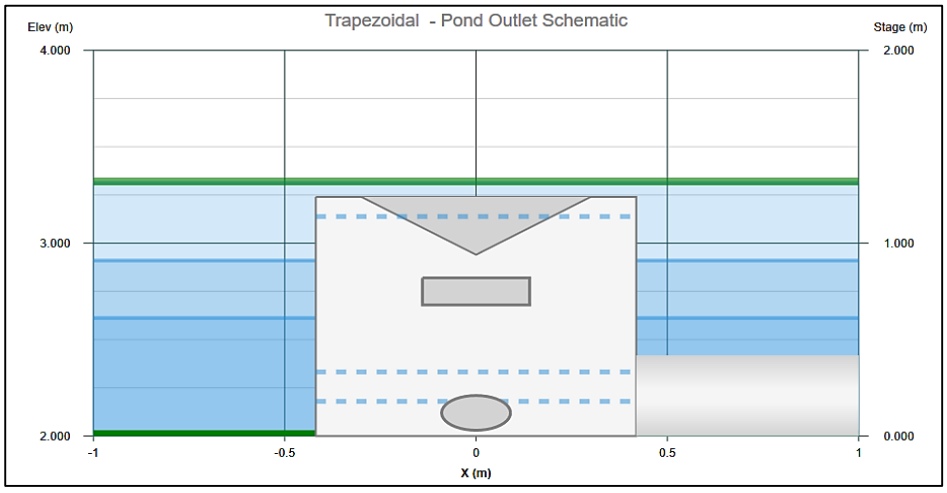

Figure E.5: Schematic of multi-stage outlet structure (Hydrology Studio, 2015)

Table E.1: Excel spreadsheet-based model for coastal regions, 400 mm MAP scenario

1	2	3							4				5			6				7				8	9	10	11	12	13
		Low Flow, 2-year control orifice m^3/s							10-year control orifice m^3/s				50-year control weir m^3/s			Pipe Flow m^3/s				Riser Flow m^3/s									
Depth, Y1 (Stage) (m)	Storage Volume (m^3)	Head h (m)	A(h)	θ (degrees)	Lw (m)	Q (m^3/s)	hs (m)	Qs (m^3/s)	Head h (m)	Q m^3/s	hs (m)	Qs m^3/s	Head h (m)	Q (m^3/s)	Qs (m^3/s)	Head on pipe, Y_2 (m)	Q: Inlet control (m^3/s)	Head on pipe, Y_2 (m)	Q: Outlet control (m^3/s)	Head h (m)	Q : Weir flow (m^3/s)	Head h (m)	Q: Orifice flow (m^3/s)	Total Q, before submergence (m^3/s)	Inlet Control: Total Q with 2- ,10- and 50-year submergence considered (m^3/s)	Total Q with 2-, 10- and 50-year submergence considered, as well as outlet control (m^3/s)	Water level in riser before 2-year orifice became submerge (m)	Water level in riser after 2-year orifice became submerge (m)	Water level in riser after 2-, 10- and 50-year orifice became submerge (m)
0.0	0.0	0.0	0.0	0.0	0.0	0.0										0.0	0.0							0.0	0.0	0.0	0.0	0.0	0.0
0.01	2.32	0.00	0.00	0.00	0.00	0.00										0.00	0.00							0.00	0.00	0.00	0.00	0.00	0.00
0.02	4.67	0.00	0.00	0.00	0.00	0.00										0.00	0.00							0.00	0.00	0.00	0.00	0.00	0.00
0.03	7.05	0.00	0.00	0.00	0.00	0.00										0.00	0.00							0.00	0.00	0.00	0.00	0.00	0.00
0.04	9.45	0.01	0.00	54.53	0.06	0.00										0.01	0.00							0.00	0.00	0.00	0.01	0.01	0.01
0.05	11.88	0.02	0.00	77.88	0.08	0.00										0.02	0.00							0.00	0.00	0.00	0.02	0.02	0.02
0.06	14.33	0.03	0.00	96.38	0.09	0.00										0.03	0.00							0.00	0.00	0.00	0.03	0.03	0.03
0.07	16.80	0.04	0.00	112.50	0.11	0.00										0.04	0.00							0.00	0.00	0.00	0.04	0.04	0.04
0.08	19.30	0.05	0.01	127.22	0.12	0.00										0.05	0.00							0.00	0.00	0.00	0.05	0.05	0.05
0.09	21.83	0.06	0.01	141.06	0.12	0.00										0.06	0.00							0.00	0.00	0.00	0.06	0.06	0.06
0.10	24.39	0.07	0.01	154.32	0.13	0.00										0.07	0.00							0.00	0.00	0.00	0.07	0.07	0.07
0.11	26.97	0.08	0.01	167.24	0.14	0.01										0.08	0.01							0.01	0.01	0.01	0.08	0.08	0.08
0.12	29.57	0.09	0.01	180.00	0.14	0.01										0.09	0.01							0.01	0.01	0.01	0.09	0.09	0.09
0.13	32.20	0.10	0.01	192.76	0.15	0.01										0.10	0.01							0.01	0.01	0.01	0.10	0.10	0.10
0.14	34.86	0.11	0.02	205.68	0.15	0.01										0.10	0.01							0.01	0.01	0.01	0.10	0.10	0.10
0.15	37.55	0.12	0.02	218.94	0.15	0.01										0.11	0.01							0.01	0.01	0.01	0.11	0.11	0.11
0.16	40.26	0.13	0.02	232.78	0.15	0.01										0.12	0.01							0.01	0.01	0.01	0.12	0.12	0.12
0.17	43.00	0.14	0.02	247.50	0.15	0.01										0.13	0.01							0.01	0.01	0.01	0.13	0.13	0.13
0.18	45.77	0.15	0.02	263.62	0.15	0.02										0.13	0.02							0.02	0.02	0.02	0.13	0.13	0.13
0.19	48.56	0.16	0.02	282.12	0.15	0.02										0.14	0.02							0.02	0.02	0.02	0.14	0.14	0.14
0.20	51.38	0.17	0.02	305.47	0.15	0.02										0.15	0.02							0.02	0.02	0.02	0.15	0.15	0.15
0.21	54.23	0.18	0.03	360.00	0.15	0.02										0.15	0.02							0.02	0.02	0.02	0.15	0.15	0.15
0.22	57.10	0.19				0.02										0.15	0.02							0.02	0.02	0.02	0.15	0.15	0.15
0.23	60.01	0.20				0.02										0.16	0.02							0.02	0.02	0.02	0.16	0.16	0.16
0.24	62.94	0.21				0.02										0.16	0.02							0.02	0.02	0.02	0.16	0.16	0.16
0.25	65.90	0.22				0.02										0.17	0.02							0.02	0.02	0.02	0.17	0.17	0.17
0.26	68.88	0.23				0.03										0.17	0.03							0.03	0.03	0.03	0.17	0.17	0.17
0.27	71.90	0.24				0.03										0.18	0.03							0.03	0.03	0.03	0.18	0.18	0.18
0.28	74.94	0.25				0.03										0.18	0.03							0.03	0.03	0.03	0.18	0.18	0.18
0.29	78.01	0.26				0.03										0.19	0.03							0.03	0.03	0.03	0.19	0.19	0.19
0.30	81.11	0.27				0.03										0.19	0.03							0.03	0.03	0.03	0.19	0.19	0.19
0.31	84.24	0.28				0.03										0.19	0.03							0.03	0.03	0.03	0.19	0.19	0.19
0.32	87.40	0.29				0.03										0.19	0.03							0.03	0.03	0.03	0.19	0.19	0.19
0.33	90.58	0.30				0.03										0.20	0.03							0.03	0.03	0.03	0.20	0.20	0.20
0.34	93.80	0.31				0.03										0.20	0.03							0.03	0.03	0.03	0.20	0.20	0.20
0.35	97.04	0.32				0.03										0.20	0.03							0.03	0.03	0.03	0.20	0.20	0.20
0.36	100.32	0.33				0.03										0.21	0.03							0.03	0.03	0.03	0.21	0.21	0.21
0.37	103.62	0.34				0.04										0.21	0.04							0.04	0.04	0.04	0.21	0.21	0.21
0.38	106.95	0.35				0.04										0.21	0.04							0.04	0.04	0.04	0.21	0.21	0.21
0.39	110.31	0.36				0.04	0.20	0.03								0.19	0.03							0.04	0.03	0.03	0.21	0.19	0.19
0.40	113.71	0.37				0.04	0.21	0.03								0.19	0.03							0.04	0.03	0.03	0.22	0.19	0.19
0.41	117.13	0.38				0.04	0.22	0.03								0.19	0.03							0.04	0.03	0.03	0.22	0.19	0.19
0.42	120.58	0.39				0.04	0.22	0.03								0.20	0.03							0.04	0.03	0.03	0.22	0.20	0.20
0.43	124.06	0.40				0.04	0.23	0.03								0.20	0.03							0.04	0.03	0.03	0.22	0.20	0.20
0.44	127.57	0.41				0.04	0.24	0.03								0.20	0.03							0.04	0.03	0.03	0.22	0.20	0.20
0.45	131.12	0.42				0.04	0.25	0.03								0.20	0.03							0.04	0.03	0.03	0.23	0.20	0.20
0.46	134.69	0.43				0.04	0.26	0.03								0.20	0.03							0.04	0.03	0.03	0.23	0.20	0.20
0.47	138.29	0.44				0.04	0.26	0.03								0.21	0.03							0.04	0.03	0.03	0.23	0.21	0.21
0.48	141.93	0.45				0.04	0.27	0.04								0.21	0.04							0.04	0.04	0.04	0.23	0.21	0.21
0.49	145.59	0.46				0.04	0.28	0.04								0.21	0.04							0.04	0.04	0.04	0.23	0.21	0.21
0.50	149.29	0.47				0.05	0.29	0.04								0.21	0.04							0.05	0.04	0.04	0.24	0.21	0.21
0.51	153.02	0.48				0.05	0.30	0.04								0.21	0.04							0.05	0.04	0.04	0.24	0.21	0.21
0.52	156.78	0.49				0.05	0.31	0.04								0.21	0.04							0.05	0.04	0.04	0.24	0.21	0.21
0.53	160.57	0.50				0.05	0.31	0.04								0.22	0.04							0.05	0.04	0.04	0.24	0.22	0.22
0.54	164.39	0.51				0.05	0.32	0.04								0.22	0.04							0.05	0.04	0.04	0.24	0.22	0.22
0.55	168.25	0.52				0.05	0.33	0.04								0.22	0.04							0.05	0.04	0.04	0.24	0.22	0.22
0.56	172.13	0.53				0.05	0.34	0.04								0.22	0.04							0.05	0.04	0.04	0.25	0.22	0.22
0.57	176.05	0.54				0.05	0.35	0.04								0.22	0.04							0.05	0.04	0.04	0.25	0.22	0.22
0.58	180.00	0.55				0.05	0.36	0.04								0.22	0.04							0.05	0.04	0.04	0.25	0.22	0.22
0.59	183.98	0.56				0.05	0.37	0.04								0.22	0.04							0.05	0.04	0.04	0.25	0.22	0.22
0.60	188.00	0.57				0.05	0.37	0.04								0.23	0.04							0.05	0.04	0.04	0.25	0.23	0.23
0.61	192.05	0.58				0.05	0.38	0.04								0.23	0.04							0.05	0.04	0.04	0.25	0.23	0.23
0.62	196.12	0.59				0.05	0.39	0.04								0.23	0.04							0.05	0.04	0.04	0.25	0.23	0.23
0.63	200.24	0.60				0.05	0.40	0.04								0.23	0.04							0.05	0.04	0.04	0.26	0.23	0.23
0.64	204.38	0.61				0.05	0.41	0.04								0.23	0.04							0.05	0.04	0.04	0.26	0.23	0.23
0.65	208.56	0.62				0.05	0.42	0.04								0.23	0.04							0.05	0.04	0.04	0.26	0.23	0.23
0.66	212.77	0.63				0.05	0.43	0.04								0.23	0.04							0.05	0.04	0.04	0.26	0.23	0.23
0.67	217.02	0.64				0.05	0.44	0.04								0.23	0.04							0.05	0.04	0.04	0.26	0.23	0.23
0.68	221.30	0.65				0.05	0.44	0.05	0.00	0.00						0.24	0.05							0.05	0.05	0.05	0.26	0.24	0.24
0.69	225.61	0.66				0.06	0.45	0.05	0.01	0.00						0.24	0.05							0.06	0.05	0.05	0.26	0.24	0.24
0.70	229.95	0.67				0.06	0.46	0.05	0.02	0.00						0.24	0.05							0.06	0.05	0.05	0.27	0.24	0.24
0.71	234.33	0.68				0.06	0.46	0.05	0.03	0.00						0.25	0.05							0.06	0.05	0.05	0.27	0.25	0.25
0.72	238.74	0.69				0.06	0.47	0.05	0.04	0.00						0.25	0.05							0.06	0.05	0.05	0.28	0.25	0.25
0.73	243.19	0.70				0.06	0.48	0.05	0.05	0.01						0.25	0.05							0.06	0.05	0.05	0.28	0.25	0.25
0.74	247.67	0.71				0.06	0.48	0.05	0.06	0.01						0.26	0.05							0.06	0.05	0.05	0.28	0.26	0.26
0.75	252.19	0.72				0.06	0.49	0.05	0.07	0.01						0.26	0.06							0.07	0.06	0.06	0.29	0.26	0.26
0.76	256.74	0.73				0.06	0.49	0.05	0.08	0.01						0.27	0.06							0.07	0.06	0.06	0.29	0.27	0.27
0.77	261.32	0.74				0.06	0.50	0.05	0.09	0.01						0.27	0.06							0.07	0.06	0.06	0.30	0.27	0.27
0.78	265.94	0.75				0.06	0.50	0.05	0.10	0.01						0.28	0.06							0.07	0.06	0.06	0.31	0.28	0.28
0.79	270.59	0.76				0.06	0.50	0.05	0.11	0.02						0.29	0.06							0.08	0.06	0.06	0.31	0.29	0.29
0.80	275.28	0.77				0.06	0.51	0.05	0.12	0.02						0.29	0.07							0.08	0.07	0.07	0.32	0.29	0.29
0.81	280.01	0.78				0.06	0.51	0.05	0.13	0.02						0.30	0.07							0.08	0.07	0.07	0.32	0.30	0.30
0.82	284.77	0.79				0.06	0.51	0.05	0.14	0.03						0.31	0.08							0.09	0.08	0.08	0.34	0.31	0.31
0.83	289.56	0.80				0.06	0.51	0.05	0.15	0.03						0.32	0.08							0.09	0.08	0.08	0.34	0.32	0.32

1	2	3							4				5			6				7				8	9	10	11	12	13
		Low Flow, 2-year control orifice m^3/s							10-year control orifice m^3/s				50-year control weir m^3/s			Pipe Flow m^3/s				Riser Flow m^3/s									
Depth, Y1 (Stage) (m)	Storage Volume (m^3)	Head h (m)	A(h)	θ (degrees)	Lw (m)	Q (m^3/s)	hs (m)	Qs (m^3/s)	Head h (m)	Q m^3/s	hs (m)	Qs m^3/s	Head h (m)	Q (m^3/s)	Qs (m^3/s)	Head on pipe, Y_2 (m)	Q: Inlet control (m^3/s)	Head on pipe, Y_2 (m)	Q: Outlet control (m^3/s)	Head h (m)	Q : Weir flow (m^3/s)	Head h (m)	Q: Orifice flow (m^3/s)	Total Q, before submergence (m^3/s)	Inlet Control: Total Q with 2- ,10- and 50-year submergence considered (m^3/s)	Total Q with 2-, 10- and 50-year submergence considered, as well as outlet control (m^3/s)	Water level in riser before 2-year orifice became submerge (m)	Water level in riser after 2-year orifice became submerge (m)	Water level in riser after 2-, 10- and 50-year orifice became submerge (m)
0.84	294.39	0.81				0.06	0.52	0.05	0.16	0.03						0.32	0.08							0.09	0.08	0.08	0.35	0.32	0.32
0.85	299.25	0.82				0.06	0.53	0.05	0.17	0.03						0.32	0.08							0.10	0.08	0.08	0.36	0.32	0.32
0.86	304.15	0.83				0.06	0.53	0.05	0.18	0.04						0.33	0.08							0.10	0.08	0.08	0.42	0.33	0.33
0.87	309.09	0.84				0.06	0.54	0.05	0.19	0.04						0.33	0.09							0.10	0.09	0.09	0.42	0.33	0.33
0.88	314.06	0.85				0.06	0.54	0.05	0.20	0.04						0.34	0.09							0.10	0.09	0.09	0.42	0.34	0.34
0.89	319.07	0.86				0.06	0.55	0.05	0.21	0.04						0.34	0.09							0.10	0.09	0.09	0.43	0.34	0.34
0.90	324.12	0.87				0.06	0.56	0.05	0.22	0.04						0.34	0.09							0.11	0.09	0.09	0.43	0.34	0.34
0.91	329.20	0.88				0.07	0.56	0.05	0.23	0.04						0.35	0.09							0.11	0.09	0.09	0.43	0.35	0.35
0.92	334.32	0.89				0.07	0.57	0.05	0.24	0.04						0.35	0.09							0.11	0.09	0.09	0.43	0.35	0.35
0.93	339.47	0.90				0.07	0.57	0.05	0.25	0.04						0.36	0.10							0.11	0.10	0.10	0.43	0.36	0.36
0.94	344.66	0.91				0.07	0.58	0.05	0.26	0.05			0.00	0.00		0.36	0.10							0.11	0.10	0.10	0.44	0.42	0.36
0.95	349.89	0.92				0.07	0.59	0.05	0.27	0.05			0.01	0.00		0.36	0.10							0.11	0.10	0.10	0.44	0.42	0.36
0.96	355.15	0.93				0.07	0.59	0.05	0.28	0.05			0.02	0.00		0.37	0.10	0.42	0.10					0.12	0.10	0.10	0.44	0.42	0.42
0.97	360.45	0.94				0.07	0.60	0.05	0.29	0.05			0.03	0.00		0.37	0.10	0.42	0.10					0.12	0.10	0.10	0.44	0.42	0.42
0.98	365.79	0.95				0.07	0.61	0.05	0.30	0.05			0.04	0.00		0.37	0.10	0.42	0.10					0.12	0.10	0.10	0.44	0.43	0.42
0.99	371.17	0.96				0.07	0.61	0.05	0.31	0.05			0.05	0.00		0.38	0.11	0.43	0.10					0.12	0.11	0.10	0.45	0.43	0.43
1.00	376.58	0.97				0.07	0.62	0.05	0.32	0.05			0.06	0.00		0.38	0.11	0.43	0.11					0.12	0.11	0.11	0.45	0.43	0.43
1.01	382.03	0.98				0.07	0.62	0.05	0.33	0.05			0.07	0.00		0.39	0.11	0.43	0.11					0.12	0.11	0.11	0.45	0.43	0.43
1.02	387.52	0.99				0.07	0.63	0.05	0.34	0.06			0.08	0.00		0.39	0.11	0.43	0.11					0.13	0.11	0.11	0.45	0.43	0.43
1.03	393.05	1.00				0.07	0.63	0.05	0.35	0.06			0.09	0.00		0.40	0.11	0.44	0.11					0.13	0.11	0.11	0.46	0.44	0.44
1.04	398.62	1.01				0.07	0.64	0.05	0.36	0.06			0.10	0.00		0.40	0.12	0.44	0.11					0.13	0.12	0.11	0.46	0.44	0.44
1.05	404.22	1.02				0.07	0.64	0.05	0.37	0.06			0.11	0.01		0.41	0.12	0.44	0.12					0.13	0.12	0.12	0.46	0.44	0.44
1.06	409.86	1.03				0.07	0.65	0.05	0.38	0.06			0.12	0.01		0.41	0.12	0.44	0.12					0.14	0.12	0.12	0.47	0.45	0.44
1.07	415.54	1.04				0.07	0.65	0.05	0.39	0.06			0.13	0.01		0.42	0.12	0.45	0.12					0.14	0.12	0.12	0.47	0.45	0.45
1.08	421.26	1.05				0.07	0.66	0.05	0.40	0.06			0.14	0.01		0.42	0.13	0.45	0.12					0.14	0.13	0.12	0.48	0.45	0.45
1.09	427.01	1.06				0.07	0.66	0.05	0.41	0.06			0.15	0.01		0.43	0.13	0.46	0.13					0.15	0.13	0.13	0.48	0.46	0.46
1.10	432.81	1.07				0.07	0.66	0.06	0.42	0.06			0.16	0.01		0.44	0.13	0.46	0.13					0.15	0.13	0.13	0.49	0.46	0.46
1.11	438.64	1.08				0.07	0.66	0.06	0.43	0.06			0.17	0.02		0.45	0.14	0.46	0.13					0.15	0.14	0.13	0.49	0.47	0.46
1.12	444.52	1.09				0.07	0.67	0.06	0.44	0.06			0.18	0.02		0.45	0.14	0.47	0.14					0.16	0.14	0.14	0.50	0.47	0.47
1.13	450.43	1.10				0.07	0.67	0.06	0.45	0.07			0.19	0.02		0.46	0.14	0.48	0.14					0.16	0.14	0.14	0.51	0.48	0.48
1.14	456.38	1.11				0.07	0.67	0.06	0.46	0.07			0.20	0.02		0.47	0.15	0.48	0.15					0.16	0.15	0.15	0.51	0.48	0.48
1.15	462.37	1.12				0.07	0.67	0.06	0.47	0.07			0.21	0.03		0.48	0.15	0.49	0.15					0.17	0.15	0.15	0.52	0.49	0.49
1.16	468.40	1.13				0.07	0.67	0.06	0.48	0.07			0.22	0.03		0.49	0.15	0.50	0.15					0.17	0.15	0.15	0.53	0.50	0.50
1.17	474.47	1.14				0.08	0.76	0.06	0.49	0.07			0.23	0.04		0.41	0.16	0.50	0.16					0.18	0.16	0.16	0.54	0.51	0.50
1.18	480.58	1.15				0.08	0.76	0.06	0.50	0.07			0.24	0.04		0.42	0.17	0.51	0.16					0.18	0.17	0.16	0.55	0.52	0.51
1.19	486.73	1.16				0.08	0.76	0.06	0.51	0.07			0.25	0.04		0.43	0.17	0.52	0.17					0.19	0.17	0.17	0.56	0.53	0.52
1.20	492.92	1.17				0.08	0.76	0.06	0.52	0.07			0.26	0.05		0.44	0.18	0.53	0.17					0.19	0.18	0.17	0.57	0.54	0.53
1.21	499.15	1.18				0.08	0.75	0.06	0.53	0.07			0.27	0.05		0.46	0.18	0.54	0.18					0.20	0.18	0.18	0.58	0.55	0.54
1.22	505.42	1.19				0.08	0.75	0.06	0.54	0.07			0.28	0.06		0.47	0.19	0.55	0.19					0.21	0.19	0.19	0.60	0.56	0.55
1.23	511.74	1.20				0.08	0.74	0.06	0.55	0.07			0.29	0.06		0.49	0.19	0.56	0.19					0.21	0.19	0.19	0.61	0.57	0.56
1.24	518.09	1.21				0.08	0.73	0.06	0.56	0.07			0.30	0.07		0.51	0.20	0.58	0.20					0.22	0.20	0.20	0.63	0.58	0.58
1.25	524.48	1.22				0.08	0.72	0.06	0.57	0.07			0.31	0.07		0.53	0.21	0.59	0.20	0.00	0.00	0.00	0.00	0.23	0.21	0.20	0.66	0.60	0.59
1.26	530.91	1.23				0.08	0.70	0.06	0.58	0.08			0.32	0.08		0.56	0.22	0.62	0.21	0.01	0.01	0.01	0.17	0.25	0.22	0.21	0.70	0.62	0.62
1.27	537.39	1.24				0.08	0.66	0.05	0.59	0.08			0.33	0.09		0.61	0.23	0.65	0.23	0.02	0.01	0.02	0.24	0.27	0.23	0.23	0.75	0.66	0.65
1.28	543.90	1.25				0.08	0.61	0.05	0.60	0.08			0.34	0.09		0.67	0.25	0.70	0.25	0.03	0.03	0.03	0.29	0.29	0.25	0.25	0.84	0.70	0.70
1.29	550.46	1.26				0.08	0.54	0.05	0.61	0.08			0.35	0.10		0.75	0.27	0.75	0.27	0.04	0.04	0.04	0.34	0.31	0.27	0.27	0.94	0.75	0.75
1.30	557.05	1.27				0.08	0.48	0.05	0.62	0.08	0.48	0.07	0.36	0.11		0.82	0.28	0.80	0.28	0.05	0.06	0.05	0.38	0.34	0.28	0.28	1.07	0.84	0.82
1.31	563.69	1.28				0.08	0.42	0.04	0.63	0.08	0.42	0.07	0.37	0.11		0.89	0.30	0.85	0.30	0.06	0.07	0.06	0.41	0.37	0.30	0.30	1.22	0.94	0.89
1.32	570.37	1.29				0.08	0.35	0.04	0.64	0.08	0.35	0.06	0.38	0.12		0.97	0.32	0.91	0.32	0.07	0.09	0.07	0.44	0.40	0.32	0.32	1.39	1.06	0.97
1.33	577.10	1.30				0.08	0.30	0.04	0.65	0.08	0.30	0.06	0.39	0.13	0.12	1.03	0.33	0.96	0.33	0.08	0.11	0.07	0.44	0.29	0.33	0.33	0.85	1.19	1.04

Where:

hs = differential head (m)

Qs = submerged flow (m^3/s)

Color scheme	
	Max depth and flow after routing
	Estimated max depth and storage
	Estimated max depth and storage (incl. additional 10%)
	Transition from weir flow to orifice flow
	Start of submerged flow
	Invert or crest height of each discharge control device
	Transition from inlet control to outlet control

Estimated required storage: 2-year RI		Estimated required storage: 20-year RI	
Vs (m^3)	198	Vs (m^3)	387
Qi (m^3/s)	0.27	Qi (m^3/s)	0.57
Qo (m^3/s)	0.05	Qo (m^3/s)	0.14
ti (sec)	1800	ti (sec)	1800
Vs (Added 10%) (m^3)	217.8	Vs (Added 10%) (m^3)	425.7
Estimated required storage: 5-year RI		Estimated required storage: 50-year RI	
Vs (m^3)	270	Vs (m^3)	459
Qi (m^3/s)	0.37	Qi (m^3/s)	0.74
Qo (m^3/s)	0.07	Qo (m^3/s)	0.23
ti (sec)	1800	ti (sec)	1800
Vs (Added 10%) (m^3)	297	Vs (Added 10%) (m^3)	504.9
Estimated required storage: 10-year RI		Estimated required storage: 100-year RI	
Vs (m^3)	324	Vs (m^3)	522
Qi (m^3/s)	0.46	Qi (m^3/s)	0.92
Qo (m^3/s)	0.1	Qo (m^3/s)	0.34
ti (sec)	1800	ti (sec)	1800
Vs (Added 10%) (m^3)	356.4	Vs (Added 10%) (m^3)	574.2

APPENDIX F: Preliminary Design Drawings of Multi-Stage Outlets (Prototypes)

Table F.1: Layout and dimensions of the prototype multi-stage outlet structure designed to attenuate different RI storms for coastal regions receiving 400 mm of MAP

<table>
<tr><th colspan="2">Classification</th><th>2-, 10-, 50- and 100-year RI storms</th><th>2-, 20-, 50- and 100-year RI storms</th></tr>
<tr><td rowspan="2">Coastal Region</td><td rowspan="2">400 mm Mean Annual Precipitation</td><td> 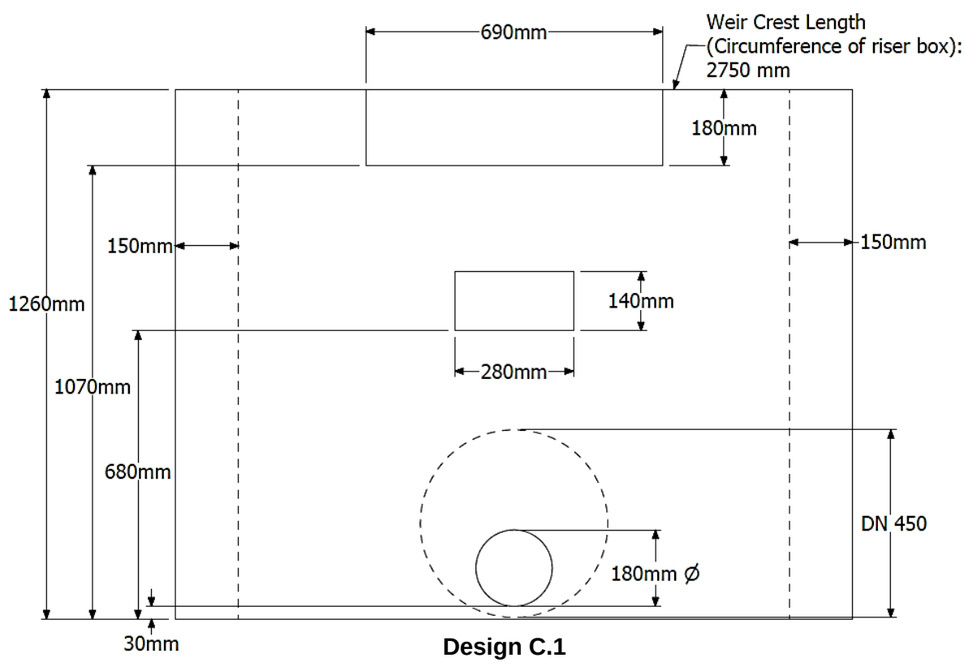

Design C.1</td><td> 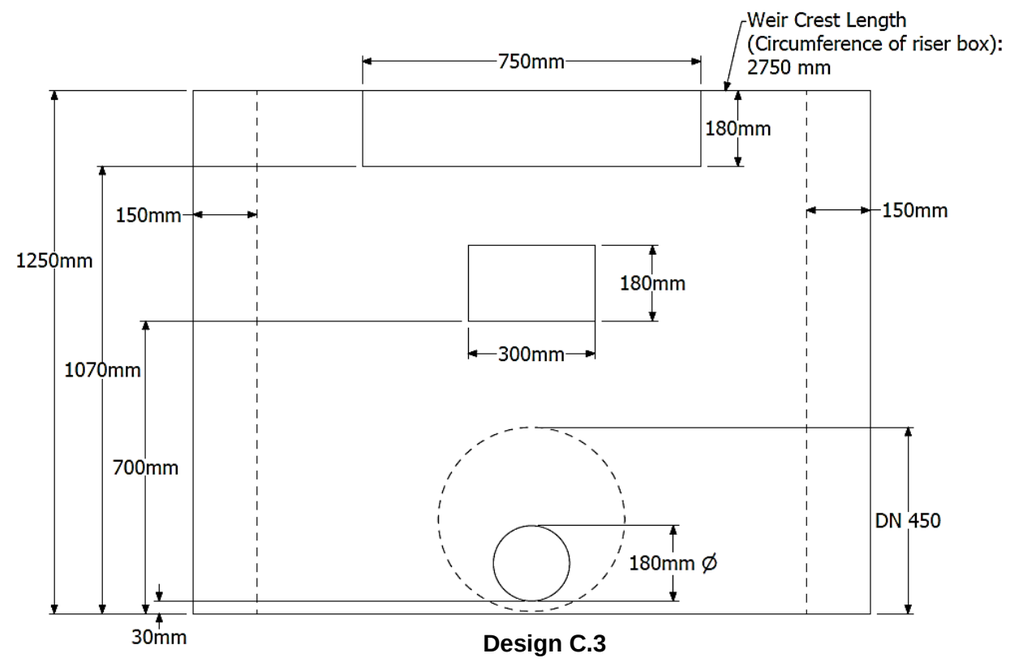

Design C.3</td></tr>
<tr><td> 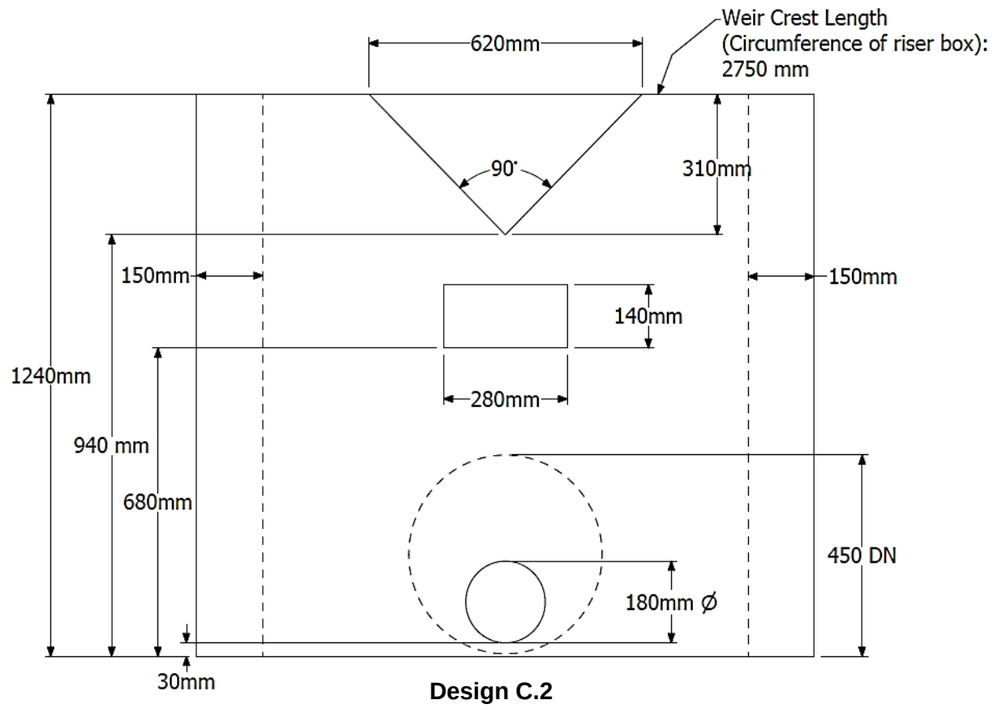

Design C.2</td><td> 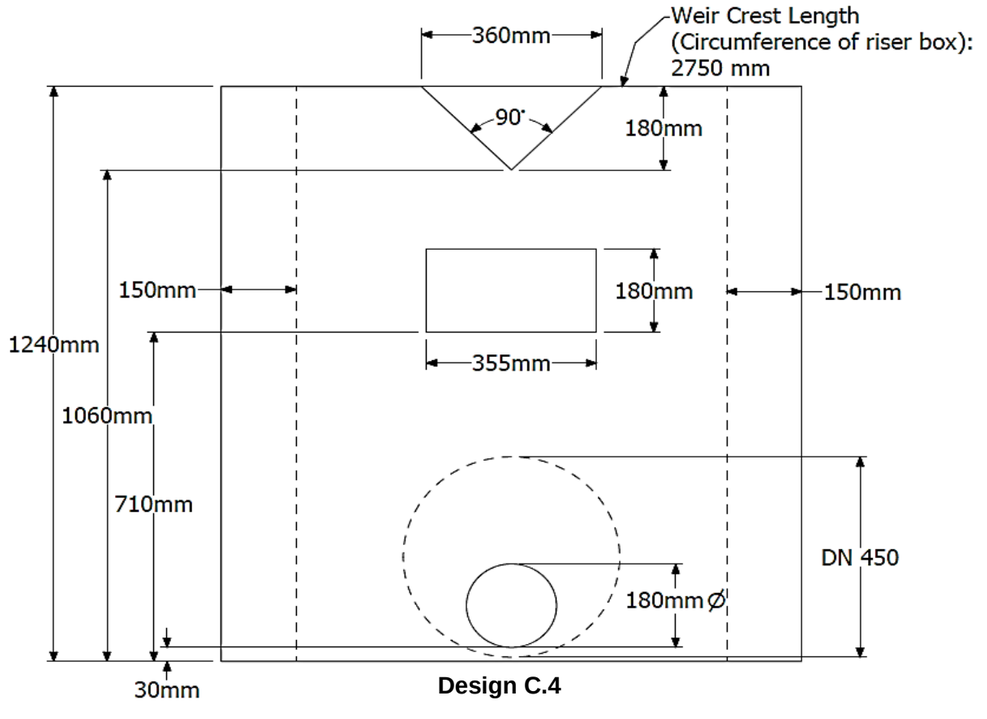

Design C.4</td></tr>
</table>

Table F.2: Layout and dimensions of the prototype multi-stage outlet structure designed to attenuate different RI storms for inland regions receiving 400 mm of MAP

<table>
<tr><th colspan="2">Classification</th><th>2-, 10-, 50- and 100-year RI storms</th><th>2-, 20-, 50- and 100-year RI storms</th></tr>
<tr><td rowspan="2">Inland Region</td><td rowspan="2">400 mm Mean Annual Precipitation</td><td> 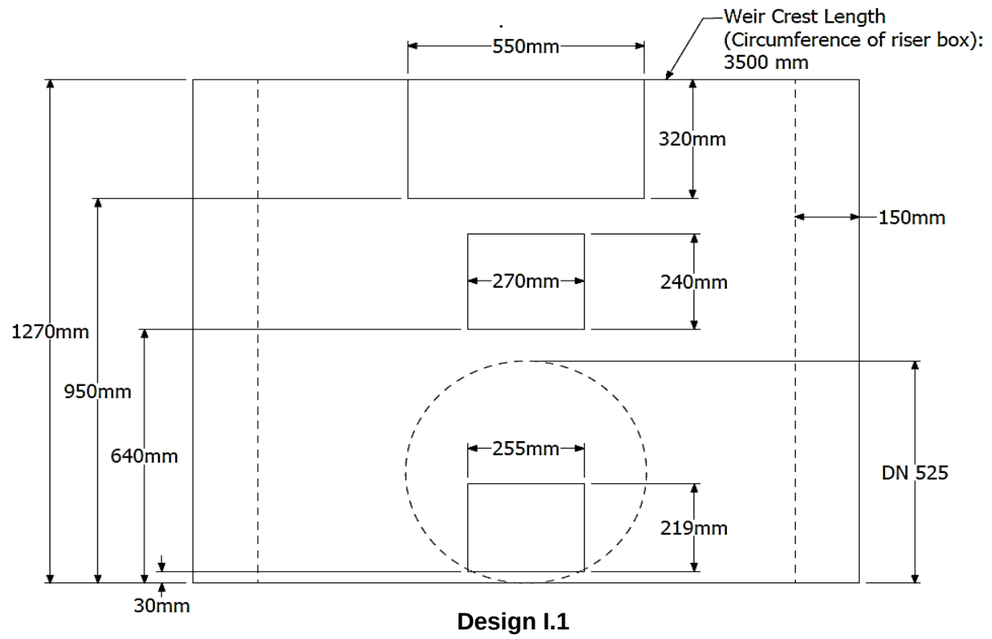

Design I.1</td><td> 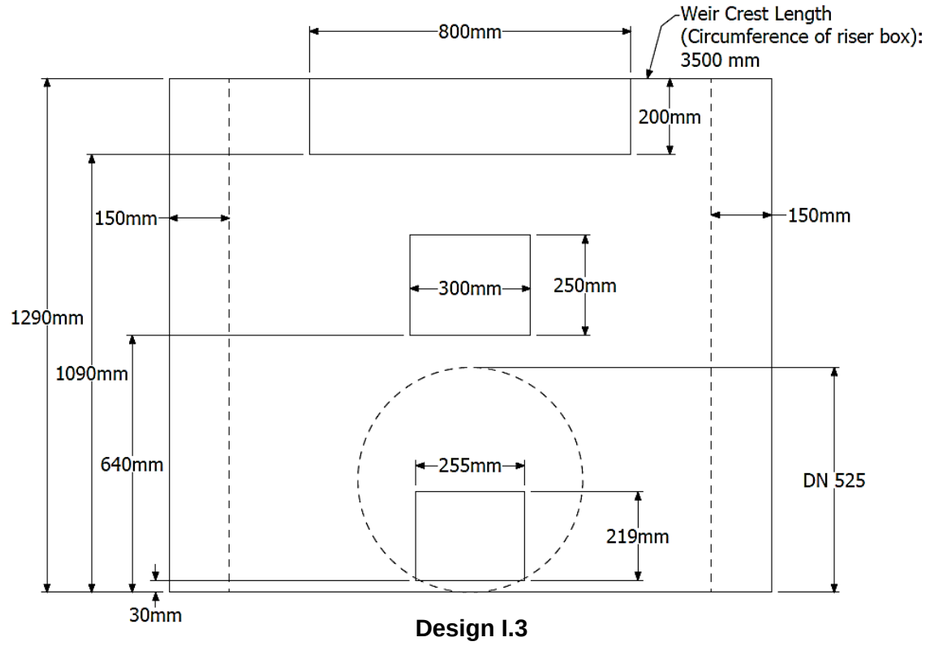

Design I.3</td></tr>
<tr><td> 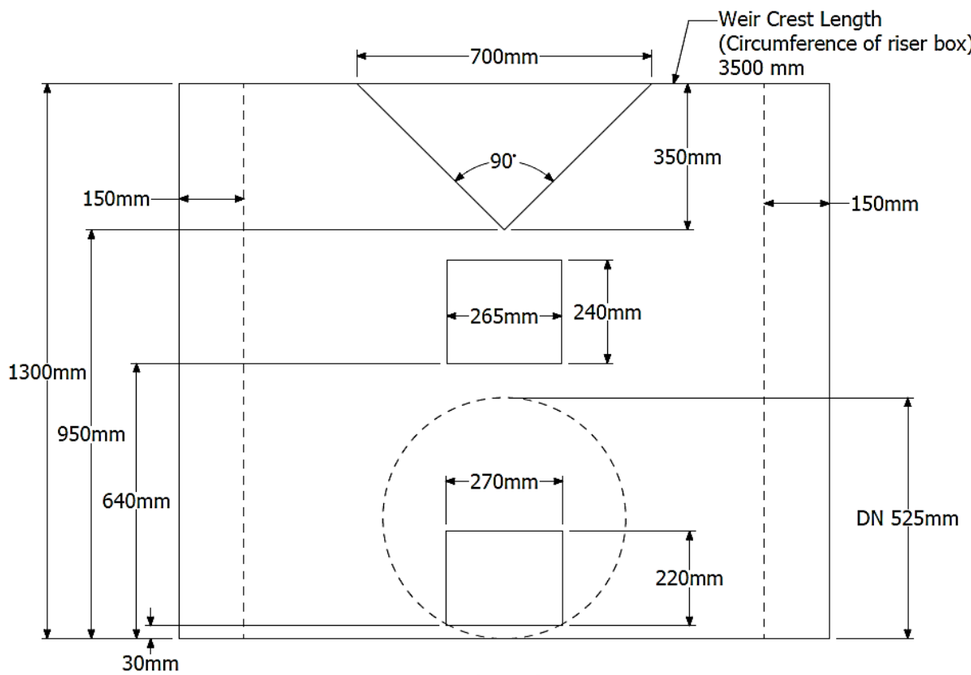

Design I.2</td><td> 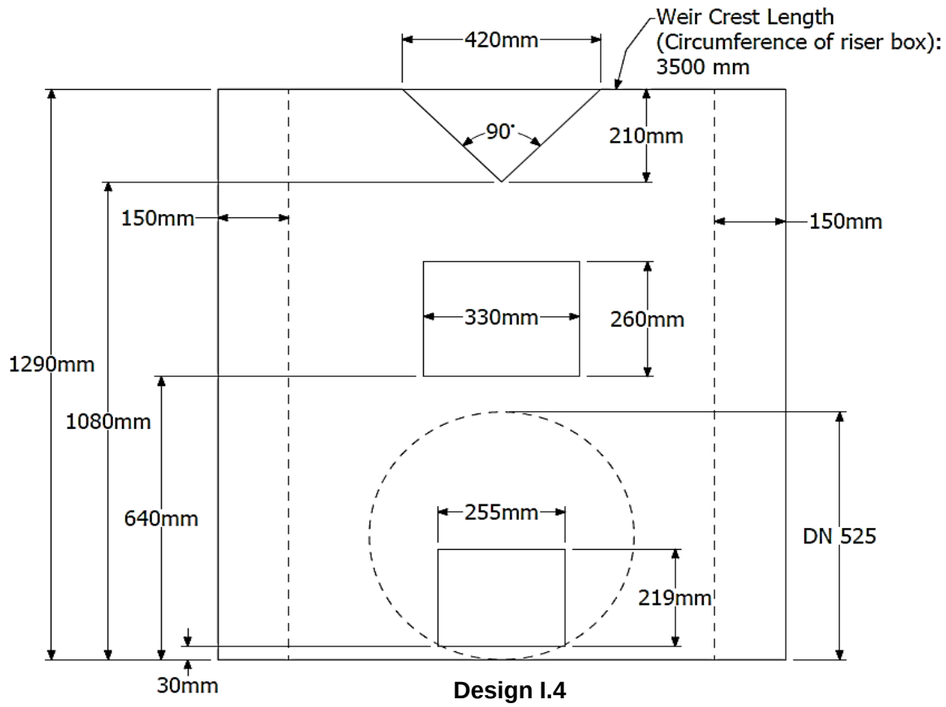

Design I.4</td></tr>
</table>

Table F.3: Layout and dimensions of the prototype multi-stage outlet structure designed to attenuate different RI storms for coastal regions receiving 700 mm of MAP

<table>
<tr><th colspan="2">Classification</th><th>2-, 10-, 50- and 100-year RI storms</th><th>2-, 20-, 50- and 100-year RI storms</th></tr>
<tr><td rowspan="2">Coastal Region</td><td rowspan="2">700 mm Mean Annual Precipitation</td><td> 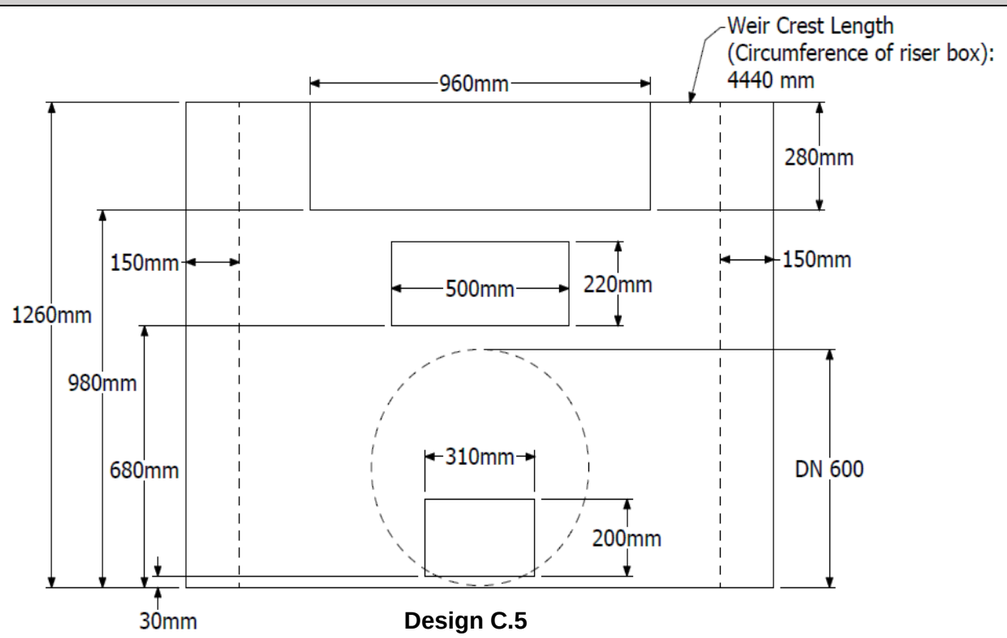

Design C.5</td><td> 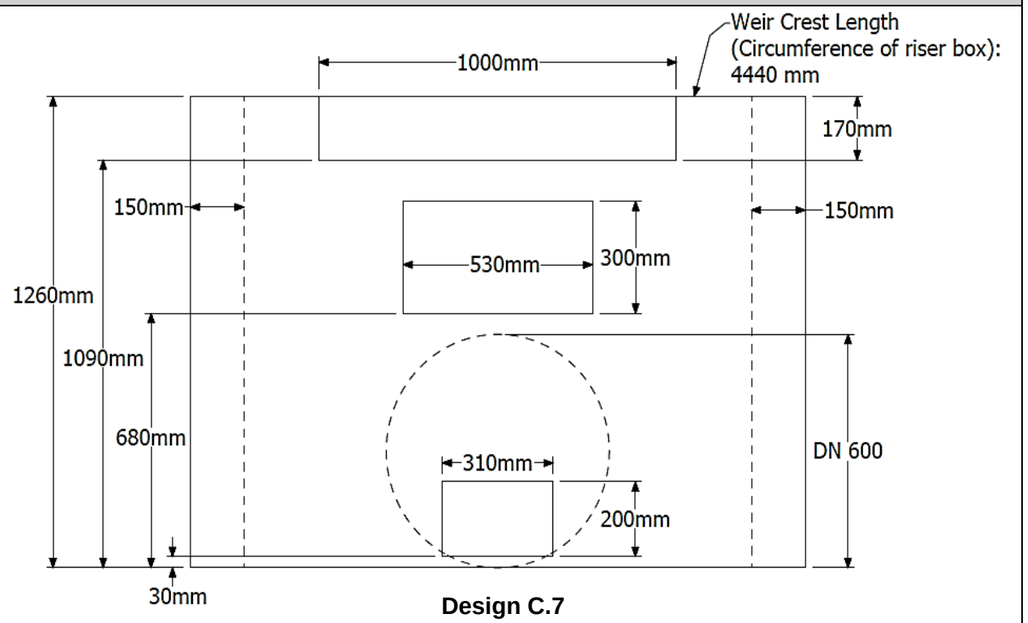

Design C.7</td></tr>
<tr><td> 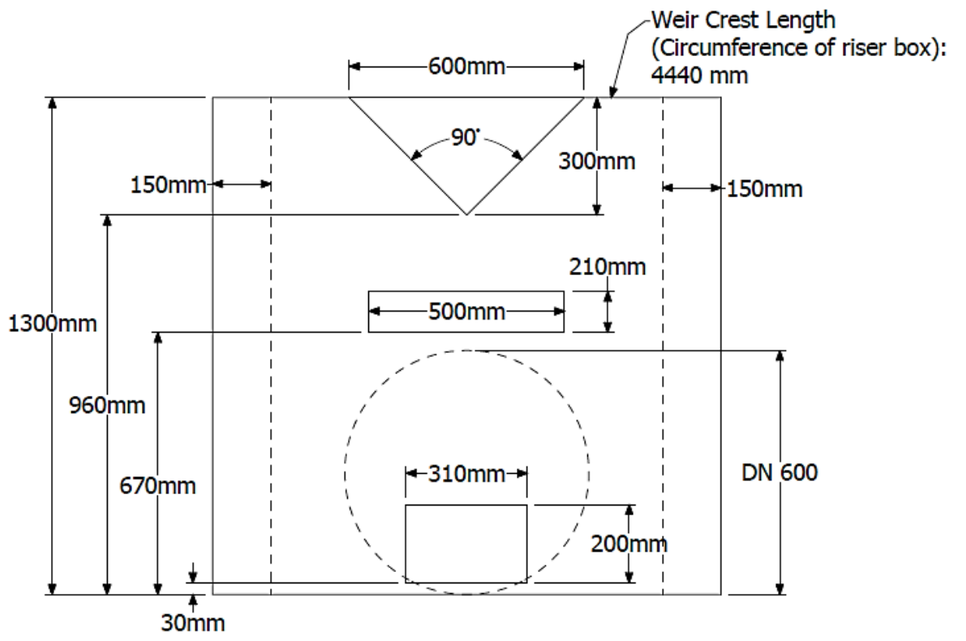

Design C.6</td><td> 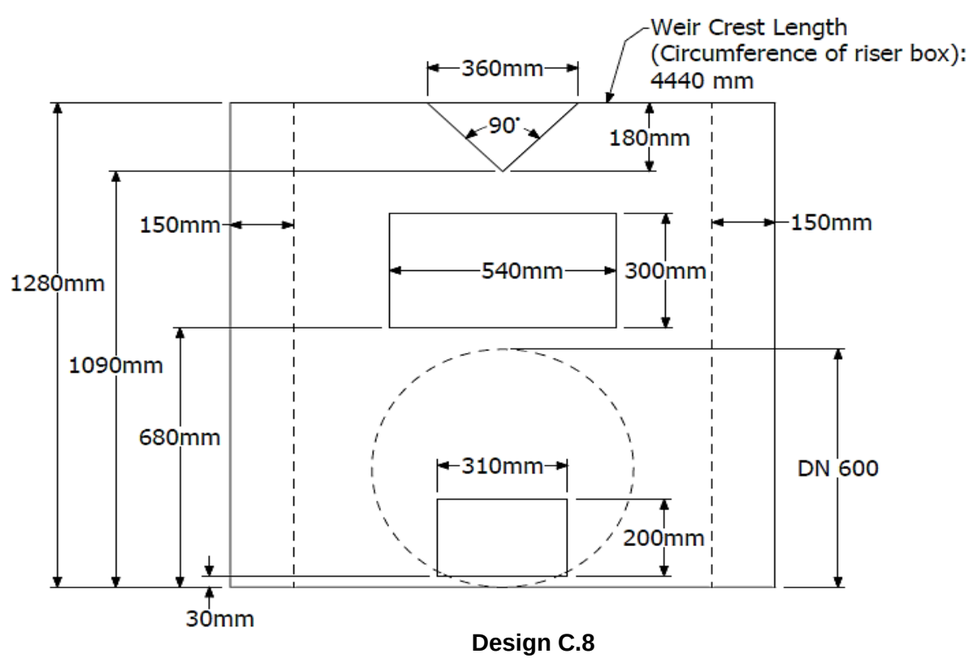

Design C.8</td></tr>
</table>

Table F.4: Layout and dimensions of the prototype multi-stage outlet structure designed to attenuate different RI storms for inland regions receiving 700mm of MAP

<table>
<tr><th colspan="2">Classification</th><th>2-, 10-, 50- and 100-year RI storms</th><th>2-, 20-, 50- and 100-year RI storms</th></tr>
<tr><td rowspan="2">Inland Region</td><td rowspan="2">700 mm Mean Annual Precipitation</td><td> 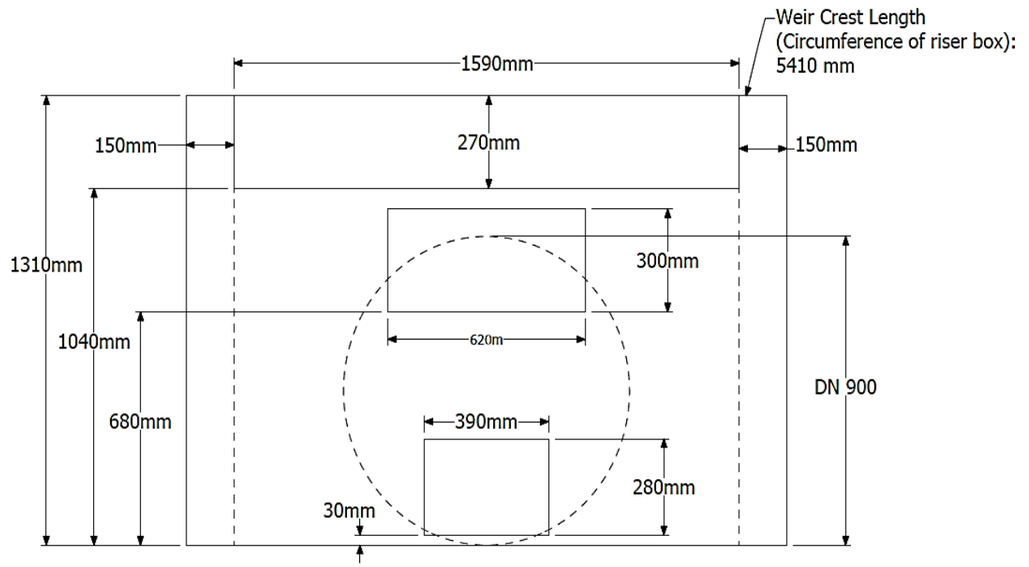

Design I.5</td><td> 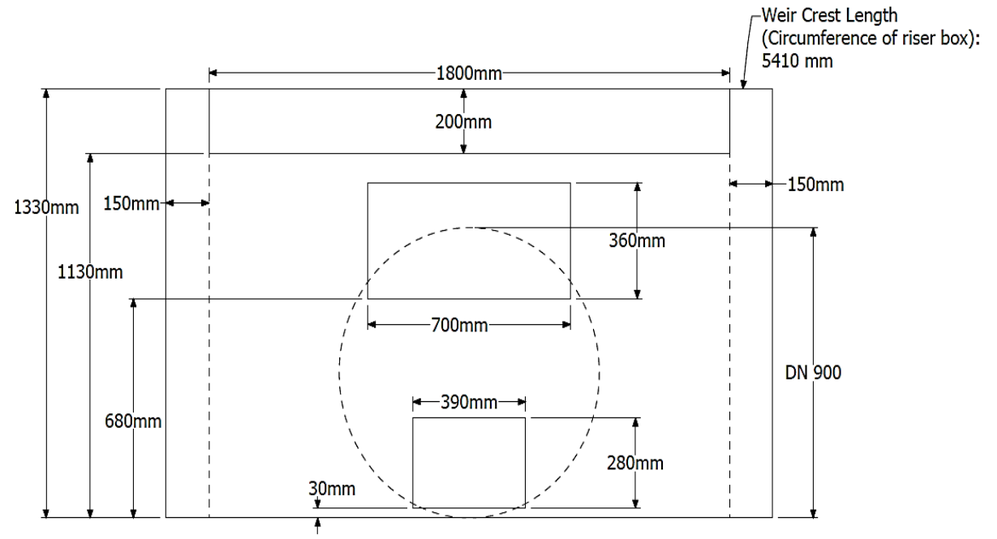

Design I.6</td></tr>
<tr><td> 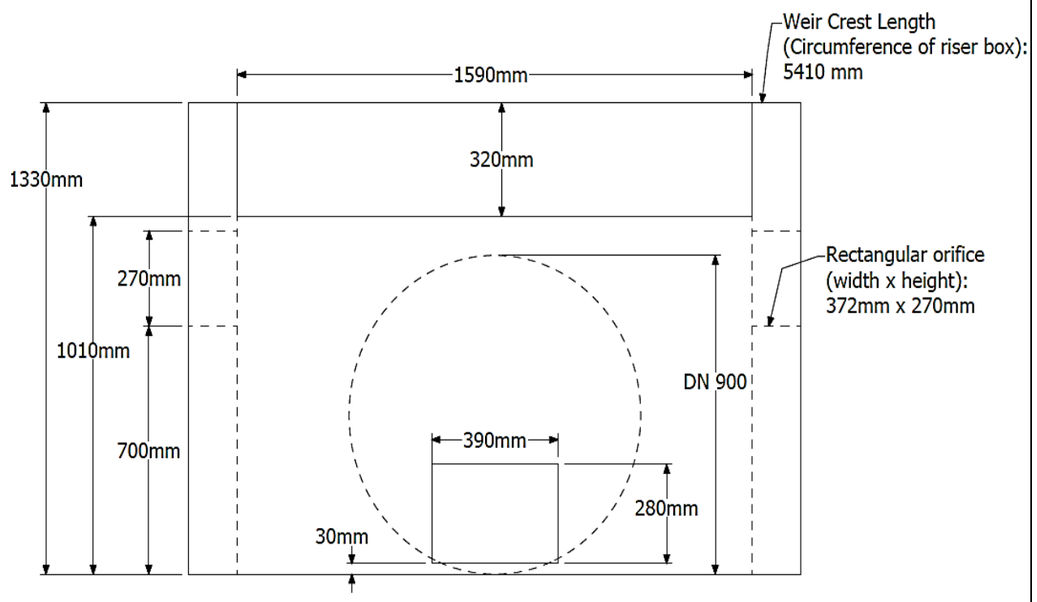

Design I.7</td><td> 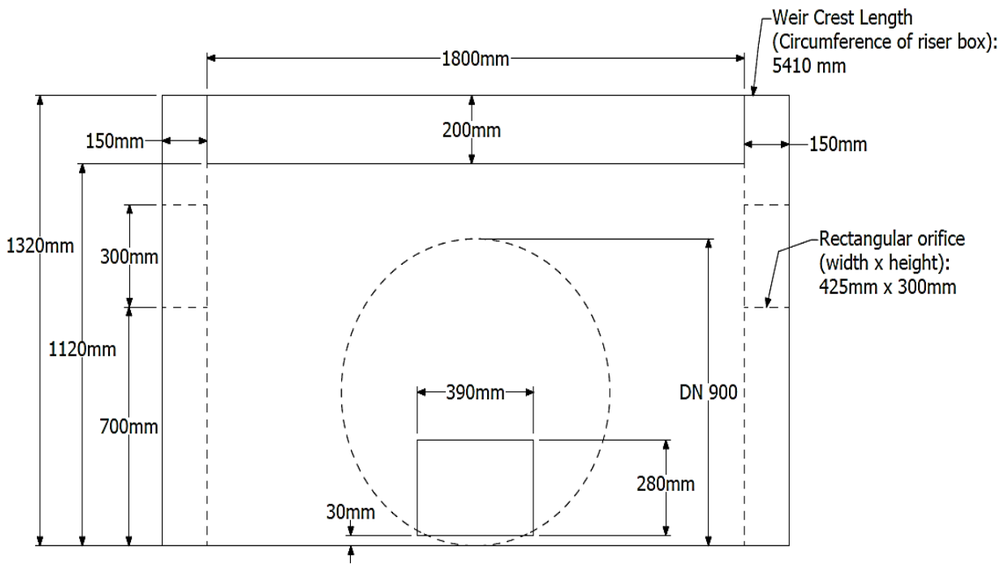

Design I.8</td></tr>
</table>

Table F.5: Layout and dimensions of the prototype multi-stage outlet structure designed to attenuate different RI storms for coastal regions receiving 1000mm of MAP

<table>
<tr><th colspan="2">Classification</th><th>2-, 10-, 50- and 100-year RI storms</th><th>2-, 20-, 50- and 100-year RI storms</th></tr>
<tr><td rowspan="2">Coastal Region</td><td rowspan="2">1000 mm Mean Annual Precipitation</td><td> 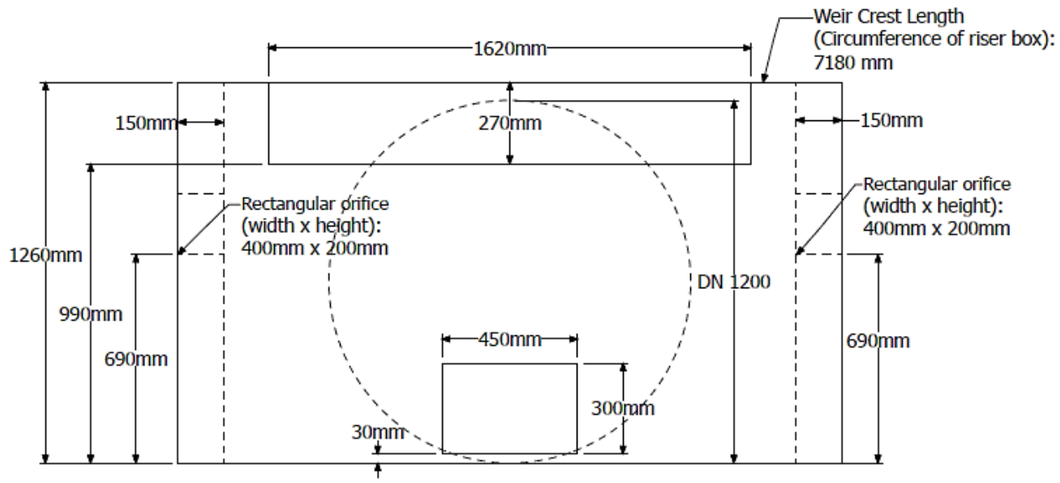

Design C.9</td><td> 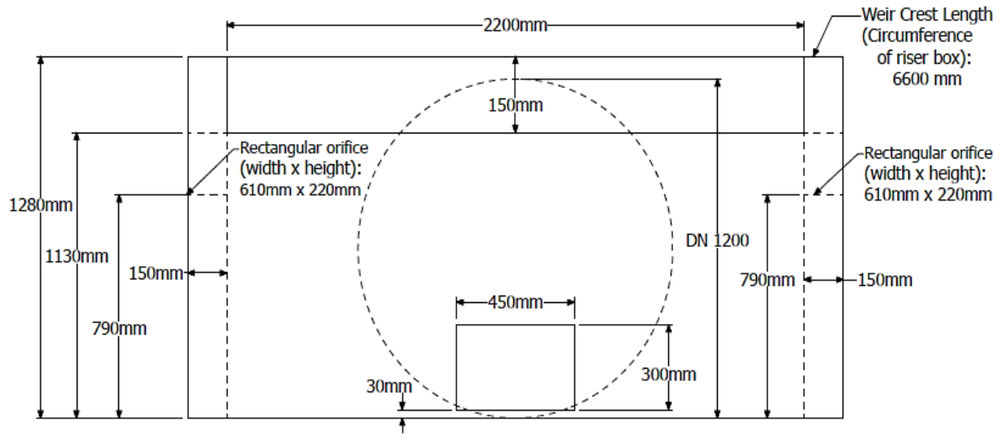

Design C.11</td></tr>
<tr><td> 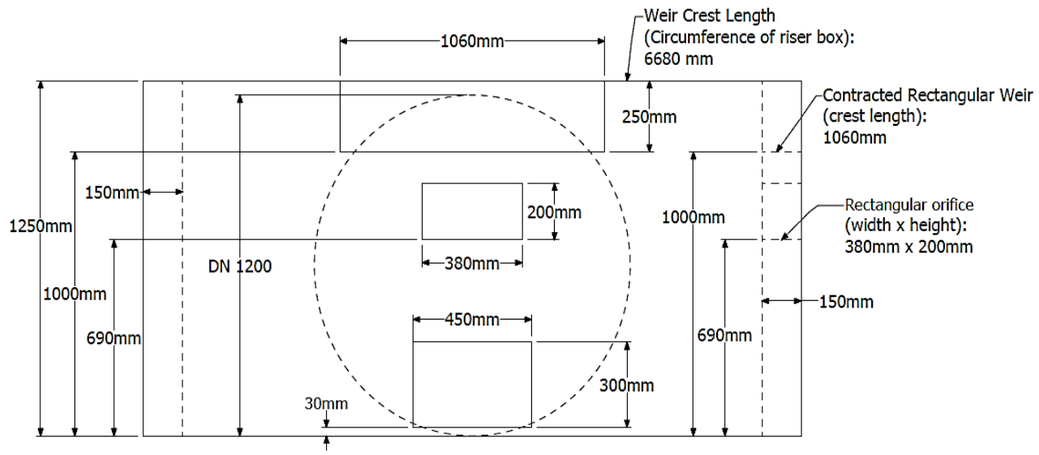

Design C.10</td><td> 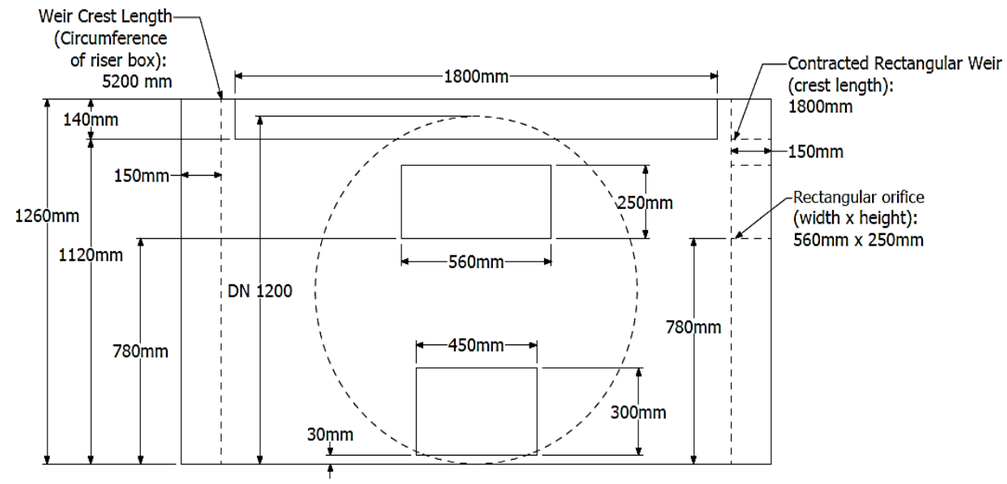

Design C.12</td></tr>
</table>

Table F.6: Layout and dimensions of the prototype multi-stage outlet structure designed to attenuate different RI storms for Inland regions receiving 1000mm of MAP

Classification		Inland Region
2-, 10-, 50- and 100-year RI storms	**1000 mm Mean Annual Precipitation**	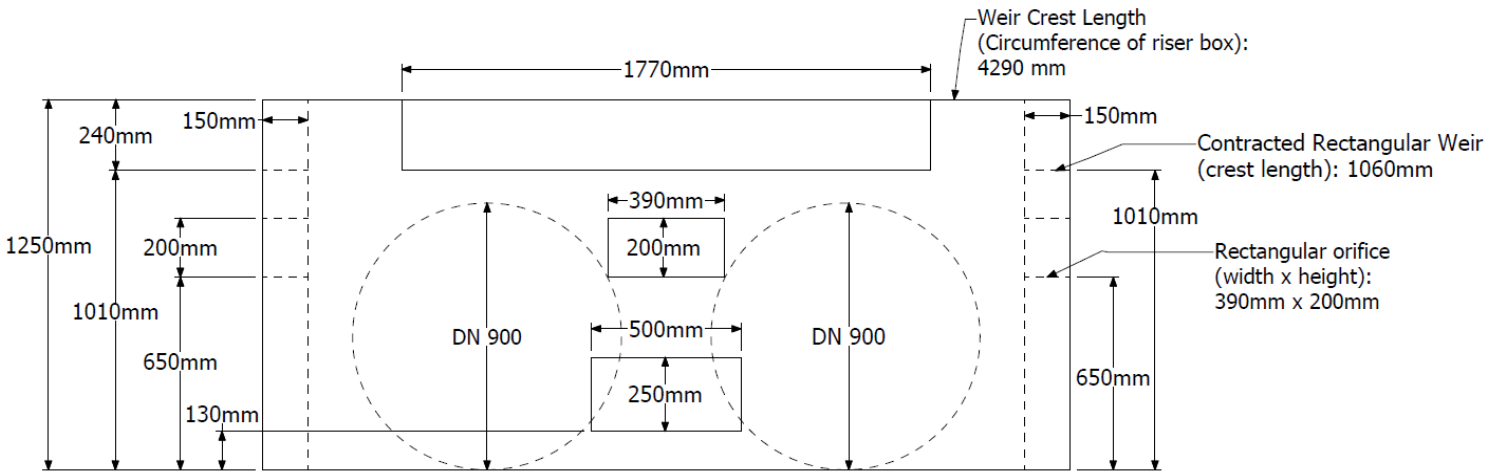 **Design I.9**
2-, 20-, 50- and 100-year RI storms	**1000 mm Mean Annual Precipitation**	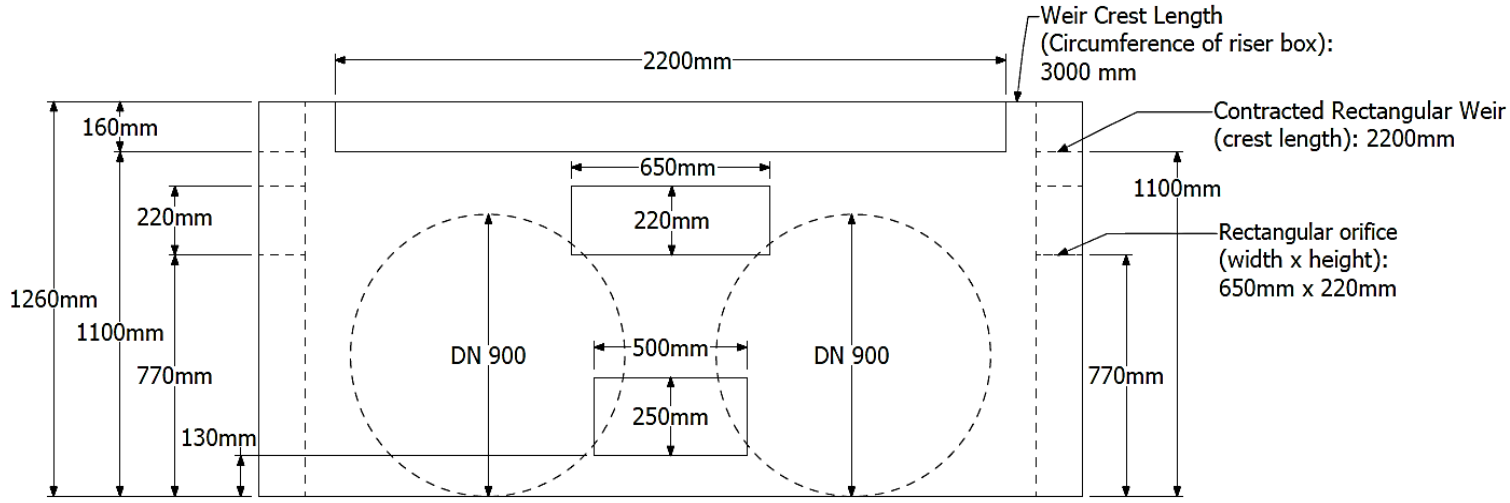 **Design I.10**

APPENDIX G: Drawings and Photographs of as-built Multi-Stage Outlet Models

Photographs of as-built multi-stage outlet models

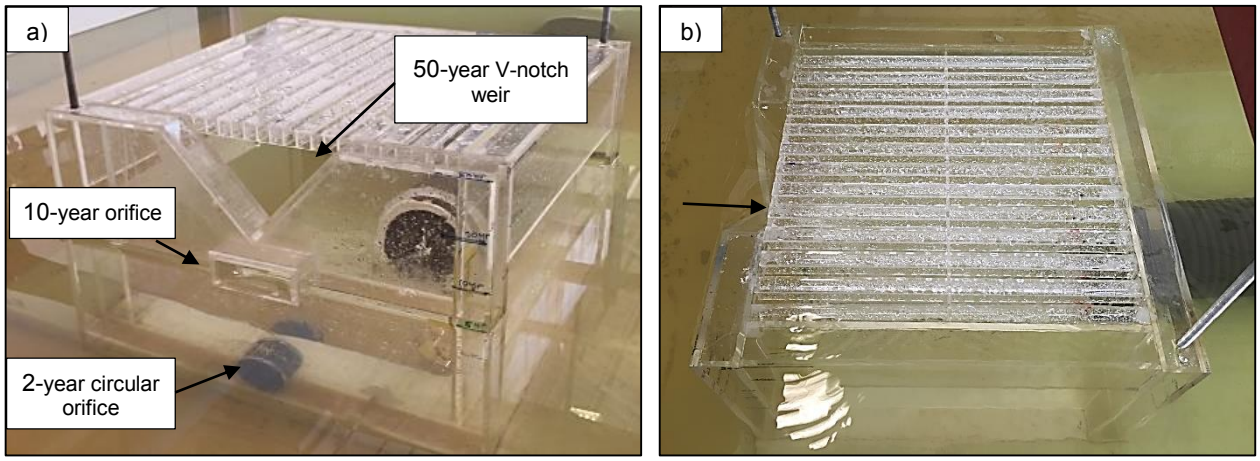

Figure G.1: Front (a) and top (b) view of Model 1 (based on flood peaks for coastal regions, 400 mm MAP class)

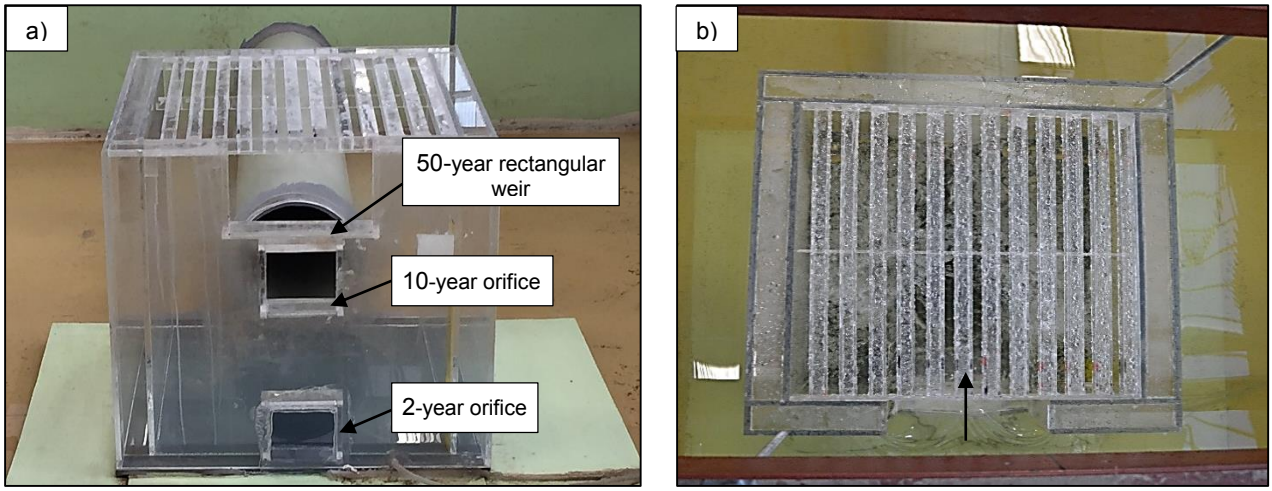

Figure G.2: Front (a) and top (b) view of Model 2 (design based on flood peaks for inland regions, 400mm MAP class)

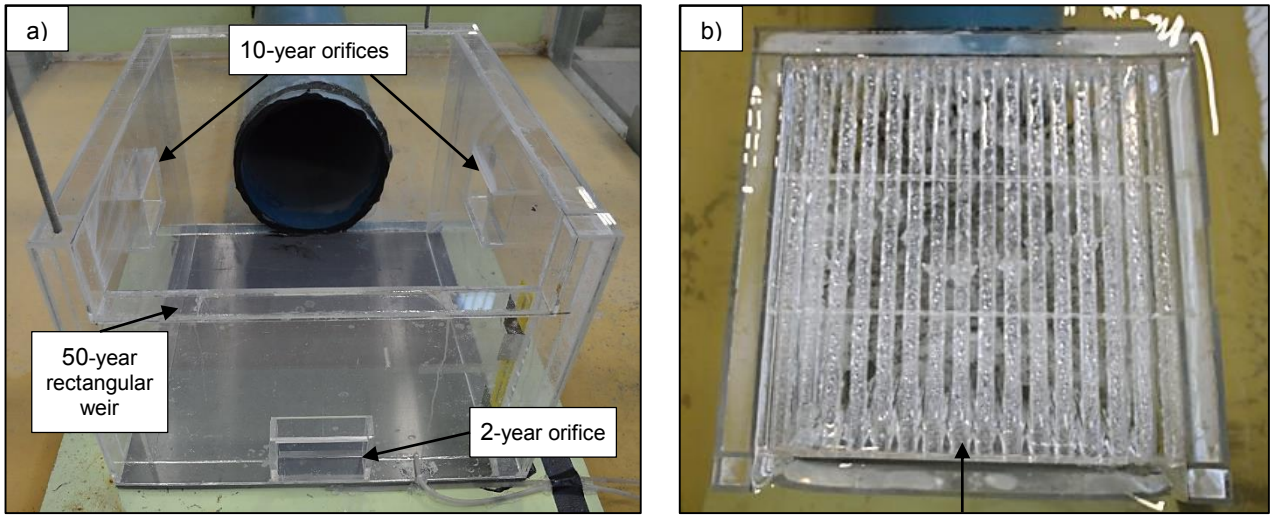

Figure G.3: Front (a) and top (b) view of Model 3 (design based on flood peaks for inland regions, 700 mm MAP class)

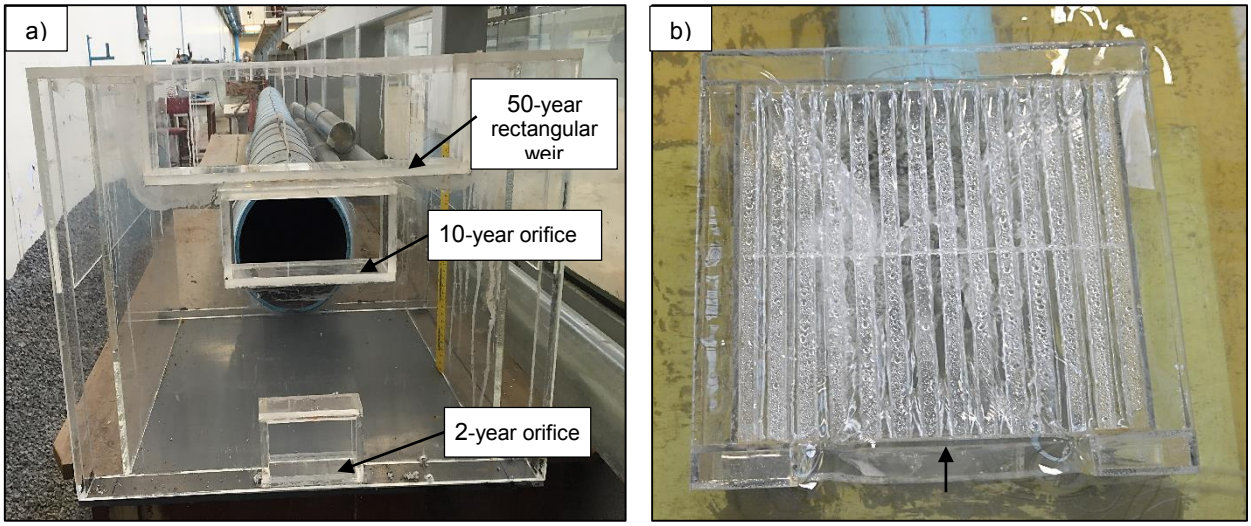

Figure G.4: Front (a) and top (b) view of Model 4 (design based on flood peaks for coastal regions, 700 mm MAP class)

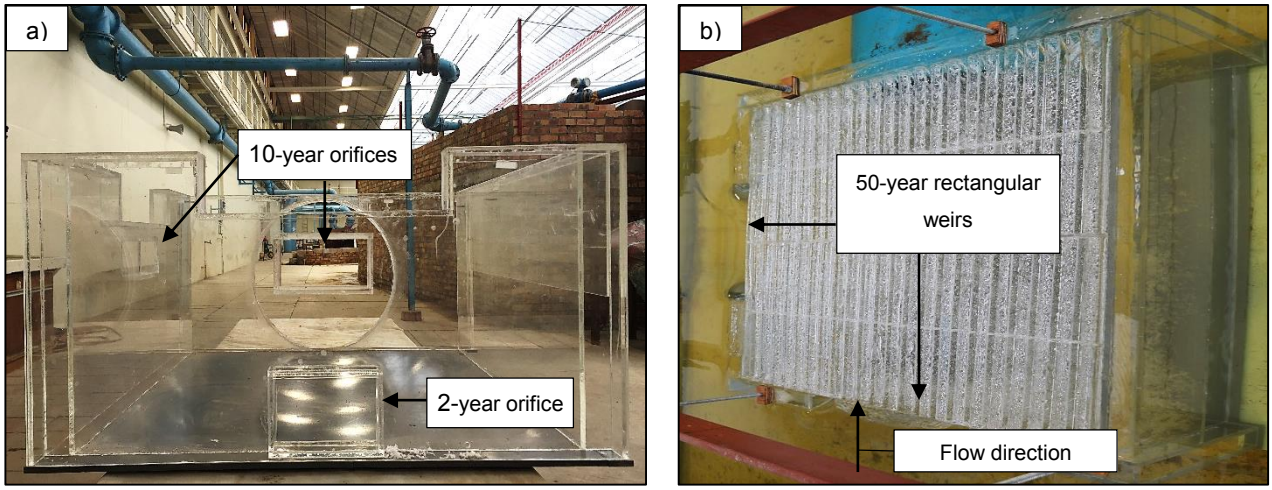

Figure G.5: Front (a) and top (b) view of Model 5 (design based on flood peaks for coastal regions, 1000 mm MAP class)

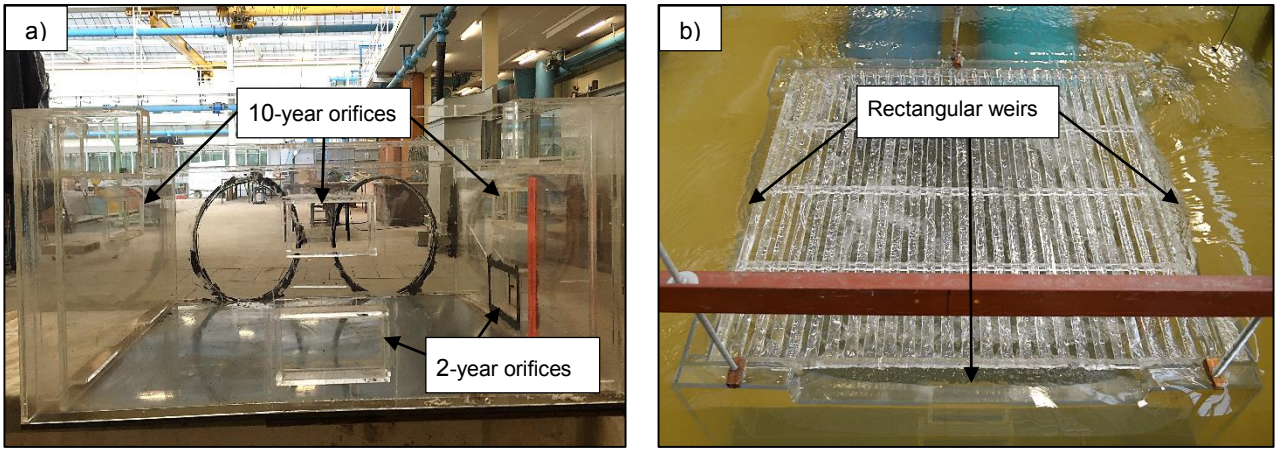

Figure G.6: Front (a) and top (b) view of Model 6 (design based on flood peaks for inland regions, 1000 mm MAP class)

Table G.1: Model and prototype dimensions of multi-stage outlet structures for coastal and inland regions with 400 mm of MAP

MAP Class	Coastal Region	Inland Region
400 mm Mean Annual Precipitation	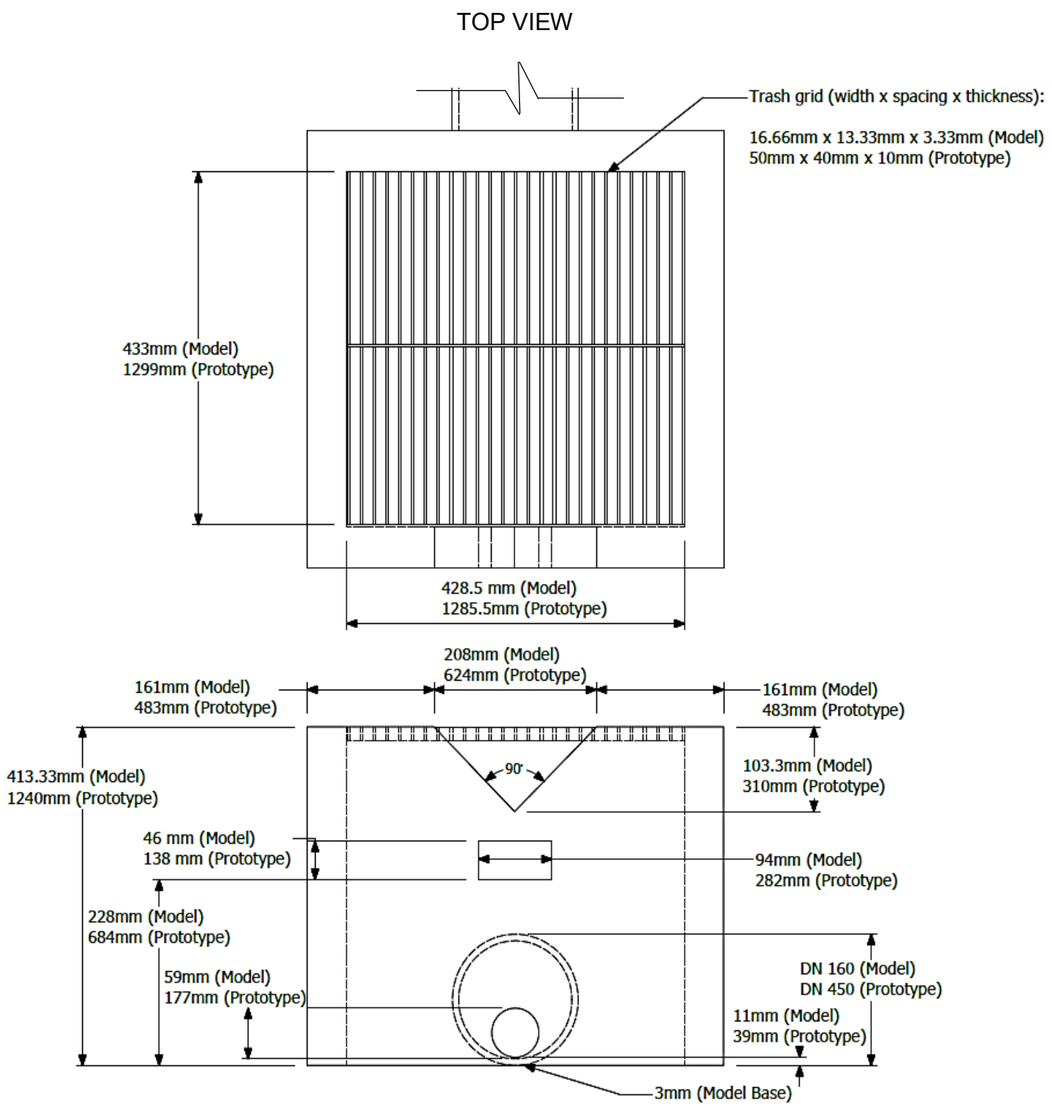	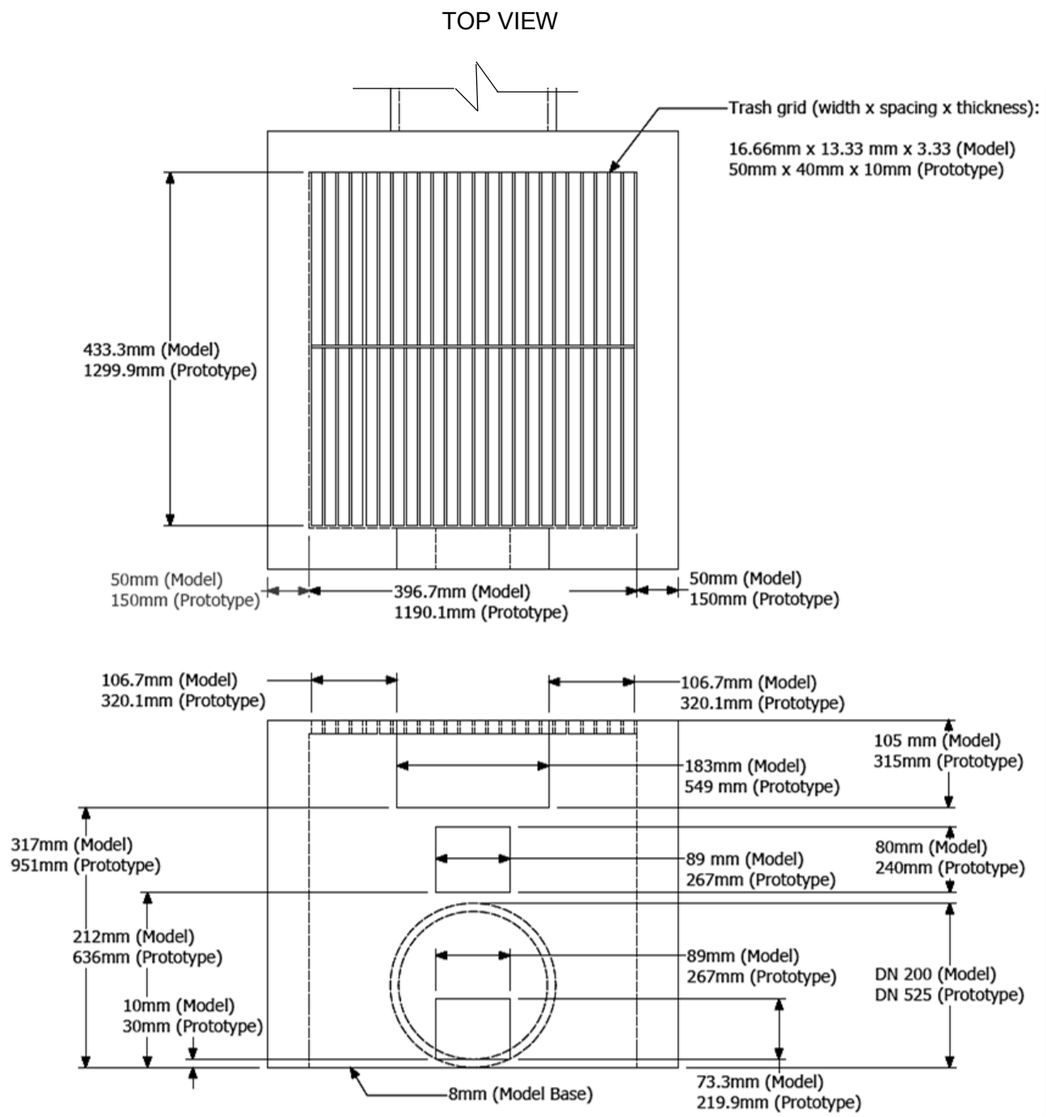

Table G.2: Model and prototype dimensions of multi-stage outlet structures for coastal and inland regions with 700 mm of MAP

MAP Class	Coastal Region	Inland Region
700 mm Mean Annual Precipitation	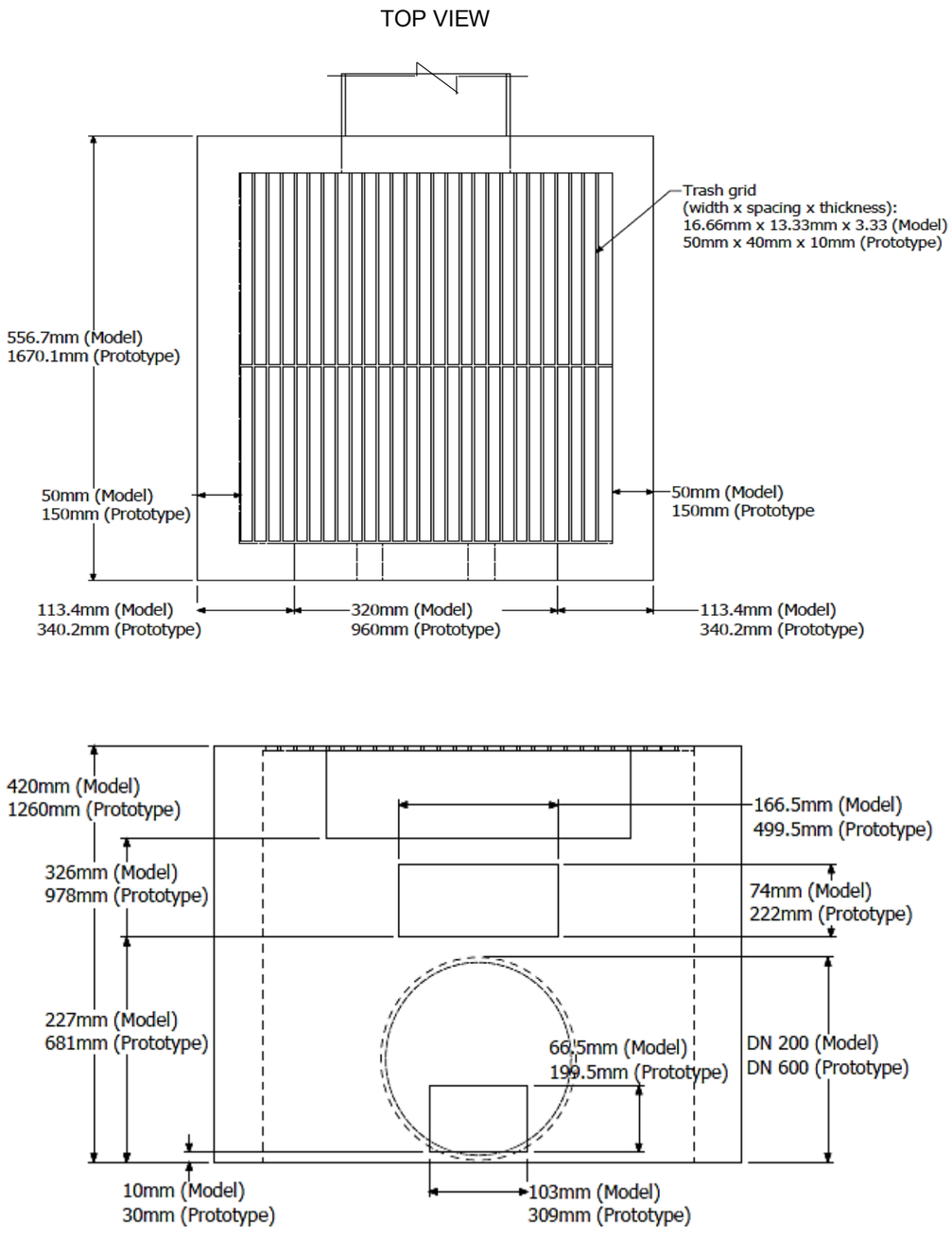	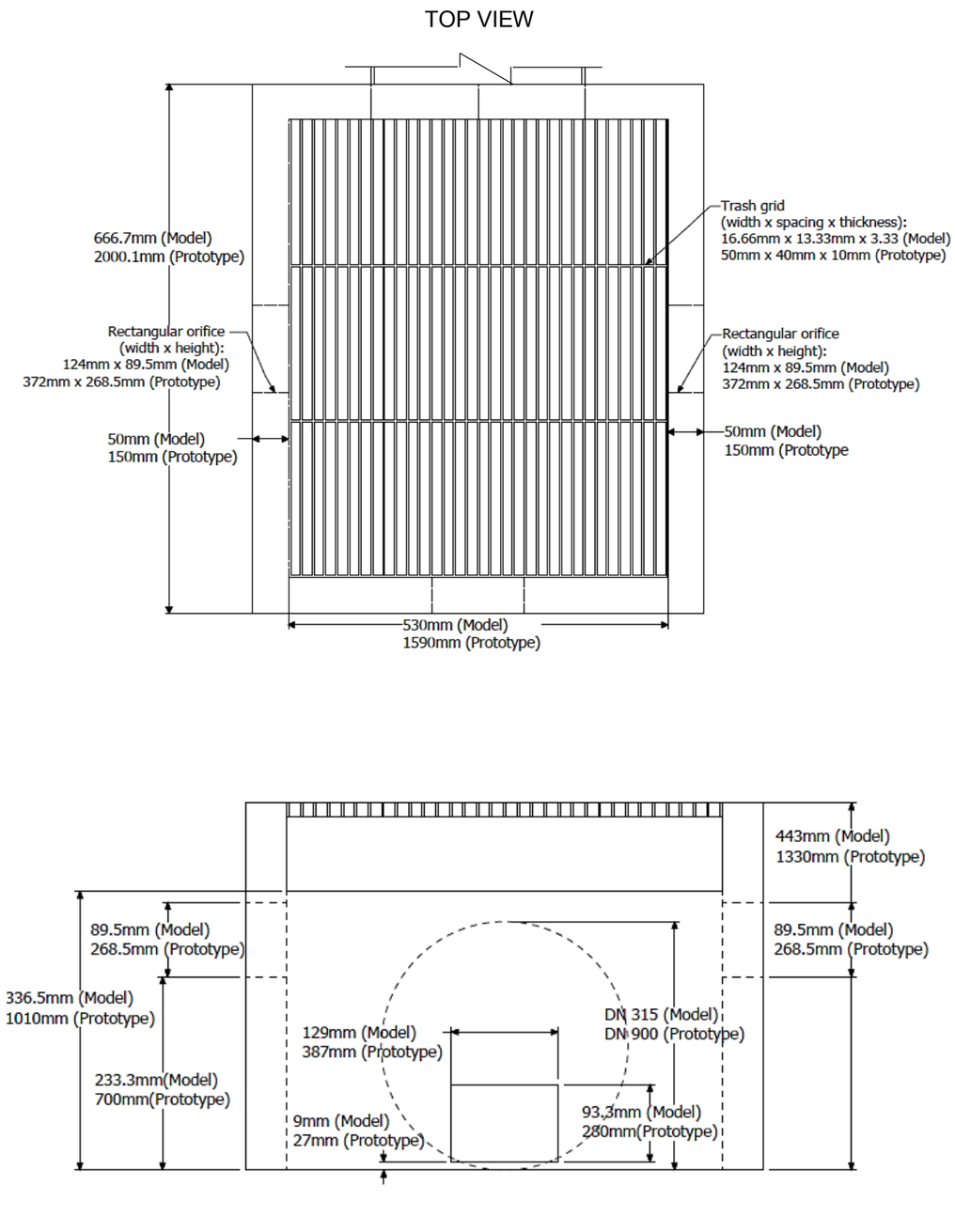

Table G.3: Model and prototype dimensions of multi-stage outlet structures for coastal and inland regions with 1000 mm of MAP

MAP Class	Coastal Region	Inland Region
1000 mm Mean Annual Precipitation	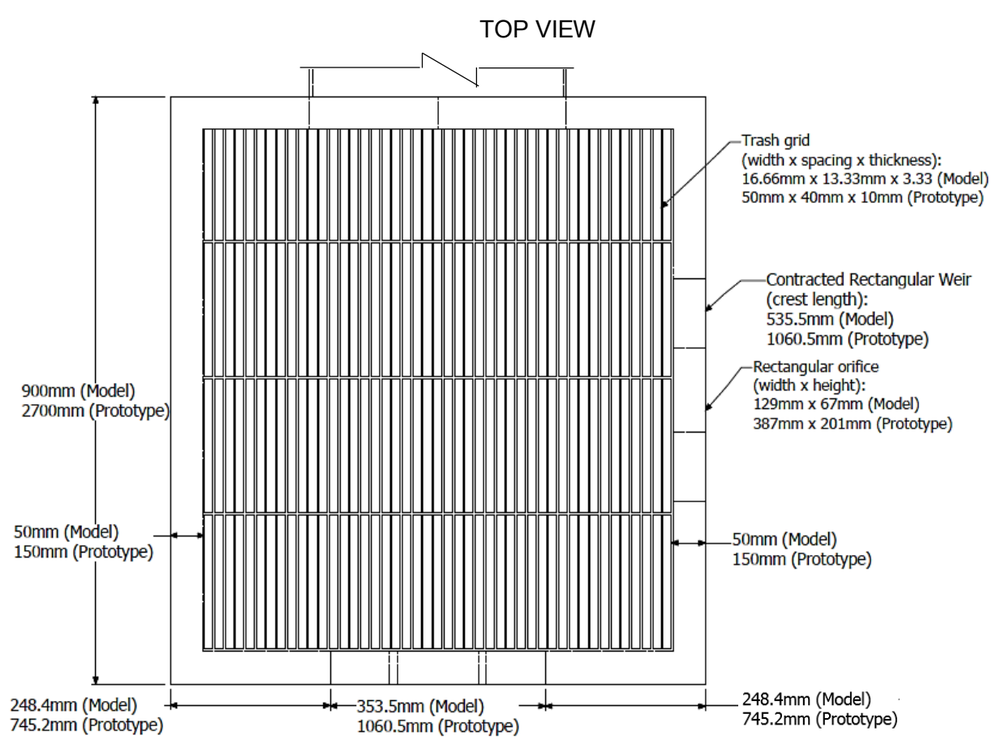	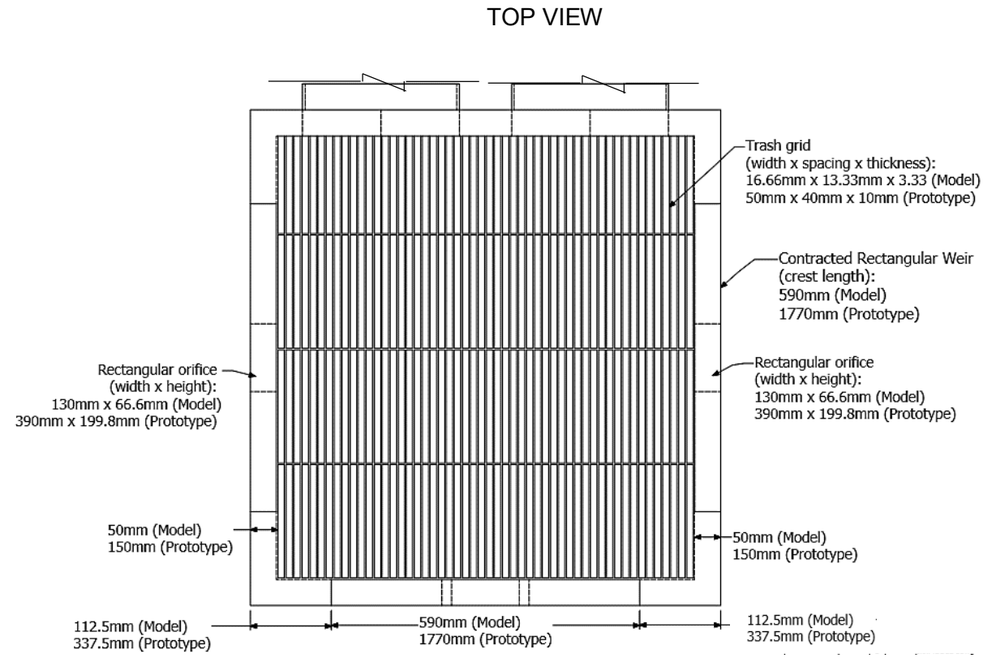
	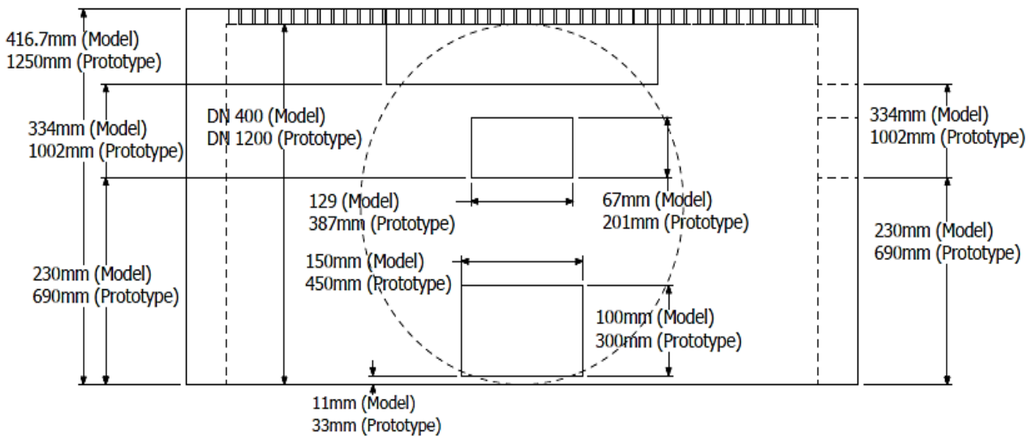 FRONT VIEW	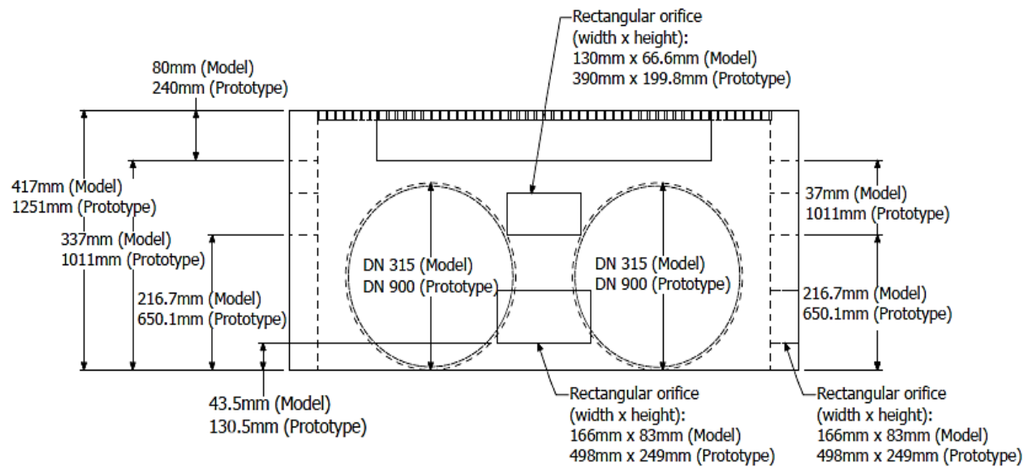 FRONT VIEW

APPENDIX H: Experimental Test Results

H. Experimental Test Results

H.1 Results of Model 1

The measured outflow of Model 1 (C.2) was plotted against the stage to determine if the outlet discharged at a rate equal to the pre-development peak flow levels, or if the target discharge (pre-development flow) was exceeded. Model 1 (C.2) was designed to control the 2-, 10-, 50-, and 100-year RI storm events for coastal regions receiving 400 mm MAP.

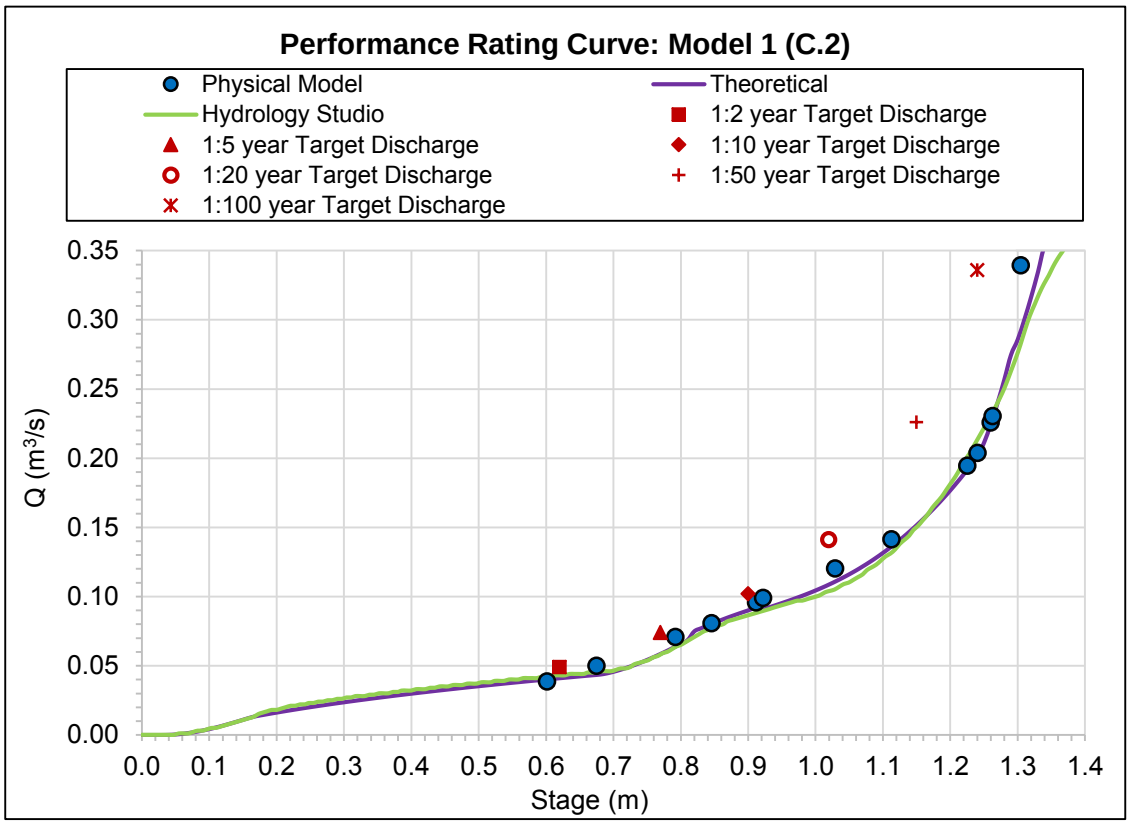

Figure H.1: Calculated and physically modelled stage-discharge curve of Model 1 (prototype dimensions)

Figure H.1 shows that the stage-discharge curve of the physical model (indicated in blue) plots below the target stage-discharge curve (indicated in red). Therefore, the physical model controlled the outflow effectively. However, the flow was released at higher stages than initially estimated. Thus, the multi-stage outlet over controlled the flow. The pond would require more storage volume than initially estimated in order for the multi-stage outlet to control the outflow at the estimated target stage. The pre-development hydrograph was approximated as a triangular shaped outflow hydrograph according to the rational method. The approximation of the pre-development hydrograph caused the maximum storage level to be underestimated; hence, the maximum head level is also underestimated.

It is evident from Figure H.1 that although Model 1 was designed to control the 2-, 10-, 50- and 100-year RI storm events, the physical model still restricted the outflow at the 5- and 20-year

maximum water surface elevation to meet or more than meet the pre-development target discharge. Table H.1 capsulate the percentage difference between the theoretical and physical model discharge.

Table H.1: Difference between the theoretical and measured discharge of Model 1

RI (years)	Stage (m)	Actual discharge of physical model(1) (m^3/s)	Theoretical calculated discharge (m^3/s)	Absolute difference (m^3/s)	Percentage difference (%)
2	0.675	0.050	0.043	-0.006	-12.92
5	0.792	0.071	0.064	-0.007	-9.86
10	0.923	0.099	0.091	-0.008	-8.27
20	1.113	0.141	0.136	-0.005	-3.43
50	1.241	0.204	0.201	-0.003	-1.34
100	1.305	0.339	0.333	-0.006	-1.86

(1) The actual discharge equals the average of the discharge measurements, taken every 10 minutes until water surface elevation stabilised

From Table H.1 it is clear that the hydraulic performance of the 2-year storm control component of the multi-stage model deviated the most from the theoretical formula. The 2-year storm control component also contributes to the amount of water released by the multi-stage outlet as the stage increased for the 5-, 10-, 20-, 50- and 100-year recurrence interval storms. The hydraulic performance of each component of the multi-stage outlet model is further investigated in Section H.1.1 to Section H.1.2.

H.1.1 Discharge Component of Model 1 Controlling the 2-year Storm Event

The physical model study indicated that the discharge coefficient for the 2-year storm control orifice varied from 0.67 to 0.98 depending on the degree of submergence. Literature recommended a constant discharge coefficient of 0.6 for circular orifices (refer to Section 2.3.1.1). Since the discharge coefficient varied during the physical model test, the discharge of the physical model increased with an increase in the stage, whereas the theoretical discharge reached an asymptotic value and then started to decrease at the highest stage, as the 100-year storm control outlet pipe became the control of the multi-stage outlet model. Figure H.2 indicates that the experimental circular 2-year storm control orifice discharged at a higher rate than determined theoretically.

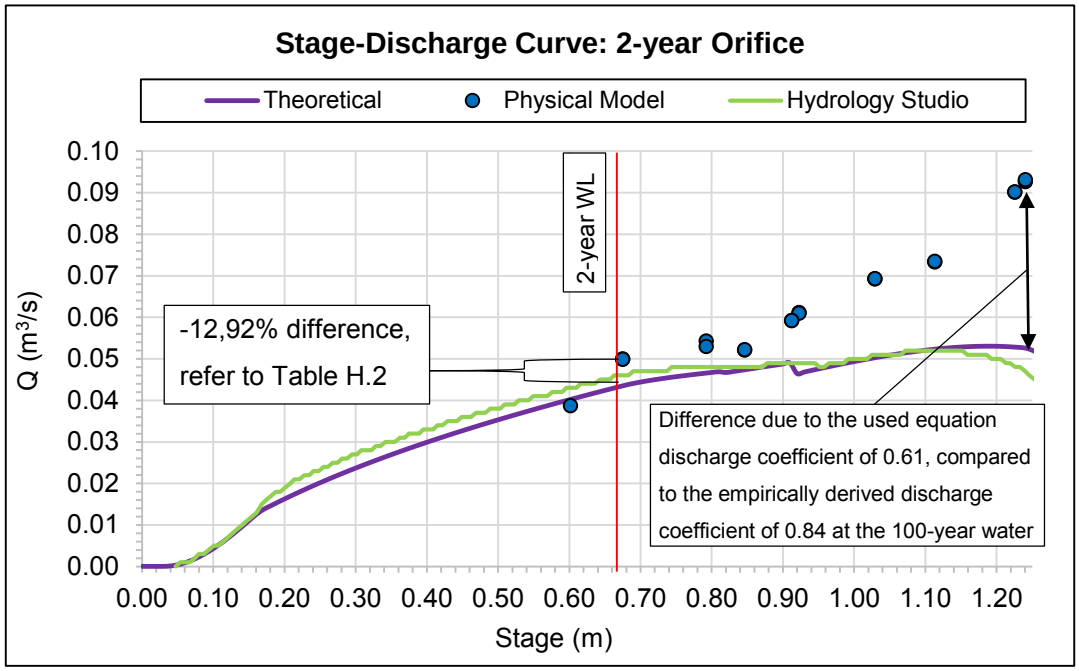

Figure H.2: Stage-discharge curve of the 2-year control component of Model 1

At the 2-year water level (WL), the 12.92% difference between the theoretical and measured discharge (refer to Table H.2) could be attributed to the discharge coefficient and the backwater head produced by the 100-year outlet pipe. The backwater head affected the differential head on the orifice. The fractional change in discharge, as a result of the difference in the theoretical and experimental discharge coefficient, as well as differential head, should equal the percentage difference between the theoretical and actual discharge of the physical model. If not, the variance between the fractional change in discharge and percentage difference between the theoretical and physically measured discharge is due to experimental error.

However, in Table H.2 the variance between the fractional change and percentage difference in discharge is -0.04%, which indicates that the magnitude of the experimental error caused by averaging the electromagnetic flow meter reading and human error that occurred during measurements of the 2-year water level, was insignificant.

Table H.2: Fractional change in discharge at the 2-year water level (stage 0.675 m)

Parameter	2-year control orifice		Fractional change in discharge (%)	Total fractional change in discharge (%)	Percentage difference in discharge from Table H.1 (%)	Error (%)
	Theoretical	Physical				
C_d	0.6	0.67	-10.45	-12.88	**-12.92**	-0.04
Δh (Eq. 6.1)	0.442	0.465	-2.43			

H.1.2 Discharge Component of Model 1 Controlling the 10-year Storm Event

The 10-year storm control orifice of the multi-stage outlet model was partially submerged upstream (u/s), therefore, acting as a weir during the 5-year design flow, see Figure H.3 (a). The mean value of the discharge coefficient of the modelled 10-year orifices was determined to be 0.345 for weir flow conditions (when the orifice is partially submerged upstream) and 0.521 for orifice flow conditions (when the orifice is fully submerged upstream), refer to Figure H.3 (b). This deviates from the discharge coefficients recommended by literature, which was 0.37 for weir flow when using Equation 2.13 and C_d= 0.6 when using the standard orifice equation.

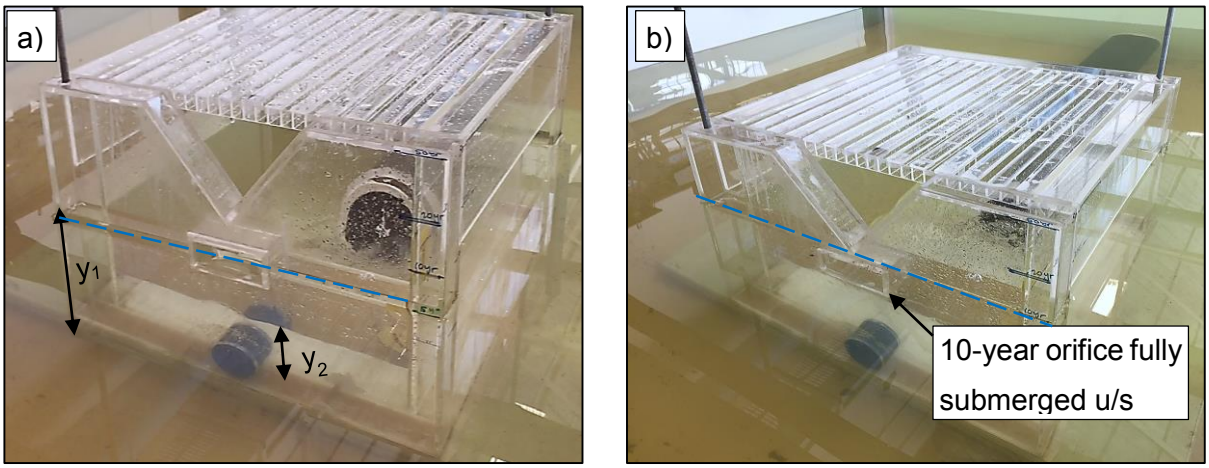

Figure H.3: a) 10-year orifice discharge as a weir b) 10-year orifice discharge under orifice flow

The area and height dimensions of the 10-year storm control orifice of Model 1 were much smaller than for the other five multi-stage models since the 10-year target discharge of Model 1 was smaller. Thus, the area from which the 10-year storm control orifice of Model 1 draws its flow was smaller in comparison to the other five physical models. This resulted in a discharge over orifice area ratio that is smaller than the other five multi-stage models. Thus, when operating under the same head as the other models, the contraction coefficient should be smaller according to Equation 2.1, with the discharge coefficient taken as a combination of the contraction and velocity coefficient.

The theoretical formula (Equation 2.1), with equation discharge coefficient of 0.6, used in the spreadsheet calculations, overestimated the discharge of the 10-year storm control orifice, as illustrated in Figure H.4. However, the shape of the stage-discharge curve of the 10-year storm control orifice of the physical model is similar to the theoretical model. The modelled 10-year storm control orifice of the physical model had a submergence ratio of 61.5% at stage 1.34 m, which explains the decrease in discharge. Where the submergence ratio is the downstream depth relative to the invert of the orifice divided by the upstream depth relative to the invert of the orifice.

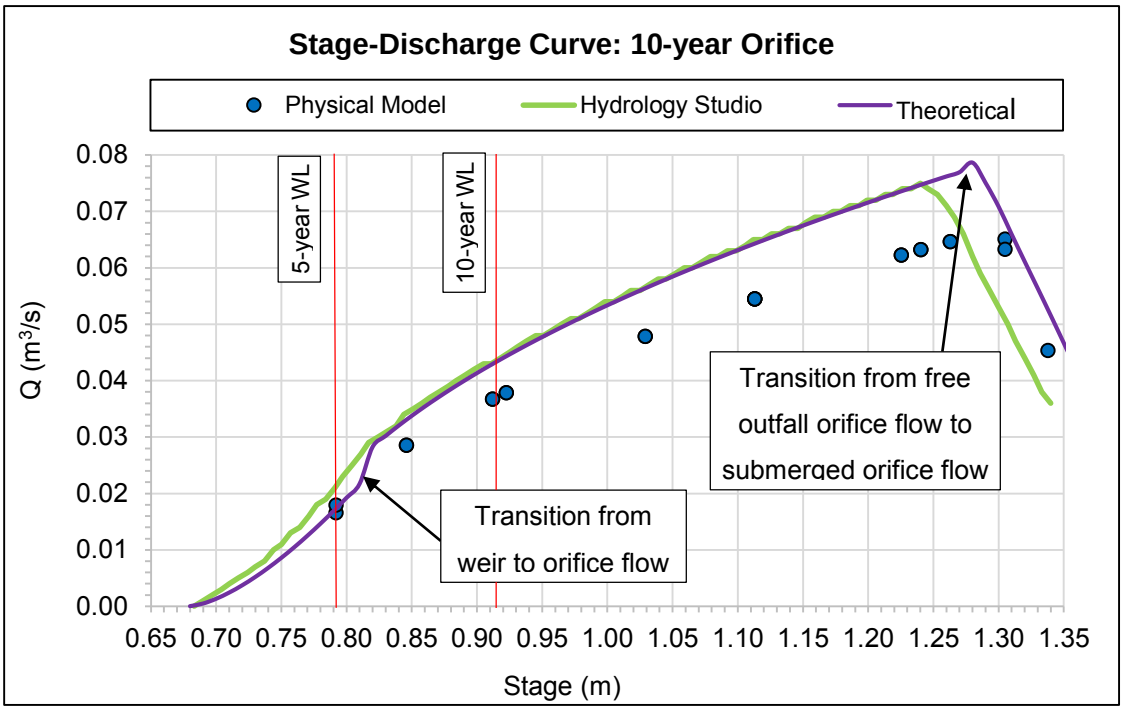

Figure H.4: Stage-discharge relationship for the 10-year control component of Model 1

Table H.3 and Table H.5 summarise the differences between the theoretical discharge and the discharge measured physically, for each control component of the multi-stage model, at the 5- and 10-year water surface elevations. Table H.4 and Table H.6 summarise the fractional change in discharge for each discharge control device.

It is evident from Table H.6 that the fractional change in the discharge of the 2- and 10-year storm control orifices, due to the difference between the theoretical equation discharge coefficient and experimental discharge coefficient, was the main attribute to the difference between the measured and calculated discharge at stage 0.923 m.

The total percentage difference between the theoretical and physical discharge determined in Table H.3 and Table H.5 varied slightly from the total fractional change in discharge determined in Table H.4 and Table H.6 respectively. The slight variance is due to experimental error since the theoretical head was rounded off and the electromagnetic flow meter readings averaged. The approach velocity of the 100-year storm control pipe was assumed negligible, which had a minor influence on the theoretical differential head.

The 2-year storm control orifice was again evaluated in Table H.3, but at the 10-year water level. The outflow of each individual discharge control device of the multi-stage outlet model, at the water level corresponding to each specific return period, required verification in order to make sure that the target discharge is never exceeded. This was done for all six multi-stage outlet models.

Table H.3: Percentage difference between theoretical and actual discharge at the 5-year water level (stage 0.792 m)

Individual components of multi-stage outlet	Stage (m)	Actual discharge of individual component, physical model (1) (m^3/s)	Theoretical discharge of individual component (m^3/s)	Percentage difference (%)
2-year component	0.792	0.054	0.047	-13.25
10-year component	0.792	0.0172	0.0173	0.52
Total		**0.071**	**0.064**	**-9.86**

(1) The actual discharge equals the average of the discharge measurements, taken every 10 minutes until water surface elevation stabilised

Table H.4: Fractional change in discharge at the 5-year water level (stage 0.792 m)

Parameter	Theoretical	Physical	Fractional change in discharge (%)	Total fractional change in discharge (Compare to Table H.3) (%)
2-year control orifice				
C_d	0.6	0.672	-10.71	-13.50
Δh (Eq. 6.1)	0.507	0.537	-2.79	
10-year control orifice				
C_d	0.37	0.345	7.25	0.84
Head (Eq. 6.1)	0.112	0.117	-6.41	

Table H.5: Percentage difference between theoretical and actual discharge at the 10-year water level (stage 0.923 m)

Individual components of multi-stage outlet	Stage (m)	Actual discharge of individual component, physical model (1) (m^3/s)	Theoretical discharge of individual component (m^3/s)	Percentage difference (%)
2-year component	0.923	0.061	0.0465	-23.85
10-year component	0.923	0.039	0.044	17.06
Total		**0.099**	**0.091**	**-8.27**

(1) The actual discharge equals the average of the discharge measurements, taken every 10 minutes until water surface elevation stabilised

Table H.6: Fractional change in discharge at the 10-year water level (stage 0.923 m)

Parameter	Theoretical	Physical	Fractional change in discharge (%)	Total fractional change in discharge (Compare to Table H.5) (%)
2-year control orifice				
C_d	0.6	0.755	-20.53	-23.54
Δh (Eq. 6.1)	0.507	0.540	-3.01	
10-year control orifice				
C_d	0.61	0.521	17.08	17.08

H.1.3 Discharge Component of Model 1 Controlling the 50-year Storm Event

Figure H.5 illustrates that the discharge from the 50-year storm control V-notch weir of the physical model was less than the theoretical discharge at consecutive stages. The reason being that the modelled thick-walled V-notch weir had an empirically derived weir discharge coefficient of 0.386 when calibrated as a V-notch weir (Equation 2.23), which is less than the typical discharge coefficient of 0.59 for a sharp-crested V-notch weir. The general expression, Equation 2.24, for discharge over a notched weir, was used for the theoretical model with a weir discharge coefficient of approximately 0.584.

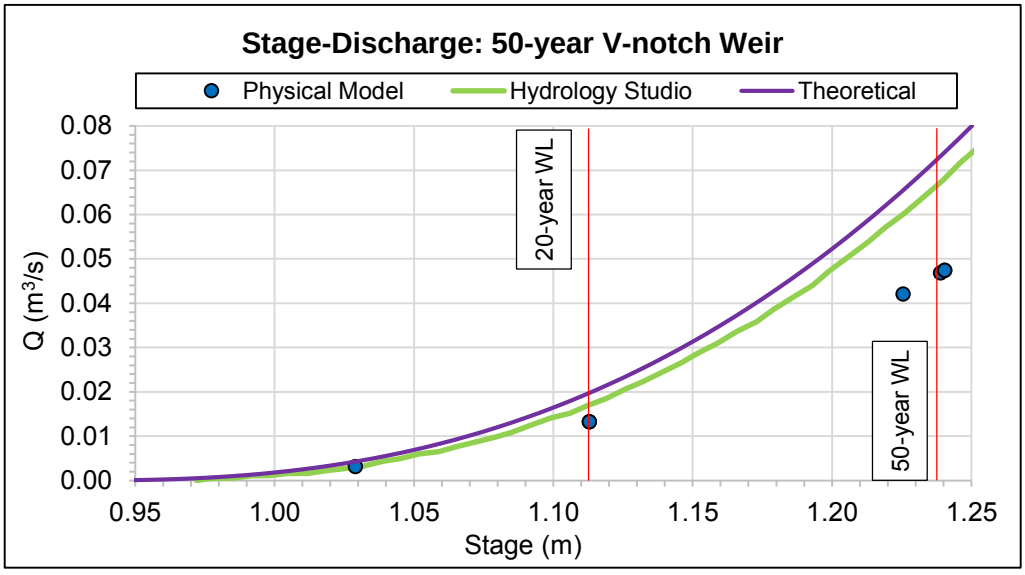

Figure H.5: Stage-discharge relationship of the 50-year control component of Model 1

The 50-year storm control V-notch weir was modelled with a crest length of 50 mm, in the direction of the flow, which is the typical thickness of concrete multi-stage outlet structures constructed in the field (150 mm prototype dimension). However, the sharp-crested or thin-plate weir is an overflow structure whose crest length, in the direction of flow, is equal or less than 2 mm (Equation 2.24), as discussed in Section 2.3.2.4. The thicker, and therefore longer crest-length in the direction of the flow, caused more contraction of the nappe during the

physical model study than theoretically estimated. This was observed during the calibration of the 50-year storm control V-notch weir in the hydraulic laboratory, as illustrated by Figure H.6.

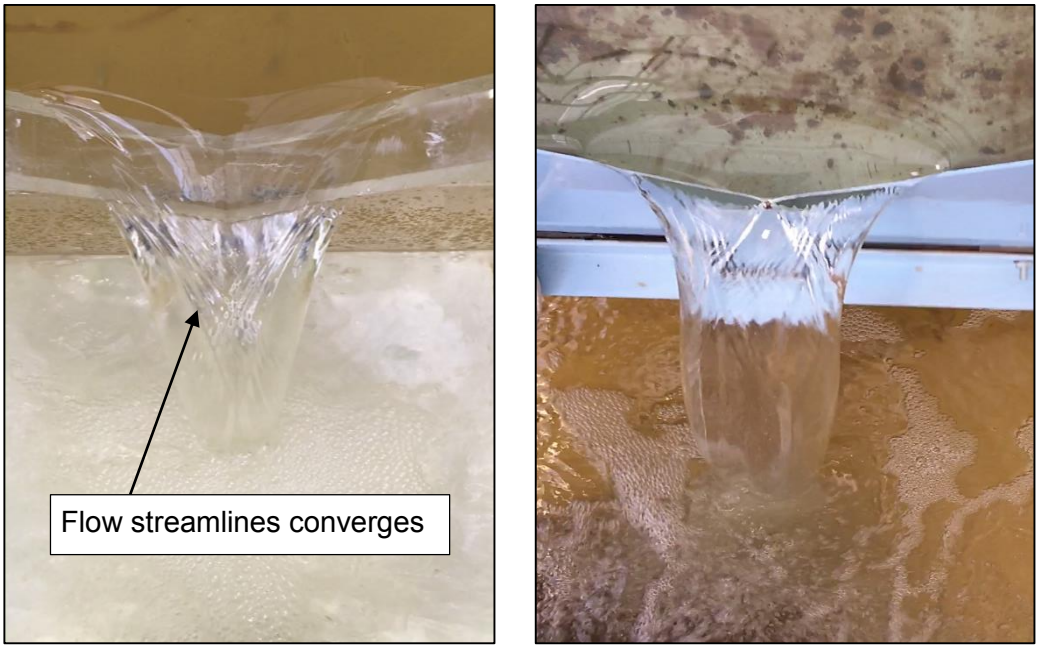

Figure H.6: Contraction of flow at a) thick-plate weir and b) thin-plate weir under the same head

Table H.7 and Table H.9 summarise the differences between the theoretical discharge and discharge measured physically, for each control component of the multi-stage model, at the 5-, 10-, and 50-year water surface elevations. Table H.8 and Table H.10 summarise the fractional change in the discharge at different water levels. From Table H.7 and Table H.9, it is evident that the hydraulic performance of the low-flow circular orifice and the 50-year control V-notch weir deviated the most from the theoretical calculations, as a result of the difference between the respective theoretical equation discharge coefficient and empirically derived discharge coefficient.

Table H.7: Percentage difference between theoretical and actual discharge at the 20-year water level (stage 1.113 m)

Individual components of multi-stage outlet	Stage (m)	Actual discharge of individual component, physical model (1) (m^3/s)	Theoretical discharge of individual component (m^3/s)	Percentage difference (%)
2-year component	1.113	0.073	0.052	-28.74
10-year component	1.113	0.054	0.064	17.94
50-year component	1.113	0.015	0.020	34.42
Total		**0.141**	**0.136**	**-3.43**

(1) The actual discharge equals the average of the discharge measurements, taken every 10 minutes until water surface elevation stabilised

Table H.8: Fractional change in discharge at the 20-year water level (stage 1.113 m)

Parameter	Theoretical	Physical	Fractional change in discharge (%)	Total fractional change in discharge (Compare to Table H.7) (%)
2-year control orifice				
C_d	0.6	0.841	-28.66	-28.77
Δh (Eq.6.1)	0.640	0.642	-0.11	
10-year control orifice				
C_d	0.61	0.521	17.08	17.08
50-year control weir				
C_d	0.58	0.386	51.32	39.60
Head (Eq. 6.1)	0.183	0.192	-11.72	

Table H.9: Percentage difference between theoretical and actual discharge at the 50-year water level (stage 1.241 m)

Individual components of multi-stage outlet	Stage (m)	Actual discharge, physical model (1) (m^3/s)	Theoretical discharge (m^3/s)	Percentage difference (%)
2-year component	1.241	0.088	0.053	-40.03
10-year component	1.241	0.063	0.075	18.08
50-year component	1.241	0.053	0.074	40.38
Total		**0.204**	**0.201**	**-1.34**

(1) The actual discharge equals the average of the discharge measurements, taken every 10 minutes until water surface elevation stabilised

Table H.10: Fractional change in discharge at the 50-year water level (stage 1.113 m)

Parameter	Theoretical	Physical	Fractional change in discharge (%)	Total fractional change in discharge (Compare to Table H.9) (%)
2-year control orifice				
C_d	0.60	0.98	-38.78	-39.63
Δh (Eq. 6.1)	0.648	0.659	-0.86	
10-year control orifice				
C_d	0.61	0.52	17.08	17.08
50-year control weir				
C_d	0.58	0.386	51.32	44.27
Head (Eq. 6.1)	0.310	0.319	-7.05	

The total percentage difference between the theoretical and physical discharge summarised in Table H.7 and Table H.9, varied slightly from the total fractional change in discharge, as

determined in Table H.8 and Table H.10, respectively. However, the 50-year storm control V-notch weir was an exception, with a variance of 3.89%. The 3.89% variance is due to the V-notch weir that was constructed with an 89° angle compared to the 90° of the theoretical model.

H.2 Results of Model 2

The measured outflow of Model 2 (I.1) was plotted against the stage to determine if the outlet is discharging at a rate equal to the pre-development peak flow levels, or if the target was exceeded. Model 2 was designed to control the 2-, 10-, 50-, and 100-year RI storm events for inland regions receiving 400 mm MAP. The outflow from Model 2 exceeded the target discharges for the more frequent storm events (2-, 5-, and 10-year RI storms). As illustrated on Figure H.7, where the blue stage-discharge curve of the physical model lies above the red target stage-discharge curve, the outflow from Model 2 exceeded the target discharge. For the less frequent storm events, such as the 20-, 50-, 100-year RI storms, the flow released by Model 2 met the target discharges. The data collected from the physical model fitted the stage-discharge curve of the spreadsheet (theoretical model) for the less frequent events.

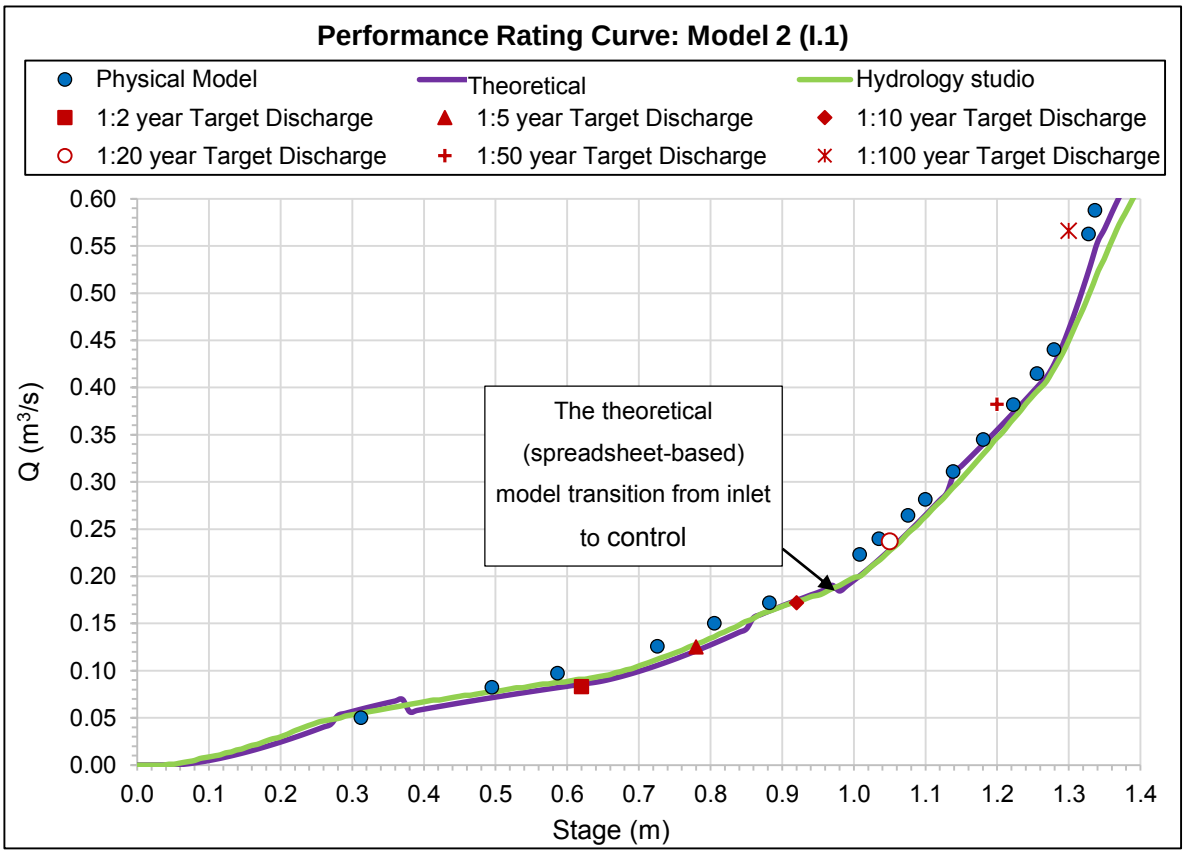

Figure H.7: Calculated and physically modelled stage-discharge relationship of Model 2 (prototype dimensions)

It is evident from Figure H.7 that although Model 2 was designed without a discharge control device that was sized to control the 20-year peak flow, the physical model still restricted the outflow at the 20-year maximum water surface elevation to almost meet the pre-development

target discharge. The main reason why the 5- and 10-year RI storms were not attenuated to meet the target discharges is due to the 2-year storm control orifice, which empirically derived discharge coefficient was larger than the recommended theoretical equation coefficient of 0.61. The hydraulic performance of each component of the multi-stage outlet model is further elaborated in Sections H.2.1 to H.2.3.

In Table H.11 the actual discharge, released by the multi-stage outlet model, was compared with the theoretical discharge, at the resultant water surface elevation measured in the hydraulic laboratory. From Table H.11 it is evident that the percentage difference in discharge for the 5-year RI was the greatest due to the hydraulic performance of the 2-year storm control component of the multi-stage model, which deviated the most from the theoretical discharge. The flow released by the 2-year storm orifice also affected the total flow released by the multi-stage outlet, as the stage increased for the 10-, 20-, 50- and 100-year RI storms.

Table H.11: Difference between theoretical discharge and physically measured discharge of Model 2

RI (years)	Stage (m)	Actual discharge of physical model(1) (m^3/s)	Theoretical discharge (m^3/s)	Absolute difference (m^3/s)	Percentage Difference (%)
2	0.495	0.082	0.073	-0.010	-12.0
5	0.726	0.126	0.107	-0.018	-14.5
10	0.882	0.172	0.165	-0.007	-3.80
20	1.035	0.240	0.220	-0.020	-8.30
50	1.223	0.382	0.371	-0.010	-2.70
100	1.328	0.563	0.525	-0.038	-6.70

(1) The actual discharge equals the average of the discharge measurements, taken every 10 minutes until water surface elevation stabilised

H.2.1 Discharge Component of Model 2 controlling the 2-year Storm Event

Figure H.8 indicates that the discharge through the 2-year storm control orifice decreased at stage 0.882 m. The reason being the 10-year storm control orifice that transitioned from weir flow to orifice flow at stage 0.882 m. This caused the water inside the riser to increase and in return reduced the differential head and discharge of the 2-year orifice. Thereafter the water inside the riser gradually increased.

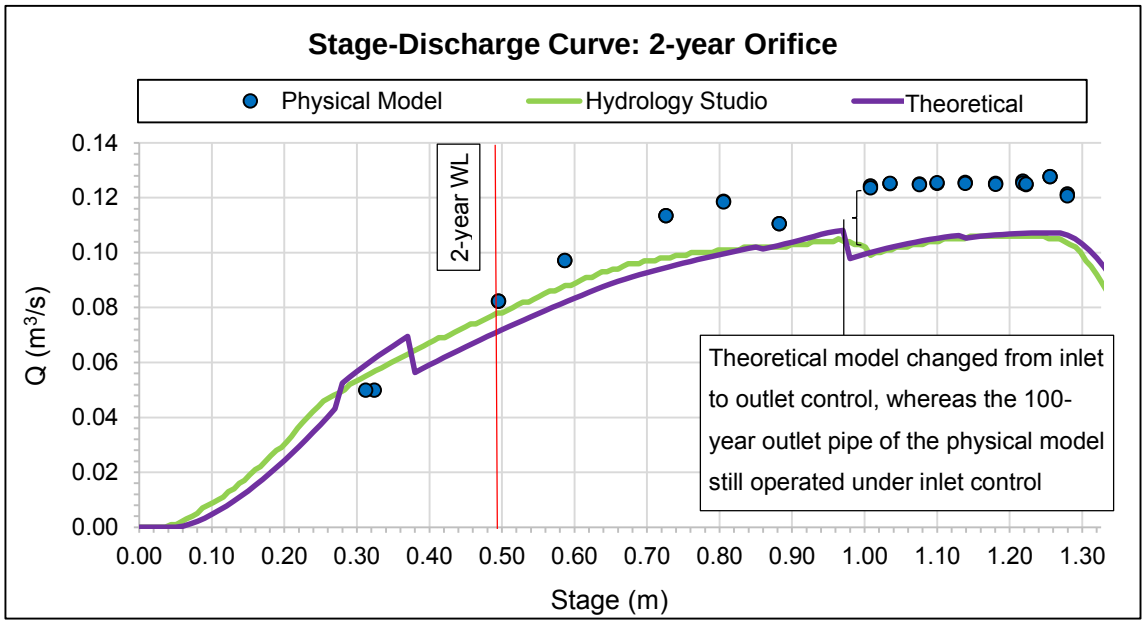

Figure H.8: Relationship between the discharge and stage for the 2-year control component of Model 2

Table H.12 indicates that the discharge released by the 2-year sized component of the physical model deviated from the theoretical discharge since the discharge coefficient varied as the differential head fluctuated per stage, while the spreadsheet (theoretical model) assumed a constant discharge coefficient of 0.61. The empirical derived discharge coefficient, based on experimentally collected data, varied from 0.67 to 0.63 as the differential head increased.

The mean of the discharge coefficients was determined to be 0.65 (refer to Table I.2 in Appendix I) and is the most probable equation coefficient based on 28 readings. This is further elaborated in Section 7. From Figure H.8 it is clear that the standard orifice equation with a single-valued discharge coefficient does not fit the empirically derived data of the physical model.

Table H.12: Fractional change in discharge at the 2-year water level (stage 0.495 m)

Parameter	2-year control orifice		Fractional change in discharge (%)	Total fractional change in discharge (%)	Percentage difference from Table H.11 (%)	Error (%)
	Theoretical	Physical				
C_d	0.61	0.67	-8.96	-12.60	**-12.00**	0.59
Δh (Eq. 6.1)	0.219	0.236	-3.66			

H.2.2 Discharge Component of Model 2 Controlling the 10-year Storm Event

Figure H.9 indicates that the 10-year storm control orifice of the physical model is in good agreement with the theoretical model once the 10-year storm control orifice was fully submerged upstream (from stage 0.882 m). The 10-year storm control orifice of the multi-stage outlet model was partially submerged upstream at the 5-year maximum water surface elevation, 0.726 m, where the 10-year orifice functioned as a weir.

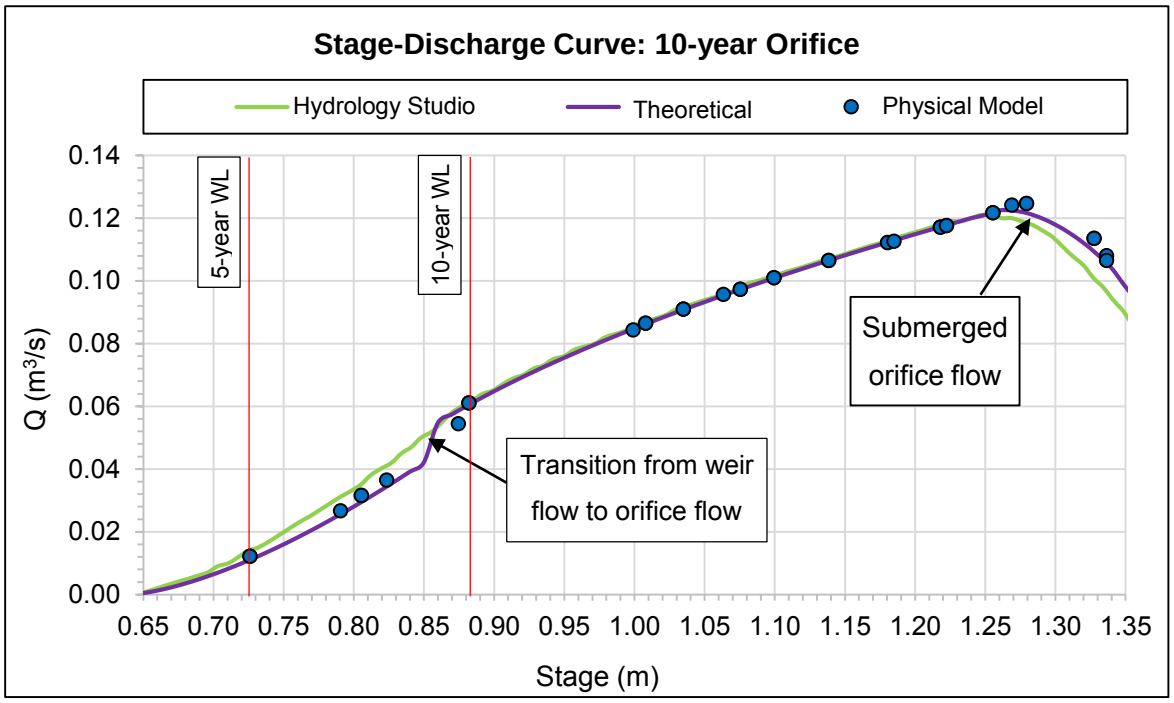

Figure H.9: Stage-discharge relationship for the 10-year control component of Model 2

The mean value of the empirically derived discharge coefficient, for the 2-year control orifice of the physical model, varied from 0.66 at the 5-year water level (stage 0.726 m) to 0.63 at the 10-year water level (stage 0.882 m). This is larger than the typical constant discharge coefficient of 0.61 used in the theoretical formula. The latter caused a large fractional change in the discharge of the modelled 2-year control orifice, as determined in Table H.14 and Table H.16.

The mean value of the discharge coefficient of the modelled 10-year orifices was determined to be 0.383 for weir flow conditions and 0.607 for orifice flow conditions, which is in good agreement with the typical discharge coefficients found in the literature (theoretical formula), refer to Table H.14 and Table H.16 respectively. The head produced by the modelled 100-year pipe (water inside the riser) was in accordance to the head calculated by the theoretical formula at the 10-year water level (stage 0.882 m). The reason was that the 10-year storm control orifice of the physical model discharged as designed and the contribution of the 2-year storm control orifice to the total flow decreased as the stage increased. Thus, the fractional change in discharge caused by the difference in differential head readings was small, as summarised in Table H.14 and Table H.16.

Table H.13: Percentage difference between theoretical and actual discharge at the 5-year water level (stage 0.726 m)

Individual components of multi-stage outlet	Stage (m)	Actual discharge of individual component, physical model (1) (m^3/s)	Theoretical discharge of individual component (m^3/s)	Percentage difference (%)
2-year component	0.726	0.1135	0.0964	-15.03
10-year component	0.726	0.0122	0.0110	-9.65
Total		0.126	0.107	**-14.50**

(1) The actual discharge equals the average of the discharge measurements, taken every 10 minutes until water surface elevation stabilised

Table H.14: Fractional change in discharge at the 5-year water level (stage 0.726 m)

Parameter	Theoretical	Physical	Fractional change in discharge (%)	Total fractional change in discharge (Compare to Table H.13) (%)
2-year control orifice				
C_d	0.61	0.66	-7.58	-15.39
Δh (Eq. 6.1)	0.3865	0.4580	-7.81	
10-year control orifice				
C_d	0.37	0.383	-3.39	-10.06
Head (Eq. 6.1)	0.086	0.090	-6.67	

Table H.15: Percentage difference between theoretical and actual discharge at the 10-year water level (stage 0.882 m)

Individual components of multi-stage outlet	Stage (m)	Actual discharge of individual component, physical model (1) (m^3/s)	Theoretical discharge of individual component (m^3/s)	Percentage difference in discharge (%)
2-year component	0.882	0.1106	0.1047	-5.29
10-year component	0.882	0.0612	0.0605	-1.127
Total		**0.172**	**0.165**	**-3.83**

(1) The actual discharge equals the average of the discharge measurements, taken every 10 minutes until water surface elevation stabilised

Table H.16: Fractional change in discharge at the 10-year water level (stage 0.882 m)

Parameter	Theoretical	Physical	Fractional change in discharge (%)	Total fractional change in discharge (Compare to Table H.15) (%)
2-year control orifice				
C_d	0.61	0.63	-3.17	-4.86
Δh (Eq. 6.1)	0.4562	0.4721	-1.69	
10-year control orifice				
C_d	0.61	0.607	0.5	-1.09
Head (Eq. 6.1)	0.1220	0.1260	-1.59	

H.2.3 Discharge Component of Model 2 Controlling the 50-year Storm Event

The 50-year storm control weir had weir discharge coefficients that ranged from 1.75 to 1.79 when calibrated as a broad-crested weir (Equation 2.14). The two downward slopes of the water surface profile, one at the beginning of the crest and again near the end of the weir crest, merged at higher stages, see Figure H.12 (b). This larger streamline curvature explains the increase in the discharge coefficient at higher stages. Equation 2.14 incorporates a varying discharge coefficient for different head values, refer to Table 2.3. Whereas the theoretical model used a constant weir coefficient of 1.84 for sharp-crested weirs, refer to Equation 2.19.

Figure H.10 illustrates the comparison of different theoretical equations, most commonly found in stormwater drainage manuals, with the results of the software, Hydrology Studio, and the physical model. The broad-crested weir equation (Equation 2.14) is in good agreement with the physical model at very low stages. The reason being that the head on the weir is small enough so that the influence of the streamline curvature is still insignificant.

The stage-discharge curve resulting from the sharp-edged suppressed rectangular weir equation, Equation 2.18, did not match the results from the physical model study at higher stages. Since Equation 2.18 made allowance for end contractions. The end contraction phenomenon arises where the width of the flow, flowing over the weir, becomes narrower than the crest width (Institute for Agricultural Engineering, 2003).

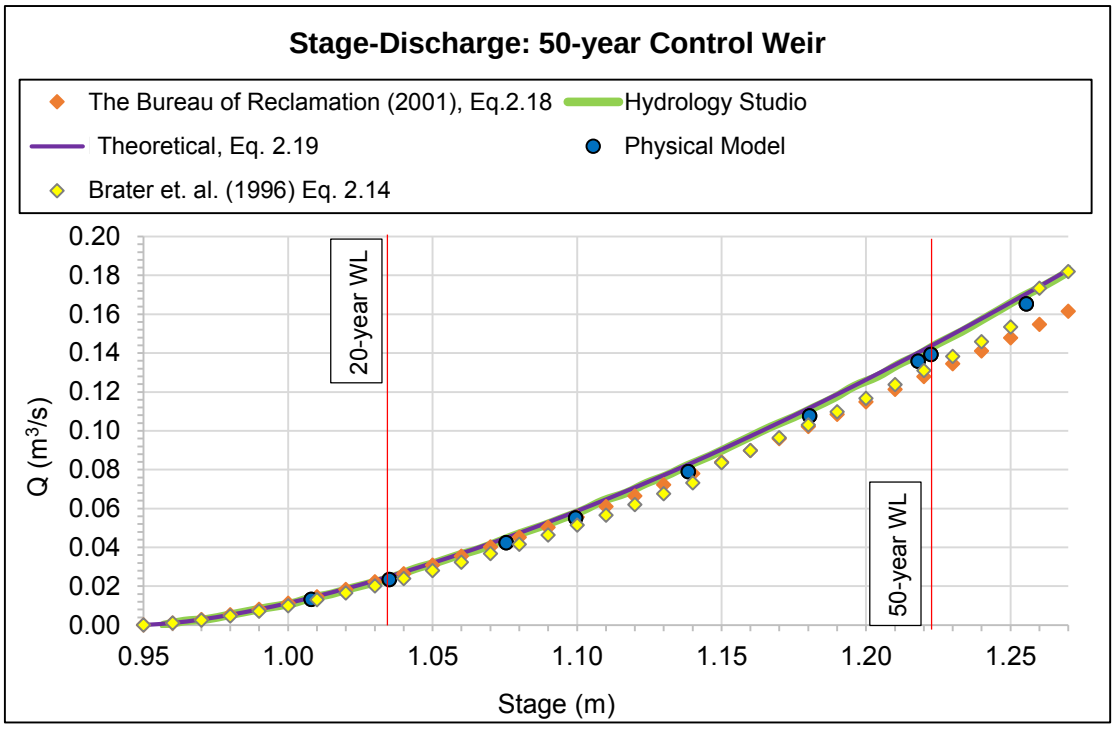

Figure H.10: Stage-discharge curve of the 50-year control component of Model 2

Figure H.11 and Figure H.12 shows the 50-year weir discharging at low and high water surface elevations respectively. After stage 1.035 m, the 20-year water level, the 100-year pipe became submerged upstream. The 10-year storm control orifice was fully submerged upstream and discharged freely downstream at stages 1.035 m and 1.223 m. The 2-year orifice operated as a submerged orifice at stage 1.035 m and stage 1.223m.

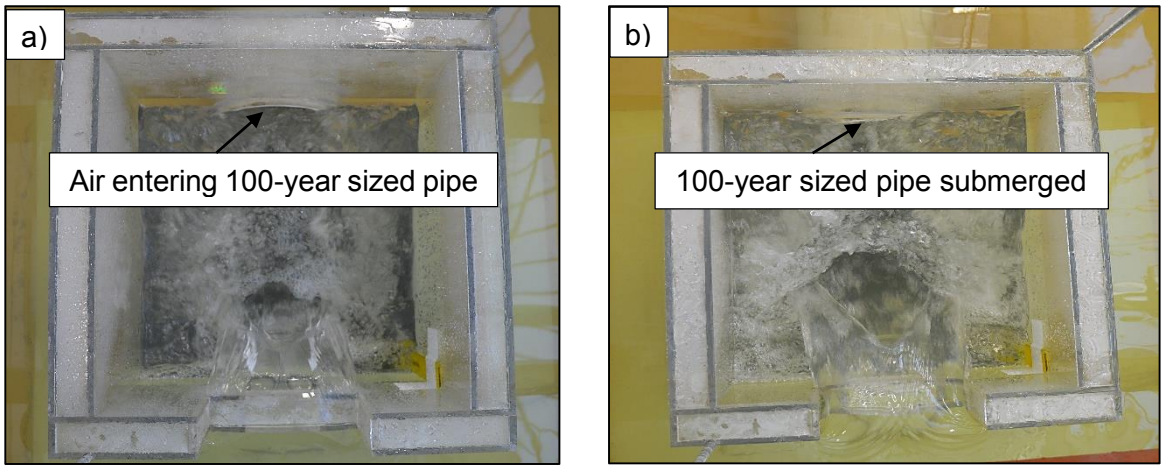

Figure H.11: a) Top view of Model 2 discharging at the 20-year water level, stage 1.035 m b) Top view of Model 2 discharging at 50-year water level, stage 1.223 m

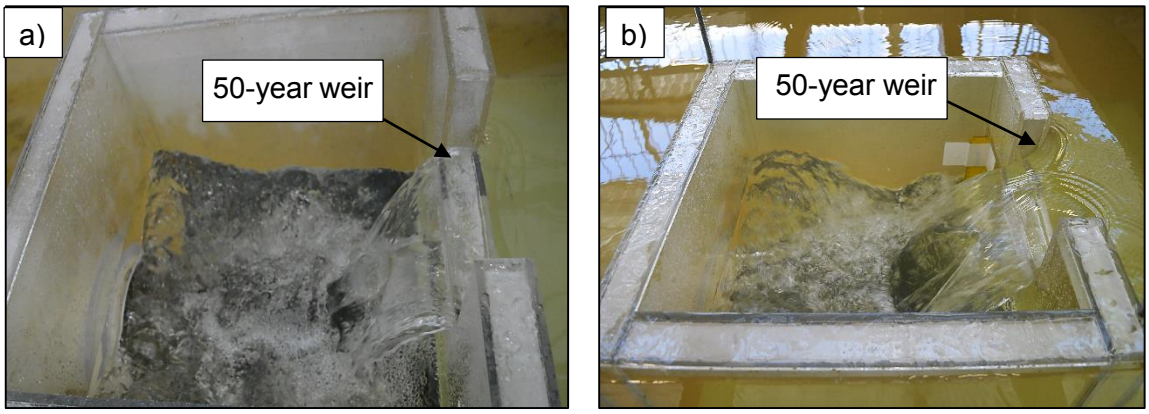

Figure H.12: a) Flow was more parallel above the crest at the 20-year water level, stage 1.035 m b) End-contraction of flow visible at 50-year water level, stage 1.223 m

Table H.17 and Table H.19 summarise the fractional change in discharge at the 20-year water level (stage 1.035 m) and the 50-year water level (stage 1.223 m) respectively, for each individual component of Model 2. These fractional changes could be attributed to the difference between the theoretical equation discharge coefficient and experimentally calibrated discharge coefficient, and differential head. The latter was the greatest for the 2-year storm control orifice. The measured outflow from the multi-stage outlet model for the 20-year storm event exceeded the theoretical discharge by 8.27%, since the 2-year storm control orifice released more flow than estimated, as indicated in Table H.18.

The total percentage difference between the theoretical and physical discharge determined in Table H.17 differs with a maximum of 0.61% (2-year component) from the total fractional change in discharge, as determined in Table H.18. Therefore, the 0.61% variance is acceptable, as an experimental error of $\pm$0.5% was expected, as mentioned in Section 5.3. The approach velocity of the 100-year storm control pipe was assumed negligible when the theoretical differential head was calculated by means of the spreadsheet-based model.

Table H.17: Percentage difference between theoretical and physical measured discharge at the 20-year water level (stage 1.035 m)

Individual components of multi-stage outlet	Stage (m)	Actual discharge of individual component, physical model (1) (m^3/s)	Theoretical discharge of individual component (m^3/s)	Percentage difference between theoretical and physical discharge (%)
2-year component	1.035	0.1252	0.1041	-16.91
10-year component	1.035	0.0910	0.0908	-0.23
50-year component	1.035	0.0234	0.0251	6.97
Total		0.240	0.220	**-8.27**

(1) The actual discharge equals the average of the discharge measurements, taken every 10 minutes until water surface elevation stabilised

Table H.18: Fractional change in discharge at the 20-year water level (stage 1.035 m)

Parameter	Theoretical	Physical	Fractional change in discharge (%)	Total fractional change in discharge (Compare to Table H.17) (%)
2-year control orifice				
C_d	0.61	0.67	-8.96	-17.52
Δh (Eq. 6.1)	0.450	0.543	-8.56	
10-year control orifice				
C_d	0.61	0.607	0.49	-0.22
Head (Eq. 6.1)	0.275	0.279	-0.72	
50-year control orifice				
C_d	1.84	1.753	4.96	6.75
Head (Eq. 6.1)	0.085	0.084	1.79	

Table H.19: Percentage difference between theoretical and actual discharge at the 50-year water level (stage 1.223 m)

Individual components of multi-stage outlet	Stage (m)	Actual discharge of individual component, physical model (1) (m^3/s)	Theoretical discharge of individual component (m^3/s)	Percentage difference in discharge (%)
2-year component	1.223	0.125	0.109	-12.07
10-year component	1.223	0.118	0.118	0.06
50-year component	1.223	0.139	0.144	3.26
Total		**0.382**	**0.371**	**-2.73**

(1) The actual discharge equals the average of the discharge measurements, taken every 10 minutes until water surface elevation stabilised

Table H.20: Fractional change in discharge at the 50-year water level (stage 1.223 m)

Parameter	Theoretical	Physical	Fractional change in discharge (%)	Total fractional change in discharge (Compare to Table H.19) (%)
2-year control orifice				
C_d	0.61	0.63	-3.17	-11.67
Δh (Eq. 6.1)	0.501	0.604	-8.49	
10-year control orifice				
C_d	0.61	0.607	0.49	0.15
Head (Eq. 6.1)	0.583	0.587	-0.34	
50-year control orifice				
C_d	1.84	1.792	2.68	3.23
Head (Eq.6.1)	0.2725	0.2715	0.55	

H.3 Results of Model 4

The measured outflow of Model 4 (C.5) is plotted against the stage to determine if the outlet s discharging at a rate equal to the pre-development peak flow levels, or if the target was exceeded. The discharge control devices of Model 4 (C.5) were designed to control the 2-, 10-, 50-, and 100-year RI storm events for coastal regions receiving 700 mm MAP.

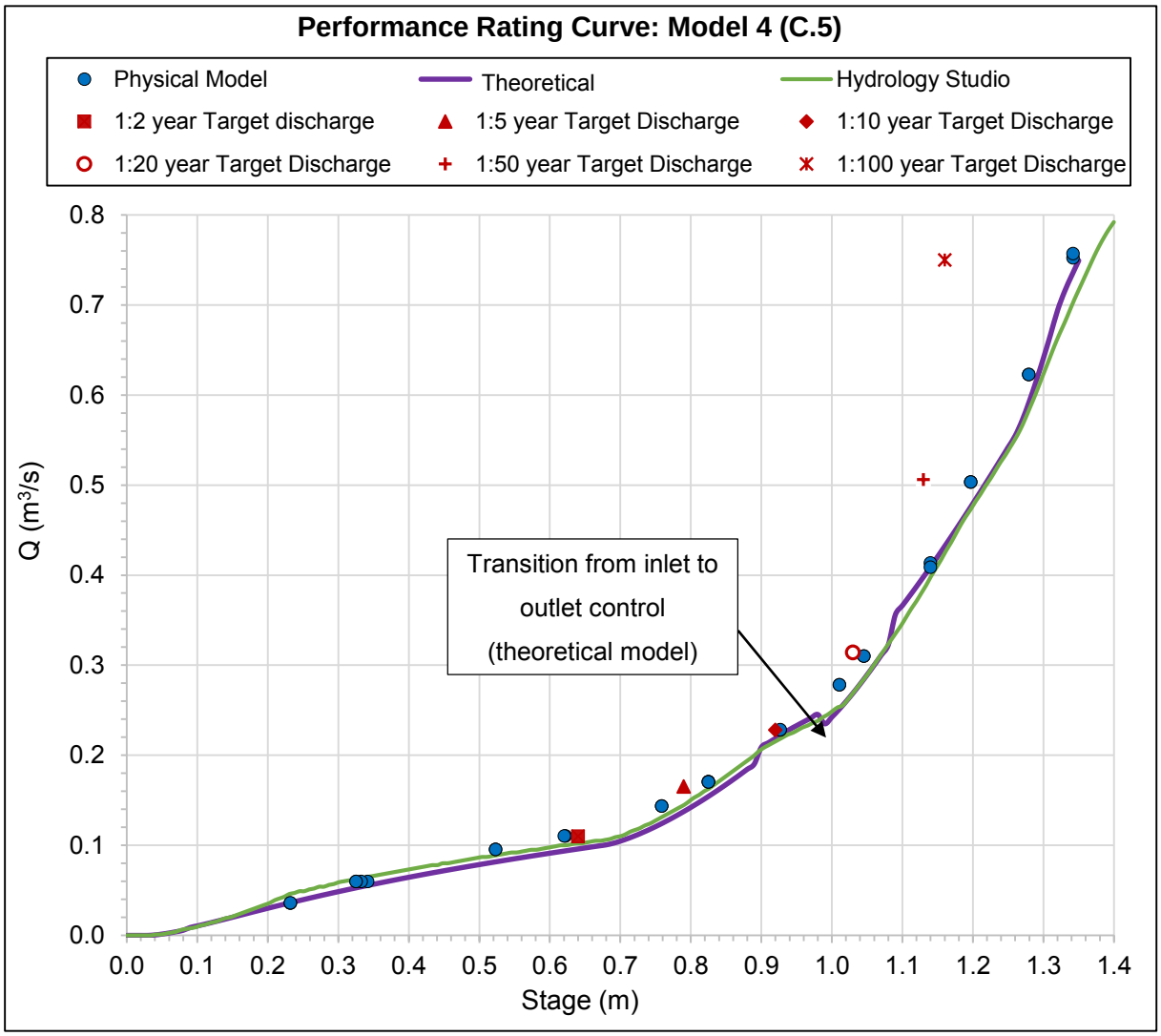

Figure H.13: Calculated and physically modelled stage-discharge relationship of Model 4 (prototype dimensions)

Figure H.13 shows that the stage-discharge curve of the physical model (blue) plots adjacent to the target stage-discharge curve (red), for the more frequent flood events. At the less frequent storm events (50- and 100-year), the stage-discharge curve of the physical model lies below the target stage-discharge curve, which indicates that the physical model controlled the outflow effectively. However, the model over controlled the flow of the less frequent storm events. It is evident from Figure H.13 that Model 4 did not restrict the outflow of the 2-year design storm to the pre-development peak flow since it released the 2-year target discharge at a stage that is 3.06% lower than the estimated maximum 2-year water surface elevation.

Model 4 was designed without individual discharge control components to limit the discharge for the 5- and 20-year recurrence interval storms. However, the 2- and 10-year discharge control components of the multi-stage outlet still controlled the amount of water released at the 5- and 20-year maximum water surface elevation. The discharge released by the physical multi-stage outlet model was compared with the theoretical discharge, at the resultant water surface elevation measured in the hydraulic laboratory, in Table H.21.

Table H.21: Difference between theoretical and actual discharge of Model 4

RI (years)	Stage (m)	Actual discharge of physical model(1) (m^3/s)	Theoretical discharge (m^3/s)	Absolute difference (m^3/s)	Percentage difference (%)
2	0.621	0.110	0.094	-0.016	-14.50
5	0.825	0.170	0.155	-0.016	-9.24
10	0.927	0.228	0.222	-0.006	-2.68
20	1.046	0.310	0.285	-0.025	-8.16
50	1.197	0.503	0.476	-0.027	-5.34
100	1.343	0.754	0.736	-0.018	-2.42

The theoretical discharge differs the most at the 2-, 5-, and 20-year water surface elevations. The flow contribution of the 2-year orifice to the total flow at consecutive stages decreases as the other control component starts to function. Thus, the influence of the 2-year orifice on the percentage difference between the theoretical and actual discharge decreases. This explains why the discharge calculated at the 5-year water surface elevation differs less (-9.24%) from the measured discharge than at the 2-year water surface elevation (-14.5%). This is further investigated in Section H.3.1 to H.3.3.

H.3.1 Discharge Component of Model 4 Controlling the 2-year Storm Event

When the water surface elevation reached 1.197 m for a flow rate of 0.503 m^3/s, the 100-year outlet pipe installed downstream of the 2-year orifice become fully submerged. From stage 1.197 m, the flow entering the multi-stage outlet was very turbulent between the overflow riser and the 100-year outlet pipe. The Reynolds number for the flow inside the riser ranged from 35 431 to 41 526 (model values) for stage 1.197 m and 1.34 m respectively. This caused fluctuations in the water surface elevation inside the riser that influenced the differential head acting on the 2-year orifice.

It is also at these high water surface elevations that the flow transitioned for free-surface flow (inlet control) at the entrance of the 100-year pipe to pressurized flow at stage 1.197 m, refer to Figure H.14. It is evident from Figure H.15 that the 2-year storm control orifice released more flow than calculated with the theoretical formulas.

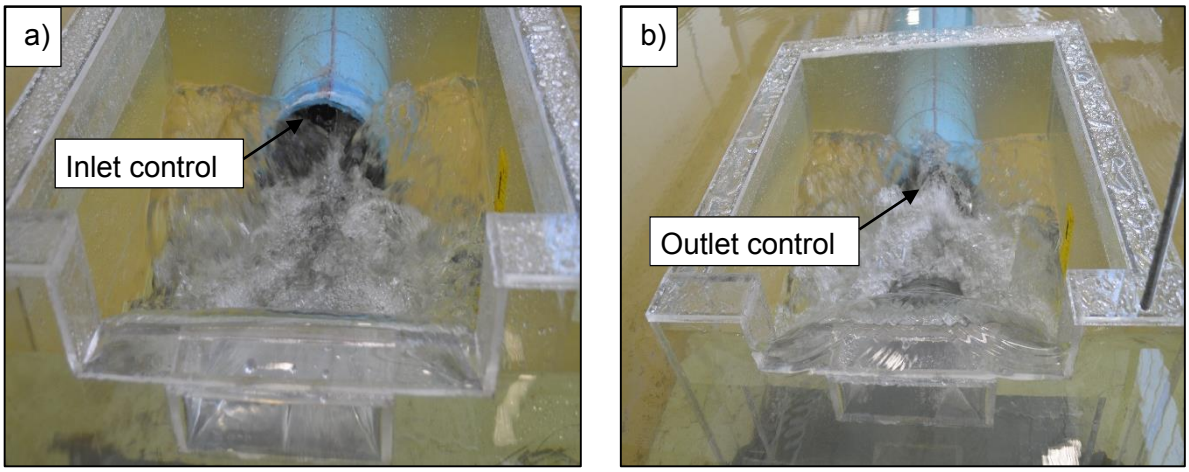

Figure H.14: a) Free surface flow (inlet control) at stage 1.046 m b) Pressurized flow (outlet control) at stage 1.197 m

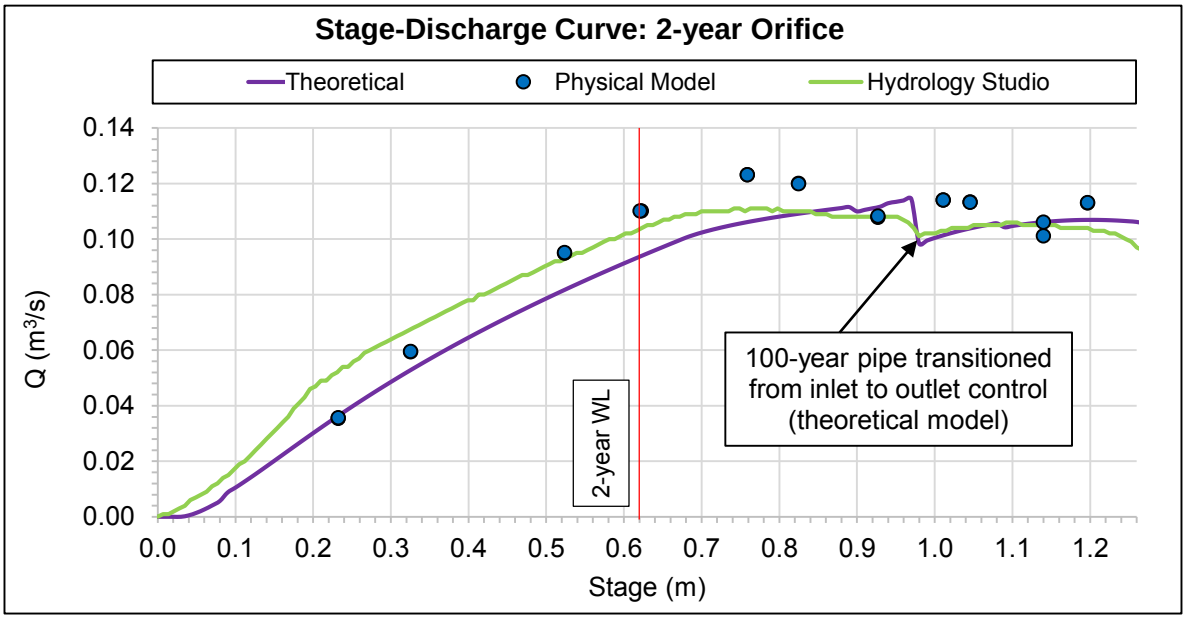

Figure H.15: Stage-discharge curve for the 2-year control component of Model 4

The fractional change in the discharge of the 2-year orifice, as a result of the difference in theoretical and measured differential head, was determined to be -9.07%, as summarised in Table H.22. The empirically derived discharge coefficient, based on experimentally collected data, varied from 0.66 to 0.59 as the differential head and discharge decreased with increase in the stage. This is further elaborated in Section 7.

The mean of the discharge coefficients was determined to be 0.63 (refer to Table I.4 in Appendix I) and is the most probable equation coefficient based on 24 readings. The theoretical equation discharge coefficient (C_d=0.61) was -6.15% different from the empirically derived discharge coefficient at stage 0.621 m, refer to Table H.22.

Table H.22: Fractional change in discharge at the 2-year water level (stage 0.621 m)

Parameter	2-year control orifice		Fractional change in discharge (%)	Total fractional change in discharge (%)	Percentage difference from Table H.21 (%)	Error (%)
	Theoretical	Physical				
C_d	0.61	0.65	-6.15	-15.22	**-14.50**	0.72
Differential head (Eq. 6.1)	0.317	0.387	-9.07			

H.3.2 Discharge Component Controlling 10-year Storm Event

It is clear from Figure H.16 that the outflow from the physical modelled 10-year storm control orifice component decreased once the water inside the riser reached the centre of the orifice at stage 1.28 m. The 10-year storm control orifice calculated with the theoretical formulas was submerged above the centre of the orifice at a lower stage (1.20 m), since the calculated head, produced by the 100-year pipe was larger than measured in the hydraulic laboratory. The reason for the decrease in the discharge, only after the orifice was submerged downstream to an elevation above the centre, is due to the average head approximation of Equation 2.1 as discussed in Section 2.3.2.1.

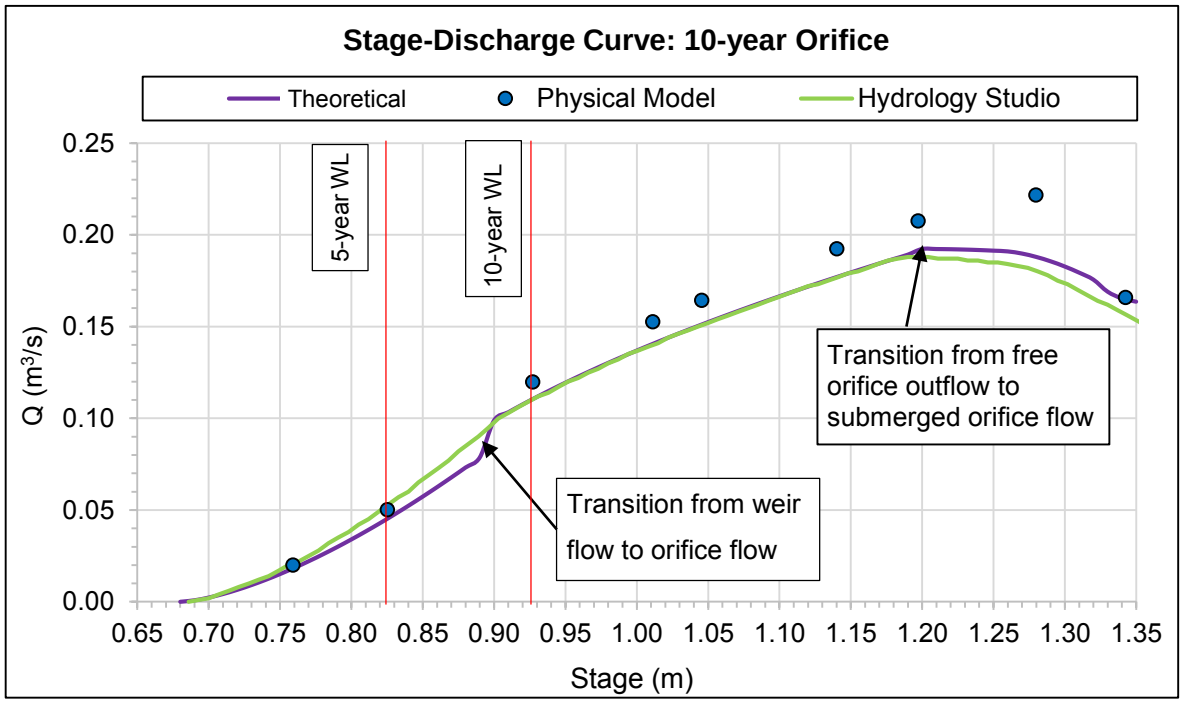

Figure H.16: Stage-discharge curve for the 10-year control component of Model 4

The mean value of the discharge coefficient of the modelled 10-year orifice was determined to be 0.415 for weir flow conditions and 0.664 for orifice flow conditions, which is both larger than the theoretical discharge coefficient, as summarised in Table H.24 and Table H.26. The mean value of the discharge coefficient for the modelled 2-year storm control orifice varied from 0.66 at stage 0.825 m to 0.60 at stage 0.927 m. From stage 0.927 m to stage 1.197 m, the empirically derived discharge coefficient was constant for the modelled 2-year storm control orifice.

The fractional change in the discharge of the 10-year storm control orifice, due to the difference between the discharge coefficient recommended in the literature (0.61) and experimentally calibrated, is the main attribute to the difference between the theoretical and actual discharge at the 5- and 10-year water levels. Refer to Table H.24 and Table H.26, which summarise the fractional change in discharge for each component of the multi-stage outlet model. Tables H.23 and H.25 summarise the amount of flow released by the individual components of the multi-stage outlet model during the physical model tests, as well as the corresponding theoretical values.

Table H.23: Percentage difference between theoretical and actual discharge at the 5-year water level (0.825 m)

Individual component of multi-stage outlet designed to control specific RI storm (years)	Stage (m)	Actual discharge of individual components, physical model(1) (m^3/s)	Theoretical discharge of individual component (m^3/s)	Percentage difference between theoretical and physical discharge (%)
2- year component	0.825	0.120	0.109	-9.03
10-year component	0.825	0.050	0.045	-9.92
Total		**0.170**	**0.154**	**-9.24**

(1) The actual discharge equals the average of the discharge measurements, taken every 10 minutes until water surface elevation stabilised

Table H.24: Contribution of discharge coefficient and differential head measurements to the percentage difference between theoretical and actual discharge at 5-year water level (stage 0.825 m)

Parameter	Theoretical	Physical	Fractional change in discharge (%)	Total fractional change in discharge (Compare to Table H.23) (%)
2-year control orifice				
C_d	0.61	0.66	-7.58	-9.90
Δh (Eq. 6.1)	0.4295	0.4504	-2.32	
10-year control orifice				
C_d	0.37	0.415	-10.84	-10.84

Table H.25: Percentage difference between theoretical and physical measured discharge at 5-year water level (stage 0.927 m)

Individual component of multi-stage outlet designed to control specific RI storm (years)	Stage (m)	Actual discharge of individual component, physical model(1) (m3/s)	Theoretical discharge of individual component (m3/s)	Percentage difference (%)
2- year component	0.927	0.1081	0.1115	3.15
10-year component	0.927	0.1200	0.1105	-7.94
Total		0.228	0.2218	**-2.68**

(1) The actual discharge equals the average of the discharge measurements, taken every 10 minutes until water surface elevation stabilised

Table H.26: Contribution of discharge coefficient and differential head measurements to the percentage difference between theoretical and actual discharge at 10-year water level (stage 0.927 m)

Parameter	Theoretical	Physical	Fractional change in discharge (%)	Total fractional change in discharge (Compare to Table H.25) (%)
2-year control orifice				
C_d	0.61	0.6	1.67	2.99
Δh (Eq. 6.1)	0.448	0.437	1.32	
10-year control orifice				
C_d	0.61	0.664	-8.1	-8.13

The compiled spreadsheet-based model, consisting of numerous theoretical formulas, was interpolated linearly across stages (0.92 m and 0.93 m) to determine the discharge at the water surface elevation that was measured in the laboratory (stage 0.927 m). Thus, in addition to experimental error, the interpolation of the theoretical water level caused the total percentage difference between the theoretical and physical discharge (Tables H.23 and H.25) to differed slightly from the total fraction change in discharge, as determined in Table H.24 and Table H.26.

H.3.3 Discharge Component of Model 4 Controlling the 50-year Storm Event

The weir discharge coefficient for the 50-year storm control weir was experimentally calibrated and ranged from 1.83 to 1.91 when modelled as a broad-crested weir (Equation 2.14). Whereas the spreadsheet used a constant weir coefficient of 1.84 for sharp-crested weirs, as given by Equation 2.19. Figure H.17 indicates that the stage-discharge curve, determined by means of Equation 2.14, with a varying discharge coefficient of 1.61 to 1.83 for different head values, after Brater et al. (1996), does not fit the data collected from the physical model. Since at larger heads, the nappe springs clear from the weir crest and discharges as a sharp-crested weir.

Equation 2.18 (The Bureau of Reclamation, 2001) represents discharge for a standard fully contracted rectangular weir and underestimated the discharge of the physical modelled 50-year storm control weir. Figure H.17 indicates that the stage-discharge curve, determined by means of Equation 2.19, with a constant discharge coefficient, best fitted the experimental data of Model 4.

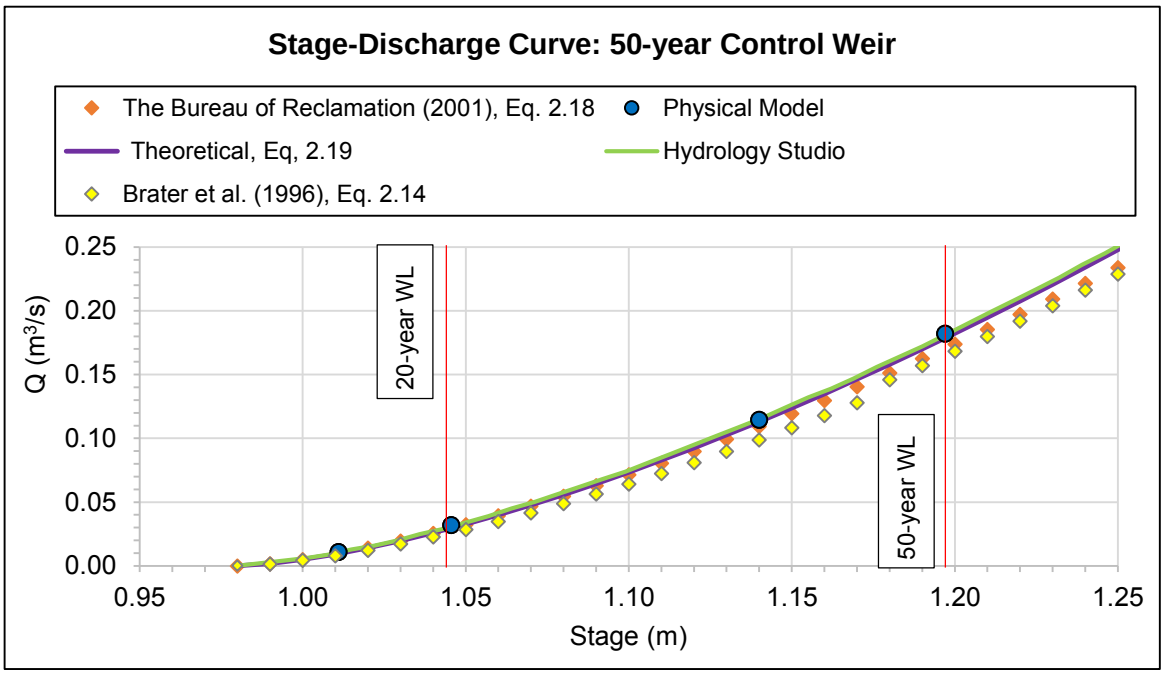

Figure H.17: Stage-discharge relationship for the 50-year control component of Model 5

Figure H.18 indicates that at stage 1.046 m (20-year water level), the 10-year storm control orifice was fully submerged upstream, discharged freely downstream, where the nappe of the 50-year sized weir collided with the jet of the 10-year control orifice. At stage 1.197 m (50-year water level), the 10-year storm control orifice was partially submerged downstream (submergence ratio of 3.8%) downstream.

The 10-year sized orifice was periodically submerged downstream due to the water surface fluctuations inside the riser box, as illustrated in Figure H.19. Figure H.18 indicates that the 50-year storm control weir also discharged at the 20-year water surface elevation, but under a low head of 0.0675 m (prototype dimension).

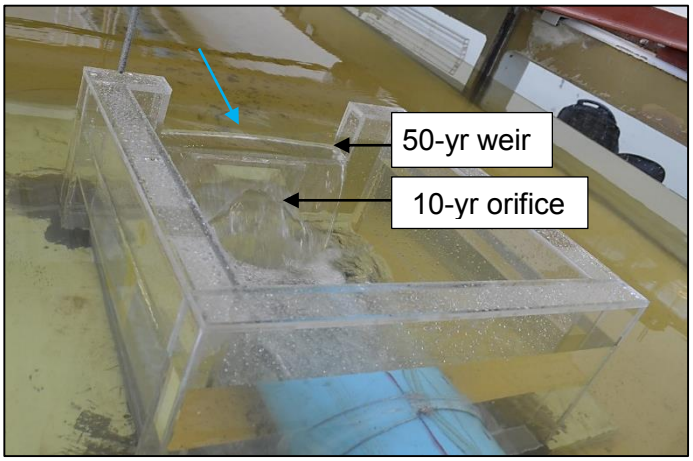

Figure H.18: 10-year sized orifice fully submerged upstream

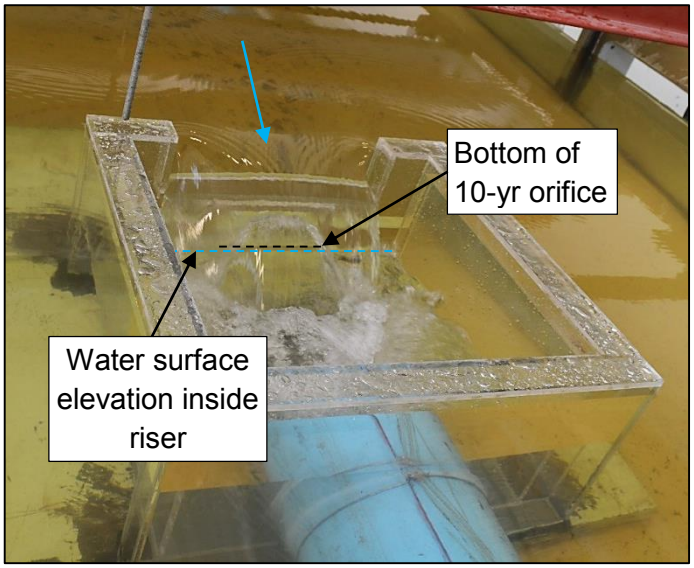

Figure H.19: Water inside riser submerged the 10-year sized orifice at stage the 50-year water level, 1.197 m

Tables H.28 and H.30 summarise the fractional change in discharge for each individual component of Model 4 at stage 1.046 m and 1.197 m respectively. These fractional changes are due to the difference between the theoretical discharge coefficient and the experimentally calibrated discharge coefficient, and differential head. The 50-year outflow was not restricted to the theoretical discharge due to the 2- and 10-year sized orifices, since the respective empirically derived discharge coefficients deviated from the recommended equation discharge coefficients, as summarised in Table H.30.

Table H.27: Percentage difference between theoretical and actual discharge at the 20-year water level (stage 1.046 m)

Individual component of multi-stage outlet designed to control specific RI storm	Stage (m)	Actual discharge of individual components, physical model(1) (m^3/s)	Theoretical discharge of individual component (m^3/s)	Percentage difference between theoretical and physical discharge (%)
2-year component	1.046	0.1133	0.1038	-8.36
10-year component	1.046	0.1642	0.1511	-7.95
50-year component	1.046	0.0322	0.0297	-7.84
Total		0.310	0.285	**-8.16**

(1) The actual discharge equals the average of the discharge measurements, taken every 10 minutes until water surface elevation stabilised

Table H.28: Fractional change in discharge at the 20-year water level (stage 1.046 m)

Parameter	Theoretical	Physical	Fractional change in discharge (%)	Total fractional change in discharge (Compare to Table H.27) (%)
2-year control orifice				
C_d	0.61	0.6	1.67	-7.62
Δh (Eq. 6.1)	0.389	0.477	-9.29	
10-year control orifice				
C_d	0.61	0.664	-8.13	-8.13
50-year control weir				
C_d	1.84	1.913	-3.82	-8.26
Head (Eq. 6.1)	0.072	0.066	-4.44	

Table H.29: Percentage difference between theoretical and actual discharge at the 50-year water level (stage 1.197 m)

Individual component of multi-stage outlet designed to control specific RI storm	Stage (m)	Actual discharge of individual components, physical model(1) (m^3/s)	Theoretical discharge of individual component (m^3/s)	Percentage difference between theoretical and physical discharge (%)
2-year component	1.197	0.113	0.106	-6.07
10-year component	1.197	0.208	0.191	-7.95
50-year component	1.197	0.182	0.179	-2.04
Total		0.503	0.476	**-5.34**

(1) The actual discharge equals the average of the discharge measurements, taken every 10 minutes until water surface elevation stabilised

Table H.30: Fractional change in discharge at the 50-year water level (stage 1.197 m)

Parameter	Theoretical	Physical	Fractional change in discharge (%)	Total fractional change in discharge (Compare to Table H.29) (%)
2-year control orifice				
C_d	0.61	0.59	3.39	-5.81
Δh (Eq. 6.1)	0.407	0.499	-9.20	
10-year control orifice				
C_d	0.61	0.664	-8.13	-8.13
50-year control weir				
C_d	1.84	1.852	-0.65	-2.02
Head (Eq. 6.1)	0.217	0.219	-1.37	

The total percentage difference between the theoretical and physical discharge, as summarised in Table H.27 and Table H.29, deviated by a maximum of -0.74% from the total fractional change in discharge, as determined in Table H.28 and Table H.30 respectively. Thus, the deviations are an indication of the magnitude of the experimental error caused by averaging the electromagnetic flow meter reading when necessary.

H.4 Results of Model 5

The actual recorded outflow of Model 5 (C.9) was plot against the stage to determine if the outlet is discharging at a rate equal to the pre-development peak flow levels, or if the target was exceeded. Model 5 (C.9) was designed to control the 2-, 10-, 50-, and 100-year RI storm events for coastal regions receiving 1000 mm MAP. From Figure H.20 it is evident that Model 5 was ineffective in restricting the 2-, 5- and 10- year design storms to the pre-development peak flow levels, since the discharge control devices of Model 5 released these target discharges at stages lower than the estimated maximum stages for the 2-, 5- and 10-year design storms.

Figure H.20 indicates that the theoretical 100-year sized pipe (purple line) operated under outlet control at stage 1.26 m. Under outlet control conditions a higher head is produced by the 100-year pipe, therefore the differential head on the 2-year control orifice was reduced, which in return reduced the discharge capacity. Whereas the 100-year pipe of the physical model (blue) operated under inlet control condition, which resulted in a larger differential head and higher discharge rates.

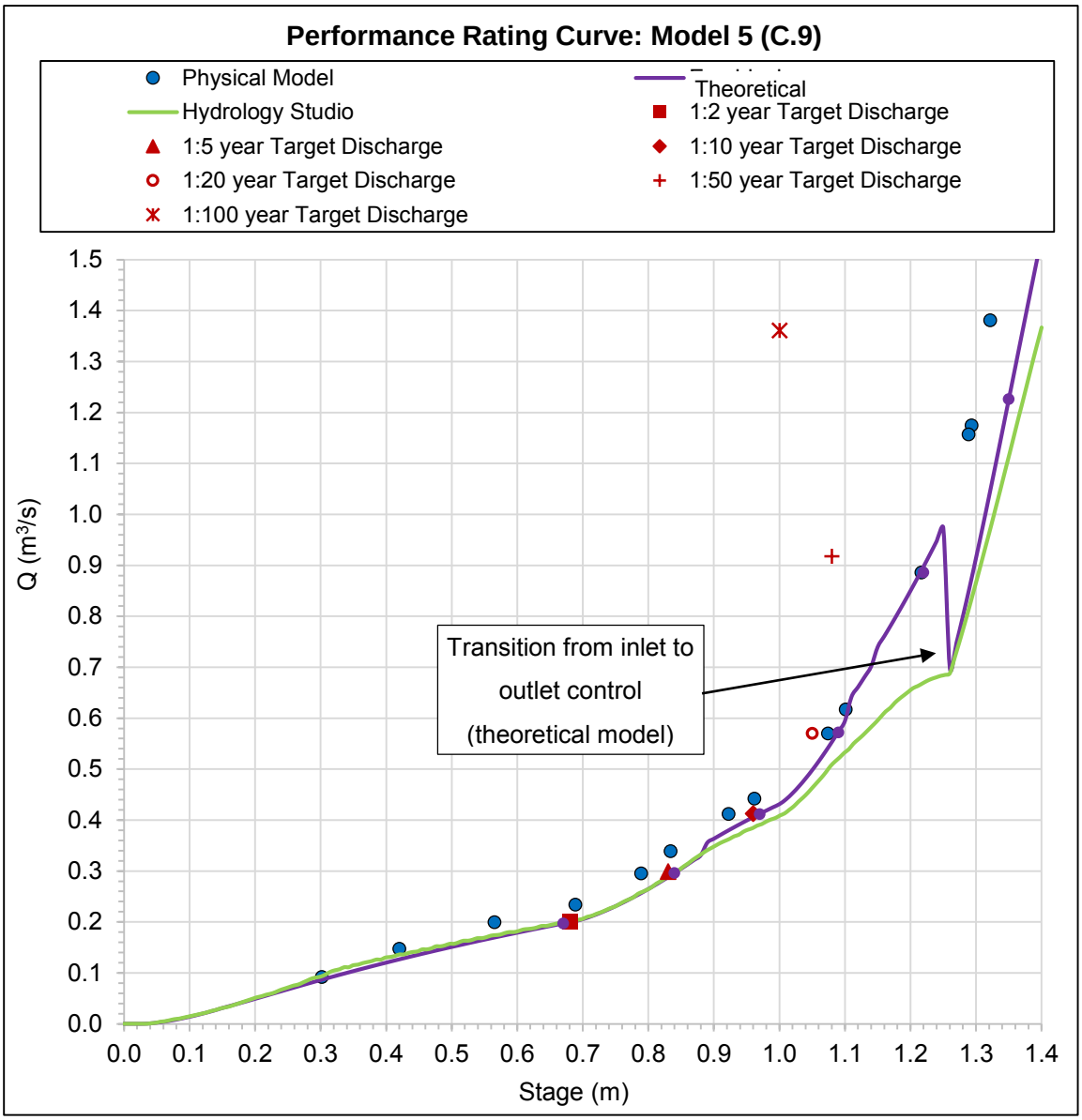

Figure H.20: Calculated and physically modelled stage-discharge relationship of Model 5 (prototype dimensions)

The results of Model 5 further indicated that the multi-stage outlet was effective in limiting the 20-, 50- and 100-year peak outflow, since the physically collected data lies on the right-hand side of the stage-target discharge curve, refer to Figure H.20. However, the model released the 20- and 50-year target flows at higher stages than the estimated maximum stages for the specific storm event. Therefore, the peak flow of the 20-,50- and 100-year design storms were reduced to the pre-development peak flow, however, more storage volume (higher maximum water surface elevation) were required than initially estimated. The latter is due to the approximation of the pre- and post-development hydrograph as a triangular shaped outflow hydrograph when estimating the storage volume, as mentioned in Section 4.2. The physically measured outflow is not triangular, but bell shaped. This approximation caused the maximum storage level to be underestimated; hence, the maximum head level was underestimated.

The stage presented in Table H.31 is the stabilised water surface elevation (prototype dimensions), relative to the base of the physical multi-stage outlet model, measured in the glass flume for a specific inflow. Table H.31 encapsulates the discharge released by the multi-stage outlet model in the hydraulic laboratory with the theoretical discharge at the corresponding stage tabulated in Table H.31.

Table H.31: Difference between theoretical discharge and physically measured discharge of Model 5

Recurrence interval (RI) (years)	Stage (m)	Actual discharge of physical model (1) (m^3/s)	Theoretical discharge (m^3/s)	Absolute difference (m^3/s)	Percentage difference (%)
2	0.566	0.199	0.170	-0.030	-14.91
5	0.789	0.295	0.257	-0.039	-13.16
10	0.923	0.413	0.380	-0.033	-8.00
20	1.074	0.571	0.542	-0.030	-5.23
50	1.217	0.884	0.889	0.005	0.60
100	1.322	1.383	1.045	-0.338	-24.43

(1) The actual discharge equals the average of the discharge measurements, taken every 10 minutes until water surface elevation stabilised

Table H.31 indicated that the hydraulic performance of the multi-stage outlet model deviated the most from the theoretical stage-discharge relationship at the 2- and 100-year water surface elevations. The 2-year storm control component had an ongoing effect on the amount released by the multi-stage outlet as the stage increased for the 5-, 10-, 20-, 50- and 100-year recurrence interval storms. The hydraulic performance of each component of the multi-stage outlet model is further elaborated in Section H.4.1 to Section H.4.3.

H.4.1 Discharge Component of Model 5 Controlling the 2-year Storm event

The fractional change in the discharge of the 2-year storm control orifice was determined to be -13.7%, as summarised in Table H.32. The discharge released by the 2-year sized component of the physical model also deviated from the theoretical discharge, since the discharge coefficient varied from 0.62 to 0.6, as the differential head increased. While the theoretical, spreadsheet-based model, assumed a constant discharge coefficient of 0.61. This is further elaborated in Section 7. From Figure H.21 it is clear that the standard orifice equation with a single-valued discharge coefficient does not fit the empirically derived data of the physical model.

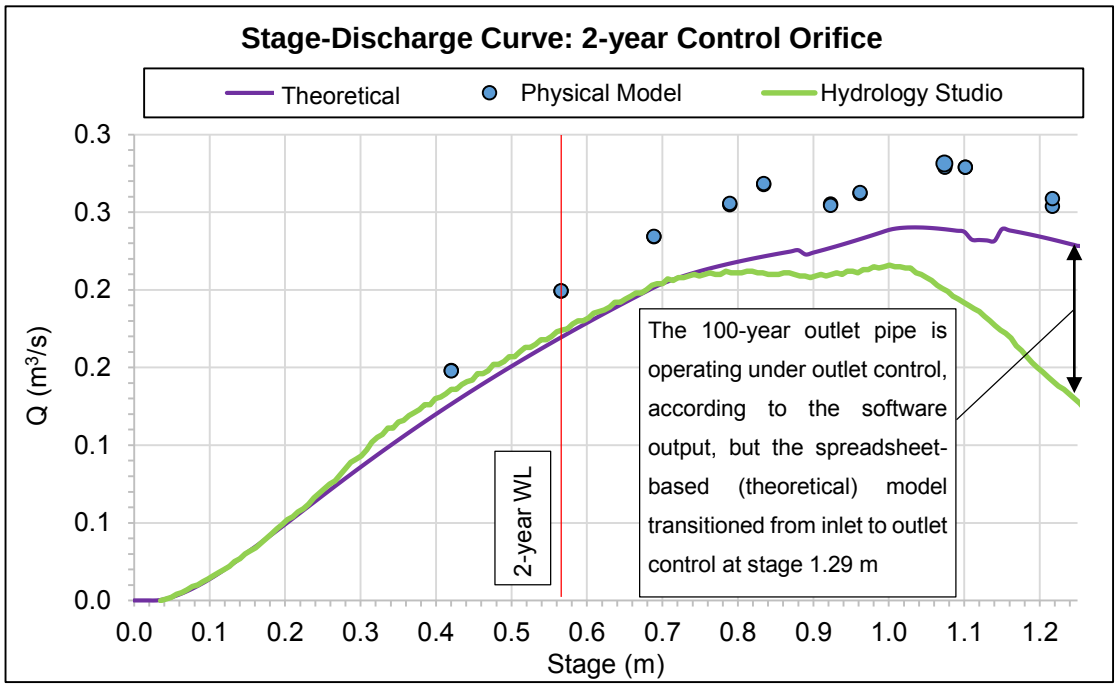

Figure H.21: Relationship between the discharge and stage for the two 2-year control component of Model 5

The mean of the discharge coefficients was determined to be 0.615 (refer to Table I.5 in Appendix I) and is the most probable equation coefficient based on 28 readings. Given in Table H.32, the theoretical discharge coefficient was -0.61% different from the empirical derived discharge coefficient at the 2-year water level, stage 0.566 m.

Table H.32: Fractional change in discharge at the 2-year water level (stage 0.566 m)

Parameter	2-year control orifice		Fractional change in discharge (%)	Total fractional change in discharge (%)	Percentage difference from Table H.31 (%)
	Theoretical	Physical			
C_d	0.61	0.61	-0.16	-13.86	**-14.91**
Differential head (Eq. 6.1)	0.216	0.297	-13.70		

H.4.2 Discharge Component of Model 5 Controlling the 10-year Storm Event

Model 5 was designed without an individual device to control the 5-year storm event. However, the 2-year storm control orifice and the two 10-year storm control orifices restricted the outflow, when operating under the 5-year maximum water surface elevation (see Figure H.22). The 10-year sized orifices of the multi-stage outlet model were partially submerged upstream at the 5-year maximum water surface elevation (0.789 m). Thus, the 10-year orifices functioned as weirs at stage 0.789 m, as illustrated by Figure H.22. After

stage 0.9 m, the 10-year storm control orifices were fully submerged upstream and discharge freely downstream. Just before stage 1.29 m, the 10-year storm control orifices operated under submerged conditions. The riser was filling up due to backwater head produced by the 100-year outlet pipe, which transitioned from inlet control to outlet control at stage 1.29 m.

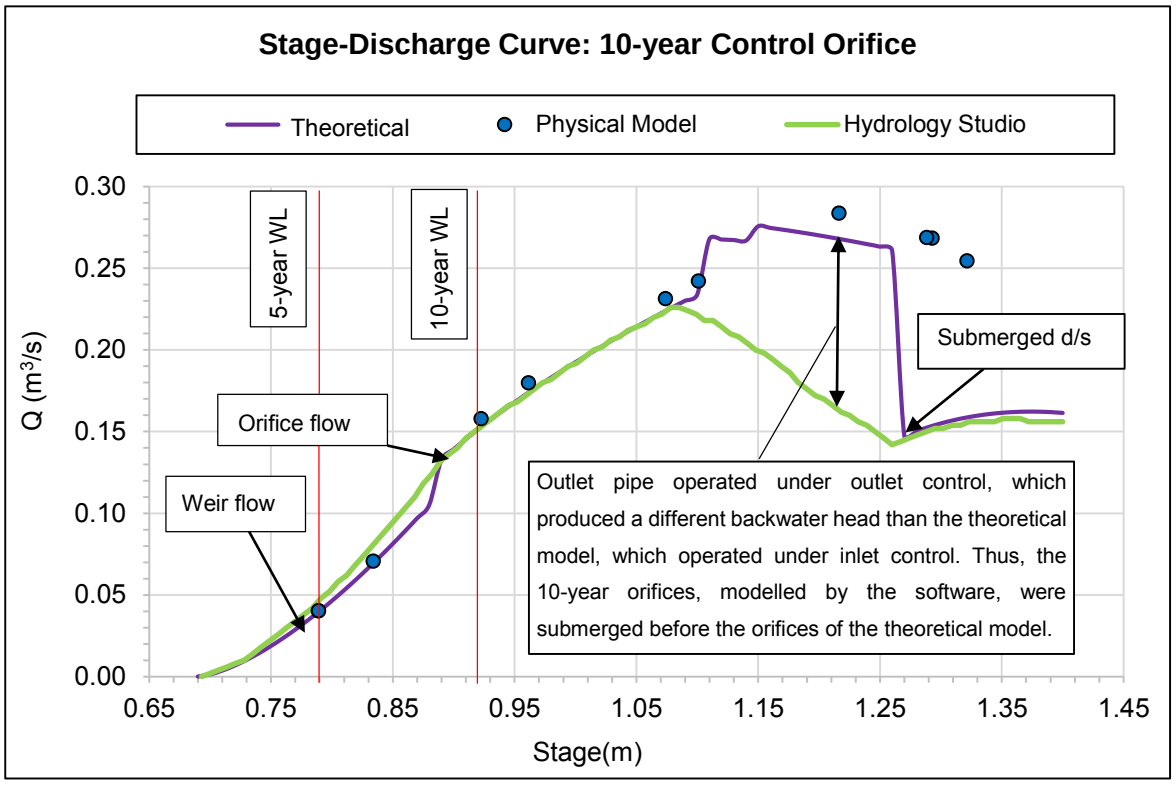

Figure H.22: Stage-discharge curve for the two 10-year control components of Model 5

The fractional change in discharge of the 2-year storm control orifice, due to the difference between the differential heads calculated and experimentally measured, caused a large (-12.70% and -11.34%) difference between the actual and calculated discharge at stage 0.789 m and 1.074 m respectively (see Tables H.34 and H.36). In addition, the mean value of the discharge coefficient of the modelled 10-year orifices was determined to be 0.377 for weir flow conditions and 0.631 for orifice flow conditions, which is both larger than the discharge coefficients used in the spreadsheet-based model, as summarised in Table H.34 and Table H.36.

Table H.33: Percentage difference between theoretical and actual discharge at stage the 5-year water level (0.789 m)

Individual component of multi-stage outlet designed to control specific RI storm	Stage (m)	Actual discharge of individual components, physical model (1) (m^3/s)	Theoretical discharge of individual component (m^3/s)	Percentage difference between theoretical and physical discharge (%)
2-year component	0.789	0.2550	0.2169	-14.95
10-year component	0.789	0.0403	0.0395	-1.87
Total		0.2953	0.2564	**-13.16**

(1) The actual discharge equals the average of the discharge measurements, taken every 10 minutes until water surface elevation stabilised

Table H.34: Fractional change in discharge at the 5-year water level (stage 0.789 m)

Parameter	Theoretical	Physical	Fractional change in discharge (%)	Total fractional change in discharge (Compare to Table H.33) (%)
2-year control orifice				
C_d	0.61	0.62	-1.61	-14.36
Δh (Eq. 6.1)	0.354	0.475	-12.70	
2x, 10-year control orifices				
C_d	0.37	0.377	-1.86	-1.86

Table H.35: Percentage difference between theoretical and physical measured discharge at 10-year water level (stage 0.923 m)

Individual component of multi-stage outlet designed to control specific RI storm (years)	Stage (m)	Actual discharge of individual components, physical model (1) (m^3/s)	Theoretical discharge of individual component (m^3/s)	Percentage difference (%)
2-year component	0.923	0.2548	0.2271	-10.89
10-year component	0.923	0.1580	0.1527	-3.34
Total		**0.413**	**0.380**	**-8.00**

(1) The actual discharge equals the average of the discharge measurements, taken every 10 minutes until water surface elevation stabilised

Table H.36: Fractional change in discharge at the 10-year water level (stage 0.923 m)

Parameter	Theoretical	Physical	Fractional change in discharge (%)	Total fractional change in discharge (Compare to Table H.35) (%)
2-year control orifice				
C_d	0.61	0.602	1.33	-10.02
Δh (Eq. 6.1)	0.387	0.501	-11.34	
Two,10-year control orifices				
C_d	0.61	0.631	-3.3	-3.33

H.4.3 Discharge Component of Model 5 Controlling the 50-year Storm Event

The multi-stage model was designed without an individual device to control the 20-year design storm. However, the low flow orifice and the two 10-year storm control orifices restricted the outflow when operating under the 20-year water surface elevation at stage 1.074 m. Figure H.23 indicates that at stage 1.074 m, the 10-year sized orifices were fully submerged upstream, discharged freely downstream. The nappe flow of the 50-year sized weir collided with the jet of the 10-year orifice at stage 1.074 m.

Figure H.23 indicates that the two 50-year storm control weirs also discharged at the 20-year maximum water surface elevation, but under a low head of 0.072 m. At stage 1.217 m (50-year water level), the 10-year sized orifices of the multi-stage model were partially submerged downstream, which resulted in a submergence ratio of 8.2%, see Figure H.24.

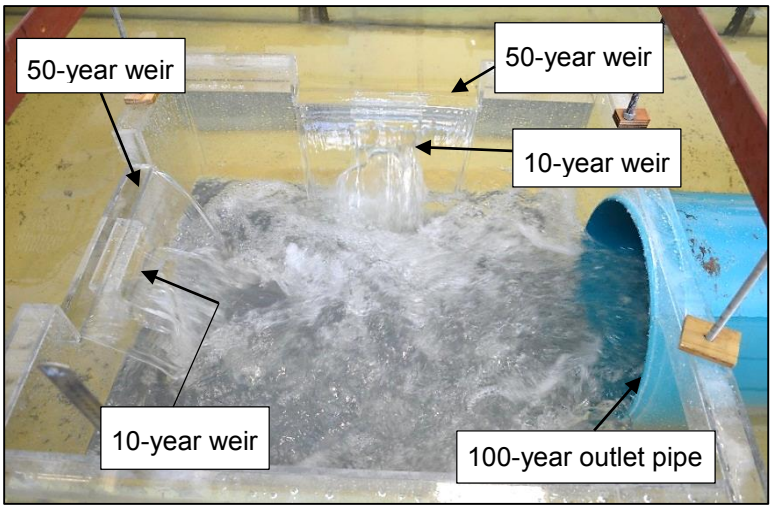

Figure H.23: Top view of Model 5 discharging at 20-year water level, stage 1.074m

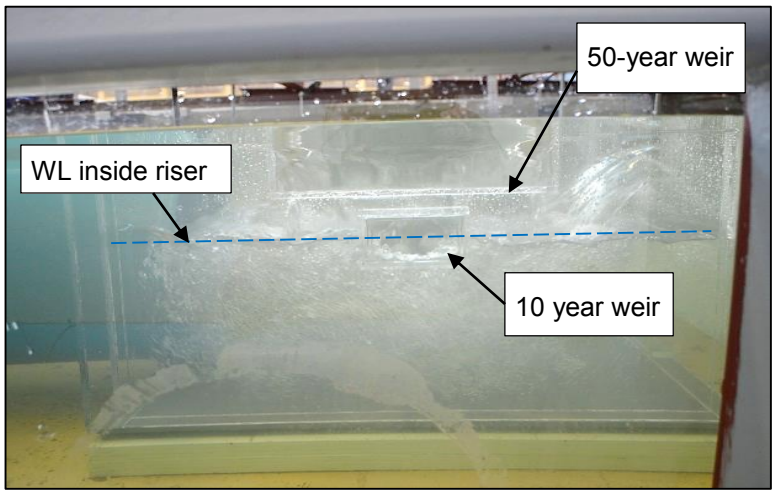

Figure H.24: Side view of Model 5 discharging at 50-year water level, stage 1.217m

The weir discharge coefficient for the 50-year storm control weirs was experimentally calibrated and ranged from 1.46 to 1.67, when modelled as broad-crested weirs (Equation 2.14). Whereas the spreadsheet used a constant weir coefficient of 1.84 for sharp-crested weirs (Equation 2.19). Figure H.25 indicates a good fit between the stage-discharge curve determined by means of Equation 2.14 and the discharge measured in the hydraulic laboratory at stage 1.074 m and 1.217 m.

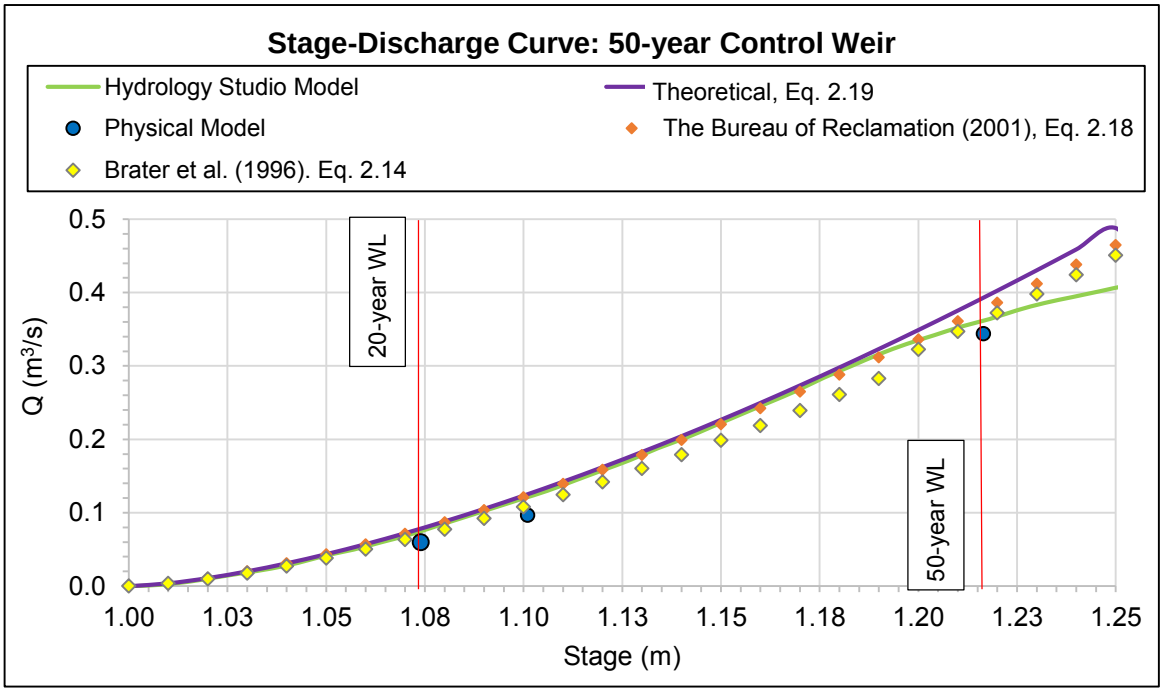

Figure H.25: Stage-discharge curve for the two 50-year control components of Model 5

The 20-year and 50-year outflow differed from the theoretical discharge due to the outflow released by the 2-year sized orifice, as indicated in Tables H.38 and H.39. Equation 2.19 overestimated the discharge of the 50-year control component of the multi-stage outlet, as indicated in Figure H.25.

Table H.37: Percentage difference between theoretical and actual discharge at the 20-year water level (stage 1.074 m)

Individual component of multi-stage outlet designed to control specific RI storm	Stage (m)	Actual discharge of individual component, physical model (1) (m^3/s)	Theoretical discharge of individual component (%)	Percentage difference (%)
2-year component	1.074	0.2801	0.239	-14.71
10-year component	1.074	0.2315	0.2240	-3.33
50-year component	1.074	0.060	0.079	31.83
Total		**0.571**	**0.542**	**-5.23**

(1) The actual discharge equals the average of the discharge measurements, taken every 10 minutes until water surface elevation stabilised

Table H.38: Fractional change in discharge at the 20-year water level (stage 1.074 m)

Parameter	Theoretical	Physical	Fractional change in discharge (%)	Total percentage change in discharge (Compare to Table H.37) (%)
C_d	0.61	0.624	-2.24	-14.13
Δh (Eq. 6.1)	0.429	0.563	-11.89	
Two, 10-year control orifice				
C_d	0.61	0.631	-3.33	-3.33
Two, 50-year control weir				
C_d	1.84	1.458	26.20	30.37
Head (Eq. 6.1)	0.072	0.0740	4.17	

Table H.39: Percentage difference between theoretical and actual discharge at the 50-year water level (stage 1.217 m)

Individual component of multi-stage outlet designed to control specific RI storm	Stage (m)	Actual discharge of individual components, physical model (1) (m^3/s)	Theoretical discharge of individual component (%)	Percentage difference between theoretical and physical discharge (%)
2-year component	1.217	0.256	0.229	-10.30
10-year component	1.217	0.284	0.266	-6.43
50-year component	1.217	0.344	0.393	14.31
Total		**0.884**	**0.889**	**0.6**

(1) The actual discharge equals the average of the discharge measurements, taken every 10 minutes until water surface elevation stabilised

Table H.40: Fractional change in discharge at the 50-year water level (stage 1.217 m)

Parameter	Theoretical	Physical	Fractional change in discharge (%)	Total fractional change in discharge (Compare to Table H.39) (%)
C_d	0.61	0.616	-0.97	-9.73
Δh (Eq. 6.1)	0.399	0.483	-8.76	
2x 10-year control orifice				
C_d	0.61	0.631	-3.33	-6.53
Δh (Eq. 6.1)	0.426	0.399	-3.2	
2x 50-year control weir				
C_d	1.84	1.673	9.98	11.38
Head (Eq. 6.1)	0.2165	0.2145	1.40	

The total percentage difference between the theoretical and physical discharge, as summarised in Tables H.37 and H.39, varied from the total fractional change in discharge, as summarised in Table H.38 and Table H.40 respectively. The maximum variance was 2.93 %, for the 50-year component of Model 5, and is an indication of the experimental error.

H.5 Results of Model 6

The physically recorded outflow of Model 6 (I.9) was plotted against the stage to determine if the outlet was discharging at a rate equal to the pre-development peak flow levels, or if the target was exceeded. Model 6 (I.9) was designed to control the 2-, 10-, 50-, and 100-year RI storm events for inland regions receiving 1000 mm MAP.

From Figure H.26 it is evident that Model 6 was ineffective in restricting the 2-year design storms to the pre-development peak flows since it released these target discharges at stages lower than the estimated maximum stage for the 2-year design storm. The 5- and 10-year discharge components of the multi-stage model released the restricted flow at a slightly lower stage than estimated during preliminary stage-storage calculations. Thus, the 2- and 10-year components did not attenuate the 5- and 10-year design storms effectively.

The performance curve of Model 6, shown in Figure H.26, further indicates that the multi-stage outlet was effective in limiting the 20-year peak outflow, despite the fact that the outlet was designed for the 10-year design storm and not the 20-year storm event. The model limited the 20-, 50- and 100-year design storms, but released the flow at higher stages than the estimated maximum stages for the specific storm event. The latter only indicates that the pond would require more storage volume than initially estimated.

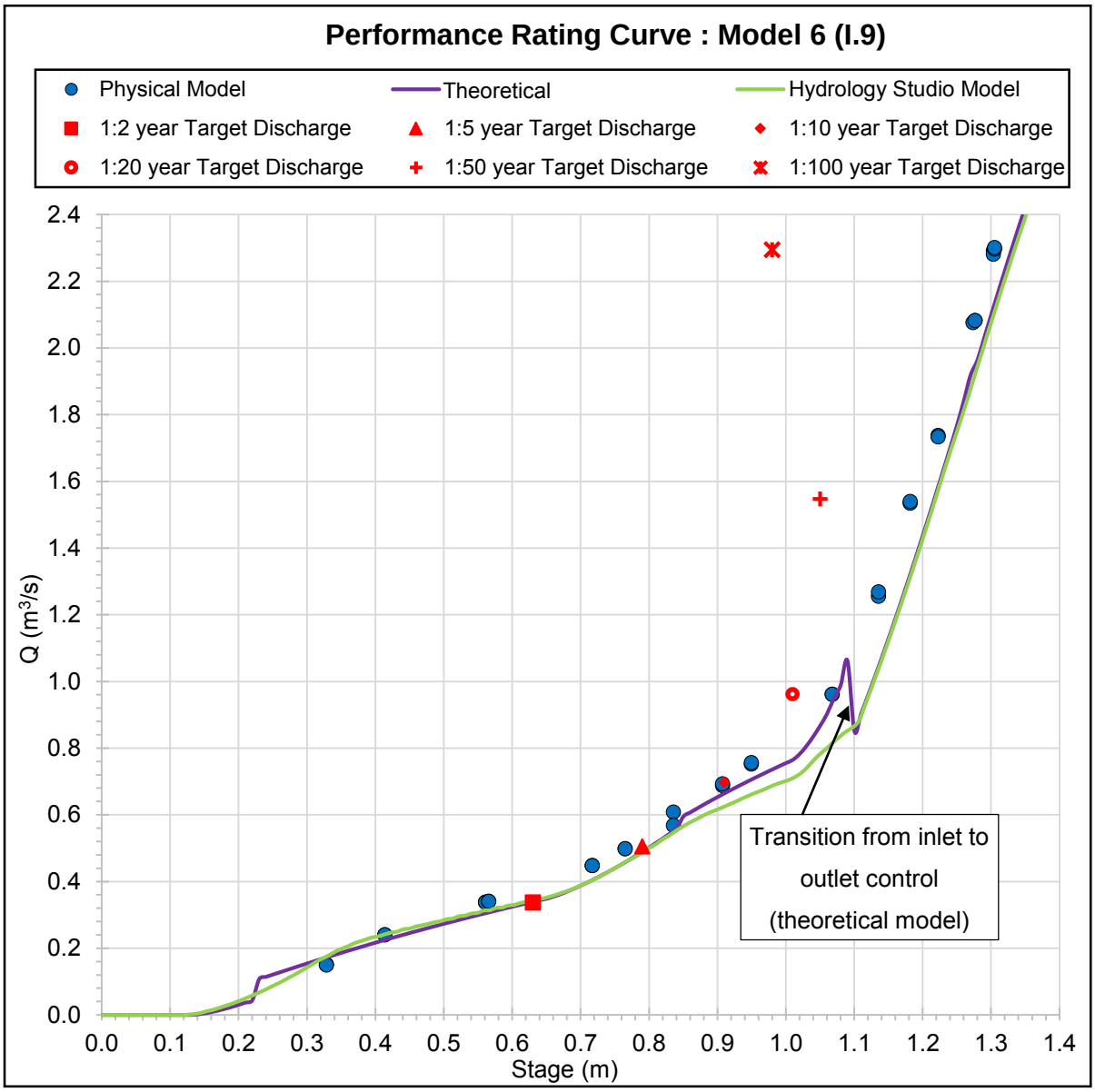

Figure H.26: Calculated and physically modelled stage-discharge relationship of Model 6 (prototype dimensions)

Figure H.26 also illustrates that the theoretical stage-discharge curve is in good agreement with the stage-discharge curve calculated with Hydrology Studio (software). The theoretical discharge starts to differ from the software output around stage 0.85 m, where after it converge again at stage 1.1 m. The reason being that the spreadsheet-based model applied outlet control only when the 100-year storm control pipe is full-flowing.

The downstream water depth at the outlet of the 100-year pipe was assumed equal to the inside diameter of the 100-year outlet pipe (0.894 m) for full flow conditions. Thus, outlet control was only applied and compared to inlet control conditions from stage 1.1 m for the theoretical determined multi-stage outlet. It is at stage 1.1 m, where it was determined, theoretically, that the water inside the riser submerged the entrance of the 100-year outlet pipe.

Hydrology Studio (2015) on the other hand, applied outlet control for full flow, partly full flow, as well as for free surface flow conditions. Free surface flow arises where neither the inlet nor the outlet end of the culvert is submerged and the pipe flows partly full over its entire length while the flow profile is subcritical. Thus, backwater calculations are required for the partly full flow conditions. For inlet control conditions, the software computed the discharge by means of Equation 2.1, whereas the spreadsheet determined the discharge for inlet control by means of Equations 2.9, 2.11 and 2.1, depending on the H_1/D condition.

The stage tabulated in Table H.41 is the stabilised water surface elevation relative to the base of the physical multi-stage outlet model, which corresponds to the measured inflow. Table H.41 encapsulates the discharge released by the multi-stage outlet model, as well as the theoretical discharge, at the corresponding stages. The percentage difference between the measured stage-discharge and the target stage-discharge curve is included in Appendix J.

Table H.41: Data comparison between theoretical and physical discharge for Model 6

Recurrence interval (RI) (years)	Stage (m)	Actual discharge of physical model (1) (m^3/s)	Theoretical discharge (m^3/s)	Absolute difference (m^3/s)	Percentage difference (%)
2	0.566	0.340	0.307	-0.032	-9.54
5	0.765	0.498	0.458	-0.040	-8.02
10	0.908	0.690	0.662	-0.028	-4.01
20	1.068	0.961	0.940	-0.021	-2.23
50	1.182	1.536	1.323	-0.214	-13.91
100	1.305	2.298	2.132	-0.166	-7.23

(1) The actual discharge equals the average of the discharge measurements, taken every 10 minutes until water surface elevation stabilised

H.5.1 Discharge Component of Model 6 Controlling the 2-year Storm Event

Figure H.27 indicates that the two rectangular orifices, sized to control the 2-year storm, discharged at a higher rate than determined theoretically. The -9.54% difference between the theoretical discharged and the measured discharge (see Table H.42) is attributed to the varying discharge coefficient and water elevation inside the riser, which the influence the differential head on the orifice.

The physical model study indicated that the discharge coefficient of the 2-year storm control orifice varied from 0.61 to 0.73 as the differential head varied at higher stages. The spreadsheet-based model assumed a constant discharge coefficient of 0.61 for a rectangular orifice. The mean of the discharge coefficients was determined to be 0.68 (refer to Table I.6 in Appendix I) and is the most probable equation coefficient based on 26 readings.

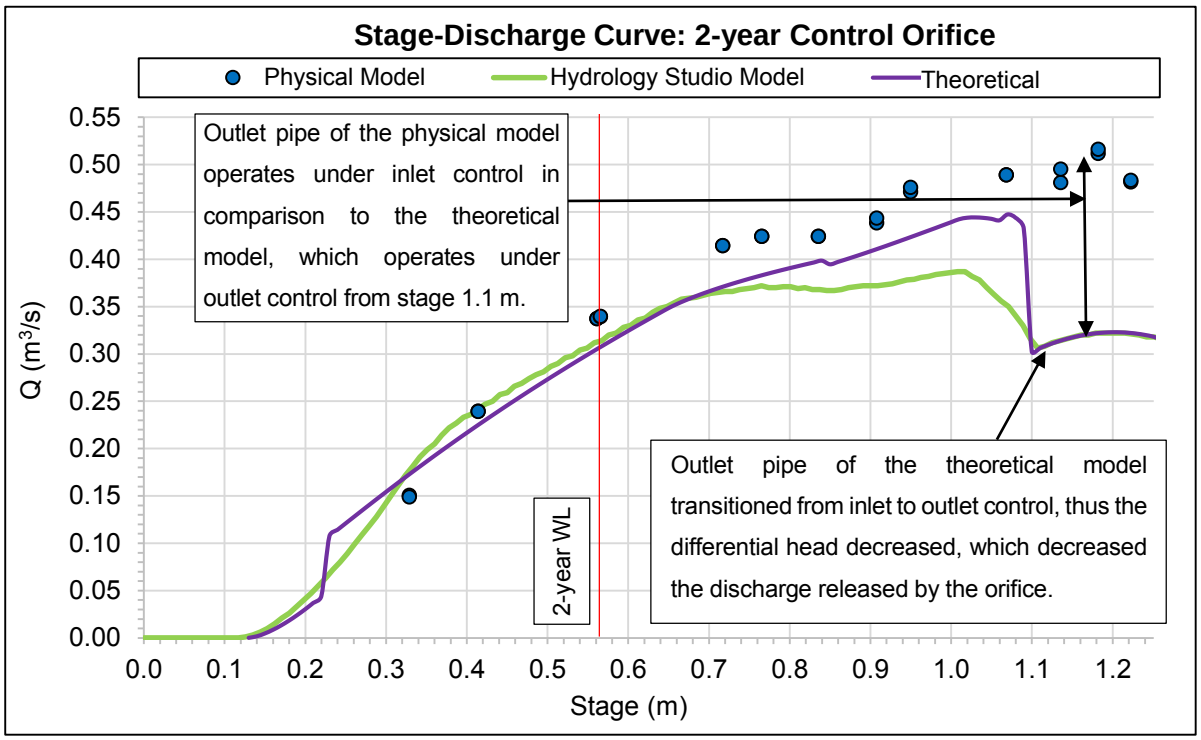

Figure H.27: Stage-discharge curve for the two, 2-year control components of the multi-stage outlet structure

From Stage 1.13 m, as indicated in Figure H.27, the modelled orifices discharge at higher rates than theoretically calculated. This is mainly due to the high water surface elevation in the riser at larger flows, causing the differential head to decrease, thus the discharge coefficient increased. The variation in the discharge coefficient is elaborated in Section 7.

The theoretical discharge coefficient was -6.15% different from the empirically derived discharge coefficient at the 2-year water level (stage 0.566 m). The 9.54% difference between the theoretical and measured discharge (see Table H.42), is a result of a fractional change of -6.15% in the discharge due to the discrepancy in discharge coefficients and a -3.33% fractional change in discharge due to the variation in differential heads. The remaining -0.05% is an indication of the experimental error. As mentioned, the experimental error (refer to Section 5.3.1) is also included in the C_d value of the 2-year orifice, since it was empirically derived from calibrated experimental data.

Table H.42: Percentage difference between theoretical and physical collected data at stage 0.566 m

Parameter	2x 2-year control orifice		Fractional change in discharge (%)	Total fractional change in discharge (%)	Percentage difference from Table H.41 (%)	Error (%)
	Theoretical	Physical				
C_d	0.61	0.65	-6.15	-9.48	**-9.54**	-0.05
Differential head (Eq. 6.1)	0.210	0.225	-3.33			

H.5.2 Discharge Component of Model 6 Controlling the 10-year Storm Event

Model 6 was designed without an individual device to control the 5-year storm event. However, the two low flow orifices (sized to control the 2-year storm event) and the three, 10-year sized orifices, restricted the outflow when operating under the 5-year water surface elevation. The 10-year sized orifices were partially submerged upstream and operated as weirs during the 5-year design flow, as illustrated Figure H.28.

The mean value of the discharge coefficient of the modelled 10-year orifices was determined to be 0.37 for weir flow conditions and 0.605 for orifice flow conditions. The empirically derived discharge coefficient correlates to the theoretical equation discharge coefficients, where C_d= 0.37 is recommended for weir flow conditions (Equation 2.13) and C_d=0.61 is used for the standard orifice equation (Equation 2.1). The 10-year orifices were fully submerged upstream at the 10-year water level, as shown in Figure H.29.

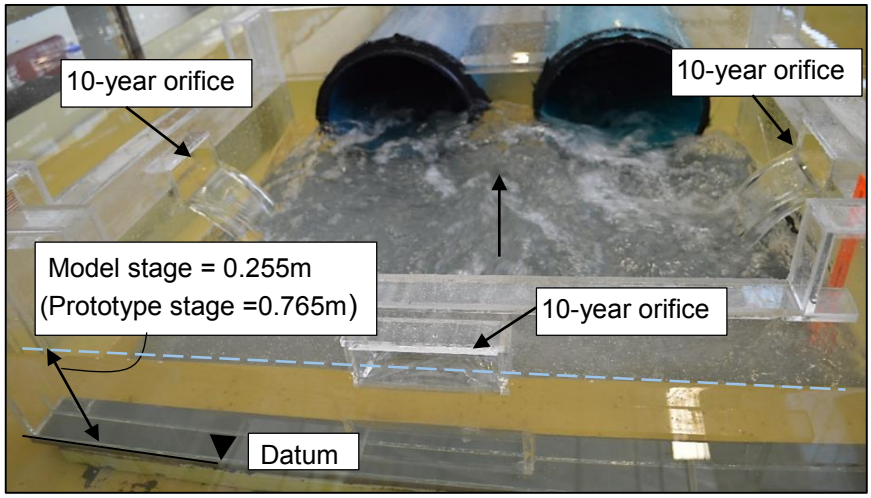

Figure H.28: 10-year control orifices, partially submerged upstream, $Q_{p\ Total}$=0.498 m^3/s

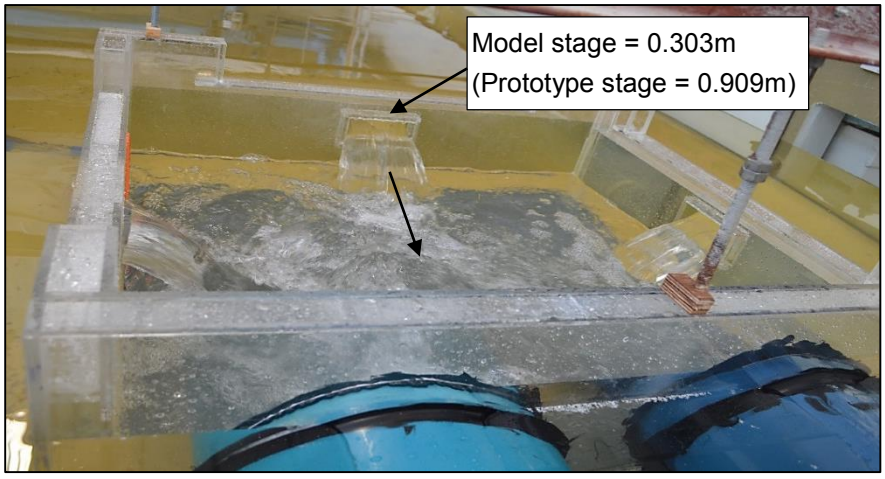

Figure H.29: Three 10- year control orifices fully submerged upstream, $Q_{p\ Total}$=0.69 m^3/s

The 10-year storm control orifices of the multi-stage outlet model deviated from the theoretical model once the orifices were submerged downstream. Since the modelled 100-year pipe operated at a lower head than determined theoretically. Therefore, the differential head on the modelled 10-year orifices is larger than calculated, which increased the capacity of the physically tested orifices. Figure H.30 illustrates the theoretical submergence of the orifices clearly at stage 1.1 m, where the stage-discharge relationship decreased, since the theoretical differential head on the orifices decreased.

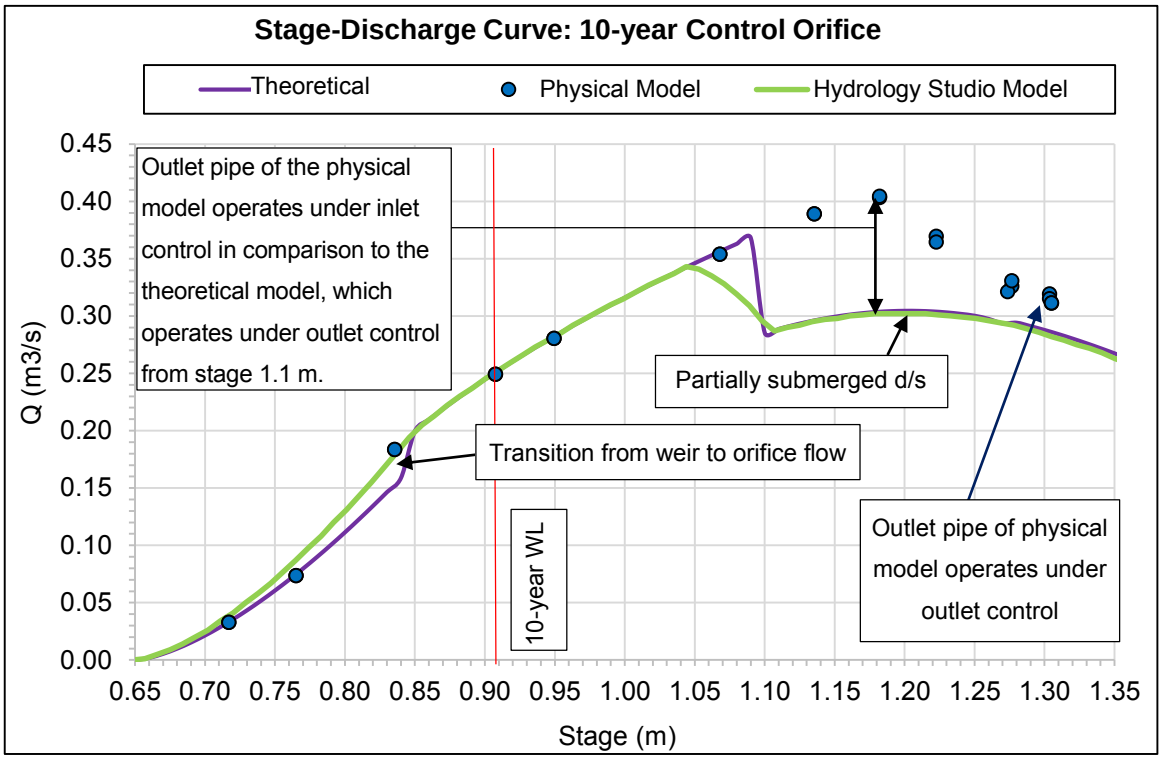

Figure H.30: Stage-discharge curve for the three 10-year control components of Model

Figure H.30 indicates that there was a good fit between the theoretical and physical model discharge at stages 0.765 m and 0.908 m, which is the respective stages where the water surface stabilised for the 5- and 10-year design flows. The discharge calculated for the 10-year orifices at stage 0.908 m (10-year water level) was only 0.8% more than the measured discharge of the modelled 10-year orifices. Table H.43 summarises the differences between the theoretical and actual discharge measured experimentally, whereas Table H.44 indicates the differences between the theoretical parameters and experimentally recorded parameters (C_d and Δh**)** that caused the difference between the theoretical and experimentally measured discharge.

Table 43: Percentage difference between theoretical and physical measured discharge at the 10-year water level (stage 0.908 m)

Individual component of multi-stage outlet designed to control specific RI storm	Stage (m)	Actual discharge of individual components, physical model(1) (m^3/s)	Theoretical discharge of individual component (m^3/s)	Percentage difference (%)
2-year component	0.908	0.441	0.411	-6.92
10-year component	0.908	0.249	0.251	0.80
Total		0.690	0.662	-4.01

(1) The actual discharge equals the average of the discharge measurements, taken every 10 minutes until water surface elevation stabilised

Table H.44: Fractional change in discharge at the 10-year water level (stage 0.908 m)

Parameter	Theoretical	Physical	Fractional change in discharge (%)	Total fractional change in discharge (Compare to Table 6.43) (%)
2x 2-year Control Orifices				
C_d	0.61	0.623	-2.09	-6.80
Δh (Eq. 6.1)	0.415	0.376	-4.71	
3x 10-year Control Orifices				
C_d	0.61	0.605	0.83	0.83

The total fractional change in discharge, as determined in Table H.44 for the 2- and 10-year storm control orifices, varied with -0.12% and 0.03% respectively, from the percentage difference, as determined in Table H.43. The variation is an indication of the experimental error that occurred during the physical model tests. The theoretical approach velocity of the 100-year storm control pipe was assumed negligible, which also had a minor influence on the differential head.

H.5.3 Discharge Component of Model 6 Controlling the 50-year Storm Event

Model 6 was designed without an individual device to control the 20-year design storm. However, the two low flow orifices and the three 10-year storm control orifices restricted the outflow when operating under the 20-year maximum water surface elevation (stage 1.068 m). The 10-year sized orifices of the multi-stage outlet model were fully submerged upstream, discharged freely downstream, and operated as discussed in Section H.5.2. The 50-year storm control weirs also discharged at the 20-year maximum water surface elevation, as illustrated by Figure H.31.

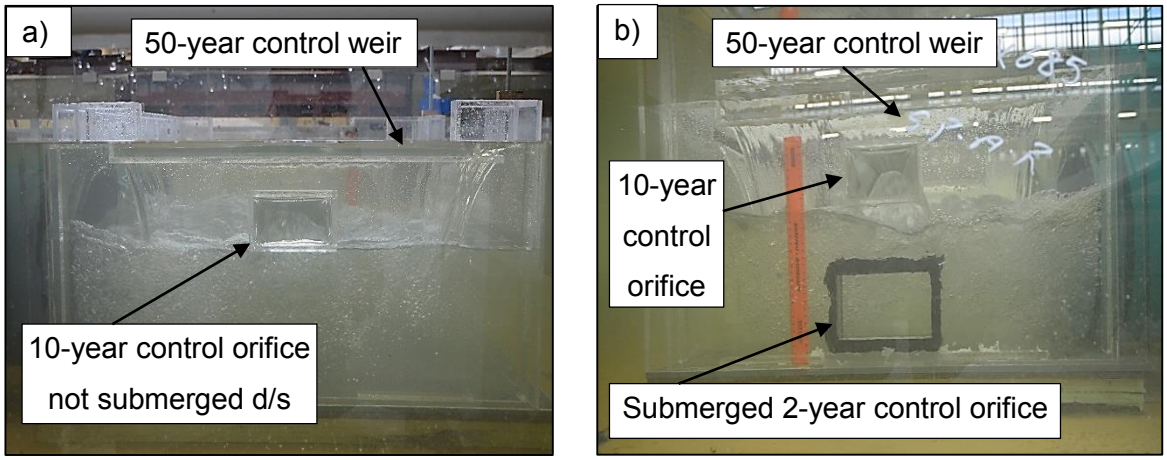

Figure H.31: a) Left side view of 10-year control orifice and 50-year weir at stage 1.068 m b) Right side view of 2-, 10- and 50-year control weir at the 20-year water level (stage 1.068 m)

The 50-year storm control weirs had weir coefficients that ranged from 1.64 to 1.71 when modelled as broad-crested weirs (Equation 2.14). Varying weir discharge coefficients, for different head levels, have been experimentally derived in previous experimental studies, as discussed in Section 2.3.2.4, after Brater *et al*. (1996:5.25). Whereas the spreadsheet used a constant weir coefficient of 1.84 for sharp-crested weirs (Equation 2.19). The stage-discharge curve determined by means of broad-crested weir equation (Equation 2.14) best fit the stage-discharge curve of the modelled 50-year storm control weir when the weir discharged under low heads, as illustrated by Figure H.32.

Furthermore, the experimentally determined discharge coefficients of the 2-year storm control orifices were 0.65 at the 20-year water level (stage 1.068 m). Thus, the three weirs restricted the flow more than theoretically calculated, but then again, the 2-year storm control orifices released more water than theoretically calculated, due to the larger discharge coefficient and differential head. Therefore, due to the 50-year weirs, Model 6 exceeded the 20-year target discharge with only 2.23%, which is less than the 4.01% exceedance of the 10-year target discharge.

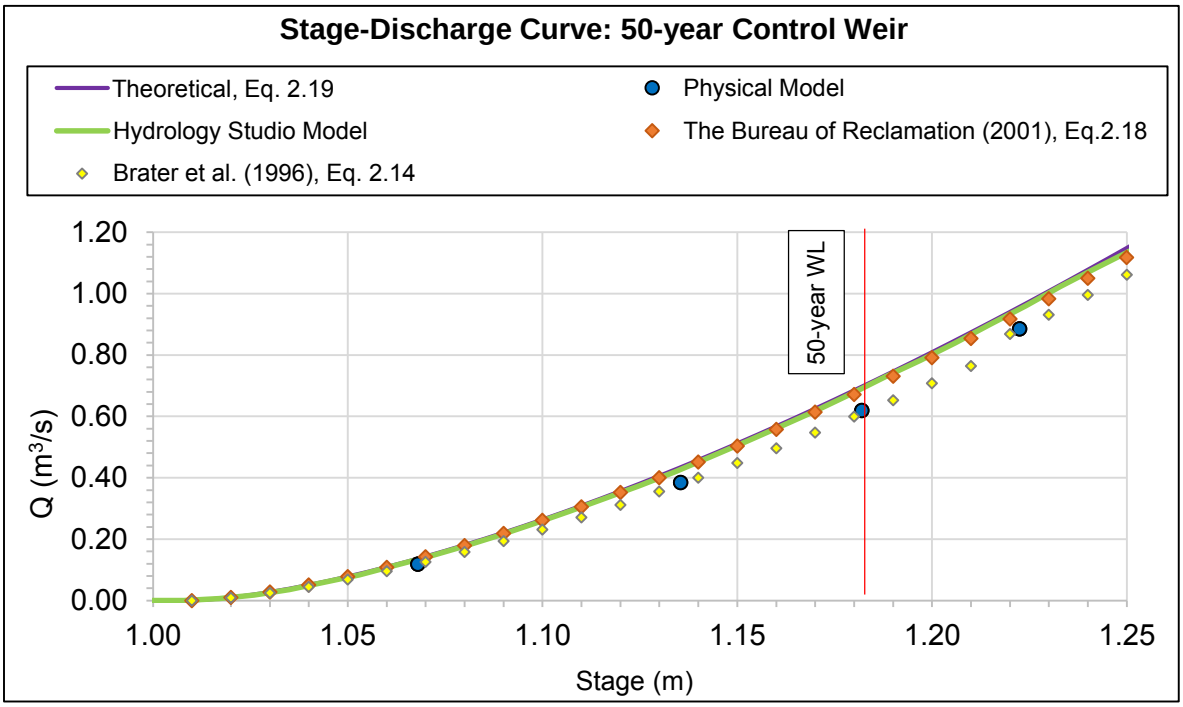

Figure H.32: Stage-discharge curve for the three 50-year control components of Model 6

The three 10-year storm control orifices were partially submerged (22%) downstream at stage 1.182 m, as illustrated in Figure H.33. The 2-year storm control orifices had a submergence ratio of 61% at stage 1.182 m. The 50-year weir operated under 0.17 m of head at stage 1.182 m and had a weir discharge coefficient of 1.65.

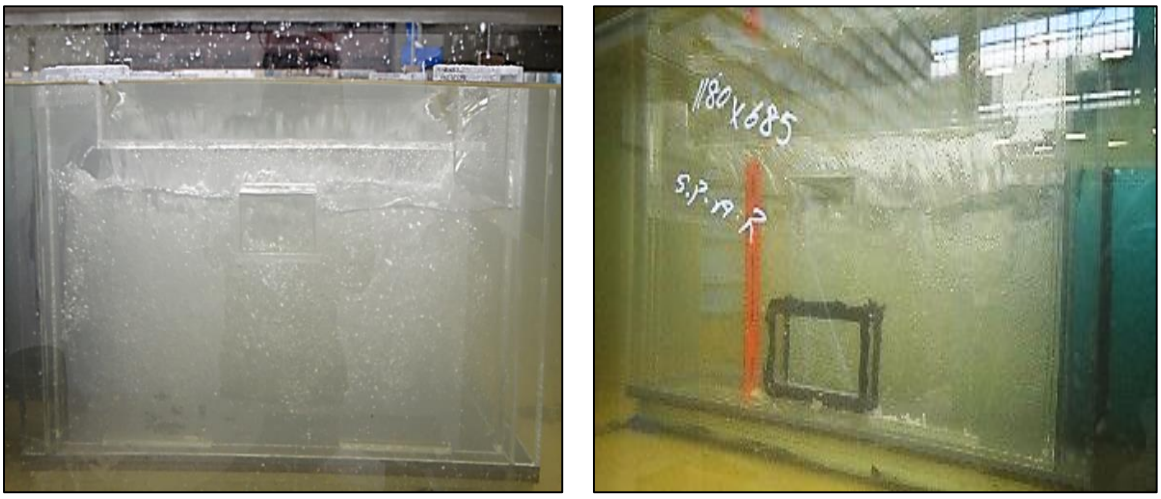

Figure H.33: 10-year control orifices, partially submerged d/s

Table H.45 summarises the differences between the theoretical and physical measured discharge of each individual control component of the multi-stage outlet, whereas Table H.46 indicates the differences between the theoretical and physical discharge coefficient, and differential head of each component, which caused the differences between the theoretical calculated and physically measured discharge.

Table H.45: Percentage difference between theoretical and physical measured discharge at the 50-year water level (stage 1.182 m)

Individual component of multi-stage outlet designed to control specific RI storm	Stage (m)	Actual discharge of individual component, physical model (1) (m^3/s)	Theoretical discharge of individual component (m^3/s)	Percentage difference between theoretical and physical discharge (%)
2-year component	1.182	0.514	0.322	-37.35
10-year component	1.182	0.403	0.304	-24.57
50-year component	1.182	0.619	0.697	12.60
Total		**1.536**	**1.323**	**-13.91**

(1) The actual discharge equals the average of the discharge measurements, taken every 10 minutes until water surface elevation stabilised

Table H.46: Fractional change in discharge at the 50-year water level (stage 1.182 m)

Parameter	Theoretical	Physical	Fractional change in discharge (%)	Total fractional change in discharge (Compare to Table H.45) (%)
Two 2-year Control Orifice				
C_d	0.61	0.727	-16.09	-38.17
Δh (Eq. 6.1)	0.231	0.414	-22.08	
Three 10-year Control Orifice				
C_d	0.61	0.605	0.83	-21.25
Δh (Eq. 6.1)	0.231	0.414	-22.08	
Three 50-year Control weirs				
C_d	1.84	1.648	11.65	13.27
Head (Eq. 6.1)	0.172	0.171	0.88	

The total percentage difference between the theoretical and physical discharge determined in Table H.45, for the 2- and 50-year storm control weirs, varied with 0.84% and -0.67%, respectively, from the total fractional change, as determined in Table H.46. The variation is an indication of the magnitude of the experimental error caused by averaging the electromagnetic flow meter reading.

The total percentage difference between the theoretical and physical discharge, determined in Tables H.45 and H.46, for the 10-year orifice, varied with -3.41%, which is larger than the above-mentioned differences for the 2- and 50-year components. The variation of -3.41% is due to the backwater head produced by the 100-year modelled pipe, at stage 1.182 m, which is lower than theoretically calculated.

The backwater head resulted in a water surface elevation inside the riser of 0.768 m above the base of the multi-stage model, which is just above the centre of the modelled 10-year orifices (0.75 m above the base of the multi-stage model). Thus, the 10-year modelled orifices had a submergence ratio of 22%. The 22% submergence ratio indicates that the modelled orifices could have been transitioning between submerged orifice flow conditions and free outfall flow conditions. Since Equation 2.1 use an average head approximation when an orifice discharge as a free outfall. The average head approximation means that the head is taken as the difference between the upstream water surface elevation and the centre of the orifice. Whereas the theoretical calculated, 10-year orifices, were fully submerged downstream to an elevation of 0.951 m, which resulted in a submergence ratio of 56.6%.

APPENDIX I: Experimental Test Data

Table I.1: Collected experimental data of Model 1

Increment	Q: flow meter (l/s)	Q: V-notch (l/s)	Reading of water level (mm)	Water level w.r.t base of model (mm)	t (min)	Δt (min)	ΔQ (l/s)	Q : outflow (l/s)	H_2 (mm)	Y_2 (mm)	Multi-stage outlet model								
											Q: 50-year V-notch (l/s)	C_d	Q: 50-year V-notch submerged (l/s)	Q: 10-year Rectangular orifice (l/s)	C_d	Q: 10-year rectangular orifice submerged (l/s)	Q: 2-year circular orifice submerged (l/s)	C_d	Q: Riser (l/s)
1	3.21	3.11	876.0	223.0	0	10	-0.02	3.23	108	69							3.21	0.68	
2	3.20	3.11	876.5	223.5	10	10	-0.02	3.22	108	69							3.20	0.67	
3	3.20	3.16	877.0	224.0	20	10	-0.02	3.22	108	70							3.20	0.67	
4	3.21	3.16	877.5	224.5	30	10	-0.02	3.23	110	71							3.21	0.68	
5	3.21	3.16	878.0	225.0	40	10	0.00	3.21	108	70							3.21	0.67	
6	3.20	3.16	878.0	225.0	50	10	0.00	3.20	108	70							3.20	0.67	
1	4.54	4.41	915.0	262.0	0	10	-0.09	4.64	124	85				1.12	0.38		3.42	0.67	
2	4.55	4.52	917.0	264.0	10	10	-0.05	4.59	123	84				1.09	0.34		3.46	0.67	
3	4.55	4.46	918.0	265.0	20	10	0.05	4.50	123	84				1.09	0.33		3.46	0.67	
4	4.55	4.46	917.0	264.0	30	10	0.00	4.55	120	81				1.06	0.33		3.49	0.67	
5	4.55	4.52	917.0	264.0	40	10	0.00	4.55	128	89				1.15	0.36		3.40	0.67	
1	6.36	6.25	960.0	307.0	0	10	-0.02	6.39	167	128				2.42	0.52		3.94	0.77	
2	6.36	6.25	960.5	307.5	10	10	0.00	6.36	168	129				2.43	0.52		3.93	0.77	
3	6.35	6.32	960.5	307.5	20	10	0.00	6.35	168	129				2.43	0.52		3.92	0.77	
4	6.34	6.32	960.5	307.5	30	10	0.00	6.34	165	126				2.43	0.52		3.92	0.76	
1	13.12	13.18	1066.0	413.0	0	10	-0.02	13.14	233	193	3.33	0.39		4.05	0.52		5.73	1.01	
2	13.05	13.18	1066.5	413.5	10	10	0.00	13.05	233	194	3.37	0.39		4.06	0.52		5.61	0.99	
3	13.08	13.18	1066.5	413.5	20	10	0.00	13.08	233	194	3.37	0.39		4.06	0.52		5.64	0.99	
1	14.78	14.84	1074.0	421.0	10	10	0.00	14.78	250	211	4.00	0.39		4.15	0.52		4.26	0.77	2.37
2	14.79	14.84	1074.0	421.0	20	10	0.00	14.79	248	209	4.00	0.39		4.15	0.52		4.27	0.77	2.37
3	14.79	14.84	1074.0	421.0	30	10	0.00	14.79	249	211	4.00	0.39		4.15	0.52		4.27	0.77	2.37
1	21.82	21.64	1088.0	435.0	0	10	0.00	21.82	299	260	5.34	0.39		4.31	0.52	4.23	3.93	0.78	8.31
2	21.79	21.64	1088.0	435.0	10	10	0.00	21.79	298	260	5.34	0.39		4.31	0.52	4.24	3.90	0.77	8.31
3	21.71	21.64	1088.0	435.0	20	10	0.00	21.71	308	269	5.34	0.39		4.31	0.52	4.12	3.93	0.80	8.31
1	26.51	26.20	1099.0	446.0	0	10	3.91	22.60	399	361	6.57	0.39	6.50	4.44	0.52	2.95	2.62	0.74	14.44
1	9.08	-	568.0	363.0	0	10	-0.24	9.08	183	148	0.68	0.39		3.38	0.52		5.09	0.91	
2	9.07	-	573	368	10	10	-0.09	9.07	190	155	0.84	0.39		3.45	0.52		4.86	0.87	
3	9.06	-	575	370	20	10	-0.05	9.06	191	156	0.91	0.39		3.48	0.52		4.76	0.85	
4	9.06	-	576	371	30	10	0.00	9.06	192	157	0.94	0.39		3.50	0.52		4.71	0.84	
5	9.06	-	576	371	40	10	0.00	9.06	191	156	0.94	0.39		3.50	0.52		4.71	0.84	
6	9.05	-	576	371	50	10	0.00	9.05	192	157	0.94	0.39		3.50	0.52		4.71	0.84	
7	9.06	-	576	371	60	10	0.00	9.06	192	157	0.94	0.39		3.50	0.52		4.71	0.84	

2-year control orifice	
C_d average	0.79
C_d at 2-year WL	0.67
C_d at 5-year WL	0.67
C_d at 10-year WL	0.76
C_d at 20-year WL	0.84
C_d at 50-year WL	0.98

Where:

H_2 = Energy head inside riser box

Y_2 = Water level inside riser box.

Table Ii.2: Collected experimental data of Model 2 (model dimensions)

Increment	Q: flow meter (l/s)	Q: V-notch (l/s)	Reading of water level (mm)	Water level w.r.t base of model (mm)	t (min)	Δt (min)	ΔQ (l/s)	Q : outflow (l/s)	H_2 (mm)	Y_2 (mm)	Multi-stage outlet model							
											Q: 50-year V-notch (l/s)	C_d	Q: 10-year Rectangular orifice (l/s)	C_d	Q: 10-year rectangular orifice submerged (l/s)	Q: 2-year circular orifice submerged (l/s)	C_d	Q: Riser (l/s)
1	3.46	3.78	789.00	122.00	0	10	0.35	3.11	126.88	79.38						3.11	0.53	
2	3.33	3.68	781.50	114.50	10	10	0.31	3.03	125.40	77.91						3.03	0.56	
3	3.21	3.39	775.00	108.00	20	10	0.19	3.02	124.94	77.45						3.02	0.61	
4	3.21	3.29	771.00	104.00	30	10	0.00	3.21	122.00	74.40						3.21	0.66	
1	5.29	5.85	854.00	187.00	0	10	0.57	4.73	133.75	85.77						4.73	0.53	
2	5.28	5.53	842.00	175.00	10	10	0.19	5.09	133.91	85.77						5.09	0.60	
3	5.29	5.47	838.00	171.00	20	10	0.14	5.15	134.44	86.28						5.15	0.63	
4	5.28	5.34	835.00	168.00	30	10	0.09	5.19	133.96	85.77						5.19	0.64	
5	5.29	5.28	833.00	166.00	40	10	0.05	5.24	134.48	86.28						5.24	0.66	
6	5.29	5.28	832.00	165.00	50	10	0.00	5.29	135.00	86.80						5.29	0.67	
7	5.29	0.92	832.00	165.00	60	10	0.00	5.29	134.00	85.77						5.29	0.67	
1	6.30	6.39	871.00	204.00	0	10	0.14	6.16	132.42	83.66						6.16	0.63	
2	6.24	6.39	868.00	201.00	10	10	0.12	6.13	134.44	85.78						6.13	0.64	
3	6.25	6.32	865.50	198.50	20	10	0.07	6.18	133.46	84.74						6.18	0.65	
4	6.25	6.25	864.00	197.00	30	10	0.02	6.22	132.49	83.70						6.22	0.65	
5	6.24	6.25	863.50	196.50	40	10	0.02	6.21	132.99	84.22						6.21	0.66	
6	6.24	6.25	863.00	196.00	50	10	0.02	6.22	132.99	84.22						6.22	0.66	
7	6.23	6.18	862.50	195.50	60	10	0.00	6.23	134.00	85.27						6.23	0.66	
8	6.23	6.18	862.50	195.50	70	10	0.00	6.23	133.50	84.75						6.23	0.66	
1	8.06	8.17	910.00	243.00	0	10	0.05	8.01	138.97	89.37			0.82	0.38		7.19	0.65	
2	8.06	8.03	909.00	242.00	10	10	0.00	8.06	139.50	89.89			0.78	0.38		7.28	0.66	
3	8.06	8.03	909.00	242.00	20	10	0.00	8.06	138.47	88.80			0.78	0.38		7.28	0.66	
1	9.64	9.77	943.00	276.00	0	10	0.09	9.55	169.96	120.94			2.44	0.38		7.11	0.64	
2	9.64	9.68	941.00	274.00	10	10	0.14	9.50	170.94	121.98			2.33	0.38		7.17	0.65	
3	9.64	9.68	938.00	271.00	20	10	0.07	9.57	151.96	102.12			2.16	0.38		7.40	0.64	
4	9.64	9.68	936.50	269.50	30	10	0.05	9.59	150.47	100.52			2.08	0.38		7.51	0.65	
5	9.64	9.59	935.50	268.50	40	10	0.00	9.64	150.50	100.52			2.03	0.38		7.61	0.66	
6	9.63	9.59	935.50	268.50	50	10	0.00	9.63	151.00	101.06			2.03	0.38		7.61	0.66	
1	11.04	11.16	960.00	293.00	0	10	-0.05	11.08	182.52	133.28			3.87	0.61		7.21	0.64	
2	11.02	11.06	961.00	294.00	10	10	0.00	11.02	187.50	138.45			3.92	0.61		7.10	0.64	
3	11.02	11.06	961.00	294.00	20	10	0.00	11.02	184.00	134.84			3.92	0.61		7.09	0.63	
1	14.37	14.27	1003.00	336.00	0	10	0.00	14.37	207.50	157.82	0.84	1.75	5.55	0.61		7.98	0.67	
2	14.32	14.38	1003.00	336.00	10	10	0.00	14.32	208.50	158.87	0.84	1.75	5.55	0.61		7.93	0.67	
1	15.39	15.18	1010.00	343.00	0	10	-0.09	15.48	211.54	161.56	1.35	1.75	5.77	0.61		8.36	0.69	
2	15.37	15.41	1012.00	345.00	10	10	0.00	15.37	213.00	163.12	1.50	1.75	5.84	0.61		8.03	0.67	
3	15.38	15.41	1012.00	345.00	20	10	-0.66	16.04	214.75	164.67	1.50	1.75	5.84	0.61		8.70	0.67	
1	17.00	16.85	1026.00	359.00	0	10	0.02	16.97	222.49	172.35	2.76	1.75	6.26	0.61		7.95	0.65	
2	16.98	16.90	1025.50	358.50	10	10	0.00	16.98	223.50	173.39	2.71	1.75	6.25	0.61		8.02	0.66	
3	16.97	16.90	1025.50	358.50	20	10	0.00	16.97	224.00	173.92	2.71	1.75	6.25	0.61		8.01	0.66	
1	18.05	17.98	1033.50	366.50	0	10	0.00	18.05	229.50	179.22	3.53	1.75	6.48	0.61		8.03	0.66	
2	18.06	17.98	1033.50	366.50	10	10	0.00	18.06	228.50	178.17	3.53	1.75	6.48	0.61		8.05	0.66	
1	19.96	19.83	1046.50	379.50	0	10	0.00	19.96	237.00	186.28	5.06	1.77	6.84	0.61		8.06	0.65	
2	19.94	19.83	1046.50	379.50	10	10	0.00	19.94	237.00	186.29	5.06	1.77	6.84	0.61		8.04	0.65	
1	22.15	21.79	1059.50	392.50	0	10	-0.05	22.19	246.02	194.82	6.77	1.78	7.18	0.61		8.25	0.65	
2	22.15	21.93	1060.50	393.50	10	10	0.00	22.15	247.50	196.38	6.91	1.78	7.20	0.61		8.04	0.64	
3	22.12	21.93	1060.50	393.50	20	10	0.00	22.12	249.00	197.96	6.91	1.78	7.20	0.61		8.01	0.64	
1	24.31	24.16	1073.00	406.00	0	10	0.00	24.31	256.50	204.94	8.71	1.79	7.51	0.61		8.09	0.64	
2	24.26	24.16	1073.00	406.00	10	10	0.00	24.26	257.00	205.49	8.71	1.79	7.51	0.61		8.04	0.64	
1	24.48	24.31	1074.00	407.00	0	10	-0.02	24.50	255.51	203.83	8.85	1.79	7.54	0.61		8.11	0.64	
2	24.48	24.31	1074.50	407.50	10	10	0.00	24.48	258.50	206.97	8.93	1.79	7.55	0.61		8.00	0.63	
3	24.50	24.31	1074.50	407.50	20	10	0.00	24.50	257.00	205.39	8.93	1.79	7.55	0.61		8.02	0.63	
1	26.61	26.85	1085.50	418.50	0	10	0.00	26.61	265.00	212.94	10.60	1.79	7.81	0.61		8.19	0.64	
2	26.61	26.68	1085.50	418.50	10	10	0.00	26.61	264.00	211.89	10.60	1.79	7.81	0.61		8.19	0.64	
1	28.25	28.50	1093.50	426.50	0	10	0.00	28.25	275.13	222.92	11.88	1.79	8.00	0.61	8.64	7.76	0.69	0.61
2	28.28	28.67	1093.50	426.50	10	10	0.00	28.28	276.50	224.35	11.88	1.79	8.00	0.61	8.61	7.79	0.61	0.61
3	28.24	28.67	1093.50	426.50	20	10	-0.71	28.94	275.76	223.32	11.88	1.79	8.00	0.61	8.63	8.45	0.61	0.61
1	36.10	34.79	1108.50	441.50	0	10	0.00	36.10	347.50	295.67	14.41	1.79	8.33	0.61	7.31	8.86	0.82	5.52
2	36.10	34.79	1108.50	441.50	10	10	-0.02	36.12	349.01	297.22	14.41	1.79	8.33	0.61	7.27	8.92	0.83	5.52
3	36.10	34.98	1109.00	442.00	20	10	-0.02	36.12	348.51	296.71	14.49	1.79	8.34	0.61	7.30	8.59	0.80	5.74
4	36.10	34.98	1109.50	442.50	30	10	0.00	36.10	349.50	297.74	14.58	1.79	8.36	0.61	7.28	8.28	0.77	5.95
5	36.10	34.98	1109.50	442.50	40	10	0.00	36.10	349.50	297.74	14.58	1.79	8.36	0.61	7.28	8.28	0.77	5.95
1	37.69	36.72	1112.50	445.50	0	10	0.00	37.69	368.00	316.40	15.11	1.79	8.42	0.61	6.88	8.40	0.83	7.31
2	37.38	36.92	1112.50	445.50	10	10	0.00	37.38	366.00	314.42	15.11	1.79	8.42	0.61	6.93	8.03	0.79	7.31
3	37.69	36.92	1112.50	445.50	20	10	0.00	37.69	369.50	317.95	15.11	1.79	8.42	0.61	6.84	8.44	0.84	7.31

2-year control orifice	
C_d average	0.65
C_d at 2-year WL	0.67
C_d at 5-year WL	0.66
C_d at 10-year WL	0.63
C_d at 20-year WL	0.67
C_d at 50-year WL	0.63

Where:

H_2: =Energy head inside riser box

Y_2 = Water level inside riser box.

Table I.3: Collected experimental data of Model 3 (model dimensions)

Increment	Q: flow meter (l/s)	Q: V-notch (l/s)	Reading of water level (mm)	Water level w.r.t base of model (mm)	t (min)	Δt (min)	ΔQ (l/s)	Q : outflow (l/s)	H_2 (mm)	Y_2 (mm)	Multi-stage outlet model								
											Q: 50-year V-notch (l/s)	C_d	Q: 50-year V-notch submerged (l/s)	Q: 10-year rectangular orifice (l/s)	C_d	Q: 10-year rectangular orifice submerged (l/s)	Q: 2-year circular orifice submerged (l/s)	C_d	Q: Riser (l/s)
1	10.16	9.95	848.5	180.5	0	10	0.047	10.11	128.50										
2	10.14	9.95	847.5	179.5	10	10	0.024	10.12	128.00										
3	10.14	9.95	847.0	179.0	20	10	0.000	10.14	128.50										
4	10.15	9.95	847.0	179.0	30	10	0.024	10.13	129.00										
5	10.16	9.95	846.5	178.5	40	10	0.000	10.16	129.00										
6	10.15	9.95	846.5	178.5	50	10	0.000	10.15	129.00										
1	11.90	11.65	878.0	210.0	0	10	-0.094	11.99	129.5										
2	11.90	11.65	880.0	212.0	10	10	-0.047	11.95	130.0										
3	11.90	11.94	881.0	213.0	20	10	0.000	11.90	129.5										
4	11.90	11.94	881.0	213.0	30	10	0.000	11.90	130.0										
5	11.90	11.94	881.0	213.0	40	10	0.000	11.90	130.0										
1	15.16	14.84	926.0	258.0	0	10	0.000	15.16	130.50					1.55	0.36				
2	15.21	15.18	926.0	258.0	10	10	0.000	15.21	129.00					1.55	0.36				
3	15.22	15.18	926.0	258.0	20	10	0.000	15.22	130.00					1.55	0.36				
1	18.03	17.98	947.5	279.5	0	10	0.000	18.03	140.00					3.98	0.36				
2	18.02	18.11	947.5	279.5	10	10	0.000	18.02	140.00					3.98	0.36				
3	18.02	18.11	947.5	279.5	20	10	0.000	18.02	141.00					3.98	0.36				
1	24.60	24.47	990.0	322.0	0	10	0.000	24.60	187.50					10.58	0.36				
2	24.57	24.47	990.0	322.0	10	10	0.000	24.57	187.50					10.58	0.36				
1	32.58	34.79	1035.5	367.5	0	10	0.000	32.58	275.00		5.18	1.79							
2	32.90	34.79	1035.5	367.5	10	10	0.000	32.90	275.00		5.18	1.79							
1	53.03	-	1084.5	416.5	0	10	0.000	53.03	336.50										
2	53.03	-	1084.5	416.5	10	10	0.000	53.03	339.00										
3	53.03	-	1084.5	416.5	20	10	0.000	53.03	335.00										
1	4.27	4.19	762.5	94.50	0	10	0.000	4.27	123.00	75.42							4.27	0.58	
2	4.26	4.24	762.5	94.50	10	10	0.000	4.26	123.00	75.42							4.26	0.58	
3	4.26	4.19	762.5	94.50	20	10	0.000	4.26	122.50	74.91							4.26	0.57	
1	8.33	8.17	814.5	146.50	0	10	-0.047	8.37	138.00	89.4							8.33	0.65	
2	8.33	8.25	815.5	147.50	10	10	0.000	8.33	137.50	88.9							8.33	0.65	
3	8.30	8.25	815.5	147.50	20	10	0.000	8.30	138.00	89.4							8.30	0.65	
1	9.99	9.86	843.5	175.50	0	10	0.000	9.99	142.00	92.9							9.99	0.65	
2	9.99	9.86	843.5	175.50	10	10	0.000	9.99	143.00	93.9							9.99	0.66	
1	11.92	11.94	880.5	212.50	0	10	0.000	11.92	141.00	90.9							11.92	0.64	
2	11.93	11.94	880.5	212.50	10	10	0.000	11.93	142.00	91.9							11.93	0.64	
1	15.33	15.30	926.5	258.50	0	10	0.000	15.33	142.00	89.7				1.60	0.36		13.73	0.63	
2	15.31	15.41	926.5	258.50	10	10	0.000	15.31	141.50	89.2				1.60	0.36		13.70	0.62	
3	15.31	15.41	926.5	258.50	20	10	0.000	15.31	142.50	90.3				1.60	0.36		13.71	0.63	
1	18.03	18.11	947.5	279.50	0	10	0.000	18.03	157.00	104.6				3.98	0.36		14.05	0.63	
2	18.03	18.11	947.5	279.50	10	10	0.000	18.03	156.50	104.1				3.98	0.36		14.05	0.63	
1	20.67	20.80	967.0	299.00	0	10	0.000	20.67	174.00	121.8				6.74	0.36		13.93	0.62	
2	20.66	20.80	967.0	299.00	10	10	0.000	20.66	174.50	122.3				6.74	0.36		13.92	0.62	
1	24.43	24.47	989.0	321.00	0	10	0.000	24.43	206.00	154.5				10.40	0.36		14.03	0.64	
2	24.42	24.47	989.0	321.00	10	10	0.000	24.42	206.00	154.5				10.40	0.36		14.02	0.64	
1	28.41	28.34	1010.5	342.50	0	10	0.000	28.41	240.50	189.4	0.44	1.79		14.89	0.60		13.07	0.63	
2	28.42	28.34	1010.5	342.50	10	10	0.000	28.42	239.50	188.4	0.44	1.79		14.89	0.60		13.08	0.62	
1	31.63	-	1031.0	363.00	0	10	0.000	31.63	280.50	230.1	4.09	1.79		17.12	0.60		10.41	0.54	
2	31.63	-	1031.0	363.00	10	10	0.000	31.63	282.50	232.1	4.09	1.79		17.12	0.60		10.41	0.54	
1	41.53	-	1060.0	392.00	0	10	0.000	41.53	324.50	273.3	12.80	1.85		19.85	0.60	20.32	8.88	0.48	
2	41.21	-	1060.0	392.00	10	10	0.000	41.21	323.00	271.8	12.80	1.85		19.85	0.60	20.45	8.56	0.46	
1	53.35	-	1085.0	417.00	0	10	0.000	53.35	350.50	297.7	22.75	1.88		21.93	0.60	20.38	10.22	0.55	
2	53.35	-	1085.0	417.00	10	10	0.000	53.35	350.00	297.2	22.75	1.88		21.93	0.60	20.42	10.17	0.55	
1	65.17	-	1113.5	445.50	0	10	0.000	65.17	375.00	320.5	35.68	1.87		24.09	0.60	20.86	8.35	0.44	0.29
2	65.49	-	1113.5	445.50	10	10	0.000	65.49	373.50	318.8	35.68	1.87		24.09	0.60	20.99	8.53	0.45	0.29
1	76.03	-	1127.5	459.50	0	10	0.000	76.03	-	-	42.76	1.87		25.08	0.60		0.00	0.00	4.87
2	76.35	-	1127.5	459.50	10	10	0.000	76.35	-	-	42.76	1.87		25.08	0.60		0.00	0.00	4.87
3	76.35	-	1127.5	459.50	20	10	0.000	76.35	-	-	42.76	1.87		25.08	0.60		0.00	0.00	4.87
4	76.35	-	1127.5	459.50	30	10	0.000	76.35	-	-	42.76	1.87		25.08	0.60		0.00	0.00	4.87
5	76.67	-	1127.5	459.50	40	10	0.000	76.67	-	-	42.76	1.87		25.08	0.60		0.00	0.00	4.87
1	80.18	-	1133.0	465.00	0	10	0.000	80.18	411.00	354.7	45.66	1.87	44.71	25.46	0.60	19.59	8.39	0.47	7.50
2	80.18	-	1133.0	465.00	10	10	0.000	80.18	411.00	354.7	45.66	1.87	44.71	25.46	0.60	19.59	8.39	0.47	7.50
1	80.82	-	1133.0	465.00	0	10	0.000	80.82	411.00	354.6	45.66	1.87	44.72	25.46	0.60	19.60	9.00	0.51	7.50
2	80.50	-	1133.0	465.00	10	10	0.000	80.50	411.00	354.7	45.66	1.87	44.82	25.46	0.60	19.60	8.59	0.49	7.50
3	80.18	-	1133.0	465.00	20	10	0.000	80.18	409.00	352.6	45.66	1.87	44.97	25.46	0.60	19.78	7.94	0.44	7.50

2-year control orifice	
C_d average	0.60
C_d at 2-year WL	0.65
C_d at 5-year WL	0.63
C_d at 10-year WL	0.645
C_d at 20-year WL	0.54
C_d at 50-year WL	0.55

Where:
H_2 =Energy head inside riser box
Y_2 = Water level inside riser box.

Table I.4: Collected experimental data of Model 4 (model dimensions)

Increment	Q: flow meter (l/s)	Q: V-notch (l/s)	Reading of water level (mm)	Water level w.r.t base of model (mm)	t (min)	Δt (min)	ΔQ (l/s)	Q : outflow (l/s)	H_2 (mm)	Y_2 (mm)	Multi-stage outlet model								
											Q: 50-year V-notch (l/s)	C_d	Q: 50-year V-notch submerged (l/s)	Q: 10-year rectangular orifice (l/s)	C_d	Q: 10-year rectangular orifice submerged (l/s)	Q: 2-year circular orifice submerged (l/s)	C_d	Q: Riser (l/s)
1	6.99	6.67	863.0	195.0	0	10	-0.21	7.20											
2	6.99	6.74	867.5	199.5	10	10	-0.12	7.11											
3	6.97	6.81	870.0	202.0	20	10	-0.07	7.04											
4	6.98	6.81	871.5	203.5	30	10	0.00	6.98											
5	6.97	6.81	871.5	203.5	40	10	0.00	6.97											
1	7.06	6.95	878.5	210.5	0	10	0.07	6.98	125.0	75.8							7.06	0.63	
2	7.06	6.95	877.0	209.0	10	10	0.05	7.01	124.5	75.3							7.06	0.64	
3	7.06	6.88	876.0	208.0	20	10	0.02	7.04	125.0	75.8							7.06	0.64	
4	7.07	6.88	875.5	207.5	30	10	0.02	7.04	125.5	76.3							7.07	0.64	
5	7.07	6.88	875.0	207.0	40	10	0.00	7.07	127.0	77.9							7.07	0.65	
1	10.93	10.78	943.0	275.0	0	10	0.00	10.93	171.5	122.5				3.22	0.41		7.71	0.65	
2	10.92	10.78	943.0	275.0	10	10	0.00	10.92	175.0	126.1				3.22	0.41		7.70	0.66	
3	10.91	10.78	943.0	275.0	20	10	0.00	10.91	175.0	126.1				3.22	0.41		7.69	0.66	
1	14.61	14.50	977.0	309.0	0	10	0.00	14.61	213.0	164.0				7.69	0.66		6.92	0.60	
2	14.64	14.50	977.0	309.0	10	10	0.00	14.64	212.0	162.9				7.69	0.66		6.95	0.60	
1	19.88	19.56	1016.5	348.5	0	10	0.00	19.88	239.0	189.2	2.07	1.91		10.54	0.66		7.27	0.60	
2	19.87	19.70	1016.5	348.5	10	10	0.00	19.87	239.5	189.7	2.07	1.91		10.54	0.66		7.27	0.60	
1	32.26	31.64	1067.0	399.0	0	10	0.00	32.26	284.0	232.1	11.69	1.85		13.32	0.66	14.81	7.25	0.59	
2	32.27	-	1067.0	399.0	10	10	0.00	32.27	285.5	233.6	11.69	1.85		13.32	0.66	14.74	7.26	0.59	
1	47.60	-	1114.5	446.5	0	10	0.00	47.60	428.0	376.9	24.80	1.85	22.50		0.66	9.56	6.23	0.78	9.30
1	48.24	-	1115.5	447.5	0	10	0.00	48.24	415.5	364.0	25.10	1.85	23.86		0.66	10.47	4.58	0.52	9.32
2	48.56	-	1115.5	447.5	10	10	0.00	48.56	413.0	361.4	25.10	1.85	24.04		0.66	10.64	4.56	0.51	9.32
1	39.93	-	1094.5	426.5	0	10	0.00	39.93	328.5	276.2	18.89	1.85			0.66	14.05	6.99	0.59	
2	39.93	-	1094.5	426.5	10	10	0.00	39.93	325.0	272.5	18.89	1.85			0.66	14.22	6.82	0.57	
1	26.51	26.85	1048.0	380.0	0	10	0.00	26.51	271.5	220.8	7.36	1.83		12.35	0.66		6.81	0.56	
2	26.19	26.68	1048.0	380.0	10	10	0.00	26.19	270.5	219.9	7.36	1.83		12.35	0.66		6.49	0.53	
1	17.82	17.86	1005.0	337.0	0	10	0.00	17.82	228.5	179.0	0.71	1.91		9.79	0.66		7.32	0.61	
2	17.82	17.73	1005.0	337.0	10	10	0.00	17.82	227.5	177.9	0.71	1.91		9.79	0.66		7.32	0.60	
1	9.18	8.99	922.0	254.0	0	10	0.05	9.14	144.0	94.6				1.36	0.41		7.83	0.65	
2	9.18	8.99	921.0	253.0	10	10	0.00	9.19	143.0	93.5				1.28	0.41		7.90	0.65	
3	9.18	8.99	921.0	253.0	20	10	0.00	9.18	145.5	96.2				1.28	0.41		7.90	0.66	
1	6.10	6.39	856.5	188.5	0	10	0.31	5.79	126.5	77.9							6.10	0.60	
2	6.10	6.18	850.0	182.0	10	10	0.19	5.91	127.5	79.0							6.10	0.63	
3	6.110	6.12	846.0	178.0	20	10	0.09	6.02	129.0	80.5							6.11	0.65	
4	6.09	6.05	844.0	176.0	30	10	0.07	6.02	127.5	79.0							6.09	0.64	
5	6.09	5.98	842.5	174.5	40	10	0.00	6.09	127.5	79.0							6.09	0.65	
6	6.10	5.98	842.5	174.5	50	10	0.00	6.10	128.0	79.5							6.10	0.65	
1	3.82	3.93	782.0	114.0	0	10	0.14	3.68	122.5	74.8							3.82	0.64	
2	3.82	3.78	779.0	111.0	10	10	0.09	3.73	122.5	74.8							3.82	0.66	
3	3.81	3.73	777.0	109.0	20	10	0.02	3.80	120.5	72.8							3.82	0.66	
4	3.81	3.73	776.5	108.5	30	10	0.00	3.82	121.0	73.3							3.82	0.67	
5	3.81	3.73	776.5	108.5	40	10	0.00	3.82	121.5	73.8							3.82	0.68	
1	2.29	2.29	747.0	79.0	0	10	0.07	2.22	113.0	65.7							2.29	0.65	
2	2.27	2.22	745.5	77.5	10	10	0.00	2.28	113.5	66.2							2.28	0.71	
3	2.29	2.22	745.5	77.5	20	10	0.00	2.29	113.5	66.2							2.29	0.71	

2-year control orifice	
C_d average	0.63
C_d at 2-year WL	0.65
C_d at 5-year WL	0.66
C_d at 10-year WL	0.60
C_d at 20-year WL	0.60
C_d at 50-year WL	0.59

Where:

H_2 = Energy head inside riser box

Y_2 = Water level inside riser box.

Table I.5: Collected experimental data of Model 5 (model dimensions)

Increment	Q: flow meter (l/s)	Q: V-notch (l/s)	Reading of water level (mm)	Water level w.r.t base of model (mm)	t (min)	Δt (min)	ΔQ (l/s)	Q : outflow (l/s)	H_2 (mm)	Y_2 (mm)	Multi-stage outlet model							
											Q: 50-year V-notch (l/s)	C_d	Q: 10-year rectangular orifice (l/s)	C_d	Q: 10-year rectangular orifice submerged (l/s)	Q: 2-year circular orifice submerged (l/s)	C_d	Q: Riser (l/s)
1	12.81	12.87	874.0	187.0	0	10	-0.05	12.85										
2	12.78	12.87	875.0	188.0	10	10	-0.02	12.80										
3	12.78	12.87	875.5	188.5	20	10	0.00	12.78	156.5	89.7						12.78	0.61	
4	12.79	12.87	875.5	188.5	30	10	0.00	12.79	156.0	89.1						12.79	0.61	
1	18.93	19.16	949.0	262.0	0	10	-0.05	18.98	170.5	102.4			2.47	0.38		16.46	0.62	
2	18.94	19.16	950.0	263.0	10	10	0.00	18.94	172.5	104.5			2.58	0.38		16.35	0.62	
3	18.98	19.16	950.0	263.0	20	10	0.00	18.98	173.0	105.0			2.58	0.38		16.40	0.62	
1	26.50	26.68	994.5	307.5	0	10	0.00	26.50	210.0	141.8			10.13	0.63		16.37	0.61	
2	26.46	26.68	994.5	307.5	10	10	0.00	26.46	207.5	139.2			10.13	0.63		16.33	0.60	
1	36.74	36.33	1045.0	358.0	0	10	0.00	36.74	237.5	168.2	3.83	1.46	14.85	0.63		18.05	0.62	
2	36.58	36.52	1045.0	358.0	10	10	0.00	36.58	241.5	172.4	3.83	1.46	14.85	0.63		17.89	0.63	
1	56.54	-	1092.5	405.5	0	10	0.00	56.54	316.0	246.2	22.06	1.63	18.21	0.63	19.28	16.28	0.61	
2	56.86	-	1092.5	405.5	10	10	0.00	56.86	312.5	242.5	22.06	1.63	18.21	0.63	19.50	16.60	0.62	
1	75.39	-	1118.0	431.0	0	10	0.00	75.39	374.5	303.9	35.73	1.67		0.63	17.22	15.62	0.66	6.81
2	75.39	-	1118.0	431.0	10	10	0.00	75.39	374.5	303.9	35.73	1.67		0.63	17.22	15.62	0.66	6.81
1	88.91	-	1127.5	440.5	0	10	0.00	88.91	398.5	326.8	41.11	1.67		0.63	16.29	18.27	0.82	13.24
2	88.59	-	1127.5	440.5	10	10	0.00	88.59	398.0	326.3	41.11	1.67		0.63	16.33	17.92	0.80	13.24
1	75.53	-	1116.5	429.5	0	10	0.00	75.53	371.0	300.3	34.91	1.67		0.63	17.37	18.03	0.75	5.22
2	74.88	-	1116.5	429.5	10	10	0.00	74.88	373.5	303.0	34.91	1.67		0.63	17.19	17.57	0.74	5.22
3	74.25	-	1116.5	429.5	20	10	0.00	74.25	372.5	302.0	34.91	1.67		0.63	17.25	16.87	0.71	5.22
1	5.55	5.53	784.0	97.0	0	10	0.00	5.55	130.0	64.3								
2	5.94	5.79	784.0	97.0	10	10	-0.14	6.08	130.0	64.2								
3	5.93	5.92	787.0	100.0	20	10	-0.02	5.95	131.5	65.8								
4	5.93	5.92	787.5	100.5	30	10	0.00	5.93	131.5	65.8								
5	5.92	5.92	787.5	100.5	40	10	0.00	5.92	130.5	64.7								
1	9.48	9.42	823.5	136.5	0	10	-0.09	9.58	146.0	79.7						9.48	0.60	
2	9.51	9.51	825.5	138.5	10	10	-0.07	9.58	146.0	79.7						9.51	0.59	
3	9.49	9.51	827.0	140.0	20	10	0.00	9.49	146.0	79.7						9.49	0.58	
4	9.48	9.51	827.0	140.0	30	10	0.00	9.48	145.5	79.2						9.48	0.58	
1	15.08	14.50	901.0	214.0	0	10	-0.42	15.50	158.6	91.0						15.08	0.65	
2	15.05	15.18	910.0	223.0	10	10	-0.24	15.28	160.6	93.1						15.05	0.63	
3	15.06	15.18	915.0	228.0	20	10	-0.05	15.11	163.0	95.8						15.06	0.62	
4	15.06	15.18	916.0	229.0	30	10	-0.02	15.08	162.0	94.7						15.06	0.62	
5	15.02	15.18	916.5	229.5	40	10	0.00	15.02	162.0	94.7						15.02	0.62	
6	15.03	15.18	916.5	229.5	50	10	0.00	15.03	163.5	96.3						15.03	0.62	
1	21.71	21.79	965.0	278.0	0	10	0.00	21.71	172.5	103.5			4.53	0.38		17.18	0.62	
2	21.76	21.79	965.0	278.0	10	10	0.00	21.76	171.5	102.4			4.53	0.38		17.22	0.62	
1	28.35	28.34	1007.5	320.5	0	10	0.00	28.35	214.5	146.1			11.53	0.63		16.81	0.61	
2	28.39	28.34	1007.5	320.5	10	10	0.00	28.39	217.5	149.2			11.53	0.63		16.85	0.61	
1	39.61	39.33	1054.0	367.0	0	10	0.00	39.61	254.0	184.8	6.18	1.46	15.54	0.63		17.89	0.63	
2	39.61	39.33	1054.0	367.0	10	10	0.00	39.61	256.5	187.5	6.18	1.46	15.54	0.63		17.89	0.64	

2-year control orifice	
C_d average	0.615
C_d at 2-year WL	0.61
C_d at 5-year WL	0.62
C_d at 10-year WL	0.60
C_d at 20-year WL	0.62
C_d at 50-year WL	0.62

Where:
H_2 = Energy head inside riser box
Y_2 = Water level inside riser box.

Table I.6: Collected experimental data of Model 6 (model dimensions)

Increment	Q: flow meter (l/s)	Q: V-notch (l/s)	Reading of water level (mm)	Water level w.r.t base of model (mm)	t (min)	Δt (min)	ΔQ (l/s)	Q : outflow (l/s)	H_2 (mm)	Y_2 (mm)	Y2	Multi-stage outlet model								
												Q: 50-year V-notch (l/s)	C_d	Q: 50-year V-notch submerged (l/s)	Q: 10-year rectangular orifice (l/s)	C_d	Q: 10-year rectangular orifice submerged (l/s)	Q: 2-year circular orifice submerged (l/s)	C_d	Q: Riser (l/s)
1	21.64	20.10	871.5	187.00	0	10	0.00	21.64	179.50	179.5	113.1							21.64	0.65	
2	21.65	20.10	871.5	187.0	10	10	0.00	21.65	180.00	180.0	113.6							21.65	0.65	
1	31.94	29.36	939.5	255.0	0	10	0.00	31.94	207.5	207.5	140.1				4.72	0.36		27.22	0.66	
2	31.94	29.36	939.5	255.0	10	10	0.00	31.94	207.0	207.0	139.6				4.72	0.36		27.22	0.66	
1	44.08	-	987.0	302.5	0	10	0.00	44.08	232.50	232.5	163.7				15.95	0.61		28.13	0.62	
2	44.40	-	987.0	302.5	10	10	0.00	44.40	233.50	233.5	164.7				15.95	0.61		28.45	0.63	
1	61.65	-	1040.5	356.0	0	10	0.00	61.65	269.00	269.0	198.7	7.59	1.64		22.67	0.61		31.39	0.65	
2	61.65	-	1040.5	356.0	10	10	0.00	61.65	269.00	269.0	198.7	7.59	1.64		22.67	0.61		31.39	0.65	
1	98.39	-	1078.5	394.0	0	10	0.00	98.39	330.00	330.0	256.3	39.70	1.65			0.61	25.84	32.85	0.73	
2	98.71	-	1078.5	394.0	10	10	0.00	98.71	329.50	329.5	255.7	39.70	1.65			0.61	25.89	33.11	0.73	
1	146.94	-	1119.0	434.5	0	10	0.00	146.94	424.00	424.0	348.3	92.39	1.71	90.98		0.61	20.44	30.18	0.84	5.34
2	146.30	-	1119.0	434.5	10	10	0.00	146.30	426.00	426.0	350.5	92.39	1.71	90.52		0.61	20.18	30.26	0.86	5.34
1	147.26	-	1119.5	435.0	0	10	0.00	147.26	428.50	428.5	353.0	93.11	1.71	90.68		0.61	19.93	31.35	0.90	5.29
2	147.58	-	1119.5	435.0	10	10	0.00	147.58	428.50	428.5	353.0	93.11	1.71	90.69		0.61	19.94	31.65	0.91	5.29
1	133.50	-	1110.0	425.5	0	10	0.05	133.45	410.00	410.0	335.6	79.90	1.71			0.61	20.88	31.00	0.85	1.72
2	133.15	-	1109.0	424.5	10	10	-0.05	133.20	411.50	411.5	337.2	78.55	1.71			0.61	20.57	32.61	0.90	1.42
3	133.50	-	1110.0	425.5	20	10	0.00	133.50	407.50	407.5	332.9	79.90	1.71			0.61	21.19	30.69	0.83	1.72
1	111.40	-	1092.0	407.5	0	10	0.00	111.40	365.50	365.5	291.9	56.81	1.71			0.61	23.67	30.92	0.75	
2	111.16	-	1092.0	407.5	10	10	0.00	111.16	368.50	368.5	295.2	56.81	1.71			0.61	23.34	31.01	0.76	
1	80.50	-	1063.0	378.5	0	10	0.00	80.50	310.00	310.0	238.5	24.67	1.65		24.96	0.61	26.05	30.88	0.68	
2	81.40	-	1063.0	378.5	10	10	0.00	81.40	308.00	308.0	236.2	24.67	1.65		24.96	0.61	26.27	31.78	0.69	
1	48.20	-	1001.0	316.5	0	10	0.00	48.20	239.00	239.0	169.7				17.96	0.61		30.24	0.65	
2	48.50	-	1001.0	316.5	10	10	0.00	48.50	239.00	239.0	169.6				17.96	0.61		30.54	0.65	
1	22.00	20.80	866.0	181.5	0	10	-0.05	22.05	180.50	180.5	114.1							22.00	0.69	
2	21.70	20.80	867.0	182.5	10	10	0.00	21.70	179.00	179.0	112.6							21.70	0.67	
1	21.81	19.29	876.0	191.5	0	10	0.14	21.66	179.50	179.5	113.1							21.80	0.64	
2	21.78	-	873.0	188.5	10	10	0.00	21.78	179.50	179.5	113.1							21.78	0.65	
3	21.79	-	873.0	188.5	20	10	0.00	21.79	180.50	180.5	114.1							21.79	0.65	
1	38.97	-	963.0	278.5	0	10	0.00	38.97	221.50	221.5	153.2				11.75	0.61		27.22	0.63	
2	38.97	-	963.0	278.5	10	10	0.00	38.97	221.00	221.5	153.3				11.75	0.61		27.22	0.63	
1	28.69	28.00	923.5	239.0	0	10	0.00	28.69	198.00	198.0	130.8				2.10	0.36		26.59	0.66	
2	28.68	-	923.5	239.0	10	10	0.00	28.68	199.00	199.0	131.9				2.10	0.36		26.59	0.67	
1	15.38	13.29	822.5	138.0	0	10	0.00	15.38	161.50	161.5	95.8							15.38	0.61	
2	15.35	13.29	822.5	138.0	10	10	0.00	15.35	161.50	161.5	95.8							15.35	0.61	
1	9.68	8.41	794.0	109.5	0	10	0.00	9.68	145.00	145.0	80.0							9.68	0.39	
2	9.57	8.41	794.0	109.5	10	10	0.00	9.57	145.00	145.0	80.1							9.57	0.38	

2-year control orifice	
C_d average	0.68
C_d at 2-year WL	0.65
C_d at 5-year WL	0.66
C_d at 10-year WL	0.62
C_d at 20-year WL	0.65
C_d at 50-year WL	0.73

Where: H_2= Energy head inside riser box and Y_2= Water level inside riser box.

APPENDIX J: Evaluation of Experimental Stage-Discharge Curve with Target (Theoretical) Stage-Discharge Curve

The reason for the difference in the theoretical and physical model discharge is because the valve in the hydraulic laboratory could only be manually controlled to supply constant inflows that is in the region of the target discharges for each recurrence interval storms. The stage tabulated in Table J.1 is the resultant stabilised water surface elevation, relative to the base of the physical multi-stage outlet model, measured in the glass flume for the specific inflow.

Table J.1: Comparison between release rate of physical model and target discharges

RI (years)	Water surface elevation (Physical) (m)	Estimated maximum water surface elevation (Theoretical) (m)	Actual discharge (Physical) (m^3/s)	Target discharge (Theoretical) (m^3/s)	Percentage difference between target and physical discharge (%)	Percentage difference between target and physical recorded stage (%)
Model 1						
2	0.675	0.620	0.050	0.049	-1.9	-8.15
5	0.792	0.770	0.071	0.074	4.4	-2.78
10	0.923	0.900	0.099	0.102	3.0	-2.44
20	1.113	1.020	0.141	0.141	-0.2	-8.36
50	1.263	1.150	0.230	0.226	-1.9	-8.95
100	1.305	1.240	0.339	0.336	-1.0	-4.98
Model 2						
2	0.495	0.620	0.082	0.083	0.65	25.25
5	0.726	0.780	0.126	0.125	-0.51	7.44
10	0.882	0.920	0.172	0.172	0.13	4.31
20	1.035	1.050	0.240	0.237	-1.15	1.45
50	1.223	1.200	0.382	0.382	0.08	-1.84
100	1.328	1.300	0.563	0.566	0.59	-2.07
Model 3						
2	0.639	0.640	0.185	0.186	0.3	0.16
5	0.893	0.800	0.281	0.279	-0.68	-10.36
10	0.966	0.940	0.383	0.385	0.47	-2.69
20	1.103	1.060	0.510	0.530	3.85	-3.85
50	1.251	1.180	0.832	0.854	2.69	-5.68
100	1.395	1.220	1.255	1.266	0.89	-12.54
Model 4						
2	0.621	0.640	0.110	0.110	0.0	3.06
5	0.825	0.790	0.170	0.165	-3.07	-4.24
10	0.927	0.920	0.228	0.228	0.04	-0.76
20	1.046	1.030	0.310	0.314	1.36	-1.48
50	1.197	1.130	0.503	0.506	0.61	-5.60
100	1.343	1.160	0.754	0.750	-0.59	-13.59
Model 5						
2	0.566	0.68	0.199	0.200	0.31	20.25
5	0.789	0.83	0.295	0.299	1.23	5.20
10	0.923	0.96	0.413	0.413	0.05	4.07
20	1.074	1.05	0.571	0.570	-0.26	-2.23
50	1.217	1.08	0.884	0.918	3.86	-11.22
100	1.322	1.00	1.383	1.361	-1.63	-24.33
Model 6						
2	0.566	0.630	0.340	0.337	-0.80	11.41
5	0.765	0.790	0.498	0.505	1.41	3.27
10	0.908	0.910	0.69	0.697	1.07	0.28
20	1.068	1.010	0.961	0.961	0.00	-5.43
50	1.182	1.050	1.536	1.547	0.70	-11.17
100	1.305	0.980	2.298	2.294	-0.18	-24.90

APPENDIX K: Dimensional Analysis of Orifice Flow

The discharge through a submerged rectangular weir is a function of the orifice area, A_o, which is the height (D) times the width (b) of the orifice, the differential head, taken as the difference between the upstream (Y_1) and downstream (Y_3) water surface elevations, and is driven by the effects of gravity. Equation K.1 gives the functional relationship between the unit discharge and the different channel and orifice parameters. Refer to Figure K.1 for a definition of the parameters. The piezo-tube in the hydraulic laboratory which determined the downstream water surface elevation, was situated directly downstream of the 2-year orifice. Water surface reading further downstream was not possible as the water surface elevation fluctuated even more near the entrance of the 100-year size pipe. Thus, the head reading on the piezo-tube were averaged.

$$q = f(Y_1, Y_3, D, b, g) \tag{K.1}$$

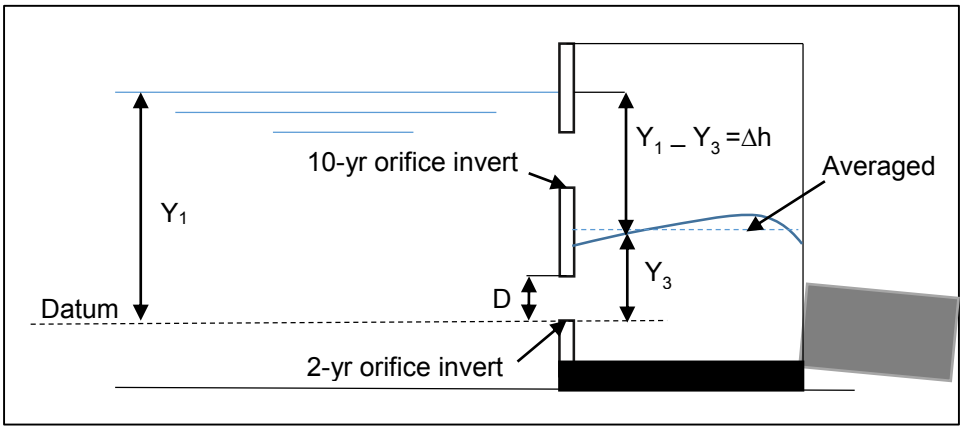

Figure K.1: Scheme of multi-stage outlet model operating under submerged flow conditions

Using the PI theorem and considering the density, gravitational acceleration and the area, as the independent variables and by neglecting viscous or compressibility effects, Equation K.2 was deduced from Equation K.1. The left-hand-side of Equation K.2 represents the dimensionless discharge coefficient (C_d) and was developed from the standard orifice equation (Equation 2.1). Equation K.3 represents the first PI group and Equation K.4 gives the discharge PI group. There is only one PI groups since there is only two dimensions (length and time) present (N= n - m = 3 - 2 = 1).

$$\frac{q}{D^{1.5}\sqrt{2}g^{0.5}} = f\left(\frac{\Delta h}{D}\right) \tag{K.2}$$

$$\Pi_1 = \frac{\Delta h}{D} \tag{K.3}$$

$$\Pi_Q = \frac{q}{D^{1.5}\sqrt{2}g^{0.5}} = f(\Pi_1) \tag{K.4}$$

By considering the cross-sectional area for a rectangular orifice and rearranging Equation 2.1 to give Equation K5, the dimensionless relationship was developed in the following steps:

$$Q = C_d(D.b)\sqrt{2g\Delta h} \tag{K.1}$$

$$\frac{\left(\frac{Q}{b}\right)}{D\sqrt{2}g^{0.5}} = C_d\sqrt{\Delta h} \tag{K.5}$$

By dividing both sides of Equation K.5 by √D, we obtain Equation K.6

$$\frac{q}{D^{1.5}\sqrt{2}\,g^{0.5}} = C_d\sqrt{\frac{\Delta h}{D}} \tag{K.6}$$

Equation K.6 could be used to compare the discharge between different rectangular orifices of different sizes, since it is equivalent to the standard orifice equation in all respects.

APPENDIX L: 50-year Control Rectangular Weir

(Individual Component of Multi-Stage Outlet Model)

Table L.1: Comparison of experimental discharge of 50-year storm control component of Model 2 with various theoretical weir equations

Physical Model 2		Characteristic dimensions of 50-year weir of Model 2				Characteristic ratios of 50-year weir of Model 2				Short-crested weir equation (Irrigation Design Manual, 2003)			Rectangular weir equation: Hamilton-Smith Formula (Chadwick *et. al*, 2004)			Short-crested weir equation (Bos, 1989)			Weir discharge coefficient, Eq. 2.13 (McCuen *et al.*, 2002)	Rectangular weir equation: Kindsvater-Carter formula *with the riser taken as width of approach channel		Rectangular weir equation: (Kindsvater-Carter, 1957)		Francis formula for rectangular weirs without end contractions (cited Institute for Agricultural Engineering, 2002)		Francis formula for rectangular weirs with end contractions (cited Institute for Agricultural Engineering, 2002)		Sharp-crested rectangular weir equation (SANRAL, 2013)		Sharp-crested weir with end contractions (SANRAL, 2013)		Contracted rectangular weir, according to British standards (Henderson, 1966)		Broad-crested weir equation (Brater *et. al*, 1996)			Broad-crested weir equation (Bos, 1989)		Broad-crested weir equation (Hager and Schwalt, 1994)		Ackers *et al*, 1978 (Chanson, 2004)
C	Q (actual discharge)	h1	Ps	Crest Length (L)	Crest breadth (bc)	h1/L	L/h1	h1/Ps	h1/bc	C	Q	% diff.	Q	% diff.	C	Q	% diff.	C	Q	% diff.		Q	% diff.	Q	% diff.	Q	% diff.	Q	% diff.	Q	% diff.	Q	% diff.	Q	% diff.	Q	% diff.	C	Q	% diff.	Q	% diff.	Q	% diff.	Q
1.80	7.59	81	364	183	50	0.44	2.26	0.223	1.62	1.63	6.27	-17.34	6.0	-21.40	0.48	7.26	-4.30	0.41	7.60	0.10	7.55	-0.50	7.76	2.26	7.08	-6.79	7.83	3.19	7.14	-5.94	7.32	-3.54	1.70	7.17	-5.52	N.A	-	7.64	0.63	N.A
1.78	7.50	81	364	183	50	0.44	2.26	0.223	1.62	1.63	6.27	-16.37	6.0	-20.49	0.48	7.19	-4.15	0.40	7.60	1.27	7.55	0.66	7.76	3.45	7.08	-5.71	7.83	4.40	7.14	-4.84	7.32	-2.41	1.70	7.17	-4.42	N.A	-	7.64	1.80	N.A
1.79	9.07	91.5	364	183	50	0.50	2.00	0.251	1.83	1.66	7.57	-16.55	6.9	-23.97	0.46	8.76	-3.49	0.40	9.11	0.37	9.05	-0.27	9.32	2.72	8.39	-7.55	9.44	4.04	8.50	-6.36	8.74	-3.68	1.83	9.27	2.17	N.A	-	9.27	2.13	N.A
1.79	9.09	91.5	364	183	50	0.50	2.00	0.251	1.83	1.66	7.57	-16.68	6.9	-24.09	0.46	8.76	-3.63	0.40	9.11	0.22	9.05	-0.41	9.32	2.57	8.39	-7.69	9.44	3.89	8.50	-6.50	8.74	-3.82	1.83	9.27	2.01	N.A	-	9.27	1.98	N.A
1.76	5.09	63	364	183	50	0.34	2.90	0.173	1.26	1.58	4.26	-16.20	4.4	-14.44	0.51	4.79	-5.94	0.40	5.24	2.95	5.21	2.39	5.32	4.66	4.96	-2.55	5.34	4.95	4.97	-2.27	5.07	-0.26	1.70	4.92	-3.30	5.03	-1.08	5.05	-0.71	N.A
1.76	3.82	52	364	183	50	0.28	3.52	0.143	1.04	1.55	3.18	-16.90	3.4	-11.49	0.53	3.48	-9.02	0.40	3.95	3.23	3.93	2.70	3.99	4.45	3.77	-1.48	3.99	4.34	3.76	-1.59	3.83	0.17	1.70	3.69	-3.49	3.57	-6.62	3.63	-5.06	N.A

Table L.2: Comparison of experimental discharge of 50-year storm control component of Model 3 with various theoretical weir equations

Physical Model 2		Characteristic dimensions of 50-year weir of Model 3				Characteristic ratios of 50-year weir of Model 2				Short-crested weir equation (Irrigation Design Manual, 2003)			Rectangular weir equation: Hamilton-Smith Formula (Chadwick *et. al*, 2004)			Short-crested weir equation (Bos, 1989)		Weir discharge coefficient, Eq. 2.13 (McCuen, *et al.*, 2002)	Rectangular weir equation: Kindsvater-Carter formula *with the riser taken as width of approach channel		Rectangular weir equation: (Kindsvater-Carter, 1957)		Francis formula for rectangular weirs without end contractions (cited Institute for Agricultural Engineering, 2002)		Francis formula for rectangular weirs with end contractions (cited Institute for Agricultural Engineering, 2002)		Sharp-crested rectangular weir equation (SANRAL, 2013)		Sharp-crested weir with end contractions (SANRAL, 2013)		Contracted rectangular weir, according to British standards (Henderson, 1966)		Broad-crested weir equation (Brater *et. al*, 1996)			Broad-crested weir equation (Bos, 1989)		Broad-crested weir equation (Hager and Schwalt, 1994)		Ackers *et al*, 1978 (Chanson, 2004)
C	Q (actual discharge)	h1	Ps	Crest Length (L)	Crest breadth (bc)	h1/L	L/h1	h1/Ps	h1/bc	C	Q	% diff.	Q	% diff.	C	Q	% diff.	C	Q	% diff.	C	Q	% diff.	Q	% diff.	Q	% diff.	Q	% diff.	Q	% diff.	Q	% diff.	Q	% diff.	C	Q	% diff.	Q	% diff.	Q	% diff.	Q
1.79	5.3	31.5	383.5	530	50	0.06	16.8	0.1	0.63	1.50	4.38	-17.50	4.9	-6.79	0.57	-	-	0.40	5.56	4.76	5.44	2.45	5.45	2.72	5.39	1.50	5.40	1.81	5.34	0.60	5.35	0.79	1.61	4.77	-10.12	4.45	-16.24	4.46	-15.95	N.A
1.80	8.2	42	383.5	530	50	0.08	12.6	0.1	0.84	1.52	6.84	-16.59	7.4	-9.94	0.55	-	-	0.41	8.48	3.37	8.28	0.86	8.39	2.30	8.26	0.68	8.35	1.75	8.22	0.14	8.22	0.17	1.70	7.76	-5.49	7.31	-10.97	7.24	-11.78	N.A
1.85	13.5	57.5	383.5	530	50	0.11	9.2	0.1	1.15	1.57	11.20	-17.01	11.3	-16.30	0.52	12.08	-10.5	0.42	13.51	0.04	13.13	-2.70	13.45	-0.40	13.15	-2.56	13.44	-0.42	13.15	-2.58	13.13	-2.76	1.70	12.4	-7.98	12.40	-8.18	12.52	-7.30	N.A
1.85	18.4	70.5	383.5	530	50	0.13	7.5	0.2	1.41	1.60	15.48	-15.80	14.7	-19.89	0.50	16.76	-8.84	0.42	18.30	-0.45	17.75	-3.45	18.25	-0.71	17.77	-3.35	18.33	-0.29	17.84	-2.95	17.78	-3.30	1.70	16.9	-8.26	17.68	-3.83	17.66	-4.18	N.A
1.88	24.24	84	383.5	530	50	0.16	6.3	0.2	1.68	1.64	20.49	-15.46	18.3	-24.38	0.48	21.97	-9.35	0.42	23.79	-1.84	23.01	-5.07	23.74	-2.06	22.99	-5.16	23.95	-1.20	23.19	-4.34	23.06	-4.86	1.83	23.6	-2.59	-	-	23.45	-3.28	N.A
1.87	27.67	92	383.5	530	50	0.17	5.76	0.24	1.84	1.66	23.73	-14.24	20.4	-26.10	0.47	29.58	6.89	0.42	27.28	-1.42	26.34	-4.82	27.21	-1.65	26.27	-5.07	27.52	-0.53	26.57	-3.99	26.39	-4.62	1.83	27.1	-2.19	-	-	27.06	-2.19	N.A

Table L.3: Comparison of experimental discharge of 50-year storm control component of Model 4 with various theoretical weir equations

Physical Model 4		Characteristic dimensions of 50-year weir of Model 3				Characteristic ratios of 50-year weir of Model 2				Short-crested weir equation (Irrigation Design Manual, 2003)			Rectangular weir equation: Hamilton-Smith Formula (Chadwick *et. al*, 2004)			Short-crested weir equation (Bos, 1989)		Weir discharge coefficient, Eq. 2.13 (McCuen, *et al*, 2002)	Rectangular weir equation: Kindsvater-Carter formula *with the riser taken as width of approach channel		Rectangular weir equation: (Kindsvater-Carter, 1957)		Francis formula for rectangular weirs without end contractions (cited Institute for Agricultural Engineering, 2002)		Francis formula for rectangular weirs with end contractions (cited Institute for Agricultural Engineering, 2002)		Sharp-crested rectangular weir equation (SANRAL, 2013)		Sharp-crested weir with end contractions (SANRAL, 2013)		Contracted rectangular weir, according to British standards (Henderson, 1966)		Broad-crested weir equation (Brater *et. al*, 1996)			Broad-crested weir equation (Bos, 1989)		Broad-crested weir equation (Hager and Schwalt, 1994)		Ackers *et al*, 1978 (Chanson, 2004)	
C	Q (actual discharge)	h1	Ps	Crest Length (L)	Crest breadth (bc)	h1/L	L/h1	h1/Ps	h1/bc	C	Q	% diff.	Q	% diff.	C	Q	% diff.	C	Q	% diff.		Q	% diff.	Q	% diff.	Q	% diff.	Q	% diff.	Q	% diff.	Q	% diff.	Q	% diff.	Q	% diff.	C	Q	% diff.	Q	% diff.	Q	% diff.	Q	% diff.
1.92	2.50	25.5	373	320	50	0.080	12.55	0.1	0.51	1.48	1.9	-24.01	2.2	-11.51	0.57			0.43	2.45	-1.86	2.42	-3.09	2.40	-3.92	2.36	-5.45	2.37	-4.95	2.33	-6.46	2.35	-5.93	1.61	2.10	-15.93	1.91	-23.4	1.92	-22.9	2.1	-15.4
1.91	2.49	25.5	373	320	50	0.080	12.55	0.1	0.51	1.48	1.9	-23.87	2.2	-11.35	0.57			0.43	2.45	-1.69	2.42	-2.91	2.40	-3.75	2.36	-5.28	2.37	-4.77	2.33	-6.29	2.35	-5.76	1.61	2.10	-15.78	1.91	-23.3	1.92	-22.8	2.1	-15.3
1.83	6.17	48	373	320	50	0.150	6.67	0.1	0.96	1.54	5.0	-18.47	5.3	-13.55	0.54	5.56	-9.81	0.41	6.17	-0.02	6.08	-1.45	6.19	0.36	6.01	-2.65	6.17	0.07	5.99	-2.93	6.02	-2.43	1.70	5.72	-7.27	5.45	-11.7	5.52	-10.6	N.A	-
1.83	6.17	48	373	320	50	0.150	6.67	0.1	0.96	1.54	5.0	-18.44	5.3	-13.51	0.54	5.56	-9.77	0.41	6.17	0.02	6.08	-1.41	6.19	0.41	6.01	-2.61	6.17	0.11	5.99	-2.89	6.02	-2.39	1.70	5.72	-7.23	5.45	-11.6	5.52	-10.6	N.A	-
1.85	11.92	74	373	320	50	0.231	4.32	0.198	1.48	1.61	9.9	-16.85	9.4	-21.17	0.49	10.93	-8.30	0.42	11.70	-1.78	11.51	-3.39	11.85	-0.52	11.30	-5.12	11.92	0.08	11.37	-4.55	11.43	-4.09	1.70	10.95	-8.09	11.65	-2.3	11.54	-3.1	N.A	-
1.86	11.95	74	373	320	50	0.231	4.32	0.198	1.48	1.61	9.9	-17.09	9.4	-21.40	0.49	10.93	-8.57	0.42	11.70	-2.07	11.51	-3.68	11.85	-0.81	11.30	-5.40	11.92	-0.21	11.37	-4.83	11.43	-4.37	1.70	10.95	-8.36	11.65	-2.5	11.54	-3.4	N.A	

Table L.5: Comparison of experimental discharge of 50-year storm control component of Model 5 with various theoretical weir equations

Physical Model 5		Characteristic dimensions of 50-year weir of Model 3				Characteristic ratios of 50-year weir of Model 2				Short-crested weir equation (Irrigation Design Manual, 2003)			Rectangular weir equation: Hamilton-Smith Formula (Chadwick *et. al*, 2004)			Short-crested weir equation (Bos, 1989)		Weir discharge coefficient, Eq. 2.13 (McCuen *et al.*, 2002)	Rectangular weir equation: Kindsvater-Carter formula *with the riser taken as width of approach channel		Rectangular weir equation: (Kindsvater-Carter, 1957)		Francis formula for rectangular weirs without end contractions (cited Institute for Agricultural Engineering, 2002)		Francis formula for rectangular weirs with end contractions (cited Institute for Agricultural Engineering, 2002)		Sharp-crested rectangular weir equation (SANRAL, 2013)		Sharp-crested weir with end contractions (SANRAL, 2013)		Contracted rectangular weir, according to British standards (Henderson, 1966)		Broad-crested weir equation (Brater *et. al*, 1996)			Broad-crested weir equation (Bos, 1989)		Broad-crested weir equation (Hager and Schwalt, 1994)		Ackers *et al*, 1978 (Chanson, 2004)	
C	Q (actual discharge)	h1	Ps	Crest Length (L)	Crest breadth (bc)	h1/L	L/h1	h1/Ps	h1/bc	C	Q	% diff.	Q	% diff.	C	Q	% diff.	C	Q	% diff.	Q	% diff.	Q	% diff.	Q	% diff.	Q	% diff.	Q	% diff.	Q	% diff.	C	Q	% diff.	Q	% diff.	Q	% diff.	Q	% diff.	Q	% diff.
1.46	2.55	29	399	353.5	50	0.08	12.19	0.07	0.58	1.49	2.56	0.44	2.9	15.71	0.57	-	-	0.33	3.23	26.88	3.22	26.36	3.21	26.22	3.16	24.15	3.18	24.94	3.13	22.89	3.14	23.55	1.61	2.81	10.44	2.62	2.92	2.60	2.29	2.83	11.10
1.55	4.6	41.5	399	353.5	50	0.12	8.52	0.10	0.83	1.52	4.44	-3.99	4.9	5.21	0.55	4.80	3.75	0.35	5.45	17.65	5.42	17.12	5.50	18.78	5.37	15.99	5.47	18.06	5.34	15.29	5.36	15.86	1.70	5.08	9.74	4.69	1.25	4.73	2.15	-	-
1.63	9.6	65	399	353.5	50	0.18	5.44	0.16	1.3	1.59	8.96	-6.27	8.9	-6.68	0.52	9.83	2.81	0.37	10.55	10.34	10.49	9.75	10.78	12.77	10.38	8.62	10.80	12.94	10.40	8.78	10.44	9.26	1.70	9.96	4.19	10.19	6.59	10.29	7.61	-	-
1.67	12.65	77	399	353.5	50	0.22	4.59	0.19	1.54	1.62	11.71	-7.40	11.1	-12.31	0.50	13.01	2.86	0.38	13.56	7.20	13.48	6.58	13.90	9.91	13.29	5.12	13.97	10.50	13.36	5.68	13.42	6.11	1.70	12.84	1.54	13.79	9.03	13.60	7.56	-	-

Table L.6: Comparison of experimental discharge of 50-year storm control component of Model 6 with various theoretical weir equations

Physical Model 6		Characteristic dimensions of 50-year weir of Model 3				Characteristic ratios of 50-year weir of Model 2				Short-crested weir equation (Irrigation Design Manual, 2003)			Rectangular weir equation: Hamilton-Smith Formula (Chadwick *et. al*, 2004)			Short-crested weir equation (Bos, 1989)		Weir discharge coefficient, Eq. 2.13 (McCuen *et al.*, 2002)	Rectangular weir equation: Kindsvater-Carter formula *with the riser taken as width of approach channel		Rectangular weir equation: (Kindsvater-Carter, 1957)		Francis formula for rectangular weirs without end contractions (cited Institute for Agricultural Engineering, 2002)		Francis formula for rectangular weirs with end contractions (cited Institute for Agricultural Engineering, 2002)		Sharp-crested rectangular weir equation (SANRAL, 2013)		Sharp-crested weir with end contractions (SANRAL, 2013)		Contracted rectangular weir, according to British standards (Henderson, 1966)		Broad-crested weir equation (Brater *et. al*, 1996)			Broad-crested weir equation (Bos, 1989)		Broad-crested weir equation (Hager and Schwalt, 1994)		Ackers *et al*, 1978 (Chanson, 2004)	
C	Q (actual discharge)	h1	Ps	Crest Length (L)	Crest breadth (bc)	h1/L	L/h1	h1/Ps	h1/bc	C	Q	% diff.	Q	% diff.	C	Q	% diff.	C	Q	% diff.	Q	% diff.	Q	% diff.	Q	% diff.	Q	% diff.	Q	% diff.	Q	% diff.	C	Q	% diff.	Q	% diff.	Q	% diff.	Q	% diff.	Q	% diff.
1.64	2.24	17.5	401	590	50	0.03	33.71	0.04	0.35	1.46	1.98	-11.55	2.4	6.24	0.59	-	-	0.37	2.62	17.20	2.60	16.17	2.51	12.37	2.50	11.71	2.48	10.82	2.46	10.16	2.47	10.58	1.61	2.2	-1.67	1.97	-11.71	1.99	-11.12	2.21	-1.09
1.65	9.8	46.5	401	590	50	0.08	12.69	0.12	0.93	1.54	8.95	-8.23	9.5	-2.44	0.54	-	-	0.37	10.81	10.83	10.69	9.64	10.89	11.63	10.71	9.87	10.84	11.12	10.67	9.37	10.66	9.31	1.70	10.1	3.14	9.58	-1.74	9.62	-1.33	-	-
1.72	18.6	69.5	401	590	50	0.12	8.49	0.17	1.39	1.60	16.89	-8.97	16.3	-12.39	0.51	18.32	-1.29	0.39	19.58	5.51	19.34	4.21	19.89	7.20	19.42	4.67	19.95	7.50	19.48	4.97	19.40	4.56	1.70	18.4	-0.96	19.27	3.83	19.20	3.45	-	-
1.71	18.5	69.5	401	590	50	0.12	8.49	0.17	1.39	1.60	16.89	-8.87	16.3	-12.30	0.51	18.32	-1.18	0.39	19.58	5.62	19.34	4.32	19.89	7.31	19.42	4.79	19.95	7.62	19.48	5.08	19.40	4.67	1.70	18.4	-0.85	19.25	3.84	19.20	3.56	-	-
1.67	12.39	54	401	590	50	0.09	10.93	0.13	1.08	1.56	11.32	-8.64	11.7	-5.94	0.53	12.24	-1.20	0.38	13.47	8.75	13.32	7.52	13.62	9.95	13.37	7.94	13.59	9.71	13.34	7.71	13.32	7.53	1.70	12.6	1.58	12.43	0.34	12.50	0.85	-	-

where:

Q = discharge (l/s)

C = discharge coefficient

h_1 = head on weir (mm)

P_s = weir crest (mm)

L = crest length of weir (mm)

b_c = crest breadth of weir in direction of flow (mm)

% diff. = percentage difference in experimental and theoretical discharge (%).

APPENDIX M: Visual Studio Program

The calculation classes, as coded by the author for the outflow from the multi-stage outlet can be seen in the written Visual Studio code (refer to CD-ROM). The .exe file could be loaded from the CD-ROM. The following output could then be obtained from the implemented Visual Studio program:

Step 1: Create the inflow (post-development) and target (pre-development) run-off hydrographs for the various RI storm events, by adding the flow value for a specific time interval. The estimated storage volume is calculated automatically from the input data.

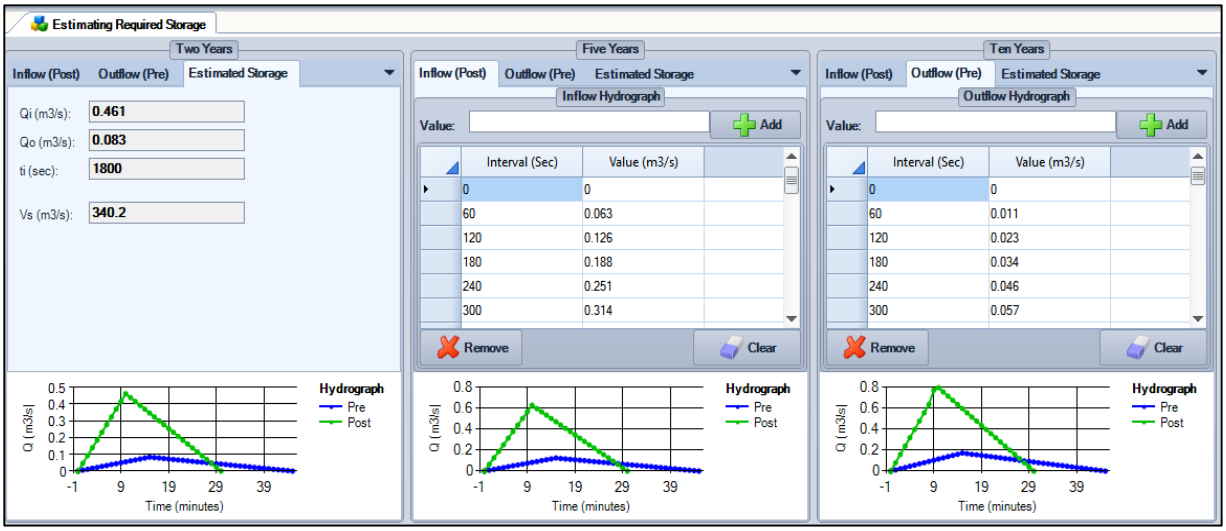

Figure M.1: Adding pre- and post-development hydrographs

Step 2: Design the trapezoidal detention pond (basin). Add the outlets. First size the culvert (pipe) and thereafter the orifice(s), weir(s) and riser. **Step 3:** After adding each outlet, run the program by clicking on the play icon under the "Process" tab. **Step 4:** Click on the "Route" button in order to perform a trail route to see the outflow from the pond before sizing the next device of the multi-stage outlet structure. Check that the actual discharges are at or below their target discharges.

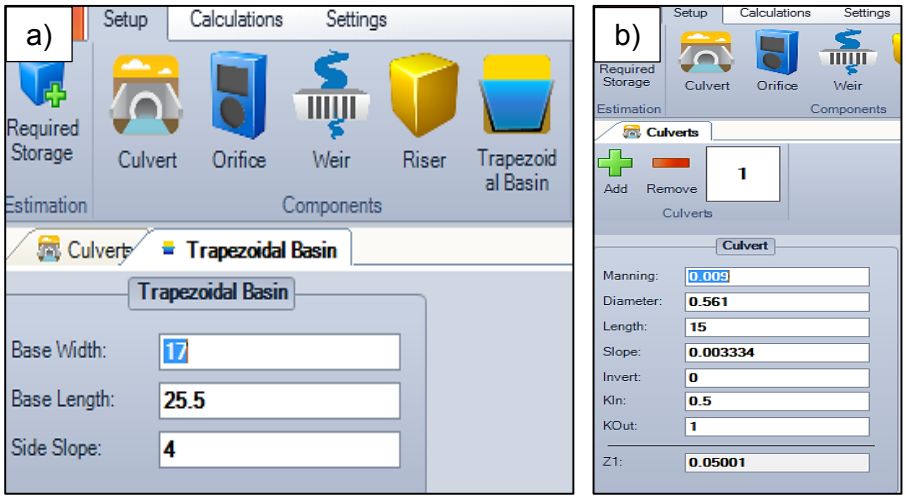

Figure M.2: Designed the trapezoidal storage pond (a) and sized the culvert first (b)

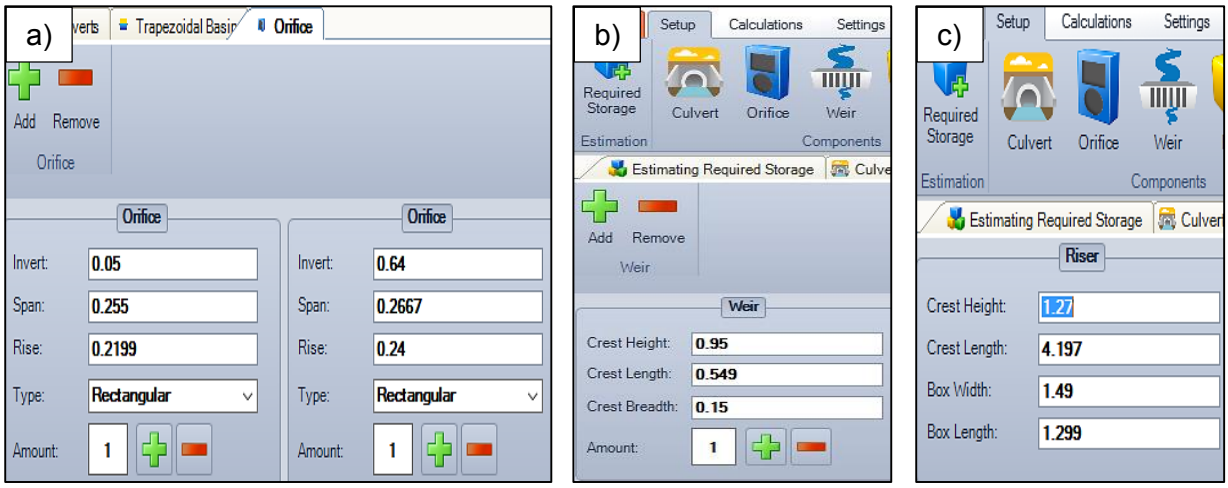

Figure M.3: Add the first orifice (2-year or 5-year RI storm control orifice). Added the next individual discharge control devices (10-year control orifice, thereafter the 50-year control weir) to the multi-stage outlet (b), lastly sized the riser (c)

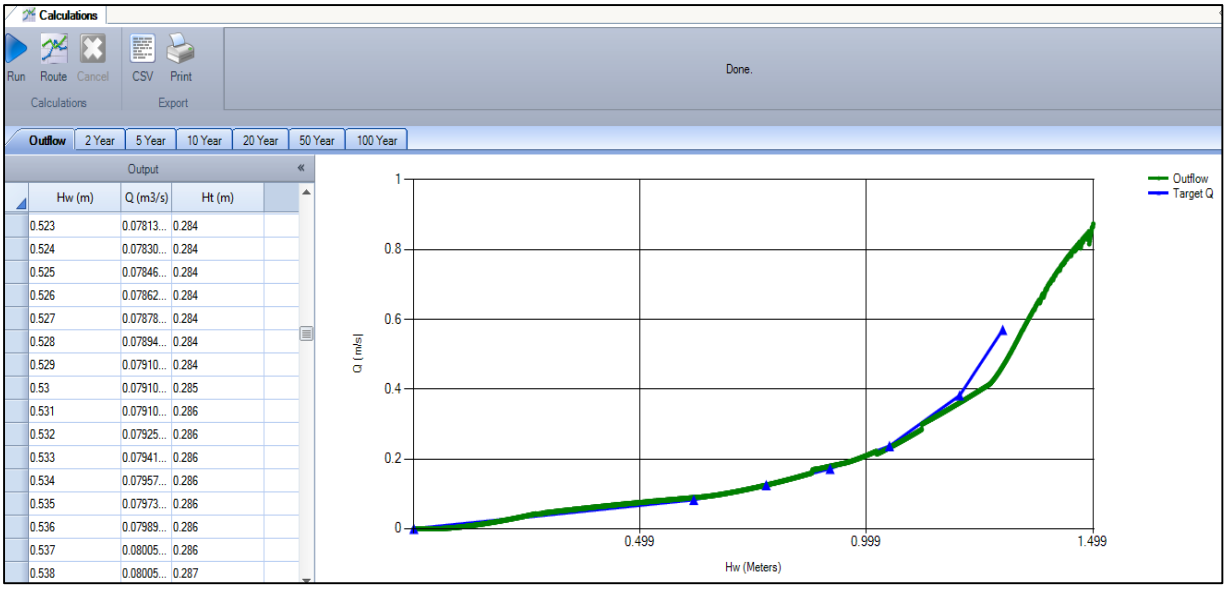

Figure M.4: Compare the outflow from the multi-stage outlet with the target discharge

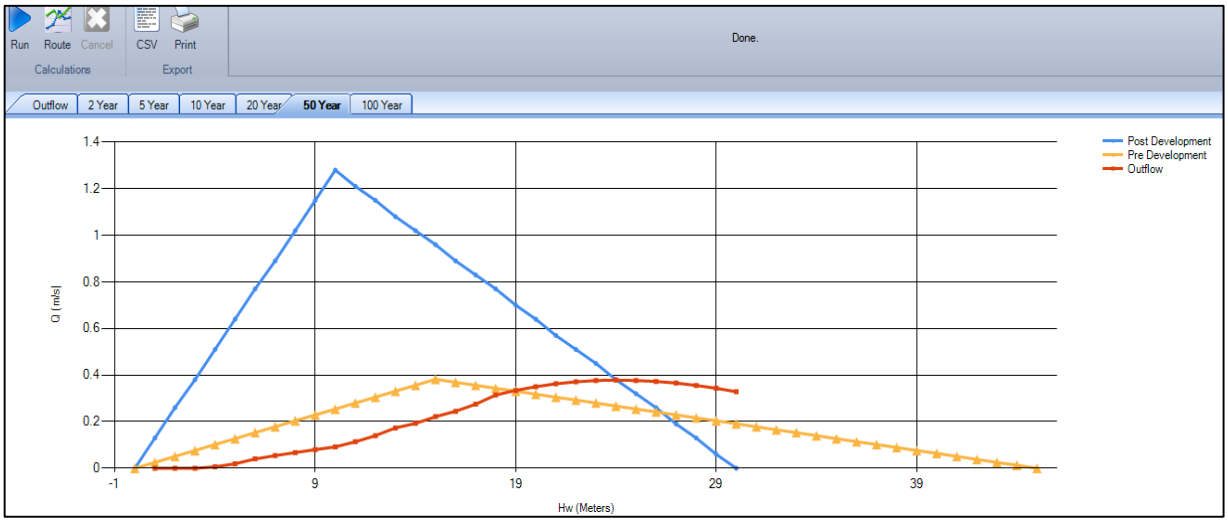

Figure M.5: Used the trail route feature to verify if the outflow for the 50-year RI storm event was restricted to the pre-development peak flow level